Cooperative Communications with Partial Channel State Information in Mobile Radio Systems

Dissertation

zur

Erlangung des akademischen Grades

Doktor-Ingenieur (Dr.-Ing.)

der Fakultät für Informatik und Elektrotechnik

der Universität Rostock

vorgelegt von

Xinning Wei, geb. in Nanjing, China

aus Rostock

Rostock, 14.07.2010

urn:nbn:de:gbv:28-diss2011-0060-4

Als Dissertation genehmigt von der
der Fakultät für Informatik und Elektrotechnik
der Universität Rostock

Gutachter:

Prof. Dr.-Ing. habil. Tobias Weber (Universität Rostock)
Prof. Dr.-Ing. Jürgen Lindner (Universität Ulm)
Prof. Dr.-Ing. habil. Volker Kühn (Universität Rostock)

Tag der öffentlichen Verteidigung:

08.03.2011

Acknowledgement

I am very fortunate to have been a member of the Institute of Communications Engineering in the Faculty of Computer Science and Electrical Engineering at the University of Rostock, where I have done my research work and have written the present thesis. I would like to express my sincere gratitude to those who have contributed in various ways to the completion of this thesis.

Foremost, I am heartily thankful to my supervisor, Prof. Dr.-Ing. habil. Tobias Weber, without whom this thesis would not have been possible. He has been guiding and supporting me from the initial to the final level to complete this thesis. He has been actively interested in my work and has always been available to advise me. His encyclopedic knowledge and his brilliant way of thinking are of a great value for me.

I wish to express my warm and sincere thanks to Prof. Dr.-Ing. Jürgen Lindner from University of Ulm. His encouragement since my graduate study in Ulm has inspired me to become a researcher in the field of wireless communications. I am also indebted to Prof. Dr.-Ing. habil. Volker Kühn who is the Head of our institute. His valuable advices and interesting discussions around my work in our institute's seminars have helped me a lot.

I am indebted to Deutsche Forschungsgemeinschaft (DFG) for sponsoring my work in the framework of the TakeOFDM project. Furthermore, I gratefully appreciate the fruitful exchange of ideas with our project partners Prof. Dr.-Ing. Anja Klein and Dipl.-Ing. Alexander Kühne from Technical University of Darmstadt and Prof. Dr. rer. nat. Hermann Rohling from Technical University of Hamburg-Harburg.

I would like to thank all my former and present colleagues in the Institute of Communications Engineering for providing an excellent and friendly working atmosphere. Particularly, I would like to thank Dr.-Ing. Shiyang Deng for his friendly help and valuable advice in my first years in Rostock. Special thanks go to my officemate Dipl.-Ing. Nico Palleit for helping me to improve my German language and for proof-reading the German version of this thesis's summary. I also wish to thank Dipl.-Ing. Nico Palleit, M.Sc. Hussein Al-Shatri, and Dipl.-Ing. Enrico Ihde, with whom I have enjoyed talking about research work, international cultures, and a lot of interesting things.

Thanks from my heart also go to all my friends throughout the years for their encouragement and support. Research work in office everyday would be pale without the people who make my experience in Germany much richer.

Finally, I owe my deepest gratitude to my parents, Guofang Wei and Xuezhen Chen, for their unconditional love, encouragement and support over the years.

Rostock, July 2010

Xinning Wei

Contents

Chapter 1

Introduction

1.1 Interference management in mobile radio cellular networks

Modern mobile radio communication systems provide data and multimedia transmission services to mobile terminal subscribers. The industry of mobile communications is significantly changing everyday life all over the world, while the increasing demand of better quality of service (QoS) is accelerating its research and development [YCCG05]. During the development of third generation (3G) mobile radio communication systems, research on beyond 3G (B3G) or 4G mobile communications has already begun. In next generation mobile radio communication systems, a rapidly increasing number of subscribers requiring a wider variety of multimedia services with higher data rate will share the limited radio spectrum. Since the scarce resource of bandwidth is quite expensive, the suitable solution is to increase the spectral efficiency. In order to increase the spectral efficiency by reusing the radio channels in different areas, most modern mobile radio networks are designed as cellular networks which are made up of geographically separate areas called cells. The communication service for the mobile terminal subscribers, i.e., mobile stations (MSs), in each cell is controlled by a base station (BS) [Sch05]. The main factors that could limit the system performance of mobile radio cellular networks are noise, fading, and interference. The effects of noise can be combated by increasing the transmit power. The effects of fading can be combated by applying diversity techniques which increase the reliability of communications by transmitting the same information through independently fading channels [TV05]. In today's interference-limited cellular systems, interference management has already become the central task to achieve spectrally efficient communications. This thesis will focus on the interference management in mobile radio cellular networks.

The remarkable capacity potential of multiple-input multiple-output (MIMO) communication systems has been theoretically indicated by some pioneering work [FG98, Tel99]. Encouraged by these theoretical discoveries, the MIMO technique applying multiple antennas at the transmitter side and at the receiver side has been widely considered in mobile radio cellular networks. For example, in the IEEE 802.16e standard, the IEEE 802.11n standard, the recent standards of both the 3G partnership project (3GPP) and the 3G partnership project 2 (3GPP2), MIMO techniques are taken into

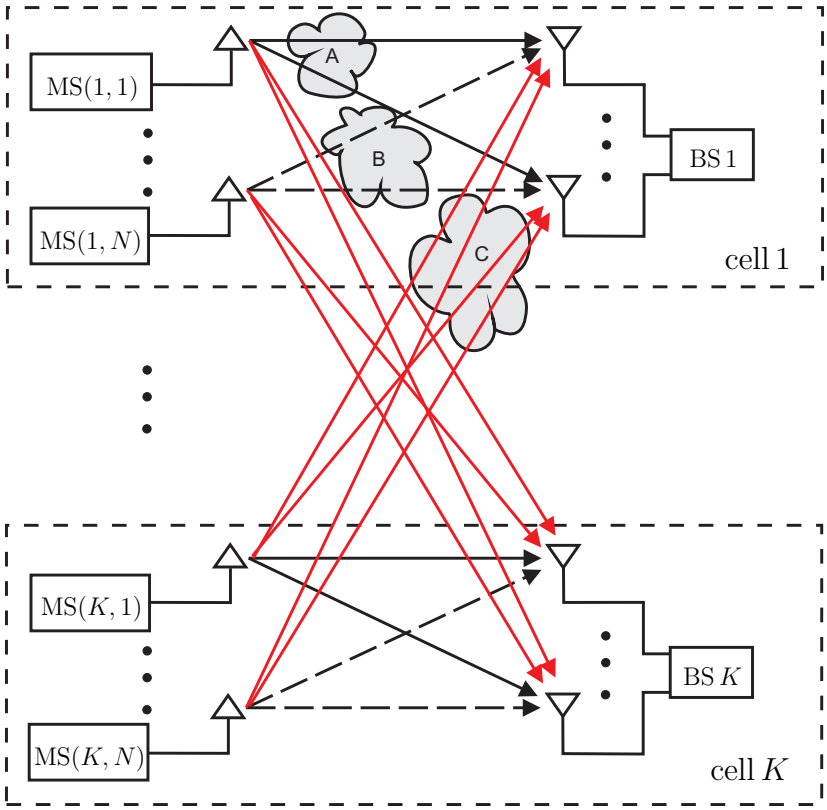

Figure 1.1. Communication in the UL of a mobile radio cellular system. A: ISI; B: intracell multiuser interference; C: intercell interference.

consideration. Considering all the antennas of the MSs on one side and all the antennas of the BSs on the other side, the mobile radio cellular networks which will be investigated in this thesis can be considered as multiuser MIMO systems.

In mobile radio cellular networks, the wireless link over which signals are transmitted from MSs to BSs is called uplink (UL), while the wireless link over which signals are transmitted from BSs to MSs is called downlink (DL). Assuming that the investigated cellular system consists of K cells, the simplified setup of data communication in the UL and in the DL of the mobile radio cellular system is generally shown in Figure 1.1 and Figure 1.2, respectively. In each cell, one BS equipped with multiple antennas and N MSs equipped with a single antenna each are considered. The multiple MSs in cell k with $k = 1 \dots K$ are indicated by $\mathrm{MS}(k, n)$ with $n = 1 \dots N$. In conventional cellular systems, it is expected that data transmissions are performed in each cell between the MSs and their own BS in the same cell. In Figure 1.1 and Figure 1.2, three types of interference are described:

- In most realistic cellular systems, there are multiple propagation paths between one BS antenna and one MS antenna. Due to different delays in different propagation paths, intersymbol interference (ISI) is caused by the overlap of received

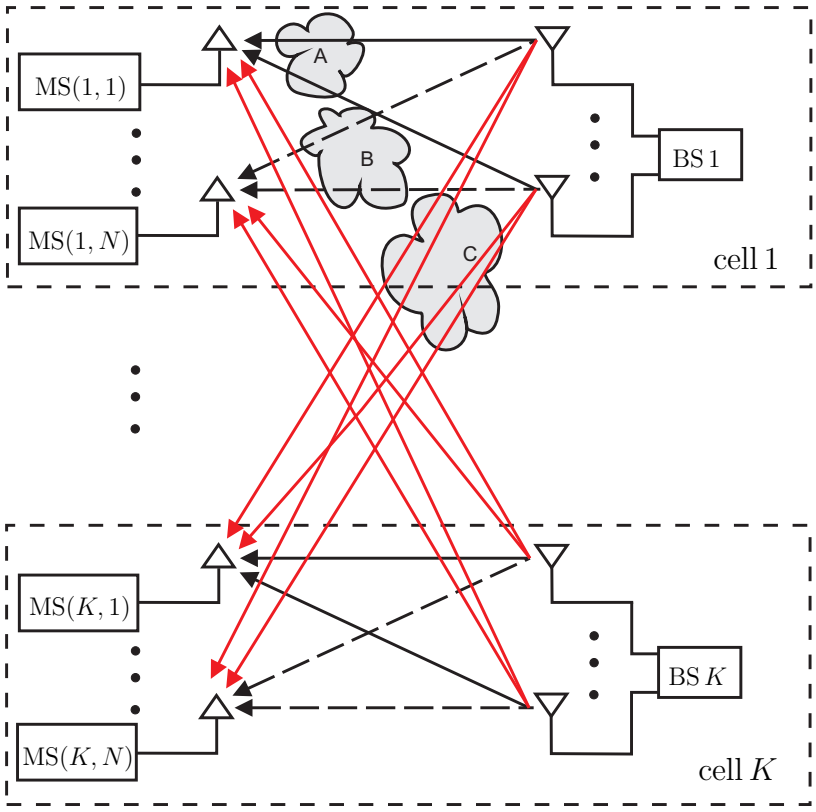

Figure 1.2. Communication in the DL of a mobile radio cellular system. A: ISI; B: intracell multiuser interference; C: intercell interference.

signals of adjacent data symbols of one user. An example of ISI for MS$(1, 1)$ in cell 1 is indicated as the type "A" interference in Figure 1.1 and Figure 1.2, respectively. On one side, ISI in frequency selective channels can be combatted with equalization. Linear equalizers such as the zero forcing (ZF) equalizer are conventional equalizers fighting against ISI. In order to avoid the noise enhancement problem inherent to linear equalizers, decision feedback equalizers (DFEs) with higher implementation complexity are better choices [Lin05]. On the other side, applying multicarrier transmission techniques such as the orthogonal frequency division multiplexing (OFDM) technique with sufficient long guard interval, all ISI can be avoided. However, the guard interval reduces the data rate of the system. Therefore, a good compromise between data rate and ISI cancellation should be considered.

- With multiple MSs in each cell, signals from different MSs arrive at the BS receiver antennas simultaneously in the UL, and the transmitted signals from the BS transmitter antennas for any MS will also go to other MSs in the DL. This kind of interference among different MSs in one cell can be named as intracell multiuser interference, and an example of it for MS$(1, 1)$ in cell 1 is indicated as the type "B" interference in Figure 1.1 and Figure 1.2, respectively. An intu-

itive idea to manage the intracell multiuser interference is to separate different users in different orthogonal resources to avoid interference among them [TV05]. Following this idea, intracell multiuser interference can be avoided by scheduling transmissions of any two users in one cell in different time and frequency resources without any overlap. In the GSM system, e.g., individual orthogonal narrowband channels are allocated to individual users in the same time slot while each narrowband channel in a certain frequency band is shared by users in a time-division manner. However, in future mobile radio cellular systems, higher data rate and better QoS need to be offered to an increasing number of users in the limited orthogonal resources [YCCG05, Tac03]. In other words, the orthogonal channels in the narrowband GSM system are not sufficient to be assigned exclusively to the users. In contrast to the poor frequency diversity in a narrowband system, in wideband OFDM systems the orthogonal frequency division multiple access (OFDMA) scheme for eliminating intracell multiuser interference is combined with the frequency/time hopping techniques for averaging intercell interference [TV05]. In wideband CDMA systems, other strategies for intracell multiuser interference management need to be applied. For example, in the UL of a CDMA system, the near-far problem which is caused by the intracell multiuser interference could exist. Due to the path loss of radio channels, the receiver at the BS can have much less received power of the MSs being far away from the BS than the MSs close to the BS if the MSs use the same transmit power. The intracell multiuser interference from the MSs close to the BS can even make the data detection of the MSs being far away from the BS impossible. Power control strategies are applied to solve the near-far problem. The minimum received power for every MS corresponding to its signal-to-interference-plus-noise ratio (SINR) threshold for data detection is maintained by carefully controlling the transmit powers. Furthermore, since intracell multiuser interference is a limiting factor in CDMA systems, intracell multiuser detection techniques are usually applied in the receivers.

- In the UL, the signals are expected to be transmitted from each MS to its corresponding BS in the same cell. However, these signals will also reach other BSs and interfere with each other. In the DL, the signals are transmitted not only from each BS to its corresponding MS in the same cell but will also cause interference to the MSs in other cells. This kind of interference is named intercell interference, and an example of it for MS$(1, 1)$ in cell 1 is indicated as the type "C" interference in Figure 1.1 and Figure 1.2, respectively. In most cellular systems, the intercell interference is simply treated as noise. In order to make this treatment more reasonable, different interference averaging strategies can be applied to make the sum of intercell interference for one MS look like white Gaussian noise and to

reduce the fluctuation of the total interference. However, the averaging method can only alleviate the influence of intercell interference in scenarios with many users in random positions of adjacent cells. Another simple idea is to increase the cluster size which is defined as the number of cells which collectively use the complete set of available frequencies [Rap01]. In this way, we can geographically separate the users sharing the same frequency channel far away from each other to reduce the intercell interference between co-channel cells. However, this is not a practical solution in realistic systems where the scarce frequency resource is quite expensive. In order to achieve the required system performance in future mobile radio cellular system, further intercell interference management to improve the spectral efficiency is inevitable in the long term. Multiuser detection in the UL and multiuser transmission in the DL for dealing with interference from the signal processing point of view could be promising solutions.

As mentioned above, in mobile radio cellular networks there are mainly three types of interference, i.e., ISI caused by the same user, intracell multiuser interference caused by different users in the same cell, and intercell interference caused by different users in different cells. In order to deal with the above interference which limits the system performance of mobile radio cellular networks, interference management becomes an essential task to improve the system performance. Some mobile radio communication strategies for interference management such as resource allocation, power control, interference averaging techniques, and interference cancellation/presubstraction signal processing techniques have been separately discussed concerning different types of interference. From a system point of view, various mobile radio communication strategies for interference management as mentioned above can be combined with each other to jointly deal with the interference. For example, in [Yen01] interference management is performed through power control, multiuser detection and beamforming for CDMA systems. In [B$^+$07], intercell interference is managed by dynamic channel allocation, scheduling and smart antennas. In [GKGØ07], adaptive transmission and resource allocation are considered simultaneously for interference management.

In the present thesis, the OFDM transmission technique is applied to eliminate all the intracell interference with respect to ISI and intracell multiuser interference in the investigated mobile radio cellular networks. Therefore, it is sufficient to assume that one active MS is contained in each cell in the considered subcarrier and time slot. The remaining interference that limits the system performance is the intercell interference. This thesis mainly contributes to the intercell interference management through cooperative communication schemes where multiuser detection and transmission techniques are applied.

1.2 Concept of cooperative communication

Based on the statement in the above section, this thesis will focus on intercell interference management in cellular networks where the OFDM transmission technique is applied. As one promising candidate for the interference management to achieve spectrally efficient communications in future mobile radio cellular networks, the cooperative communication scheme will be introduced in this section. In order to explain different communication schemes in cellular networks in a simple way, firstly a 3-cell cellular system with one BS and one MS in each cell as shown in Figure 1.3 is taken as an exemplary scenario.

In conventional cellular systems with a cluster size of $r = 1$ as shown in Figure 1.3 (a), data detection and transmission are designed considering only intracell communications. Each BS acts as a central unit (CU) to detect the data symbols from the MS in the same cell in the UL and to design the transmitted signals intended for the MS in the same cell in the DL. It is found that the capacity in such a point-to-point link grows linearly with the minimum number of the transmit and receiver antennas [FG98,Tel99]. Therefore, the MIMO technique applying multiple antennas at both the transmitter side and the receiver side can significantly improve the system throughput. For example, the single user MIMO technique has already been proposed in the current 3GPP long-term evolution (LTE) Release 8 for cellular networks [IMW+09]. However, in conventional cellular networks without cooperation between different cells, the intercell interference caused by the signals from the MSs in other cells to the considered BS in the UL and the transmitted signals from the considered BS to the MSs in other cells in the DL can strongly limit the system performance [CDG00, Blu03, DMP04]. In order to obtain a better system performance, one simple idea is to spatially separate the co-channel users to be far away from each other by increasing the cluster size of the cellular system. For example, the cellular system in Figure 1.3 (b) has a cluster size of $r = 3$. However, on one side the cluster size can not be increased without considering the cost for the scarce frequency resource, and in realistic cellular systems with a small cluster size the remaining intercell interference still limits the system performance. On the other side, in future mobile radio cellular systems with more and more users, higher data rate and better QoS need to be offered in the limited orthogonal resources [YCCG05, Tac03]. Therefore, it is necessary to apply better interference management strategies with small cluster sizes.

The cooperative communication scheme where BSs cooperate with each other to perform a cooperative signal processing for MSs in different cells is considered as a promising candidate for the interference management in multicell cellular systems. The co-

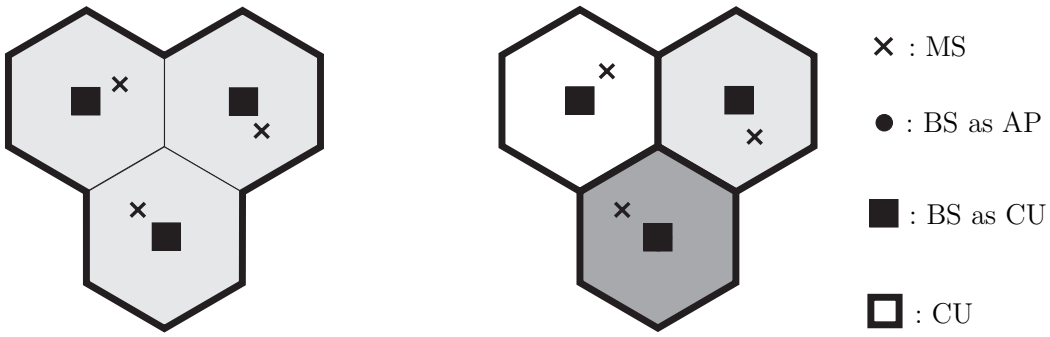

(a) conventional cellular system, $r = 1$

(b) conventional cellular system, $r = 3$

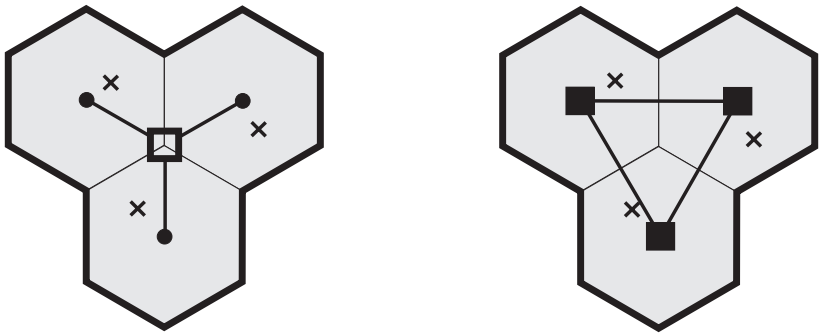

(c) cooperative cellular system based on a centralized implementation, $r = 1$

(d) cooperative cellular system based on a decentralized implementation, $r = 1$

Figure 1.3. Conventional cellular system versus cooperative cellular system.

operation of BSs in a mobile radio network can be implemented either in a centralized way or in a decentralized way. In Figure 1.3 (c), a centralized cooperative communication scheme is shown in the exemplary 3-cell cellular system. It is assumed that the BSs are connected to the CU via high speed backhaul links with high capacity. Individual BSs play the role as access points (APs) which receive signals from MSs in the UL and transmit signals to the MSs in the DL. The cooperation of the BSs is realized with the help of a CU. The CU coordinates all the BSs and performs a joint signal processing of the whole system to detect the data symbols of the MSs in the UL and to design the transmitted signals to the MSs in the DL. In Figure 1.3 (d), a decentralized cooperative communication scheme based on coordinated BSs without a CU is shown in the exemplary 3-cell cellular system. Distributed BSs not only receive and transmit signals but also act as CUs to perform a multi-cell cooperative signal processing together. The BSs are connected to each other via high speed backhaul links with high capacity, and they exchange information, e.g., channel-state information (CSI) and intermediate calculation results, between each other for the cooperative signal processing. As discussed in the following, both the information-theoretic works

and the practical considerations of the realistic system performance potentials show that the cooperative communication scheme is a very promising candidate for future mobile radio cellular networks.

Theoretically, the main effect of cooperative communication is to extend the single-user MIMO concept in a single cell with remarkable capacity potential as shown in [FG98, Tel99] to multiuser cellular systems. With perfect BS cooperation, a multicell system can be considered as a MIMO multiple access channel (MAC) in the UL and a MIMO broadcast channel (BC) in the DL [GJJV03]. The capacity region of the MAC has already been well studied by researchers [CV93, CT06, TH98, Tel99, VJG01, VTA01, YRBC04], and has been summarized in [GJJV03] for both the constant channels and the fading channels with different levels of knowledge of CSI. However, it has been a challenging task for quite a long time to find the capacity region of a general BC. Recently, it has been suggested in [CS03] that the dirty-paper coding (DPC) strategy in [Cos83] could be applied for transmitting signals in BC. The achievable rate region for a BC applying the DPC strategy could be named as the DPC rate region. The DPC rate region for a Gaussian MIMO BC with multiple transmitter antennas and a single antenna at each receiver was found in [CS03]. The DPC rate region for a Gaussian MIMO BC with an arbitrary number of antennas at each receiver was found in [YC04], which has also shown that the DPC rate region achieves the sum capacity of this BC. The duality of the capacity region of the Gaussian MIMO MAC and the DPC rate region of the Gaussian MIMO BC has been investigated in [VJG03]. Similar to the signal-user MIMO system with a great capacity potential in proportion to the number of antennas, the above work about the MIMO MAC and the MIMO BC has shown that the sum capacity of a multiuser system increases linearly with the increment of the number of transmitter antennas or receiver antennas [GJJV03]. Performance improvements of a cellular network applying the cooperative communication scheme as compared to that applying the single-user communication scheme have been shown with respect to the achievable rate region [SZ01, ZD04, KFV06, J$^+$08, KFVY06].

In practice, the multiuser MIMO system applying cooperative communication is not only a simple shift of the MIMO paradigm from a single-user point-to-point system to a multiuser cellular system. The multiuser MIMO system has some inherent advantages over the single-user MIMO system [GKH$^+$07]:

- The theoretically promised capacity of the MIMO system increases with the minimum of the number of the transmit and receiver antennas, i.e., the number of spatial degrees of freedom [TV05, FG98, Tel99]. However, in realistic systems we can't equip as many antennas as we want at the MSs or at the BSs without considering the space constraints and the cost limitations. Especially, the MSs, e.g.,

mobile phones of customers, are always required to have low complexity, low cost and small size from a practical point of view. Therefore, the system performance of the single-user MIMO scheme is limited by the small number of antennas at the MS in reality. In contrast, the multiuser MIMO system inherently has much more spatial degrees of freedom than the single-user MIMO system. For example, in a K-cell cellular system with one BS and one MS in each cell, even though each MS is equipped with only a single antenna, at least the system with full cooperation of all the BSs has K spatial degrees of freedom thanks to the multiuser diversity.

- Many previous information-theoretic works that exploit the capacity of the MIMO system are under the assumption of independent and identically distributed (i.i.d.) fading channels connecting pairs of transmitter and receiver antennas [FG98]. However, in realistic single-user MIMO systems, due to the poor scattering environment and the insufficient spacing between the antennas, the fading channels are correlated and the achievable capacity is significantly reduced [SFGK00, IUN03]. Fortunately, in cellular networks which can be considered as multiuser MIMO systems, distributed coordinated BSs in different cells form a distributed antenna array which can offer rich scattering and large antenna spacing. Even though the single-user diversity is limited by the correlated fading, the great capacity potential of the MIMO system still can be achieved by exploiting the multiuser spatial multiplexing.

- As indicated in [FG98, Tel99], the input signal-to-noise ratio (SNR) has a great influence on the capacity of MIMO channels. In realistic cellular networks, the single-user MIMO communication is performed treating all the multiuser interference as noise. Therefore, the low input SNR can strongly limit the system performance. However, in the multiuser cooperative MIMO system exploiting the multiuser interference, the interference is converted from barriers to opportunities to improve the system performance. For every user, its multiuser interference will not be accounted as noise, and hence the input SNR only depends on the background Gaussian noise. Therefore, the multiuser MIMO system with a high input SNR can fully enjoy the benefit of the MIMO techniques.

Generally, cooperative communication can be described as cooperative reception in the UL and cooperative transmission in the DL through a cooperative signal processing for the MSs in different cells based on coordinated BSs. The cooperative signal processing algorithm for joint detection (JD) in the UL [KKB96, Ver98, Poo04, LDYT05] and joint transmission (JT) in the DL [MBW$^+$00, Fis02] is considered as the core technology in the concept of cooperative communication.

In the UL, various multiuser detection strategies to detect data symbols from multiple users in a communication network considered as a multiuser MIMO MAC can be used as candidates for JD [Ver98, Poo04]. In order to minimize the probability of erroneous detection, the optimum multiuser detectors choose the most likely transmitted data vector following the maximum-a-posteriori (MAP) criterion or the maximum likelihood (ML) criterion, where the received vector and a priori information of the data vector are known. However, such a multiuser sequence detection considering all the possible data vectors has very high complexity, and is not suitable for practical applications in cellular networks. Therefore, suboptimum multiuser data detection which makes a tradeoff between complexity and performance is of more interest. Following strategies such as ZF or minimum mean squared error (MMSE), one class of the suboptimum detectors named as conventional linear multiuser detectors have been well investigated in [KB93, MH94, Kle96, KKB96, Mos96, Ver98]. Aiming at the multiuser interference cancellation, the ZF detector, i.e., the so-called decorrelator, turns out to be a promising solution in interference-limited systems with weak noise. However, noise enhancement is considered as the main drawback of the ZF detector. The MMSE detector, i.e., the so-called Wiener filter, which approaches the performance of a matched filtering (MF) receiver in systems with strong noise, makes a good compromise between interference cancellation and SNR improvement. Although the complexity of linear multiuser detectors is much smaller than that of optimum multiuser detectors, a pseudo inversion of the system matrix typically required in the computation can still cause great computational complexity. Fortunately, linear algebra indicates that the linear system of equations requiring matrix inversion can be solved in an iterative way following methods such as the Jacobi method or the Gauss-Seidel method [HJ85]. Following this idea, linear iterative multiuser detectors which have lower complexity but generally comparable performance as compared to the conventional linear multiuser detectors have been proposed [Mos96, Poo04, Küh06]. Improved performance can be obtained by the nonlinear iterative multiuser detectors which follow the same ideas as the linear iterative multiuser detectors but additionally make intermediate soft or hard decisions by exploiting the discrete data alphabet in each iteration to obtain refined data estimates [VA90, DSR98, Ver98, Poo04, Küh06]. Among the iterative multiuser detectors known as interference cancellers, the parallel interference cancellation (PIC) detector and the successive interference cancellation (SIC) detector have gained most attention [Ver98, WBR$^+$, WRB$^+$02, Poo04, Küh06, AWWD07]. Furthermore, alternative nonlinear multiuser detectors named as turbo multiuser detectors, which exploit the knowledge concerning the forward error correcting (FEC) coding and follow the turbo principle [Hag97] to achieve optimum data estimate refinement, have received a considerable attention [Moh98, WP99, Poo00, Poo04].

In the DL, with the help of the coordinated BSs or the CU connected to the BSs, a multiuser MIMO BC is formed. The cooperative signal processing task is shifted to the transmitter side to make the MSs as simple as possible. With the knowledge of the receiver structure and the CSI of the system, the process to generate transmitted signals at the transmitters is called precoding [VJ98, Fis02]. From an information-theoretic point of view, DPC is considered as the optimum precoding strategy [CS00, YC04]. However, its high computational complexity limits its application in realistic networks. From a practical point of view, precoding techniques with less computational complexity are of more interest for the realistic cooperative communication scheme. As the counterparts of the conventional linear multiuser detectors, ZF multiuser transmitters [VJ98, MBW+00, KM00] and MMSE multiuser transmitters [JKG+02, NB02] have been proposed. Their corresponding iterative versions, e.g., iterative ZF JT, are of great interest for practical applications in the DL of cellular networks to predict and presubtract interference [WWAD07, WWA07]. As one representative nonlinear successive interference canceller in the DL, the Tomlinson-Harashima precoding (THP) transmitter which was initially proposed for the equalization of ISI in single-input single-output (SISO) channels [Tom71,HM72] has been extended to MIMO channels [FWLH02,Fis02]. The basic idea of THP is to shift the decision-feedback equalizer (DFE) from the receiver side to the transmitter side, and a modulo device is considered to limit the transmit power.

1.3 State of the art and open questions

In recent years the concept of cooperative communication has received considerable attention from researchers all over the world because of its potential to achieve high spectral efficiency with affordable implementation complexity in realistic systems [WMSL02, ZD04, ZTZ+05, TXX+05, WSM06, KFV06, KFVY06, AEH06, WWAD07, KM07, MF07b, J+08, SSSP08, MF08, NEHA08, KF08, KRF08, WWC08, HZW08, PBGH08, PGH08, XZ09, ZCA+09, MF09b, MF09a, TPK09, ZHG09, PHG09, WJLY09, JTW+09, IMW+09, WHG+10]. The scheme of the joint transmission and detection integrated network (JOINT) was initially proposed for beyond 3G systems in [WMSL02], and as a generic proposal many degrees of freedom concerning the implementation of JOINT exist. Assuming that full perfect CSI is available, a cooperative processing scheme at BSs in a small size cellular system was proposed in [ZD04]. The study in [KFV06] has shown the theoretical performance gains of cooperative communication to encourage further studies striving toward these gains in practice. The same concept of cooperative communication has been intensively investigated under

various names such as "cooperative base stations" in [NEHA08], "multicell cooperative processing" in [PBGH08, PGH08, PHG09], "distributed base station processing" in [AEH06], "joint multi-cell processing" in [SSSP08], "distributed beamforming coordination" in [ZHG09], "networked MIMO" in [ZCA+09], and "coordinated multipoint transmission (CoMP)" in [XZ09, TPK09, WJLY09, WHG+10]. In some national projects for next generation communication systems, schemes based on this concept have already been applied. In China, a scheme under the name "group cell" has already been applied under the framework of the FuTURE (Future Technologies for Universal Radio Environment) project for beyond 3G mobile communication systems in the TDD Special Work Group [ZTZ+05, TXX+05]. In Germany, a similar concept about cooperative communication under the name of CoMP has been considered in the project Enablers for Ambient Services and Systems-Part C wide area coverage (EASY-C) [MF09b, IMW+09]. In this project, the first real-time trial test of the CoMP scheme in the largest testbed worldwide for LTE-Advanced systems has been performed recently [JTW+09]. In the 3GPP standards for LTE-Advanced, the concept of cooperative communication under the name of CoMP is considered as a promising candidate for the physical layer [TR309].

The key point of current research on cooperative communication is how to apply this concept in realistic mobile radio cellular networks under practical constraints such as the implementation complexity and the ability to track the CSI. The theoretical predicted excellent system performance obtained through cooperative communication with perfect CSI of the whole cellular system is limited in reality. In realistic cellular systems with a large area containing a huge number of cells, on one hand the joint signal processing based on full CSI of the whole system is almost infeasible with respect to the computational load. On the other hand, the speed and the capacity of the backhaul links interconnecting all the BSs in the decentralized scheme or connecting all the BSs to the CU in the centralized scheme can not increase without limit. Taking these practical constraints into consideration, research on cooperative communication is going on. A topological architecture allowing only links between adjacent BSs was proposed in [AEH06] to limit the backhaul network traffic. Mixed local and central signal processing was proposed in [SSSP08] to distribute the computational load to BSs and the CU with limited-capacity backhaul network. However, the above proposals are inadequate in large networks since high speed communication links between BSs and the CU are still required and full CSI is still required for every MS. One promising concept is to perform cooperative communication with partial CSI, i.e., part of the available full CSI, in separate subsystems, i.e., cooperative clusters. In this way, the computational load can be reduced as only a part of the full CSI is required for every MS, and the communication load of the backhaul links

is also reduced as only the local information needs to be exchanged in each subsystem. Following this idea, on one side, with respect to the geographical structure of the cellular system, the concept of service areas (SAs) containing several APs and a CU applying joint signal processing of the users in each small group of cells has been proposed in [WMSL02]. Similar concepts under the names "group cell" and "cooperative cluster" have been proposed in [ZTZ+05, TXX+05, ZCA+09]. On the other side, with respect to the strongly constrained backhaul, schemes for selecting users or channels considered in subsystems to reduce the backhaul communication load of the cooperative communication scheme have been proposed in [MF08, KF08, KRF08]. Last but not the least concerning the practical constraints, the limited ability to track the CSI has to be considered. The influence of imperfect CSI on the multiuser MIMO systems applying cooperative communication has been paid more attention in recent years [WSM06, WWC08, HZW08, PHG09].

Nevertheless there are still a number of roadblocks on the way to the implementation of the cooperative communication concept in realistic cellular systems. Some open questions concerning this interesting concept discussed in this thesis are listed in the following.

Firstly, the information-theoretic performance of the coordinated cellular networks applying cooperative communication with full perfect CSI has been studied in [ZD04, KFV06, SZ01, KFVY06, GJJV03, J+08]. Researchers have also paid attention to the achievable rates of the cellular systems applying cooperative communication with limited backhaul capacity or imperfect knowledge of CSI [GJJV03, SSSP08, SSPS09, MF09b, MF09a]. However, the basic information-theoretic background of the cooperative communication with partial CSI has not yet been well studied. The capacity loss due to partial CSI instead of full perfect CSI considered in the cooperative communication scheme is not precisely known.

Secondly, in order to implement the theoretical concept of cooperative communication in realistic systems, a good tradeoff between system performance and implementation complexity has to be made. As mentioned above, a practical cooperative communication scheme is based on an efficient cooperative signal processing technique considering partial CSI for every MS. Some issues concerning the practical cooperative communication scheme will be discussed in this thesis:

- In most of the state of the art techniques on cooperative communication with partial CSI, significant channels for each MS considered in JD/JT are selected according to the static geographical structure. Taking a 12 cell cellular system as

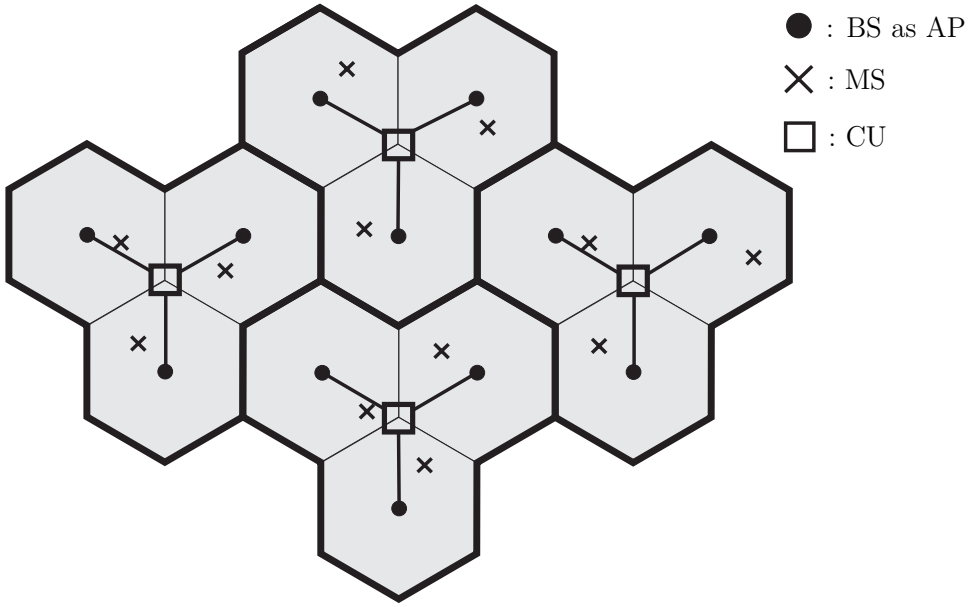

Figure 1.4. SA architecture with SA size 3 in a cellular system with cluster size 1.

an exemplary scenario, the SA scheme considering 3 cells in each SA is shown in Figure 1.4. Selecting all the channels inside every SA as significant channels for all the MSs inside this SA, the CU in this SA preforms intra-SA JD in the UL and intra-SA JT in the DL. In this scheme, MSs close to the boundary of a SA can strongly suffer from the inter-SA interference. With the static structure-oriented significant channel selection strategies, the computation complexity is significantly reduced at the price of severe performance degradation. In the opposite direction aiming at good system performance, recently various dynamic significant channel selection strategies have been proposed. In [PGH08], significant channels are selected to form disjoint graphs which maximize the sum-capacity. In [MF07b], significant channel selection in the form of user grouping is considered with respect to the overall optimization of capacity under a constrained backhaul traffic. In [KM07], significant channel selection corresponding to BS selection is performed by applying SNR sorting and exhaustive search. With these dynamic performance-oriented significant channel selection strategies, the computation complexity is very high, and this is not a practical solution to realize cooperative communication. Therefore, a practical significant channel selection strategy which can make a good compromise between system performance and implementation complexity needs to be developed. As shown in Figure 1.5, based on the high speed and high capacity backhaul links connecting the BSs, the significant CSI considered for each MS could correspond to certain channels from a dynamic area. A practical decentralized cooperative communication scheme which can make full use of the significant CSI corresponding to the dynamically

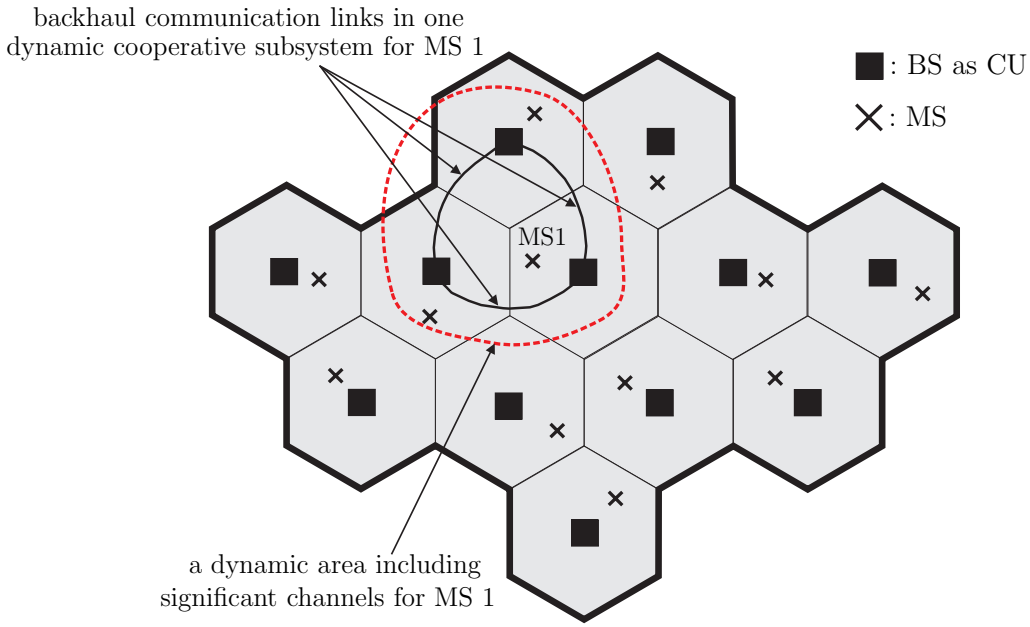

Figure 1.5. Decentralized cooperative communication scheme in a cellular system with cluster size 1.

selected significant channels is needed.

- Although various multiuser detection and multiuser transmission strategies for multiuser MIMO systems have already been proposed, a practical JD/JT algorithm which is good at dealing with interference based on the selected significant CSI has to be developed. A practical implementation of the cooperative signal processing for JD/JT needs to be designed based on the infrastructure of coordinated BSs in realistic cellular networks. System performance of the cooperative communication scheme with interference cancellation/presubstraction considering significant CSI for each MS needs to be assessed. The implementation complexity of the cooperative communication scheme with respect to the computational load and the backhaul communication load needs to be evaluated.

- It is interesting to investigate the influence of the BS-antenna-layout on the performance of cooperative communication applying various signal processing techniques. A suitable BS-antenna-layout for the cooperative communication scheme with partial CSI needs to be found. Whether the performance gain from the intelligent signal processing technique and that from the smart BS-antenna-layout can be added up in the cooperative communication scheme is an open question to be answered.

Thirdly, although a lot of research work has been done to investigate the influence of imperfect CSI on multiuser MIMO systems considering full CSI [WSM06, PHG09],

the impact of imperfect CSI on multiuser MIMO systems considering only significant CSI has rarely been mentioned in the literature. Since in realistic cellular systems due to channel estimation errors or CSI feedback errors only imperfect CSI is available, it is quite necessary to investigate whether the proposed cooperative communication scheme with significant CSI is robust in realistic systems considering the imperfectness of CSI [WWKK09]. Especially, in the practical cooperative communication scheme the question about how much significant CSI should be considered in JD/JT to achieve optimum system performance under different levels of the imperfectness of CSI is another interesting open question.

1.4 Thesis outline

In the present thesis, time division duplexing (TDD) multiuser cellular systems applying the OFDM transmission technique are investigated [vNP00]. As a promising candidate for interference management in future mobile radio cellular networks, cooperative communication is investigated as the main topic of this thesis. Generally, the aim of this thesis is to contribute to the cooperative communication concept considering practical constraints in realistic cellular systems, e.g., implementation complexity, backhaul communication load and the limited ability to track the CSI. In this thesis, the concept of cooperative communication is reconsidered from a point of view of partial CSI, i.e., significant CSI for each MS in contrast to full CSI of the whole system and imperfect CSI in realistic systems in contrast to perfect CSI. The main content of this thesis is outlined in this section.

In Chapter 2, a brief description of the considered mobile radio channel model is given. The principle of the OFDM transmission technique and the alternative BS-antenna-layouts, based on which the proposed cooperative communication scheme is established, are introduced. Finally, the system model of a general multiuser MIMO cellular system for the investigation of cooperative communication is described.

In Chapter 3, the information-theoretic background of multiuser MIMO systems is investigated based on a two-user communication channel model [Sat77]. Four typical multiuser communication schemes with no cooperation, cooperative reception, cooperative transmission, and full cooperative transmission and reception are investigated with respect to the achievable rate region. Especially, from the information-theoretic point of view, cooperative reception at the receiver side forms a MAC model, while cooperative transmission at the transmitter side forms a BC model. With the help

of some simplified information-theoretic models, the capacity gain thanks to cooperation and the capacity loss due to partial knowledge of CSI are evaluated. The work in Chapter 3 encourages practical work achieving the promising information-theoretic performance gain of cooperative communication.

Cooperative reception in the UL is investigated in Chapter 4. In the first part of Chapter 4, some multiuser detection strategies as theoretical candidates for the signal processing algorithm in the cooperative reception scheme are discussed. The principles of optimum detection strategies, e.g., MAP and ML, and the linear multiuser detection strategies, e.g., MF and ZF, are briefly introduced. Especially, the iterative interference cancellation strategies, e.g., PIC and SIC, are discussed for the investigated interference-limited cellular systems. The discussion of multiuser detection strategies in the UL is completed by developing several advanced data detection schemes following the ideas of statistical signal processing to achieve optimum system performance based on the soft information. The second part of Chapter 4 starts with a discussion of design guidelines for practical cooperative communication schemes. Based on the design guidelines, a general framework of cooperative communication suitable for both the cooperative reception scheme in the UL and the cooperative transmission scheme in the DL is shown. The practical cooperative communication scheme is expected to not only reduce the computational load and the backhaul communication load as compared to the scheme with full CSI, but also to be beneficial to the system performance. Then, a practical cooperative reception scheme as a promising solution to intercell interference management in the UL of realistic cellular systems is proposed step by step. Significant channel selection, interference cancellation, and decentralized signal processing are discussed, respectively. In the proposed MS-oriented dynamic significant channel selection scheme, the significant useful channels are distinguished from the significant interfering channels for each MS according to the functionality of the channels. An iterative ZF JD algorithm with significant CSI corresponding to the MS-oriented significant channels is proposed for intercell interference cancellation. The decentralized implementation of the cooperative signal processing is based on coordinated BSs connected by high speed backhaul links. Without a CU, the cooperative signal processing is efficiently performed at coordinated BSs. During the cooperative signal processing considering the MS-oriented significant CSI, only a limited amount of information is exchanged between neighbouring BSs through backhaul links.

Cooperative transmission in the DL is investigated in Chapter 5. From the theoretical point of view, some multiuser transmission strategies as candidates for the precoding algorithm in the cooperative transmission scheme are discussed in the first part of Chapter 5. After a brief introduction of the principle of the capacity-achieving DPC strategy, some multiuser transmitters following the linear precoding strategies,

e.g., MF transmitter and ZF transmitter, are described. As promising precoding candidates for interference-limited cellular systems, iterative interference presubstraction schemes, e.g., parallel interference presubstraction and THP as a nonlinear successive precoding technique, are discussed. Then, in the second part of Chapter 5, a practical cooperative transmission scheme for the DL of realistic cellular systems is proposed as the counterpart of the cooperative reception scheme in the UL. Due to the channel reciprocity of the investigated TDD systems, significant channels in the DL are selected following the same mathematical criterion as in the UL. An iterative ZF JT algorithm with significant CSI is proposed for interference presubstraction at the BSs. Similar to the case in the UL, the cooperative signal processing for JT in the DL is also implemented in a decentralized way based on coordinated BSs.

Whether the proposed cooperative communication scheme can offer good system performance with moderate implementation complexity is assessed in Chapter 6. The implementation complexity is evaluated with respect to the computational load and the backhaul communication load. Concerning the system performance, analytical calculations and numerical simulations are performed. The limiting values of the data estimates in the iterative JD/JT algorithm and the resulting output SINR are analytically calculated. Based on numerical simulations taking a 21-cell cellular system as the reference scenario, the system performance is investigated with respect to the following aspects for both the UL and the DL. Firstly, the system performances considering various significant channel selection schemes with different numbers of significant channels are compared. Then, the performance gains from alternative smart BS-antenna-layouts in combination with different signal processing techniques are assessed. Finally, the impact of the imperfectness of the CSI on the system performance is assessed. The corresponding performance degradations due to the imperfectness of CSI used in the significant channel selection and in JD/JT with partial CSI are evaluated. The question about how much CSI should be considered as a function of the extent of the imperfectness of the CSI in order to achieve optimum system performance with moderate complexity is answered based on numerical results.

The above chapters are summarized in Chapter 7.

Chapter 2
System model

2.1 Mobile radio channel model

In communication systems, the channel is the medium used to convey information from a transmitter to a receiver. A suitable channel model is essential for the design of a system architecture, the optimization of system parameters, and the assessment of the system performance. Therefore, before starting the discussion about the cooperative communication concept, let's first have a look at the mobile radio channel in which wireless communications are performed. Generally, it is difficult to characterize the mobile radio channels in cellular networks since the propagation of electromagnetic signals in the mobile radio channels is influenced by the physical environment and suffers from many effects such as reflection, diffraction, scattering and motion of the transmitter or the receiver [Par92, Rap01, Sch05, Gol05]. Typically, the mobile radio channel can be described in a statistical fashion by the average path gain corresponding to the phenomenon of path loss, the slow fading corresponding to the phenomenon of shadowing and the fast fading corresponding to the phenomenon of multipath propagation. Correspondingly, the propagation in a mobile radio channel is roughly described in Figure 2.1 with respect to the logarithmic path gain G versus the logarithmic distance between the transmitter and the receiver. The logarithmic path gain G is the path gain g measured in dB as

$$G/\mathrm{dB} = 10\log_{10}(g) \ , \tag{2.1}$$

and the path gain g is the ratio of the receive power to the transmit power. As the most representative characteristics of the mobile radio channel, the average path gain, the slow fading and the fast fading will be discussed respectively in the following. Then, the simplified mobile radio channel model considered in this thesis will be presented.

The average path gain is generally described as a function of the propagation distance by various path loss models which are used to characterize the attenuation of signal propagation between a transmitter and a receiver. The parameters in such path loss models mainly depend on the physical environment, carrier frequency and antenna characteristics. For example, the free-space path loss model is a simplified model considering the line-of-sight (LOS) path without obstruction [Par92,Sch05,Gol05]. The two-ray model considers a LOS ray and a single ground reflection ray [Par92, Sch05, Gol05]. Empirical path loss models, e.g., the piecewise linear model [Sch05, Gol05], the Okumura model [OOF68], the Hata model [Hat80] and the COST 231 model [COS91],

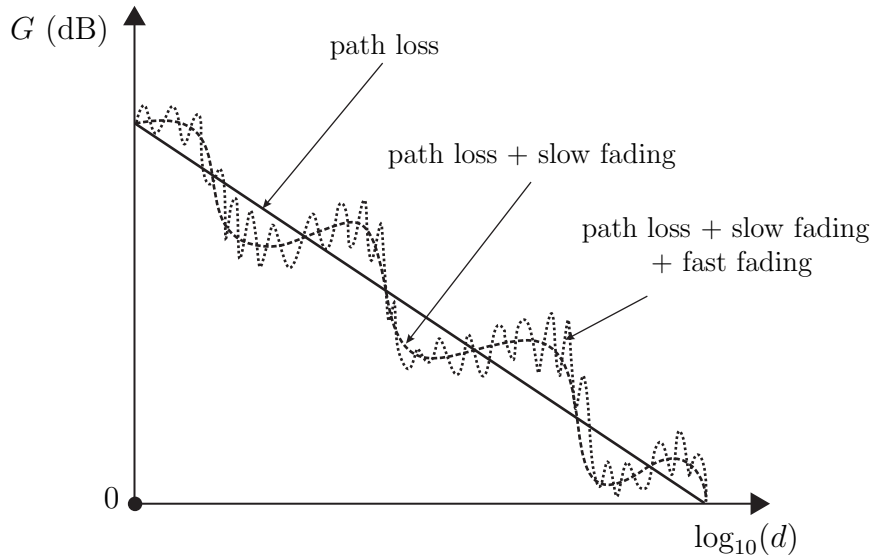

Figure 2.1. The logarithmic path gain G versus the logarithmic distance between the transmitter and the receiver considering path loss, slow fading and fast fading.

are developed based on measurements in a given physical environment over a certain distance and in a certain frequency. In the following, the dual slope model described in [Ste96] which is a special case of the piecewise linear model is taken as an example to show the typical relation between the average path gain $\bar{G}$ and the propagation distance d. With the wavelength λ, the transmit antenna gain g_{T} and the receive antenna gain g_{R}, the dual slope model can be described by

$$\bar{G}/\mathrm{dB} = \begin{cases} -\alpha_1 10\log_{10}\left(\frac{4\pi d}{\lambda}\right) + 10\log_{10}\left(g_{\mathrm{T}} g_{\mathrm{R}}\right) & \text{for } \; 0 \leq d < d_{\mathrm{B}} \\ -\alpha_1 10\log_{10}\left(\frac{4\pi d_{\mathrm{B}}}{\lambda}\right) + 10\log_{10}\left(g_{\mathrm{T}} g_{\mathrm{R}}\right) - \alpha_2 10\log_{10}\left(\frac{d}{d_{\mathrm{B}}}\right) & \text{for } \; d \geq d_{\mathrm{B}} \end{cases} . \tag{2.2}$$

Two different attenuation exponents α_1 and α_2 are used to characterize the decay of receive power with respect to the propagation distance d considering a certain measured breakpoint distance d_{B}.

Due to the shadowing effect which is mainly caused by obstacles in the wireless channel between the transmitter and the receiver, the receive power could have random variation even for a constant given propagation distance. A suitable statistical model used to characterize the shadowing effect is known as the slow fading model which can be described by a log-normal distribution of the path gain. More specifically, the logarithmic path gain G follows a Gaussian distribution as

$$\mathrm{p}(G) = \frac{1}{\sqrt{2\pi}\sigma_{\mathrm{G}}} \exp\left\{\frac{(G-\bar{G})^2}{2\sigma_{\mathrm{G}}^2}\right\} \tag{2.3}$$

with mean $\bar{G}$ and variance σ_{G}^2.

Both path loss and shadowing are usually referred to as the large-scale fading effect since they occur over relatively large distances. However, multipath propagation will cause fast fading which is often referred to as the small-scale fading effect characterizing the rapid signal variation over short distances in the order of a wave length. Due to multipath propagation as a consequence of reflection, scattering and diffraction of the transmitted waves, the constructive and destructive superposition of received signal components at the receiver results in a rapid variation of the received signal. The delay spread is used to describe the time difference between the arrival of the first received signal component and the last received signal component resulting from a single transmitted pulse [Gol05]. The larger the delay spread is, the more substantial the signal distortion will be. Additionally, Doppler spreading as a consequence of moving objects, e.g., the transmitter, the receiver and the scatters, in the propagation path leads to the time variant nature of the multipath propagation. Assuming a large number of wavefronts with i.i.d. Gaussian inphase and quadrature components contributing to the received signal, the most common statistical model used to describe fast fading without a LOS is the Rayleigh fading model. In this statistical model, it is assumed that the channel transfer function $\underline{H}(f,t) \sim \mathcal{CN}\left(0, \sigma_{\mathrm{H}}^2\right)$ has a uniformly distributed phase which is independent of its Rayleigh distributed magnitude $A = |\underline{H}(f,t)|$. The probability density function (PDF) of the magnitude A is

$$\mathrm{p}(A) = \frac{2A}{\sigma_{\mathrm{H}}^2} e^{-\frac{A^2}{\sigma_{\mathrm{H}}^2}} \tag{2.4}$$

with $\mathrm{E}\{A^2\} = 2\sigma_{\mathrm{H}}^2$ and $A \geq 0$. Additionally, it is worth pointing out that if multipath propagation contains a LOS, the Rice fading model is a more suitable model to describe fast fading [Par92, Sch05, Gol05].

Without resorting to complicated channel models, a simplified mobile radio channel model which captures the most significant characteristics of signal propagation related to the cooperative communication concept is applied in the present thesis. Ignoring slow fading, the considered mobile radio channel model focuses on path loss and fast fading. The average path gain in the path loss model is described by

$$\bar{g}(d) = \left(\frac{4\pi d}{\lambda}\right)^{-\alpha} g_{\mathrm{T}} g_{\mathrm{R}} \ . \tag{2.5}$$

This simplified path loss model can be treated as a special case of the channel model of (2.2) where a single slope model is considered with the relation $\bar{G}/\mathrm{dB} = 10\log_{10}(\bar{g})$. In the present thesis, the wavelength $\lambda = 0.0545\,\mathrm{m}$ is assumed corresponding to a carrier frequency of 5.5 GHz. Unit transmit antenna gain $g_{\mathrm{T}} = 1$ and unit receive antenna gain $g_{\mathrm{R}} = 1$ are assumed. The typical value of the attenuation exponent $\alpha = 3$ is used. Applying the OFDM transmission technique which will be introduced in the

next section, flat fast fading is assumed in the considered subcarrier and time slot in the channel model. Referring to the Rayleigh fading model of (2.4), the channel transfer function is described as

$$\underline{H}(f,t) = \sqrt{\bar{g}}\left(\underline{H}_{\mathrm{I}}(f,t) + j * \underline{H}_{\mathrm{Q}}(f,t)\right) \quad , \tag{2.6}$$

where $\underline{H}_{\mathrm{I}}(f,t)$ and $\underline{H}_{\mathrm{Q}}(f,t)$ are i.i.d. Gaussian variables with zero-mean and a variance of 1/2 to keep the average value of the channel gain unmodified.

2.2 OFDM transmission technique

Multipath propagation in realistic mobile radio channels can cause ISI. In other words, consecutive data symbols transmitted through the channel with multipath propagation may overlap with each other at the receiver. Especially in the frequency selective fading channel where the bandwidth of the signal is larger than the coherence bandwidth of the channel, data transmission could severely suffer from ISI due to the time dispersion corresponding to the frequency selectivity. Instead of applying complicated equalizers to eliminate ISI, multicarrier transmission is a very promising alternative approach to combat ISI [vNP00,FK03]. The wideband frequency selective fading channel is converted into many flat fading subchannels, i.e., subcarriers, in which individual narrowband data substreams are transmitted. In this way, the bandwidth of the substream is much smaller than the coherence bandwidth of the channel. Namely, the symbol duration of each data substream is much larger than the channel delay spread. Therefore, ISI for every data substream can be significantly reduced.

As a representative candidate for multicarrier transmission schemes, the OFDM transmission technique can offer high spectral efficiency without causing any inter-channel interference (ICI) or ISI thanks to the orthogonality between the signals in time as well as in frequency domain. The fundamental ideas of the OFDM transmission technique using the discrete Fourier transform (DFT) were firstly proposed around 40 years ago [Cha66, WE71]. With the development of digital signal processing techniques, the multicarrier modulation and demodulation in an OFDM system with a large number of subcarriers can be efficiently implemented by using inverse DFT (IDFT) and DFT which are computed by the inverse fast Fourier transform (IFFT) and fast Fourier transform (FFT) algorithms with low computational complexity. Therefore, the OFDM transmission technique became more and more popular and has gained a lot of attention in wideband wireless communication systems [Bin90, vNP00, FK03]. The first OFDM-based standard, i.e., the digital audio broadcasting (DAB) standard, was set

in Europe [ETS97b]. Then, the successful story of OFDM continues in the digital subscriber line (DSL) technology in the USA [CTC91], in the terrestrial digital video broadcasting (DVB-T) standard in Europe [ETS97a], in wireless metropolitan area network (MAN) applications, e.g., WiMAX [Har06], and in many wireless local area network (WLAN) standards such as the HIPERLAN/2, the IEEE 802.11a and the IEEE 802.11g [ETS99, 80203, 80299]. In the recently published IEEE 802.11n standard for next generation WLAN, OFDM has also been considered. Nowadays, OFDM is a promising candidate for the wireless personal area network (PAN) in the framework of the IEEE 802.15.3a, and for the 4G air interface. As every coin has two sides, OFDM also has its disadvantages such as the high peak-to-average power ratio (PAPR), the high demands on time and frequency synchronization, and the high sensitivity to Doppler spreading [vNP00, FK03].

For interference management in cellular networks, the cooperative communication scheme proposed in Chapter 4 and Chapter 5 dealing with intercell interference is based on the application of the OFDM transmission technique which can preliminarily eliminate all the intracell interference. In the following, the basic principle of the OFDM transmission technique will be briefly described based on Figure 2.2. The corresponding mechanism to eliminate intracell interference with respect to ISI and ICI in a single cell with multiple users will be shown. It is assumed that the available bandwidth in the investigated system is divided into N_{F} subcarriers which are allocated to $N_{\mathrm{us}} = N_{\mathrm{F}}$ users in a single cell. The original data symbols $\underline{d}^{(n_{\mathrm{us}})}$, $n_{\mathrm{us}} = 0, \ldots, N_{\mathrm{us}}-1$, in one cell are transmitted in every OFDM symbol including N_{F} transmitted data symbols $\underline{s}^{(n_{\mathrm{F}})} = \underline{d}^{(n_{\mathrm{us}})}$ in individual subcarriers n_{F}, $n_{\mathrm{F}} = 0, \ldots, N_{\mathrm{F}} - 1$. The mapping between the indices n_{F} and n_{us} depends on the employed random or adaptive subcarrier allocation techniques [KH95, OR05, WCLM99, KK08b, KK08a], which are beyond the scope of the present thesis. Let T_{d} denote the original symbol duration in the serial data stream. The OFDM symbol duration in every subcarrier is obtained as $T_{\mathrm{s}} = N_{\mathrm{F}} \cdot T_{\mathrm{d}}$.

The OFDM multicarrier modulation can be easily implemented using the IDFT which can be computed by the IFFT algorithm. The input of the IDFT is the transmitted vector $\underline{\mathbf{s}} = \left(\underline{s}^{(0)}, \ldots, \underline{s}^{(N_{\mathrm{F}}-1)}\right)^{\mathrm{T}}$ including the transmitted data symbols $\underline{s}^{(n_{\mathrm{F}})}$ in individual subcarriers with frequency spacing of $\Delta f = 1/T_{\mathrm{s}}$. Transforming from the frequency domain to the time domain with the sampling rate of $N_{\mathrm{F}}/T_{\mathrm{s}}$, $\underline{\mathbf{x}} = \left(\underline{x}^{(0)}, \ldots, \underline{x}^{(N_{\mathrm{F}}-1)}\right)^{\mathrm{T}}$ is obtained as the output of the IDFT with

$$\underline{x}^{(\mu)} = \left[\mathcal{F}^{-1}(\underline{\mathbf{s}})\right]_{\mu} = \frac{1}{\sqrt{N_{\mathrm{F}}}} \sum_{n_{\mathrm{F}}=0}^{N_{\mathrm{F}}-1} \underline{s}^{(n_{\mathrm{F}})} e^{j2\pi\mu n_{\mathrm{F}}/N_{\mathrm{F}}} \quad , \tag{2.7}$$

where $[\cdot]_{\mu}$ returns the μ-th element of its argument with $\mu = 0, \ldots, N_{\mathrm{F}}-1$. It is assumed that the discrete length of the channel impulse response is N_{g}. In order to eliminate all

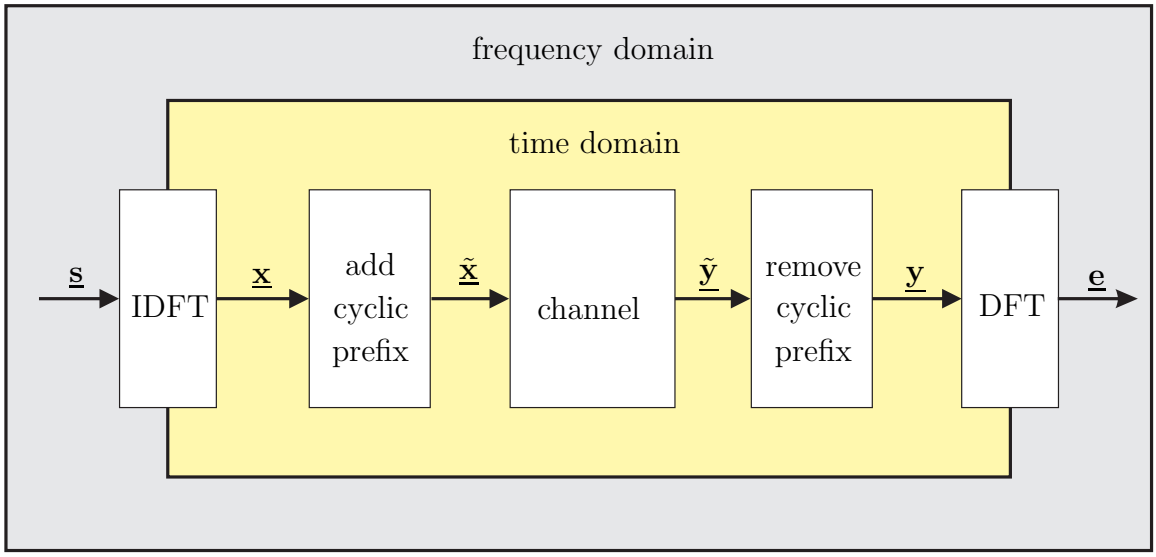

Figure 2.2. Data transmission in a single-cell OFDM system.

ISI between OFDM symbols, a guard interval with a discrete length of $N_\mathrm{g}-1$ could be inserted between adjacent OFDM symbols. Noteworthy, a cyclic prefix (CP) which is a copy of the last $N_\mathrm{g}-1$ data symbols in each OFDM symbol is considered as its guard interval. Namely, adding a CP in front of $\underline{\mathbf{x}}$, the channel input vector is obtained as

$$\begin{aligned}\underline{\tilde{\mathbf{x}}} &= \left(\underline{\tilde{x}}^{(-N_\mathrm{g}+1)},\ \ldots,\ \underline{\tilde{x}}^{(-1)},\ \underline{\tilde{x}}^{(0)},\ \ldots,\quad \underline{\tilde{x}}^{(N_\mathrm{F}-1)}\right)^\mathrm{T} \\ &= \left(\underline{x}^{(N_\mathrm{F}-N_\mathrm{g}+1)},\ \ldots,\ \underline{x}^{(N_\mathrm{F}-1)},\ \underline{x}^{(0)},\ \ldots,\ \underline{x}^{(N_\mathrm{F}-1)}\right)^\mathrm{T} \quad . \end{aligned} \tag{2.8}$$

The CP enables a circular convolution of the channel impulse response and the OFDM symbol, and it helps to achieve the orthogonality between individual subcarriers. The channel input vector $\underline{\tilde{\mathbf{x}}}$ is transmitted through the mobile radio channel considering multipath propagation and additive noise. On the receiver side, the CP of length $N_\mathrm{g}-1$ is removed from the channel output vector $\underline{\tilde{\mathbf{y}}}$ of length $N_\mathrm{F}+N_\mathrm{g}-1$, and one can obtain the vector $\underline{\mathbf{y}}$ of length N_F. Considering the finite channel impulse response vector $\underline{\mathbf{h}} = (\underline{h}^{(0)},\ldots,\underline{h}^{(N_\mathrm{g}-1)})^\mathrm{T}$ and the noise vector $\underline{\mathbf{w}} = (\underline{w}^{(0)},\ldots,\underline{w}^{(N_\mathrm{F}-1)})^\mathrm{T}$, every discrete output symbol $\underline{y}^{(\mu)}$, $\mu = 0,\ldots,N_\mathrm{F}-1$, included in $\underline{\mathbf{y}}$ reads

$$\underline{y}^{(\mu)} = \sum_{k=0}^{N_\mathrm{g}-1} \underline{h}^{(k)}\,\underline{\tilde{x}}^{(\mu-k)} + \underline{w}^{(\mu)} = \left[\underline{\mathbf{h}} \circledast \underline{\mathbf{x}} + \underline{\mathbf{w}}\right]_\mu = \left[\underline{\mathbf{h}} \circledast \underline{\mathbf{x}}\right]_\mu + \underline{w}^{(\mu)} \quad , \tag{2.9}$$

where $\circledast$ indicates the circular convolution. The corresponding OFDM multicarrier demodulation is implemented through the DFT which can be computed by the FFT algorithm. Transforming from the time domain to the frequency domain, the received

signal in the n_{F}-th subcarrier can be calculated as

$$\begin{aligned}
\underline{e}^{(n_{\mathrm{F}})} &= \left[\mathcal{F}\left(\underline{\mathbf{y}}\right)\right]_{n_{\mathrm{F}}} \\
&= \frac{1}{\sqrt{N_{\mathrm{F}}}} \sum_{\mu=0}^{N_{\mathrm{F}}-1} \left[\underline{\mathbf{h}} \circledast \underline{\mathbf{x}}\right]_{\mu} e^{-j2\pi\mu n_{\mathrm{F}}/N_{\mathrm{F}}} + \frac{1}{\sqrt{N_{\mathrm{F}}}} \sum_{\mu=0}^{N_{\mathrm{F}}-1} \underline{w}^{(\mu)} e^{-j2\pi\mu n_{\mathrm{F}}/N_{\mathrm{F}}} \\
&= \sqrt{N_{\mathrm{F}}} \cdot \left[\mathcal{F}(\underline{\mathbf{h}})\right]_{n_{\mathrm{F}}} \cdot \left[\mathcal{F}(\underline{\mathbf{x}})\right]_{n_{\mathrm{F}}} + \left[\mathcal{F}(\underline{\mathbf{w}})\right]_{n_{\mathrm{F}}} \\
&= \underline{H}^{(n_{\mathrm{F}})} \cdot \underline{s}^{(n_{\mathrm{F}})} + \underline{n}^{(n_{\mathrm{F}})} \ , \qquad (2.10)
\end{aligned}$$

where the circular convolution theorem is applied, and $[\cdot]_{n_{\mathrm{F}}}$ returns the n_{F}-th element of its argument with $n_{\mathrm{F}} = 0, \ldots, N_{\mathrm{F}} - 1$. With $\underline{H}^{(n_{\mathrm{F}})} = \sqrt{N_{\mathrm{F}}} \cdot \left[\mathcal{F}(\underline{\mathbf{h}})\right]_{n_{\mathrm{F}}}$ indicating the channel transfer function in subcarrier n_{F} scaled by $\sqrt{N_{\mathrm{F}}}$ and $\underline{n}^{(n_{\mathrm{F}})} = \left[\mathcal{F}(\underline{\mathbf{w}})\right]_{n_{\mathrm{F}}}$ indicating the noise in subcarrier n_{F}, the transmission of an OFDM symbol in N_{F} subcarriers is free of ISI and ICI. Based on Figure 2.2, the OFDM transmission in the frequency domain can be described in the matrix-vector notation as

$$\begin{aligned}
\underline{\mathbf{e}} &= \begin{pmatrix} \underline{e}^{(0)} \\ \vdots \\ \underline{e}^{(N_{\mathrm{F}}-1)} \end{pmatrix} = \begin{pmatrix} \underline{H}^{(0)} & 0 & \ldots & 0 \\ 0 & \underline{H}^{(1)} & \vdots & 0 \\ \vdots & & \ddots & \vdots \\ 0 & 0 & \ldots & \underline{H}^{(N_{\mathrm{F}}-1)} \end{pmatrix} \cdot \begin{pmatrix} \underline{s}^{(0)} \\ \vdots \\ \underline{s}^{(N_{\mathrm{F}}-1)} \end{pmatrix} + \begin{pmatrix} \underline{n}^{(0)} \\ \vdots \\ \underline{n}^{(N_{\mathrm{F}}-1)} \end{pmatrix} \\
&= \underline{\mathbf{H}} \cdot \underline{\mathbf{s}} + \underline{\mathbf{n}} \qquad (2.11)
\end{aligned}$$

with the channel matrix $\underline{\mathbf{H}}$, the transmitted vector $\underline{\mathbf{s}}$, the received vector $\underline{\mathbf{e}}$, and the noise vector $\underline{\mathbf{n}}$.

Obviously, all the original data symbols $\underline{d}^{(n_{\mathrm{us}})}$ of multiple users in a single cell which are assigned to individual subcarriers as elements $\underline{s}^{(n_{\mathrm{F}})}$ of every OFDM symbol are transmitted free of interference. In a word, all the intracell interference is eliminated when applying the above OFDM transmission technique, and only intercell interference is left to be dealt with.

2.3 Cellular networks with alternative BS-antenna-layouts

The fundamental idea of cellular networks is to increase the system capacity by reusing the channels in geographically distinct areas [Sch05]. These distinct areas named as cells are controlled by BSs which provide access for MSs to the wired core network. Therefore, cellular networks are infrastructure-based wireless networks, and they are distinguished from ad-hoc wireless networks which have no core network infrastructure. In cellular networks with high SNR, the system performance is mainly limited by

interference. Applying the OFDM transmission technique, it is assumed that all the intracell interference is cancelled, and the only left interference is intercell interference. Intuitively, the intercell interference can be reduced by increasing the cluster size in cellular networks. However, the cluster size is limited by the scarce frequency resource in future mobile radio networks. Therefore, it is quite necessary to consider how to perform spectrally efficient communications in cellular networks with a small cluster size. In the present thesis, universal frequency reuse with the cluster size $r = 1$ is considered. In order to improve spectral efficiency in cellular networks, on one side intelligent signal processing techniques can be applied in the cooperative communication scheme which will be investigated in detail in Chapter 4 and Chapter 5. On the other side, smart BS-antenna-layouts can be utilized to inherently suppress some part of the intercell interference and to fit in the cooperative communication scheme with intelligent signal processing techniques. The BS-antenna-layouts refer to different types of BS antennas at different positions in cells. Two types of antennas, i.e., omnidirectional antennas with uniform antenna pattern in all directions and directional antennas, are distinguished from each other in cellular networks. The application of smart antenna techniques which make use of directional antennas can enhance the useful signal in an expected direction and reduce the interference in a given direction [Win98, LR99, God01, KBB+05]. The most commonly used directional antennas are sectorized antennas which in the ideal case have uniform sectorized antenna pattern [Gol05]. Additionally, multiple antennas in the cells form a distributed antenna array in the whole cellular network, and therefore the system performance can benefit from diversity and multiplexing. Generally, a mobile radio communication system which is equipped with multiple antennas with a significant distance from each other and applies a joint signal processing based on these antennas can be named as distributed antenna system (DAS).

In the present thesis, DASs with three types of BS-antenna-layouts named as omni-DAS, sector-DAS I and sector-DAS II are investigated based on the reference scenario of a 21-cell cellular system as shown in Figure 2.3. Different cell layouts with BS antennas located in cell centers or at cell vertices are combined with two types of antennas, i.e., omnidirectional antennas and 120 degree sectorized antennas. For simplicity, uniform antenna pattern is assumed in the investigated DASs. In order to make a fair comparison of the system performances of different types of DASs, it is assumed that each cell is served by the same number of BS antennas. For example, 3 BS antennas per cell are assumed in the reference scenario.

In the omni-DAS, 3 omnidirectional BS antennas are located in the center of each cell. In the sector-DAS I, 3 distributed 120 degree sectorized antennas are located in 3 vertices of each cell and point towards the cell center. The transformation between

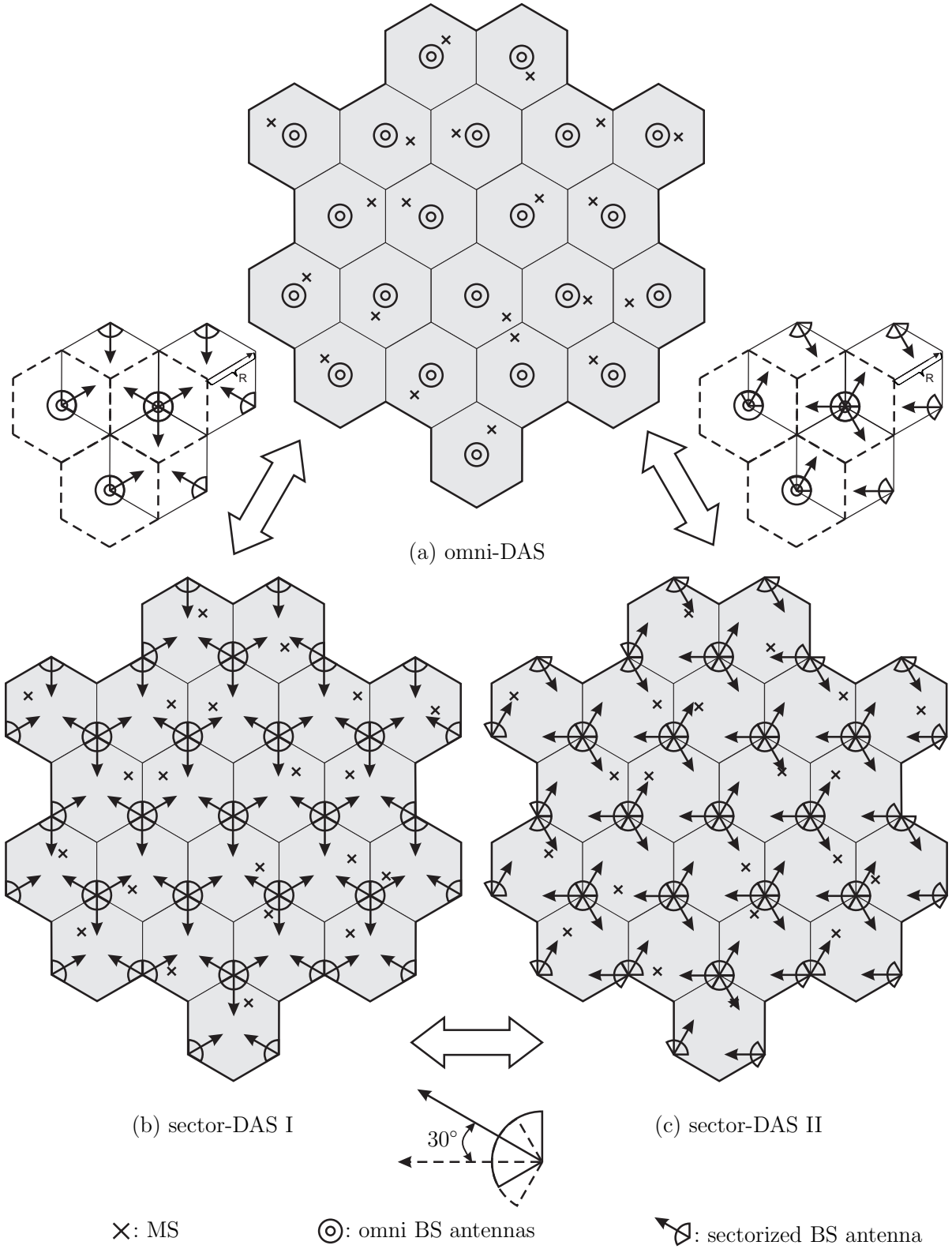

Figure 2.3. The reference scenario of a 21-cell cellular system with cluster size $r = 1$ applying different BS-antenna-layouts.

the omni-DAS and the sector-DAS I is visualized using a 3-cell scenario in Figure 2.3. Namely, the sector-DAS I can be easily obtained from the omni-DAS by shifting the cell layout of the omni-DAS by a distance of the cell radius R in the direction of the arrow and replacing the 3 omnidirectional antennas at each BS with 3 sectorized antennas separately pointing towards the centers of 3 neighbouring cells in the original network. Although after the above transformation the BS antennas for each cell are served by 3 BSs in different physical locations, the total number of BSs and the total number of BS antennas are unmodified. In reverse, the omni-DAS can also be easily obtained from the sector-DAS I. Under the assumption that antenna gains of sector antennas are zero at the directions more than 60 degrees with respect to the boresight, for each MS in the sector-DAS I there are many ineffective antennas which have no influence on this MS. Therefore, less intercell interference inherently exists in the sector-DAS I as compared to the omni-DAS due to the ineffective sectorized BS antennas in other cells for every MS in the sector-DAS I. Obviously, the useful signals for the MSs close to their own BS antennas could be very strong. Therefore, comparing the above two BS-antenna-layouts, the omni-DAS is expected to offer a better system performance for the MSs close to the cell centers, while the sector-DAS I is expected to offer a better system performance for the MSs close to the cell vertices where sectorized BS antennas could be located.

One more alternative sector-DAS, i.e., sector-DAS II, is also considered in the present thesis for comparison with sector-DAS I. The transformation between the sector-DAS I and the sector-DAS II is nothing else but a rotation of all the sectorized BS antennas. Keeping the positions of the BS antennas unmodified, the sector-DAS II can be obtained from the sector-DAS I by rotating of all the sectorized BS antennas by 30 degrees counterclockwise. Similarly, the sector-DAS I can be obtained from the sector-DAS II by rotating of all the sectorized BS antennas by 30 degrees clockwise. Obviously, every sectorized BS antenna in the sector-DAS I points toward one of the other BSs at a distance of $3R$ from it, while every sectorized BS antenna in the sector-DAS II points toward one of its neighboring BSs at a distance of $\sqrt{3}R$ from it. Every sectorized BS antenna in the sector-DAS I serves one cell close to it and some other cells far away, while every sectorized BS antenna in the sector-DAS II serves two cells close to it and some other cells far away. Therefore, it could be expected that less intercell interference inherently exists in the sector-DAS I as compared to the sector-DAS II. Additionally, the transformation between sector-DAS II and omni-DAS which is similar to the transformation between sector-DAS I and omni-DAS except the directions of the sectorized BS antennas is also visualized using a 3-cell scenario in Figure 2.3.

In conventional cellular networks without multicell cooperation, the above-mentioned three types of DASs with different BS-antenna-layouts have their inherent advantages

and disadvantages for MSs in different positions in each cell with respect to the system performance such as SNR and signal-to-interference ratio (SIR). It is expected that the inherent characteristics of the different types of DASs will also play an important role in the cooperative communication scheme for future cellular networks. In the present thesis, cooperative reception in the UL and cooperative transmission in the DL considering intelligent signal processing techniques based on various BS-antenna-layouts, i.e., the above-mentioned three types of DASs, will be investigated.

Noteworthy, in DASs applying the state of the art remote radio head (RRH) optical transmission technologies, the digital BSs containing the baseband processing functions and RRHs containing the radio functions of traditional BSs are separated. The controlling BSs and the RRHs, i.e., BS antennas, are connected by optical fiber links through interfaces following specifications for open base station architectures such as the open base station architecture initiative (OBSAI) [OBS09] and the common public radio interface (CPRI) [CRP09]. Distances between MSs and BS antennas can be shortened by distributing BS antennas which are traditionally attached at central BSs in every cell throughout the whole cell area. BS antennas in the form of RRHs can be deployed in a flexible and cost-effective manner.

2.4 Multiuser OFDM-MIMO cellular systems

The above introduced 21-cell cellular system with various BS-antenna-layouts, i.e., omni-DAS, sector-DAS I and sector-DAS II, as shown in Figure 2.3 is taken as the reference scenario of the present thesis. The concept of cooperative communication with cooperative reception in the UL and cooperative transmission in the DL will be applied to the reference scenario. In this section, without limitation to any special BS-antenna-layout or a certain number of cells, a general system model for the multiuser cellular system applying the OFDM transmission technique under the cooperative communication concept will be described.

Generally speaking, a realistic TDD cellular system including K cells with one BS per cell is considered in the present thesis. Applying the OFDM transmission technique introduced in Section 2.2, there is no interference between different subcarriers in the data transmission as indicated by (2.11). In other words, the data transmissions in different subcarriers can be considered as independently. Therefore, it is reasonable to perform a subcarrierwise investigation of the cellular system with moderate computational effort. Based on the above statements, it is sufficient to consider a single active MS contained in each cell in the considered subcarrier and time slot since all

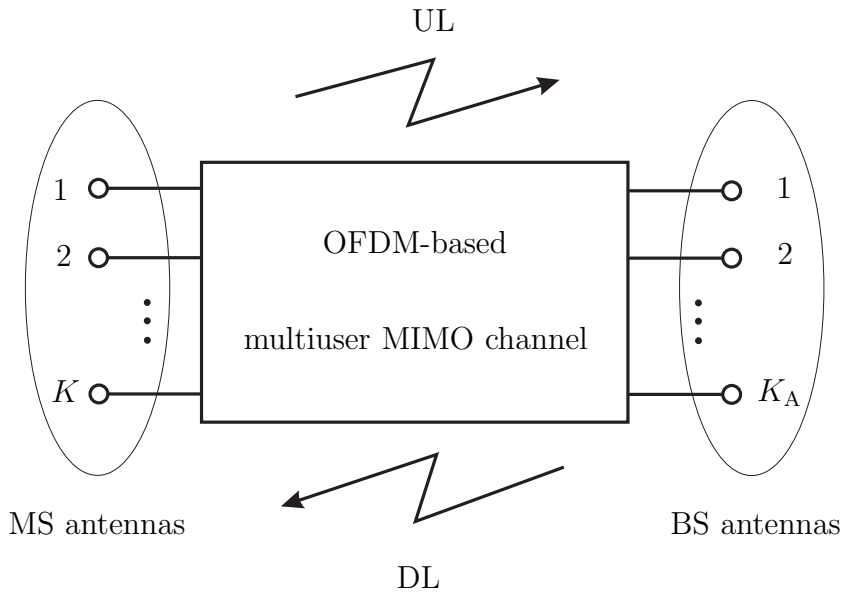

Figure 2.4. An OFDM-based multiuser MIMO system model representing the considered cellular system.

the intracell interference can be eliminated by utilizing the OFDM transmission technique. Applying multiple antennas in the cellular network, the whole system can be considered as a multiuser MIMO system with all the antennas of the MSs on the one side and all the antennas of the BSs on the other side. Considering that low-cost and low-power MSs are required in realistic mobile radio systems, each MS is equipped with a single antenna, and each BS is equipped with multiple antennas to benefit from space diversity. In the proposed cooperative communication scheme, all the computational complexity is shifted to the BSs by assigning the cooperation task to the BSs, and MSs are kept as simple as possible. However, without loss of generality, the following system model considering a single antenna at each MS can be easily extended to the case that each MS is equipped with multiple antennas.

In the system model of a K-cell cellular system as described above with one BS and one MS per cell,

$$K_{\mathrm{B}} = K \tag{2.12}$$

BSs with the indices $k_{\mathrm{B}} = 1, \ldots, K_{\mathrm{B}}$ and

$$K_{\mathrm{M}} = K \tag{2.13}$$

MSs with the indices $k_{\mathrm{M}} = 1, \ldots, K_{\mathrm{M}}$ are considered. Assuming that each BS is equipped with the same number N_{A} of antennas with the indices $n_{\mathrm{A}} = 1, \ldots, N_{\mathrm{A}}$, in the whole system

$$K_{\mathrm{A}} = N_{\mathrm{A}} \cdot K \tag{2.14}$$

BS antennas with the indices $k_\mathrm{A} = 1, \ldots, K_\mathrm{A}$ are considered. The unique antenna index k_A in the whole system for the n_A-th antenna at BS k_B reads

$$k_\mathrm{A} = N_\mathrm{A} \cdot (k_\mathrm{B} - 1) + n_\mathrm{A} \ . \tag{2.15}$$

Since only a single antenna is available at each active MS in every cell, the whole system has $K_\mathrm{M} = K$ MS antennas. For the sake of simplicity, the index of each MS, which is the index of this MS's antenna, and the index of the cell where this MS is located can be represented by the same index k, $k = 1, \ldots, K$.

Thanks to the OFDM transmission technique based on which data transmission is performed, a point-to-point transmission between one MS and one BS can be simply expressed in a subcarrierwise way as described by (2.11). For the sake of simplicity of the notation, the index n_F of the investigated subcarrier will be omitted in the following. Data transmission in an OFDM-based multiuser MIMO system is nothing else but an extension of the point-to-point OFDM transmission to a multipoint-to-multipoint OFDM transmission. As generally described in Figure 2.4, the signals are transmitted between K points at the MS side and K_A points at the BS side through the OFDM-based multiuser MIMO channel with opposite transmission directions in the UL and in the DL. In order to fairly assess the system performance in the UL and in the DL, the same data vector

$$\underline{\mathbf{d}} = (\underline{d}^{(1)}, \ldots, \underline{d}^{(K)})^\mathrm{T} \tag{2.16}$$

of dimension K is assumed in the UL and in the DL. The data vector contains i.i.d. data symbols $\underline{d}^{(k)}$ with zero-mean and variance $P_\mathrm{d}/2$ of the real and the imaginary parts. The noise signals $\underline{n}^{(k_\mathrm{A})}$ in the noise vector $\underline{\mathbf{n}}$ of dimension K_A in the UL and the noise signals $\underline{n}^{(k)}$ in the noise vector $\underline{\mathbf{n}}$ of dimension K in the DL are assumed to be i.i.d. Gaussian variables with zero-mean and the same variance $\sigma^2/2$ of real and imaginary parts. In the system model, the signals are described by their complex amplitudes and the channels are described by their transfer functions.

In the UL, simple OFDM transmitters are applied at the MSs without any pre-processing. If it is required, an adjustment of the transmit power can be considered in the transmitters. For simplicity, a unit scaling factor is applied, and therefore the transmitted signals $\underline{s}^{(k)}$ contained in the transmitted vector $\underline{\mathbf{s}}$ are equivalent to the data symbols $\underline{d}^{(k)}$. The transmitted vector can be written as

$$\underline{\mathbf{s}} = (\underline{s}^{(1)}, \ldots, \underline{s}^{(K)})^\mathrm{T} = \underline{\mathbf{d}} \ . \tag{2.17}$$

Every signal $\underline{s}^{(k)}$ is transmitted from the MS antenna k to the K_A BS antennas. The OFDM-based multiuser MIMO channel can be described by a channel matrix $\underline{\mathbf{H}}_\mathrm{UL}$ of

dimensions $K_{\mathrm{A}} \times K$ as

$$\underline{\mathbf{H}}_{\mathrm{UL}} = \begin{pmatrix} \underline{H}_{\mathrm{UL}}^{(1,1)} & \cdots & \underline{H}_{\mathrm{UL}}^{(1,K)} \\ \vdots & & \vdots \\ \underline{H}_{\mathrm{UL}}^{(K_{\mathrm{A}},1)} & \cdots & \underline{H}_{\mathrm{UL}}^{(K_{\mathrm{A}},K)} \end{pmatrix} . \tag{2.18}$$

Any one entry $\underline{H}_{\mathrm{UL}}^{(k_{\mathrm{A}},k)}$ in the channel matrix $\underline{\mathbf{H}}_{\mathrm{UL}}$ is the channel transfer function corresponding to the channel between MS antenna k and BS antenna k_{A} in the investigated subcarrier. The received vector $\underline{\mathbf{e}}$ comprising the received signals $\underline{e}^{(k_{\mathrm{A}})}$ at the corresponding BS antennas k_{A}, $k_{\mathrm{A}} = 1, \ldots, K_{\mathrm{A}}$, reads

$$\underline{\mathbf{e}} = (\underline{e}^{(1)}, \ldots, \underline{e}^{(K_{\mathrm{A}})})^{\mathrm{T}} = \underline{\mathbf{H}}_{\mathrm{UL}} \cdot \underline{\mathbf{s}} + \underline{\mathbf{n}} \ . \tag{2.19}$$

In the UL of conventional cellular systems, the antennas of the BSs k_{B}, $k_{\mathrm{B}} = 1, \ldots, K_{\mathrm{B}}$, are expected to receive only the signals from their corresponding MSs $k = k_{\mathrm{B}}$ in the same cell. However, in fact as indicated by (2.19) considering the channel matrix $\underline{\mathbf{H}}_{\mathrm{UL}}$, any one received signal $\underline{e}^{(k_{\mathrm{A}})}$ contains the contributions from all the MSs k, $k = 1, \ldots, K$. In most of the existing cellular systems, it is suggested that data detection for each MS is performed separately at its corresponding BS by treating the interference from other MSs as noise. Therefore, the intercell interference could greatly limit the system performance in conventional cellular systems. Fortunately, the concept of cooperative communication in the UL has been proposed to jointly receive the useful signals for every MS and to eliminate the interference among MSs [KFV06, MF07a, KRF08, PHG09, WW10]. Thanks to the development of hardware techniques for the backhaul infrastructure connecting the BSs, the concept of cooperative communication becomes realizable to a certain extent in realistic cellular networks. In the UL, the estimated data vector

$$\hat{\underline{\mathbf{d}}} = \left(\hat{\underline{d}}^{(1)}, \ldots, \hat{\underline{d}}^{(K)}\right)^{\mathrm{T}} \tag{2.20}$$

comprising the data estimates $\hat{\underline{d}}^{(k)}$ is obtained through cooperative reception which is implemented by JD in the proposed cooperative communication scheme. As mentioned in Section 1.2, various multiuser detection strategies based on available CSI can be applied in the JD. In Chapter 4, some commonly used multiuser detection strategies and especially those for interference cancellation will be reviewed in more detail, some advanced multiuser detection algorithms based on statistical signal processing will be investigated, and a practical cooperative reception scheme with JD will be proposed.

In the DL, the transmitted signals $\underline{s}^{(k_{\mathrm{A}})}$ from BS antennas k_{A}, $k_{\mathrm{A}} = 1, \ldots, K_{\mathrm{A}}$, contained in the transmitted vector

$$\underline{\mathbf{s}} = \left(\underline{s}^{(1)}, \ldots, \underline{s}^{(K_{\mathrm{A}})}\right)^{\mathrm{T}} \tag{2.21}$$

are transmitted to the K MS antennas through the OFDM-based multiuser MIMO channel which can be described by a channel matrix $\underline{\mathbf{H}}_{\mathrm{DL}}$ of dimensions $K \times K_{\mathrm{A}}$ as

$$\underline{\mathbf{H}}_{\mathrm{DL}} = \begin{pmatrix} \underline{H}_{\mathrm{DL}}^{(1,1)} & \cdots & \underline{H}_{\mathrm{DL}}^{(1,K_{\mathrm{A}})} \\ \vdots & & \vdots \\ \underline{H}_{\mathrm{DL}}^{(K,1)} & \cdots & \underline{H}_{\mathrm{DL}}^{(K,K_{\mathrm{A}})} \end{pmatrix} . \tag{2.22}$$

Any one entry $\underline{H}_{\mathrm{DL}}^{(k,k_{\mathrm{A}})}$ in the channel matrix $\underline{\mathbf{H}}_{\mathrm{DL}}$ is the channel transfer function corresponding to the channel between BS antenna k_{A} and MS antenna k in the investigated subcarrier. The received vector $\underline{\mathbf{e}}$ comprising the received signals $\underline{e}^{(k)}$ at the corresponding MS antennas k, $k = 1, \ldots, K$, is described by

$$\underline{\mathbf{e}} = (\underline{e}^{(1)}, \ldots, \underline{e}^{(K)})^{\mathrm{T}} = \underline{\mathbf{H}}_{\mathrm{DL}} \cdot \underline{\mathbf{s}} + \underline{\mathbf{n}} \ . \tag{2.23}$$

In the DL of conventional cellular systems, the signals are expected to be transmitted from BSs k_{B}, k_{B}=1, …, K_{B}, to their corresponding MSs k with $k = k_{\mathrm{B}}$ in the same cell. However, in fact as indicated by (2.23) considering the channel matrix $\underline{\mathbf{H}}_{\mathrm{DL}}$, the signals from BSs k_{B} will also reach other MSs k'_{M}, $k'_{\mathrm{M}} \neq k_{\mathrm{B}}$, and interfere with each other in conventional multiuser cellular systems. Similar to the UL, the concept of cooperative communication, which makes use of the advantages of the multiuser MIMO system such as spatial diversity and avoids the disadvantages of the multiuser MIMO system such as crosstalk, is considered in the DL as a promising candidate for intercell interference management. From a practical point of view, it is much easier to implement the cooperation among BSs connected by a fixed network backhaul infrastructure than to implement the cooperation among moving MSs with changing positions. Therefore, the concept of cooperative communication in the DL, i.e., cooperative transmission, is applied at the coordinated BSs, and the cooperative transmission is implemented by JT in the proposed cooperative communication scheme. Unlike in the UL, the transmitted vector $\underline{\mathbf{s}}$ in the DL is not simply equal to the data vector $\underline{\mathbf{d}}$, but is obtained from the data vector $\underline{\mathbf{d}}$ through JT considering the available CSI of the multiuser MIMO system. JT at the BSs can be considered as a certain kind of precoding scheme for the multiuser MIMO system. In Chapter 5, some commonly used linear and nonlinear multiuser transmission strategies and especially those based on interference cancellation as candidates for JT will be discussed, and a practical cooperative transmission scheme with JT will be proposed. Since we have shifted the computational load of cooperative communication to the BS side, simple OFDM receivers are applied at the MSs. A scaling of the receive power can be applied to obtain the estimated data vector $\underline{\hat{\mathbf{d}}}$ from the received vector $\underline{\mathbf{e}}$ described in (2.23).

Considering the channel reciprocity between the UL and the DL in the investigated TDD system, the notations can be simplified in the present thesis. The channel matrix

of the investigated multiuser MIMO system $\underline{\mathbf{H}}$ is defined to be equivalent to the UL channel matrix. The relationship between the UL channel matrix $\underline{\mathbf{H}}_{\mathrm{UL}}$ and the DL channel matrix $\underline{\mathbf{H}}_{\mathrm{DL}}$ can be written as

$$\underline{\mathbf{H}}_{\mathrm{UL}} = \underline{\mathbf{H}}_{\mathrm{DL}}^{\mathrm{T}} = \underline{\mathbf{H}} = \begin{pmatrix} \underline{H}^{(1,1)} & \dots & \underline{H}^{(1,K)} \\ \vdots & & \vdots \\ \underline{H}^{(K_{\mathrm{A}},1)} & \dots & \underline{H}^{(K_{\mathrm{A}},K)} \end{pmatrix} \tag{2.24}$$

with the entries

$$\underline{H}^{(k_{\mathrm{A}},k)} = \underline{H}_{\mathrm{UL}}^{(k_{\mathrm{A}},k)} = \underline{H}_{\mathrm{DL}}^{(k,k_{\mathrm{A}})} \tag{2.25}$$

denoting the channel transfer functions of the mobile radio channels between BS antennas k_{A} and MS antennas k in the investigated subcarrier.

The system model of cooperative communication in the investigated cellular network based on coordinated BSs applying cooperative reception in the UL and cooperative transmission in the DL is summarized in Figure 2.5. Different levels of knowledge of CSI, which could be considered in JD/JT to implement the concept of cooperative communication, are generally described as follows:

A) full perfect CSI: Under the ideal assumption that full perfect CSI of the whole system is available to the BSs, JD/JT based on full perfect CSI which is described by the full channel matrix $\underline{\mathbf{H}}$ of the whole system could be performed. Although this assumption without considering practical implementation limitations is unrealistic, the system performance based on perfect full CSI can be theoretically calculated and treated as the upper bound reference in the system performance assessment.

B) significant CSI: As discussed in Section 1.3, most of the state of the art cooperative communication schemes are performed based on only part of the full CSI in order to reduce the implementation complexity and the backhaul communication load. It has been suggested that for each MS the CSI in a certain subsystem of the cellular system selected according to the static geographical architecture could be considered in JD/JT [WMSL02, ZTZ+05, TXX+05, ZCA+09]. In the present thesis, in order to improve the system performance the significant channels are dynamically selected from the point of view of each MS in the form of significant useful channels and significant interfering channels with respect to the functionality of the channels. Based on suitable significant channel selection algorithms, significant CSI which is mathematically described by the significant useful channel matrix $\underline{\mathbf{H}}_{\mathrm{U}}$ corresponding to significant useful channels for all MSs and the MS specific significant interfering channel matrices $\underline{\mathbf{H}}_{\mathrm{I},k}$ corresponding to

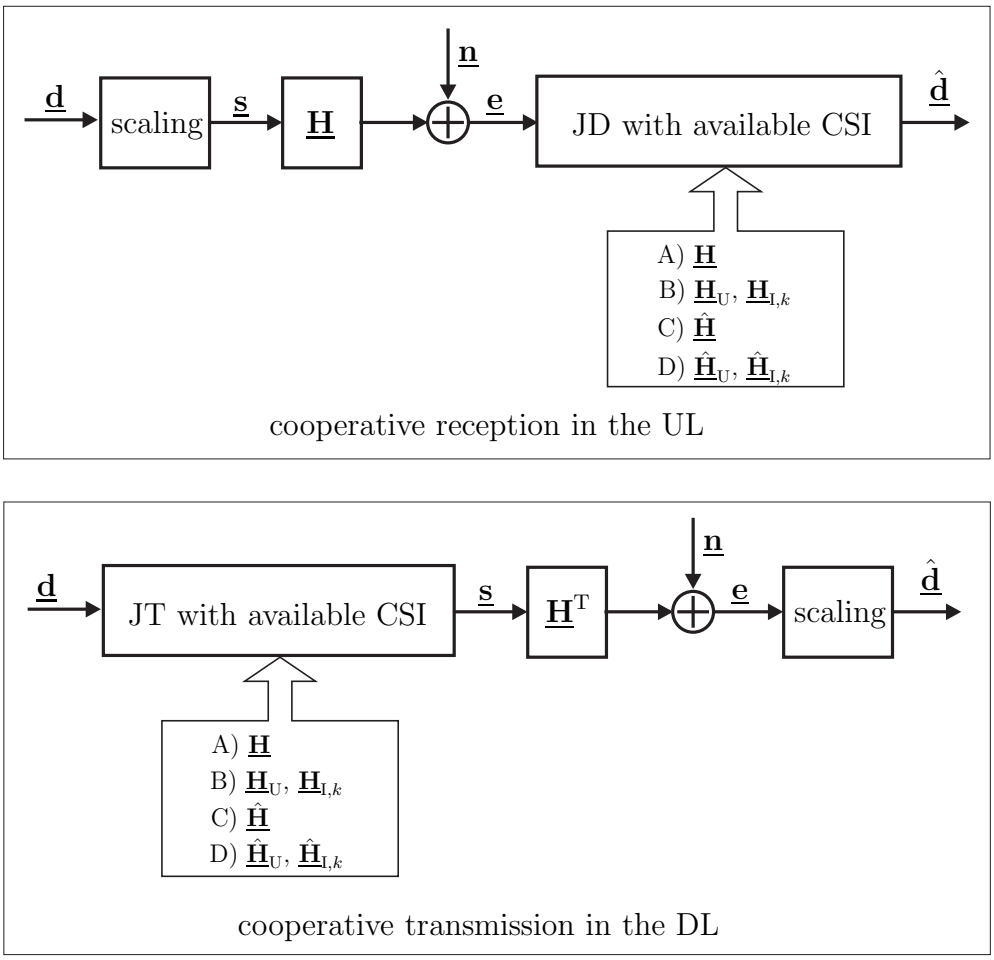

Figure 2.5. System models of cooperative communication in the UL and in the DL of cellular systems.

significant interfering channels for individual MSs is obtained from full CSI and applied in JD/JT.

C) imperfect CSI: In realistic systems considering the limited ability to track the CSI, only imperfect CSI is available to the BSs. Considering all the channels in the whole system, JD/JT could be performed based on the imperfect full CSI of the whole system described by the estimated channel matrix

$$\underline{\hat{\mathbf{H}}} = \underline{\mathbf{H}} + \underline{\boldsymbol{\Delta}} \tag{2.26}$$

with the channel-error matrix $\underline{\boldsymbol{\Delta}}$. The elements of $\underline{\boldsymbol{\Delta}}$ are assumed to be i.i.d. Gaussian variables with zero-mean and the variance $\sigma_{\Delta}^2/2$ of real and imaginary parts.

D) imperfect significant CSI: In reality, practical issues such as implementation complexity, backhaul load, and limited ability to track the CSI have to be considered in cellular systems. Therefore, in the proposed cooperative communication

scheme JD/JT is performed based on the estimated significant CSI in the form of the estimated significant useful channel matrix $\hat{\underline{\mathbf{H}}}_{\mathrm{U}}$ and the estimated MS specific significant interfering channel matrices $\hat{\underline{\mathbf{H}}}_{\mathrm{I},k}$. The estimated significant CSI is obtained from the estimated channel matrix $\hat{\underline{\mathbf{H}}}$ based on suitable significant channel selection algorithms.

In the present thesis, one key issue is that the concept of cooperative communication is reconsidered from the point view of partial CSI with respect to significant CSI and imperfect CSI. Details of cooperative communication based on different levels of knowledge of CSI will be discussed in Chapter 4 and Chapter 5. It should be emphasized that due to the channel reciprocity between the UL and the DL of the investigated TDD system as described in (2.24), the same significant channels are selected according to the same mathematical selection criteria in the UL and in the DL. Therefore, the same CSI described by the channel matrices $\underline{\mathbf{H}}$, $\underline{\mathbf{H}}_{\mathrm{U}}$, $\underline{\mathbf{H}}_{\mathrm{I},k}$, $\hat{\underline{\mathbf{H}}}$, $\hat{\underline{\mathbf{H}}}_{\mathrm{U}}$, and $\hat{\underline{\mathbf{H}}}_{\mathrm{I},k}$ is considered in both JD in the UL and JT in the DL.

Chapter 3

Information-theoretic view on cooperative communication

3.1 Preliminary remarks

In this chapter, the information-theoretic background of various multiuser communication schemes with no cooperation, cooperative reception, cooperative transmission, and full cooperative transmission and reception is investigated. An exemplary two-user communication channel is taken as the reference model. The system model of cellular networks can be considered as a generalization of this reference model.

Interference is the performance limiting phenomenon in mobile radio communication systems with several users sharing the same resource. Without any cooperation between the transmitters or between the receivers, the two-user communication channel is a two-user interference channel (IC). The two-user IC is a representative model to investigate the IC capacity region, and the characterization of its capacity region is considered as the basic issue in the information theory for multiuser communications [Sat77, Car78, Kra06]. However, except some special cases, e.g., the two-user IC with strong or very strong interference [Car75, Sat81], the fundamental information-theoretic problem initiated by Shannon in [Sha61] about the capacity region of a general two-user IC is still not fully characterized today. Fortunately, Han and Kobayashi presented an achievable rate region as an inner bound for the capacity region of the two-user IC in [HK81]. Recently, it has been shown that the Han-Kobayashi type scheme can achieve rates within one bit/s/Hz of the capacity for all values of the channel parameters [ETW08]. As the up to now best known inner bound for the two-user IC capacity region, the Han-Kobayashi achievable rate region is often used to describe the information-theoretic performance of the two-user IC.

In order to achieve spectrally efficient communications in interference-limited multiuser cellular systems, a cooperative communication scheme with partial CSI for interference management is proposed in the present thesis. From the information-theoretic point of view, in this chapter the Han-Kobayashi achievable rate region for the two-user IC is taken as the performance reference for comparing different cooperative communication strategies. Specifically, the achievable rate region for the two-user communication channel applying different communication schemes from the following two aspects is investigated:

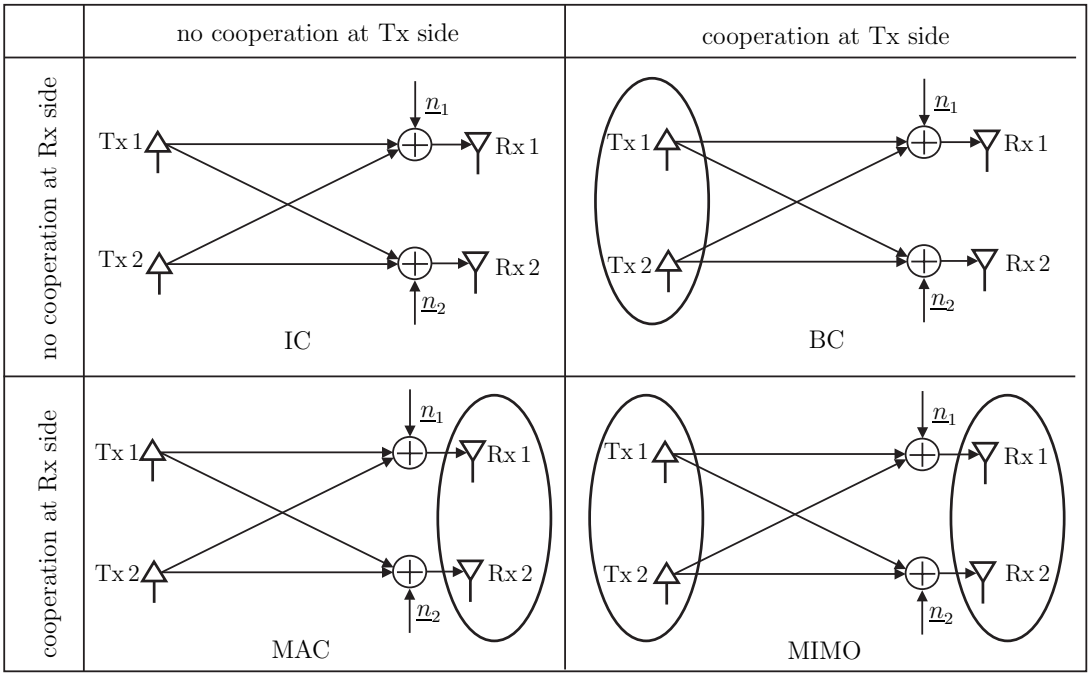

Figure 3.1. Two-user communication channels without cooperation and with cooperative communication strategies.

A) Cooperative communication strategies: The two-user communication channels applying four basic communication schemes without cooperation and with different cooperative communication strategies are briefly depicted in Figure 3.1. In the case of no cooperation, the two-user Gaussian IC [Cos85] can be taken as the information-theoretic model for this two-user communication channel. As introduced in the system model in Chapter 2, cooperative reception in the UL and cooperative transmission in the DL are applied in the proposed cooperative communication scheme based on coordinated BSs. In the UL, the IC with cooperative reception which is implemented by JD at BSs can be considered as a MAC with multiple antennas at the common receiver. In the DL, the IC with cooperative transmission which is implemented by JT at BSs can be considered as a BC with multiple antennas at the common transmitter. Based on the knowledge about the achievable rate regions for the multiuser MIMO MAC and the multiuser MIMO BC [JVG04, VJG03, TV05], the achievable rate regions for the IC with cooperative reception in the UL and the IC with cooperative transmission in the DL can be derived, respectively. Theoretically, in the extreme case that cooperation happens both in the transmitter side and in the receiver side, the sum-rate of the multiuser system can be calculated by considering the whole system as a single-user MIMO channel. As compared to the IC without cooperative communication, performance gains from different cooperative communication strategies with respect to the achievable rate region are assessed.

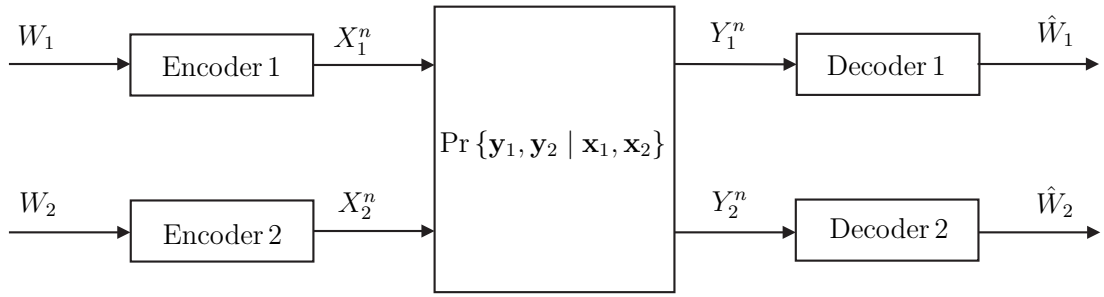

Figure 3.2. General two-user IC model.

B) Levels of the knowledge of CSI: In conventional cellular systems without cooperative communication, the intracell CSI instead of the full CSI of the whole system is considered in data detection and transmission for every user. In realistic cellular systems, cooperative communication based on significant CSI is considered as a practical solution to achieve good system performance with moderate computational complexity. In a word, communication schemes with partial CSI instead of full CSI are very common in realistic systems. Naturally, the question about how much the performance loss is due to partial CSI instead of full CSI considered in different communication schemes arises. In this chapter, this question is answered from an information-theoretic point of view. The achievable rate regions for the two-user communication channel applying different communication schemes with partial CSI are obtained with the help of some appropriately simplified information-theoretic channel models.

3.2 Interference channel - without cooperation

3.2.1 Definitions of capacity and achievable rate region

The conventional cellular system without cooperation can be considered as a general IC. The basic model for investigating the information-theoretic characteristics of the IC is the two-user IC model in which two transmitter-receiver pairs share a common communication channel. The communication between a transmitter and its corresponding receiver interferes with the communication between the other pair of transmitter and receiver. In the two-user IC model as shown in Figure 3.2, it is assumed that the random variables W_1 and W_2 are two independent messages with values w_1 and w_2 which are uniformly distributed on the two independent message sets $\mathcal{W}_1 = \{1, 2, \cdots, M_1\}$ and $\mathcal{W}_2 = \{1, 2, \cdots, M_2\}$, respectively. Let $\mathcal{X}_i^n$, $i = 1, 2$, denote the finite input codeword sets of the two-user IC. In the corresponding encoders i, $i = 1, 2$, applying the

encoding functions

$$f_i: \quad \mathcal{W}_i = \{1, 2, \cdots, M_i\} \;\rightarrow\; \mathcal{X}_i^n, \qquad i = 1, 2, \tag{3.1}$$

M_i codewords $\mathbf{x}_i \in \mathcal{X}_i^n$ with code length n for individual users i, $i = 1, 2$, are obtained.

Random vector variables X_i^n, $i = 1, 2$, with vector values $\mathbf{x}_i \in \mathcal{X}_i^n$ are transmitted as the inputs of the IC from the corresponding transmitters i, $i = 1, 2$. Let $\mathcal{Y}_i^n$, $i = 1, 2$, denote the finite output vector sets. The output random vector variables Y_i^n with vector values $\mathbf{y}_i \in \mathcal{Y}_i^n$ are obtained at the corresponding receivers i, $i = 1, 2$, through the IC with conditional probabilities $\Pr\{\mathbf{y}_1, \mathbf{y}_2 \mid \mathbf{x}_1, \mathbf{x}_2\}$. Considering a memoryless two-user IC,

$$\Pr\{\mathbf{y}_1, \mathbf{y}_2 \mid \mathbf{x}_1, \mathbf{x}_2\} = \prod_{t=1}^{n} \Pr\left\{y_1^{(t)}, y_2^{(t)} \mid x_1^{(t)}, x_2^{(t)}\right\} \tag{3.2}$$

can be obtained with

$$\mathbf{x}_i = \left(x_i^{(1)}, x_i^{(2)}, \cdots, x_i^{(n)}\right) \in \mathcal{X}_i^n, \qquad \mathbf{y}_i = \left(y_i^{(1)}, y_i^{(2)}, \cdots, y_i^{(n)}\right) \in \mathcal{Y}_i^n, \quad i = 1, 2. \tag{3.3}$$

Therefore, a discrete memoryless two-user IC can be denoted by a quintuple $(\mathcal{X}_1, \mathcal{X}_2, \widetilde{\mathcal{P}}, \mathcal{Y}_1, \mathcal{Y}_2)$, where $\mathcal{X}_i$, $i = 1, 2$, indicate the finite input signal sets, and $\mathcal{Y}_i$, $i = 1, 2$, indicate the finite output signal sets. $\widetilde{\mathcal{P}}$ is the set of conditional probabilities $\Pr\{y_1, y_2 \,|\, x_1, x_2\}$ that $y_i \in \mathcal{Y}_i$, $i = 1, 2$, as output signals are received when $x_i \in \mathcal{X}_i$, $i = 1, 2$, as input signals are transmitted.

The output random variables with vector values $\mathbf{y}_i \in \mathcal{Y}_i^n$, $i = 1, 2$, are mapped to the estimated message $\hat{W}_i$ with values $\hat{w}_i \in \mathcal{W}_i$, $i = 1, 2$, in the corresponding decoders i applying the decoding functions

$$g_i: \quad \mathcal{Y}_i^n \;\rightarrow\; \mathcal{W}_i = \{1, 2, \cdots, M_i\}, \qquad i = 1, 2 \;. \tag{3.4}$$

Based on the above description, a code $(M_1, M_2, n, \epsilon_n)$ for this two-user IC can be obtained with the error probability

$$\epsilon_n = \frac{\epsilon_{1,n} + \epsilon_{2,n}}{2} \;, \tag{3.5}$$

where the error probabilities for individual users i are

$$\epsilon_{i,n} = \frac{1}{M_1 M_2} \sum_{w_1, w_2} \Pr\left\{\hat{W}_i = g_i^n(\mathbf{y}_i) \neq w_i \mid W_1 = w_1, W_2 = w_2\right\}, \quad i = 1, 2 \;. \tag{3.6}$$

If the error probability ϵ_n of the code $(\lceil 2^{nR_1} \rceil, \lceil 2^{nR_2} \rceil, n, \epsilon_n)$ with a rate pair (R_1, R_2) goes to 0 as the code length n increases to infinity, the rate pair (R_1, R_2) is said to be achievable. The capacity region of this two-user channel is defined as the closure of the set of all achievable rate pairs. In case that the capacity region of the channel can not be fully characterized, the achievable rate region which is the union of all the known achievable rate pairs can be established as an inner bound for the capacity region.

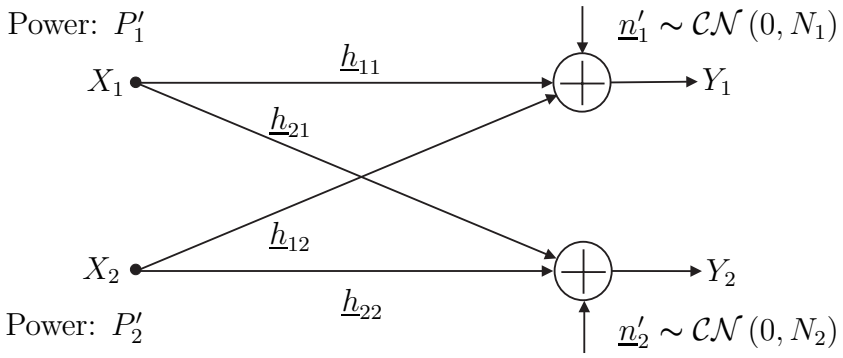

Figure 3.3. General two-user complex-valued Gaussian IC model.

3.2.2 Two-user Gaussian interference channel

As stated in [TV05], there is no conceptual difficulty to extend the framework of the IC with discrete-valued inputs and outputs to the IC with continuous-valued inputs and outputs. Even in analog memoryless channels, the communication process is still digital. In the research on the achievable rate region for the memoryless IC, the two-user real-valued Gaussian IC is frequently used as a reference model [Car75, Sat77, Car78, Sat81, HK81, Kra06]. In this chapter, a more general model, i.e., the two-user complex-valued Gaussian IC, is considered for a comparison between the performance of this IC and that of other two-user complex-valued communication channels applying different cooperative communication strategies. As depicted in Figure 3.3, this two-user complex-valued Gaussian IC considers input random variables X_i with values $\underline{x}_i \in \mathcal{X}_i$, $i = 1, 2$, and output random variables Y_i with values $\underline{y}_i \in \mathcal{Y}_i$, $i = 1, 2$, where $\mathcal{X}_1 = \mathcal{X}_2 = \mathcal{Y}_1 = \mathcal{Y}_2 = \mathbb{C}$ is the set of complex numbers. The channel inputs have to satisfy the average power constraints on codewords $\underline{\mathbf{x}}_i$ with a given block length n as

$$\frac{1}{n}\sum_{t=1}^{n}\left|\underline{x}_i^{(t)}\right|^2 \leq P_i' \quad i = 1, 2. \tag{3.7}$$

In this memoryless channel, at every time slot the channel PDF $\mathrm{p}(\underline{y}_1, \underline{y}_2 \mid \underline{x}_1, \underline{x}_2)$ can be calculated using

$$\begin{aligned} \underline{y}_1 &= \underline{h}_{11}\,\underline{x}_1 + \underline{h}_{12}\,\underline{x}_2 + \underline{n}_1' \\ \underline{y}_2 &= \underline{h}_{21}\,\underline{x}_1 + \underline{h}_{22}\,\underline{x}_2 + \underline{n}_2' \end{aligned} \tag{3.8}$$

with channel coefficients $\underline{h}_{ij} \in \mathbb{C}$, $i = 1, 2$, $j = 1, 2$. The noise signals $\underline{n}_1' \sim \mathcal{CN}(0, N_1)$ and $\underline{n}_2' \sim \mathcal{CN}(0, N_2)$ are assumed as i.i.d. Gaussian random variables.

Referring to [ETW08], although the capacity region of the two-user complex-valued Gaussian IC may depend on the phases of the channel coefficients, the achievable rate

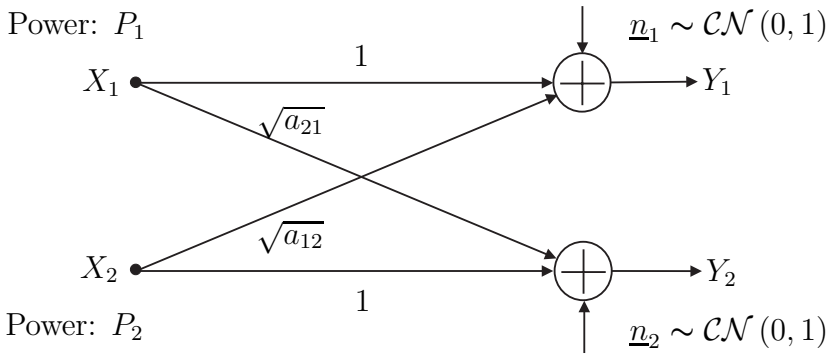

Figure 3.4. The standard form of the two-user Gaussian IC model.

regions for this IC which have been found until now only depend on the magnitudes of the channel coefficients. Therefore, the two-user IC with complex-valued channel coefficients described by (3.8) has the same up to now best known achievable rate region as the two-user IC with real-valued channel coefficients described by

$$\begin{aligned} \underline{y}_1 &= |\underline{h}_{11}|\, \underline{x}_1 + |\underline{h}_{12}|\, \underline{x}_2 + \underline{n}'_1 \\ \underline{y}_2 &= |\underline{h}_{21}|\, \underline{x}_1 + |\underline{h}_{22}|\, \underline{x}_2 + \underline{n}'_2. \end{aligned} \tag{3.9}$$

Considering real-valued channel coefficients, each use of the two-user IC in complex dimension can be considered as two uses of the two-user IC in real dimension [TV05]. Therefore, the achievable rate region for the two-user IC described by (3.9) can be easily derived from the achievable rate region for the real-valued Gaussian IC. Similar to the two-user real-valued Gaussian IC, through elementary scaling transformations the two-user Gaussian IC described by (3.9) can be converted to its standard form as shown in Figure 3.4. This standard form is described by

$$\begin{aligned} \underline{y}_1 &= \underline{x}_1 + \sqrt{a_{12}}\, \underline{x}_2 + \underline{n}_1 \\ \underline{y}_2 &= \sqrt{a_{21}}\, \underline{x}_1 + \underline{x}_2 + \underline{n}_2 \end{aligned} \tag{3.10}$$

with the channel gains

$$a_{12} = \frac{|\underline{h}_{12}|^2 N_2}{|\underline{h}_{22}|^2 N_1}, \qquad a_{21} = \frac{|\underline{h}_{21}|^2 N_1}{|\underline{h}_{11}|^2 N_2}, \tag{3.11}$$

the average power constraints of the input signals

$$P_1 = \frac{|\underline{h}_{11}|^2}{N_1} P'_1, \qquad P_2 = \frac{|\underline{h}_{22}|^2}{N_2} P'_2, \tag{3.12}$$

and i.i.d. additive Gaussian noises $\underline{n}_1 \sim \mathcal{CN}(0,1)$ and $\underline{n}_2 \sim \mathcal{CN}(0,1)$ with a unit variance. From the information-theoretic point of view, the standard form of the IC has the same achievable rate region as the IC described by (3.9), and therefore it has

the same best known achievable rate region as the general two-user complex-valued Gaussian IC described by (3.8). In the present thesis, the IC described by (3.10) is treated as the standard form for investigating the information-theoretic performance of the two-user Gaussian IC without cooperation.

3.2.3 Capacity region of the interference channel in special cases

The standard form of the two-user Gaussian IC in Figure 3.4 considers direct links with unit channel gains and noise signals with unit variance at both receivers. The capacity region of this IC depends on the power constraints P_1, P_2 and the channel gains a_{21}, a_{12} of the crosstalk links. According to different conditions of these parameters, several classes of interference in the investigated two-user Gaussian IC are defined as follows.

- No interference:
$$a_{12} = a_{21} = 0. \tag{3.13}$$
- Moderate or weak interference:
$$0 < a_{12} < 1, \quad 0 < a_{21} < 1. \tag{3.14}$$
- Strong interference:
$$a_{12} \geq 1, \quad a_{21} \geq 1. \tag{3.15}$$
- Very strong interference:
$$a_{12} \geq 1 + P_1, \quad a_{21} \geq 1 + P_2. \tag{3.16}$$

The above classification of the interference is determined with respect to the ratio of the interfering channel gain of the crosstalk link to the useful channel gain of the direct link. Since unit channel gains of the direct links are considered, the interfering channel gains a_{12} and a_{21} can fully describe this ratio. The cases of no interference, strong interference and very strong interference as the special cases where the capacity region of the two-user IC is fully characterized are discussed in this section.

Capacity region of the interference channel with no interference

Obviously, the investigated two-user communication channel without crosstalk links indicated by (3.13) can be considered as two independent complex-valued additive white Gaussian noise (AWGN) channels.

Theorem 3.1. [TV05, Cos85] The capacity region of the two-user Gaussian IC in its standard form for the case of no interference is the closure of all rate pairs (R_1, R_2) satisfying:

$$0 \leq R_1 \leq \log_2(1 + P_1) \triangleq C_1 \tag{3.17}$$
$$0 \leq R_2 \leq \log_2(1 + P_2) \triangleq C_2 \ . \tag{3.18}$$

Capacity region of the interference channel with strong interference

Intuitively, it would be expected that the stronger the interference is, the more harmful effect on communications it has. However, this statement is true only when the interference is treated as additive noise without considering any interference cancellation techniques. It should be emphasized that the harmfulness of interference is not so much due to its power or intensity, but due to its uncertainty with respect to the entropy from an information-theoretic point of view. If the interference is strong enough to be distinguishable from the useful signal, with a suitable interference cancellation technique it may be easier to eliminate strong interference than to eliminate weak interference. Therefore, a better quality of communications in the IC with strong enough interference can be achieved as compared to that in the IC with weak interference. This conjecture coincides with the knowledge about the capacity region of IC from the information-theoretic point of view. Based on the work in [Sat81, HK81] about the capacity region of the real-valued IC with strong interference, the capacity region of the two-user complex-valued Gaussian IC in its standard form with strong interference can be easily obtained.

Theorem 3.2. The capacity region of the two-user Gaussian IC in its standard form under the strong interference conditions as defined by (3.15) is a closure of all rate pairs (R_1, R_2) satisfying:

$$\begin{aligned} 0 &\leq R_1 \leq \log_2(1+P_1) && (3.19)\\ 0 &\leq R_2 \leq \log_2(1+P_2) && (3.20)\\ R_1+R_2 &\leq \min\{\log_2(1+P_1+a_{12}P_2),\, \log_2(1+P_2+a_{21}P_1)\}\ . && (3.21) \end{aligned}$$

(3.21) shows that the sum-capacity increases with the channel gains, i.e., a_{12} and a_{21}, until it reaches the maximum value $\log_2(1+P_1)+\log_2(1+P_2)$ which is limited by (3.19) and (3.20).

Theorem 3.2 shows that the capacity region of the investigated two-user IC is the intersection of the capacity regions of the two MACs corresponding to the two equations of (3.10), respectively. A simple argument for the above result is given in the following, while details of the information-theoretic proofs can be found in [Sat81, HK81]. On one side, the intersection of the capacity regions of the two MACs is the capacity region of the two-user channel when both messages are required at both receivers [Ahl74], and therefore it is an inner bound for the capacity region of the two-user IC where every message is required at its own receiver. On the other side, it has been proven that the intersection of the capacity regions of the two MACs is also an outer bound for the capacity region of the two-user IC in the case of strong interference [Sat81]. The basic

idea of this proof is as follows. It is assumed that in the two-user IC every receiver i can reliably decode the message W_i from its corresponding transmitter i, $i = 1, 2$, with a data rate pair (R_1, R_2) . At receiver 1 which can reliably decode W_1 with the data rate R_1, the received signal can be artificially rewritten as

$$\underline{y}_1' = \sqrt{a_{21}}\,\underline{x}_1 + \underline{x}_2 + \frac{\underline{n}_1}{\sqrt{a_{12}}}. \tag{3.22}$$

Considering the condition of strong interference as defined by (3.15), $\underline{y}_1'$ is equivalent to the received signal $\underline{y}_2$ at receiver 2 as described by (3.10) with a reduced noise variance. Therefore, if the message W_2 can be reliably decoded at receiver 2 with the data rate R_2, it can also be reliably decoded at receiver 1 with the data rate R_2. Similarly, receiver 2 can reliably decode message W_1 with the data rate R_1. Therefore, any rate pair in the capacity region of the two-user IC is also achievable in both MACs in which messages of both users have to be decoded at every receiver. Since the intersection of the capacity regions of the two MACs is both an inner bound and an outer bound for the capacity region of the two-user IC, it is the capacity region of the two-user IC.

Furthermore, in discrete memoryless IC the strong interference conditions can be expressed in terms of mutual information as

$$\begin{aligned} I(X_1; Y_1 \mid X_2) &\leq I(X_1; Y_2 \mid X_2) \\ I(X_2; Y_2 \mid X_1) &\leq I(X_2; Y_1 \mid X_1) \end{aligned} \tag{3.23}$$

with independent inputs X_1 and X_2 for all distributions of the probability $\Pr\{x_1\} \cdot \Pr\{x_2\}$. Each inequality of (3.23) shows that for each user in the two-user IC with strong interference the conditional mutual information in the direct link is smaller than that in the crosstalk link. The capacity region of the Gaussian IC of Theorem 3.2 can be extended to the general discrete memoryless IC.

Theorem 3.3. [CG87] The capacity region of the discrete memoryless two-user IC under the strong interference conditions as defined by (3.23) is the union of the rate pairs (R_1, R_2) which satisfy

$$0 \leq R_1 \leq I(X_1; Y_1 \mid X_2, Q) \tag{3.24}$$

$$0 \leq R_2 \leq I(X_2; Y_2 \mid X_1, Q) \tag{3.25}$$

$$R_1 + R_2 \leq \min\{I(X_1, X_2; Y_1 \mid Q),\, I(X_1, X_2; Y_2 \mid Q)\} \tag{3.26}$$

over all distributions of the probability $\Pr\{q\} \cdot \Pr\{x_1 \mid q\} \cdot \Pr\{x_2 \mid q\} \cdot \Pr\{y_1, y_2 \mid x_1, x_2\}$, where the variable Q with value q is a time-sharing parameter of cardinality 4. The cardinality bound on the time-sharing random variable Q is a consequence of applying Caratheodorys theorem on convex sets represented by (3.24)–(3.26) [Egg69].

The proofs for the achievability and the converse of the above capacity region can be found in [CG87]. In a word, the capacity region of the discrete memoryless two-user IC with strong interference can be exactly characterized.

Capacity region of the interference channel with very strong interference

In the above case of strong interference as defined by (3.15), the stronger the interference is, the larger the capacity region is until the interference becomes very strong [Sat81, HK81, CG87]. As a special case of strong interference, very strong interference as defined by (3.16) can result in the same capacity region as that derived in Theorem 3.1 for the case of no interference [Car75]. In the following, firstly let's have a look at the capacity region of the two-user Gaussian IC with very strong interference, and then the result will be extended to the discrete memoryless two-user IC. Based on the work in [Car75, Sat81] about the capacity region of the real-valued IC with very strong interference, the capacity region of the complex-valued IC with very strong interference can be easily obtained.

Theorem 3.4. The capacity region of the two-user Gaussian IC in its standard form under the very strong interference conditions as defined by (3.16) is a closure of all the rate pairs (R_1, R_2) satisfying:

$$\begin{aligned} 0 &\leq R_1 \leq \log_2(1+P_1) && (3.27)\\ 0 &\leq R_2 \leq \log_2(1+P_2)\ . && (3.28) \end{aligned}$$

A simple argument for the above result is as follows. For every user, an upper bound of the data rate with which its message can be reliably decoded at its own receiver is obtained when the interference from the other user is totally cancelled. Under the very strong interference conditions, the signal from every user in the crosstalk link is so strong that its transmitted message at the maximum data rate still can be reliably decoded at the other user's receiver even if it treats its own intended signal as noise. This means that the interfering signal from a user can always be totally cancelled at the other user's receiver. Therefore, the very strong interference will not reduce the capacity region as compared to the two-user communication channel with no interference.

From an information-theoretic point of view, in discrete memoryless IC the very strong interference conditions can be expressed in terms of mutual information as

$$\begin{aligned} I(X_1; Y_1 \mid X_2) &\leq I(X_1; Y_2) \\ I(X_2; Y_2 \mid X_1) &\leq I(X_2; Y_1) && (3.29) \end{aligned}$$

with independent inputs X_1 and X_2 for all distributions of the probability $\Pr\{x_1\} \cdot \Pr\{x_2\}$. Each inequality of (3.29) shows that for the detection of a user in the two-user IC with very strong interference the conditional mutual information flowing in the direct link with the knowledge about the message of the other user is smaller than the mutual information flowing in the crosstalk link with no knowledge about the message of the other user. The conditions of (3.29) is obviously stronger than the conditions of (3.23) due to the inequalities $I(X_1; Y_2) \leq I(X_1; Y_2 \mid X_2)$ and $I(X_2; Y_1) \leq I(X_2; Y_1 \mid X_1)$ with independent X_1 and X_2. Based on the work in [CG87], the capacity region of the discrete memoryless two-user IC with very strong interference as a special case of the discrete memoryless IC with strong interference can be easily obtained.

Theorem 3.5. The capacity region of the discrete memoryless two-user IC under the very strong interference conditions as defined by (3.29) is the union of the rate pairs (R_1, R_2) which satisfy

$$0 \leq R_1 \leq I(X_1; Y_1 \mid X_2, Q) \tag{3.30}$$

$$0 \leq R_2 \leq I(X_2; Y_2 \mid X_1, Q) \tag{3.31}$$

over all distributions of the probability $\Pr\{q\} \cdot \Pr\{x_1|q\} \cdot \Pr\{x_2|q\} \cdot \Pr\{y_1, y_2|x_1, x_2\}$, where the variable Q with value q is a time-sharing parameter of cardinality 4.

In summary, the capacity region of the two-user IC with very strong interference can be fully characterized. Since all the interference can be removed in the two-user IC with very strong interference at all data rate pairs inside the capacity region of the two-user communication channel with no interference, no capacity loss in the two-user IC with very strong interference occurs as compared to the interference-free case.

3.2.4 Han-Kobayashi achievable rate region for the interference channel

In this section, the achievable rate region for the general two-user IC will be investigated. The intensity of interference is not limited by special conditions, e.g., strong or very strong, as in the above section. In fact, in realistic cellular systems, interference is usually weak. It is known that in the two-user IC when the interference is not strong enough, reliable communications can not always be achieved with all data rate pairs inside the capacity region of the two-user interference-free communication channel. Namely, the interference will cause a capacity loss [Cos85]. However, until today the exact capacity loss due to weak interference and the encoding-decoding

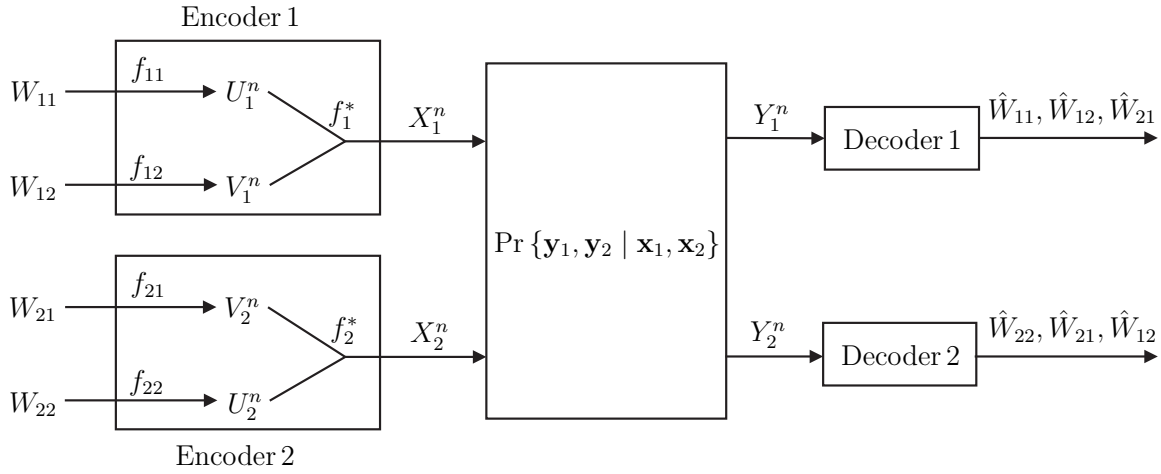

Figure 3.5. Modified two-user IC model applying the Han-Kobayashi strategy.

scheme to achieve all data rate pairs for reliable communications with weak interference are still unknown. Although the capacity region of the IC with weak interference is still not fully characterized, several achievable rate regions have been established [Sat77, Car78, HK81, Cos85]. The best known achievable rate region for the IC with weak interference, i.e., the best inner bound for the capacity region, is obtained by applying the strategy proposed by Han and Kobayashi in [HK81]. Recently, a simplified expression of the Han-Kobayshi rate region for the two-user IC has been presented in [CMGEG08]. Based on the two-user IC model in Figure 3.2, the modified two-user IC model applying the Han-Kobayashi strategy is shown in Figure 3.5. In this section, the main principle and key features of the Han-Kobayashi strategy for the two-user IC will be presented.

One key feature of the Han-Kobayashi strategy is the rate-splitting. The transmitted message W_i for each user i in message set $\mathcal{W}_i = \{1, 2, \cdots, M_i\}$ is split into two parts: the private message W_{ii} in the message set $\mathcal{W}_{ii} = \{1, 2, \cdots, M_{ii}\}$ and the common message W_{ij} in the message set $\mathcal{W}_{ij} = \{1, 2, \cdots, M_{ij}\}$, $i = 1, 2$, $j = 1, 2$, $i \neq j$. The private message W_{ii} intended for user i is expected to be decoded at its intended receiver i, while the common message W_{ij} which is intended for user i can be decoded at both receiver i and receiver j. In this way, at each user's intended receiver some part of the interference, i.e., the interference which corresponds to the common message of the other user, can be cancelled out with the decoded common message. Let $\mathcal{C}_{\mathrm{m}}$ denote the modified two-user IC in Figure 3.5, and let $\mathcal{C}$ denote the general two-user IC in Figure 3.2. In [HK81], it has been shown that if there is a code $(M_{11}, M_{12}, M_{22}, M_{21}, n, \epsilon_n)$ for $\mathcal{C}_{\mathrm{m}}$, then there is a code $(M_{11}{\cdot}M_{12},\ M_{22}{\cdot}M_{21},\ n, \epsilon_n)$ for $\mathcal{C}_{\mathrm{m}}$. If the error probability ϵ_n of the above code $(\lceil 2^{nS_1} \rceil, \lceil 2^{nT_1} \rceil, \lceil 2^{nS_2} \rceil, \lceil 2^{nT_2} \rceil, n, \epsilon_n)$ with a quadruple (S_1, T_1, S_2, T_2) for $\mathcal{C}_m$ goes to 0 as the code length n increases to infinity, the quadruple (S_1, T_1, S_2, T_2) is

said to be an achievable rate quadruple for $\mathcal{C}_{\mathrm{m}}$. Correspondingly, $(R_1 = S_1 + T_1, R_2 = S_2 + T_2)$ is an achievable rate pair for $\mathcal{C}$.

Let U_i and V_i, $i=1,2$, denote random variables defined on arbitrary finite sets $\mathcal{U}_i$ and $\mathcal{V}_i$. The variables U_i and V_i are used to carry the private message W_{ii} and the common message W_{ij} for user i, $i=1,2$, respectively. The encoding function $f_i : \mathcal{W}_i \to \mathcal{X}_i^n$ for each user i, $i=1,2$, is divided into three functions

$$f_{ii}: \quad \mathcal{W}_{ii} \to \mathcal{U}_i^n, \quad i=1,2, \tag{3.32}$$

$$f_{ij}: \quad \mathcal{W}_{ij} \to \mathcal{V}_i^n, \quad i=1,2;\ j=1,2;\ i\neq j, \tag{3.33}$$

$$f_i^*: \quad \mathcal{U}_i^n \times \mathcal{V}_i^n \to \mathcal{X}_i^n, \quad i=1,2. \tag{3.34}$$

In fact, the above rate-splitting scheme in the Han-Kobayashi strategy is a generalization of superposition coding which was originally developed in [Cov72] by Cover and firstly applied in Gaussian IC to split message in [Car78] by Carleial. A restricted version of superposition coding with a sequential decoder is applied in [Car78] in the way that each receiver i firstly decodes V_1 or V_2 corresponding to the common message W_{12} or W_{21} and then decodes U_i corresponding to its private message W_{ii}, $i=1,2$. In contrast to this, the Han-Kobayashi strategy performs a simultaneous superposition coding in the multi-variable case applying a more powerful joint decoder in each receiver i to decode V_1 and V_2 corresponding the common messages W_{12} and W_{21}, and U_i corresponding to its private message W_{ii} simultaneously.

Another key feature of the Han-Kobayashi strategy is the time-sharing scheme. Let Q denote a random variable defined on an arbitrary finite set $\mathcal{Q}$. The variable Q is used as the time-sharing parameter which allows time-sharing between the arbitrary splits of the transmitted message into private and common messages. For a given Q with value $q \in \mathcal{Q}$, one deterministic private message W_{ii} and one deterministic common message W_{ij} can be generated from every transmitted message W_i for each user i, $i=1,2$, $j=1,2$, $i\neq j$. Through the deterministic functions of (3.32)–(3.34) for deterministic private and common messages, one U_i with value $u_i \in \mathcal{U}_i$, one V_i with value $v_i \in \mathcal{V}_i$, and therefore one X_i with value $x_i \in \mathcal{X}_i$, $i=1,2$, are obtained. Over all distributions of the probability $\Pr\{q\}$ of the variable Q with value $q \in \mathcal{Q}$, time-sharing between multiple rate splitting schemes, i.e., between the corresponding multiple deterministic encoding functions, can be performed. Considering all possible rate splitting schemes and time-sharing strategies, all the rate pairs achieved by the Han-Kobayashi strategy could form an achievable rate region [HK81]. However, the optimization among the myriads of probability distributions of the time-sharing variable is still an open question [CMGEG08, ETW08]. It is still prohibitively complex to characterize the full Han-Kobayashi achievable rate region [MK09].

Let $\mathcal{P}^*$ denote the set of all distributions of the probability $Z = \Pr\{q\}\cdot\Pr\{u_1|q\}\cdot\Pr\{v_1|q\}\cdot\Pr\{u_2|q\}\cdot\Pr\{v_2|q\}\cdot\Pr\{x_1|u_1,v_1,q\}\cdot\Pr\{x_2|u_2,v_2,q\}$. For a fixed $Z \in \mathcal{P}^*$, let $\mathcal{G}_1(Z)$ be the set of all quadruples (S_1, T_1, S_2, T_2) with nonnegative real values concerning receiver 1 satisfying:

$$\begin{aligned}
S_1 &\leq I(Y_1; U_1 \mid V_1V_2Q) && (3.35)\\
T_1 &\leq I(Y_1; V_1 \mid U_1V_2Q) && (3.36)\\
T_2 &\leq I(Y_1; V_2 \mid U_1V_1Q) && (3.37)\\
S_1 + T_1 &\leq I(Y_1; U_1V_1 \mid V_2Q) && (3.38)\\
S_1 + T_2 &\leq I(Y_1; U_1V_2 \mid V_1Q) && (3.39)\\
T_1 + T_2 &\leq I(Y_1; V_1V_2 \mid U_1Q) && (3.40)\\
S_1 + T_1 + T_2 &\leq I(Y_1; U_1V_1V_2 \mid Q)\ . && (3.41)
\end{aligned}$$

The above formulas correspond to different conditional mutual information between the output variable at receiver 1 and some input variables carrying private or common messages with a given Q and with certain decoded private or common messages. Similarly, let $\mathcal{G}_2(Z)$ be the set of all quadruples (S_1, T_1, S_2, T_2) with nonnegative real values concerning receiver 2 satisfying the above equations from (3.35) to (3.41) with indices 1 and 2 exchanged with each other everywhere. The Han-Kobayashi achievable rate region $\mathcal{R}_{\mathrm{HK}}$ for the general two-user IC $\mathcal{C}$ is obtained with the help of the modified two-user IC $\mathcal{C}_{\mathrm{m}}$.

Theorem 3.6. [HK81, CMGEG08] Any element of

$$\mathcal{G} = \text{ closure of } \bigcup_{Z\in\mathcal{P}^*} (\mathcal{G}_1(Z) \cap \mathcal{G}_2(Z)) \tag{3.42}$$

is achievable for the modified two-user IC $\mathcal{C}_{\mathrm{m}}$. For any $Z \in \mathcal{P}^*$, let $\mathcal{R}(Z)$ denote the set of all (R_1, R_2) such that $R_1 = S_1 + T_1$ and $R_2 = S_2 + T_2$ for some $(S_1, T_1, S_2, T_2) \in (\mathcal{G}_1(Z) \cap \mathcal{G}_2(Z))$. Any element of

$$\mathcal{R}_{\mathrm{HK}} = \text{ closure of } \bigcup_{Z\in\mathcal{P}^*} \mathcal{R}(Z) \tag{3.43}$$

is achievable for the general two-user IC $\mathcal{C}$.

Let $\mathcal{R}_{\mathrm{HK}}$ denote the Han-Kobayashi achievable rate region obtained by using the time-sharing scheme considering all probability distributions of Q. Let $\mathcal{R}_{\mathrm{CH}}$ denote the achievable rate region obtained by using the convex-hull operation of $\mathcal{R}(Z)$ without applying time-sharing, i.e., considering a constant value of Q. In [HK81], numerical results in an exemplary Gaussian IC suggest that $\mathcal{R}_{\mathrm{HK}}$ strictly extends $\mathcal{R}_{\mathrm{CH}}$. As a special case, the achievable rate region for the IC applying the TDM/FDM strategy

which is not included in $\mathcal{R}_{\mathrm{CH}}$ is included in $\mathcal{R}_{\mathrm{HK}}$. In [HK81], it has been shown that the Han-Kobayashi strategy outperforms the scheme proposed by Sato in [Sat77] and the scheme proposed by Carleial in [Car78] to achieve a larger rate region. Until today, the Han-Kobayashi achievable rate region is still the best known inner bound for the capacity region of the general two-user IC [CMGEG08, ETW08, MK09].

A simplified explicit expression to compute $\mathcal{R}(Z)$ is presented in Appendix A.1, and then the shape of $\mathcal{R}(Z)$ can be determined by its extreme points. The Han-Kobayashi strategy can be directly applied to the two-user Gaussian IC which is a basic representative IC model as introduced in Section 3.2.2. Due to the prohibitive computational effort required to characterize the whole Han-Kobayashi achievable rate region, the following customary restriction could be put on the input signals to obtain a computable achievable rate region. Let $\mathcal{P}(P_1, P_2)$ denote a subclass of $\mathcal{P}^*$. $\mathcal{P}(P_1, P_2)$ is defined by $Z = \Pr\{q\} \cdot \Pr\{u_1|q\} \cdot \Pr\{v_1|q\} \cdot \Pr\{u_2|q\} \cdot \Pr\{v_2|q\} \cdot \Pr\{x_1|u_1, v_1, q\} \cdot \Pr\{x_2|u_2, v_2, q\} \in \mathcal{P}(P_1, P_2)$ if and only if $Z \in \mathcal{P}^*$, the time-sharing variable $Q = \phi$ has a constant value, U_1, V_1, U_2 and V_2 are Gaussian variables, and the input signals $X_1 = U_1 + V_1$ and $X_2 = U_2 + V_2$ have the average power constraints P_1 and P_2 defined as $\sigma^2(X_1) \leq P_1$ and $\sigma^2(X_2) \leq P_2$. Considering the standard form of the two-user Gaussian IC model in Figure 3.4, its computable rate region

$$\mathcal{R}'_{\mathrm{HK}} = \text{ convex closure of } \bigcup_{Z \in \mathcal{P}(P_1, P_2)} \mathcal{R}(Z), \tag{3.44}$$

which is a subset of the full Han-Kobayashi achievable rate region can be numerically computed by applying Theorem A.1 with $Z \in \mathcal{P}(P_1, P_2)$ as presented in Appendix A.1.

The numerical results of the achievable rate region for the IC with full CSI are put in the next section in order to be compared with the achievable rate region for the IC with partial CSI.

3.2.5 Achievable rate region for the interference channel with partial CSI

As mentioned in Section 3.1, in reality it is quite common that data transmissions and receptions are performed with partial CSI of the whole system. Corresponding to conventional cellular systems in which only intracell CSI is considered for each user, the achievable rate region for the two-user IC is obtained considering only the CSI of the direct links at the related transmitters and receivers. If more knowledge of CSI is available in the two-user IC, e.g., CSI of one crosstalk link is considered, a larger achievable rate region can be expected. Corresponding to the cellular system with no

cooperation but considering full CSI of the whole system for each user, the best known achievable rate region for the two-user IC with full CSI is obtained by applying the Han-Kobayashi strategy. The present section answers the question about how much the performance loss is due to partial CSI instead of full CSI being considered at the transmitters and the receivers in the two-user IC. In other words, the performance gain thanks to more knowledge of CSI at the transmitters and the receivers in the two-user IC can be revealed as well. Taking the standard form of the two-user Gaussian IC in Figure 3.4 as the reference model, the unit channel gains $a_{11} = a_{22} = 1$ in the direct links, the unit noise variance, and the average power constraints P_1 and P_2 of the input signals are assumed to be known. The investigation concerning partial CSI is performed in terms of different levels of the channel knowledge of the crosstalk links with respect to a_{12} and a_{21}. The information-theoretic performance of the two-user IC with different levels of the channel knowledge is obtained with the help of some simplified equivalent channel models. In the following, 4 different levels of the channel knowledge of the crosstalk links are distinguished, and the corresponding simplified equivalent channels are introduced. It is worth emphasizing that in the following simplified equivalent channels the effect of the lack of channel knowledge of a crosstalk link is simply modelled as enhanced noise at the related receiver. This simplified modeling provides only an estimate of the achievable rate region for the two-user IC with partial CSI. In realistic systems even though the exact instantaneous value of a channel coefficient is unknown, the statistical knowledge of the CSI can be exploited. Therefore, the simplified equivalent channel model which simply treats the signal from the crosstalk link with unknown CSI as noise underestimates the capacity region of the IC.

A) Full knowledge about a_{12} and a_{21}: This channel is nothing else but the two-user Gaussian IC in its standard form which has been described by (3.10). Let "IC" denote this channel in the following investigations.

B) a_{12} is known, a_{21} is unknown: This channel is modelled by a simplified equivalent channel, i.e., one-sided Gaussian IC with enhanced noise at receiver 2, as shown in Figure 3.6. This channel can be described by

$$\begin{aligned} \underline{y}_1 &= \underline{x}_1 + \sqrt{a_{12}}\,\underline{x}_2 + \underline{n}_1 \\ \underline{y}_2 &= \underline{x}_2 + \underline{n}_2 \end{aligned} \tag{3.45}$$

with i.i.d. Gaussian additive noises $\underline{n}_1 \sim \mathcal{CN}(0,1)$ and $\underline{n}_2 \sim \mathcal{CN}(0, 1 + a_{21}P_1)$. Let "$Z_1$ channel" denote this channel in the following investigations.

C) a_{21} is known, a_{12} is unknown: Similar to the above case of Z_1 channel, this channel is modelled by a simplified equivalent channel, i.e., one-sided Gaussian

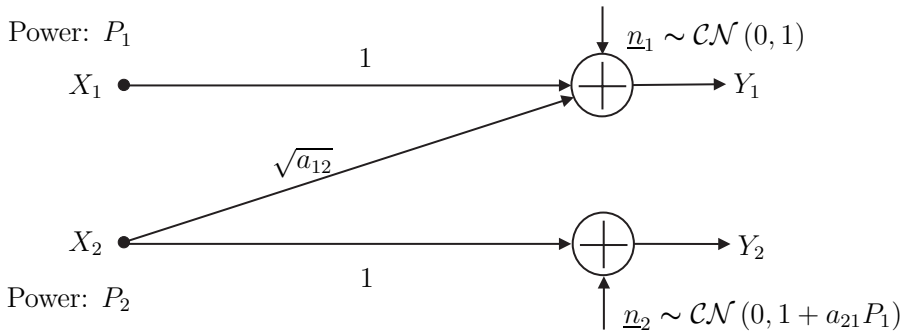

Figure 3.6. Simplified equivalent channel for the two-user Gaussian IC without knowledge about a_{21}, denoted as "Z_1 channel".

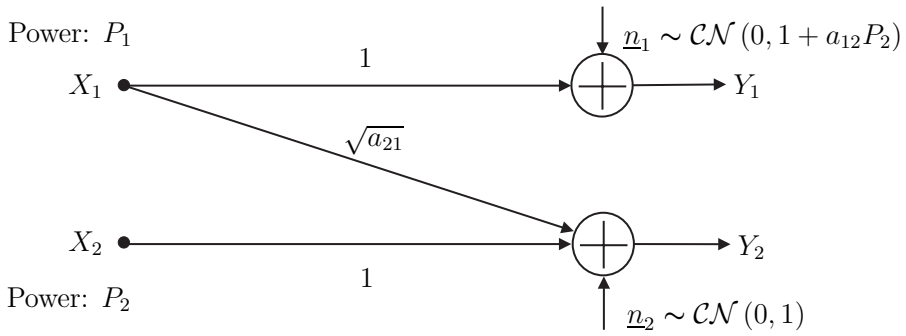

Figure 3.7. Simplified equivalent channel for the two-user Gaussian IC without knowledge about a_{12}, denoted as "Z_2 channel".

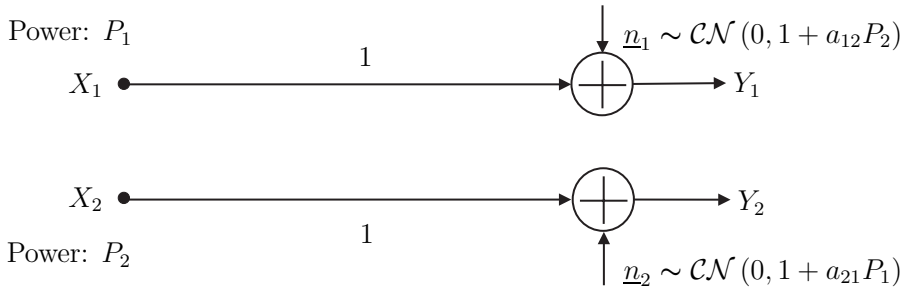

Figure 3.8. Simplified equivalent channel for the two-user Gaussian IC without knowledge about a_{12} and a_{21}, denoted as "S channel".

IC with enhanced noise at receiver 1, as shown in Figure 3.7. This channel can be described by

$$\begin{aligned} \underline{y}_1 &= \underline{x}_1 + \underline{n}_1 \\ \underline{y}_2 &= \sqrt{a_{21}}\,\underline{x}_1 + \underline{x}_2 + \underline{n}_2 \end{aligned} \tag{3.46}$$

with i.i.d. Gaussian additive noises $\underline{n}_1 \sim \mathcal{CN}(0, 1 + a_{12}P_2)$ and $\underline{n}_2 \sim \mathcal{CN}(0,1)$. Let "$Z_2$ channel" denote this channel in the following investigations.

D) No knowledge about a_{12} and a_{21}: As a combination of the above two cases of Z_1 channel and Z_2 channel, this channel can be modelled as two parallel Gaussian SISO channels with enhanced noise at both receivers. Let "S channel" denote this simplified equivalent channel in the following investigations. As shown in Figure 3.8, this channel can be described by

$$\begin{aligned} \underline{y}_1 &= \underline{x}_1 + \underline{n}_1 \\ \underline{y}_2 &= \underline{x}_2 + \underline{n}_2 \end{aligned} \tag{3.47}$$

with i.i.d. additive Gaussian noises $\underline{n}_1 \sim \mathcal{CN}(0, 1 + a_{12}P_2)$ and $\underline{n}_2 \sim \mathcal{CN}(0, 1 + a_{21}P_1)$.

Concerning the case where a_{12} and a_{21} are known, i.e., the two-user IC with full CSI, the strategy to investigate its information-theoretic performance has already been discussed in Section 3.2.3 and Section 3.2.4. Concerning the case where a_{12} and a_{21} are unknown, the information-theoretic performance of this channel can be obtained with the help of the S channel consisting of two SISO channels, whose capacity region can be easily characterized. In the following, the case where the CSI of one crosstalk link is unknown will be further investigated. Without loss of generality, the Z_1 channel is considered for this case. Then, numerical results of the achievable rate regions for the two-user IC with the above 4 different levels of channel knowledge will be presented and compared.

Since in the two-user IC there is no cooperation between the two users and the message for each user is decoded at its corresponding receiver, the functionality of the crosstalk link can only be the one of an interfering channel. In the two-user Gaussian IC without knowledge about a_{21}, i.e., no knowledge about the CSI of one crosstalk channel, the corresponding interference through this crosstalk link from transmitter 1 can not be cancelled at receiver 2. Meanwhile, no information can be obtained from this crosstalk link with unknown CSI. Therefore, the mixture of the interference and the noise at receiver 2 is simply modelled as enhanced Gaussian noise with a variance of $1 + a_{21}P_1$. The Z_1 channel in Figure 3.6 which is a one-sided two-user Gaussian IC with enhanced noise at receiver 2 is treated as the equivalent channel in this case. The standard form of the one-sided Gaussian IC with unit noise variance has been investigated by Costa in [Cos85] and by Sason in [Sas04]. Maintaining the same capacity region, the Z_1 channel described by (3.45) can be rewritten in the standard form of the one-sided Gaussian IC by applying (3.11) and (3.12) as

$$\begin{aligned} \underline{y}_1 &= \underline{x}_1 + \sqrt{a_{12}(1 + a_{21}P_1)}\,\underline{x}_2 + \underline{n}_1 \\ \underline{y}_2 &= \underline{x}_2 + \underline{n}_2 \end{aligned} \tag{3.48}$$

with average power constraints P_1 and $P_2/(1+a_{21}P_1)$ for the input signals and i.i.d. Gaussian noises $\underline{n}_1 \sim \mathcal{CN}(0,1)$ and $\underline{n}_2 \sim \mathcal{CN}(0,1)$. The results on the capacity region of the IC with strong interference in Section 3.2.3 can be easily extended to the Z_1 channel with the help of the standard form of the one-sided Gaussian IC of (3.48).

Theorem 3.7. The capacity region of the Z_1 channel in Figure 3.6 under the condition of $a_{12}(1+a_{21}P_1) \geq 1$ is a closure of all the rate pairs (R_1, R_2) satisfying

$$\begin{aligned} 0 &\leq R_1 \leq \varphi(P_1) && (3.49)\\ 0 &\leq R_2 \leq \varphi\left(\frac{P_2}{1+a_{21}P_1}\right) && (3.50)\\ R_1+R_2 &\leq \varphi(P_1+a_{12}P_2)\ . && (3.51) \end{aligned}$$

$\varphi(x) = \log_2(1+x)$ is considered in the above expressions.

However, if $a_{12}(1+a_{21}P_1) < 1$, the capacity region of the Z_1 channel is still not fully characterized. Fortunately, with the help of a degraded Gaussian IC which has the same capacity region as the Z_1 channel, the sum-capacity of the Z_1 channel in this case is exactly known. Roughly speaking, a two-user IC is said to be degraded if one output can be regarded as the output of a hypothetical channel whose input is the other output of the IC [Sat78a]. In [Cos85], Costa has shown that for every one-sided Gaussian IC with weak interference, there is a degraded Gaussian IC with the same capacity region. In other words, these two channels are equivalent with respect to the capacity region. Details of the proof has been presented in [Cos85]. Basically, the equivalence between these two channels is established by proving that if a rate pair is achievable for the first channel, it is also achievable for the second one, and vice versa. In the proof, scaling of the output signals and the Fano's inequality [CT06] are considered. Referring to [Cos85], the degraded Gaussian IC which has the same capacity region as the Z_1 channel is depicted in Figure 3.9. Maintaining the same capacity region, the degraded Gaussian IC in Figure 3.9 can be rewritten in the standard form of a two-user IC as

$$\begin{aligned} \underline{y}_1 &= \underline{x}_1 + \sqrt{a_{12}(1+a_{21}P_1)}\,\underline{x}_2 + \underline{n}_1\\ \underline{y}_2 &= \frac{1}{\sqrt{a_{12}(1+a_{21}P_1)}}\,\underline{x}_1 + \underline{x}_2 + \underline{n}_2 \end{aligned} \qquad (3.52)$$

with average power constraints P_1 and $P_2/(1+a_{21}P_1)$ for the input signals and i.i.d. Gaussian noises $\underline{n}_1 \sim \mathcal{CN}(0,1)$ and $\underline{n}_2 \sim \mathcal{CN}(0,1)$. It has been stated that the standard form of a two-user Gaussian IC is degraded if and only if the product of the channel gains of two crosstalk links is 1 [Sas04]. Obviously, the two-user Gaussian IC described by (3.52) fulfills this statement. According to the work in [Sas04, MK09] on the sum-capacity of the degraded two-user Gaussian IC in its standard form, the sum-capacity of

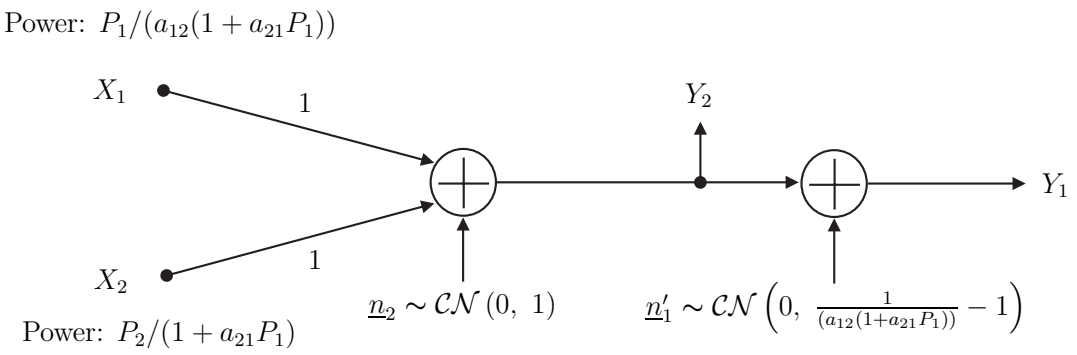

Figure 3.9. Equivalent channel for Z_1 channel with $a_{12}(1+a_{21}P_1) < 1$.

the channel described by (3.52) is attained at the rate pair $\left(\varphi\left(\frac{P_1}{1+a_{12}P_2}\right), \varphi\left(\frac{P_2}{1+a_{21}P_1}\right)\right)$, which is an extreme point in its capacity region. Since the standard form of the degraded Gaussian IC of (3.52) has the same capacity region as the Z_1 channel, the sum-capacity of the Z_1 channel under the condition that $a_{12}(1+a_{21}P_1) < 1$ is also obtained. Consequently, considering different conditions of the weak interference, of the strong interference and of the very strong interference with respect to the parameters in the standard form of the degraded Gaussian IC of (3.52), the sum-capacity of the Z_1 channel in Figure 3.6 is

$$\max(R_1+R_2) = \begin{cases} \varphi\left(\frac{P_1}{1+a_{12}P_2}\right) + \varphi\left(\frac{P_2}{1+a_{21}P_1}\right) & \text{for } 0 \le a_{12}(1+a_{21}P_1) < 1 \\ \varphi\left(P_1 + a_{12}P_2\right) & \text{for } 1 \le a_{12}(1+a_{21}P_1) < 1+P_1 \\ \varphi(P_1) + \varphi\left(\frac{P_2}{1+a_{21}P_1}\right) & \text{for } a_{12}(1+a_{21}P_1) \ge 1+P_1 \end{cases} . \tag{3.53}$$

In the following, the achievable rate regions for the standard form of the two-user complex-valued Gaussian IC in Figure 3.4 with different levels of knowledge of CSI are numerically computed. In Figure 3.10 the two-user IC under the condition of strong interference with parameters $P_1 = P_2 = 2$ and $a_{12} = a_{21} = 1.5$ is investigated, while in Figure 3.11 the two-user IC under the condition of moderate/weak interference with parameters $P_1 = P_2 = 6$ and $a_{12} = a_{21} = 0.55$ is investigated. Generally, the achievable rate regions for the two-user IC with the above considered different levels of knowledge of CSI can always be obtained by applying the Han-Kobayashi strategy. Even for the two-user IC with partial knowledge of CSI, the corresponding simplified equivalent channels can be considered as special cases of the two-user IC with some modified parameters. The obtained different achievable rate regions for the IC with different

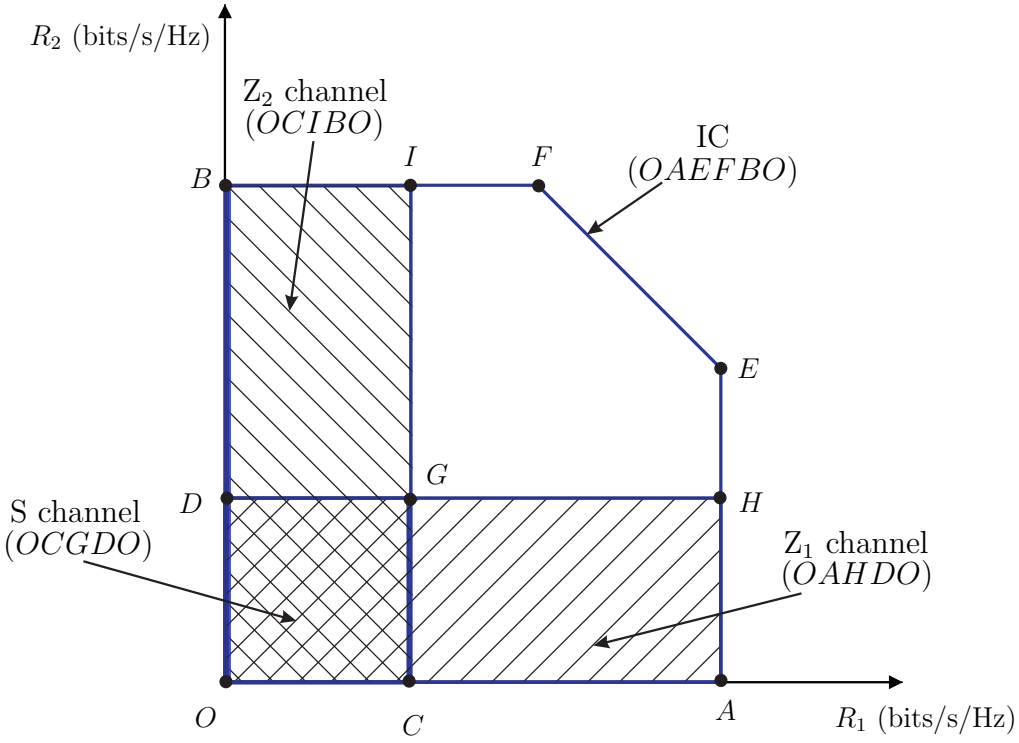

Figure 3.10. Achievable rate region for the two-user Gaussian IC in the standard form with $P_1 = P_2 = 2$ and $a_{12} = a_{21} = 1.5$ considering different levels of channel knowledge.

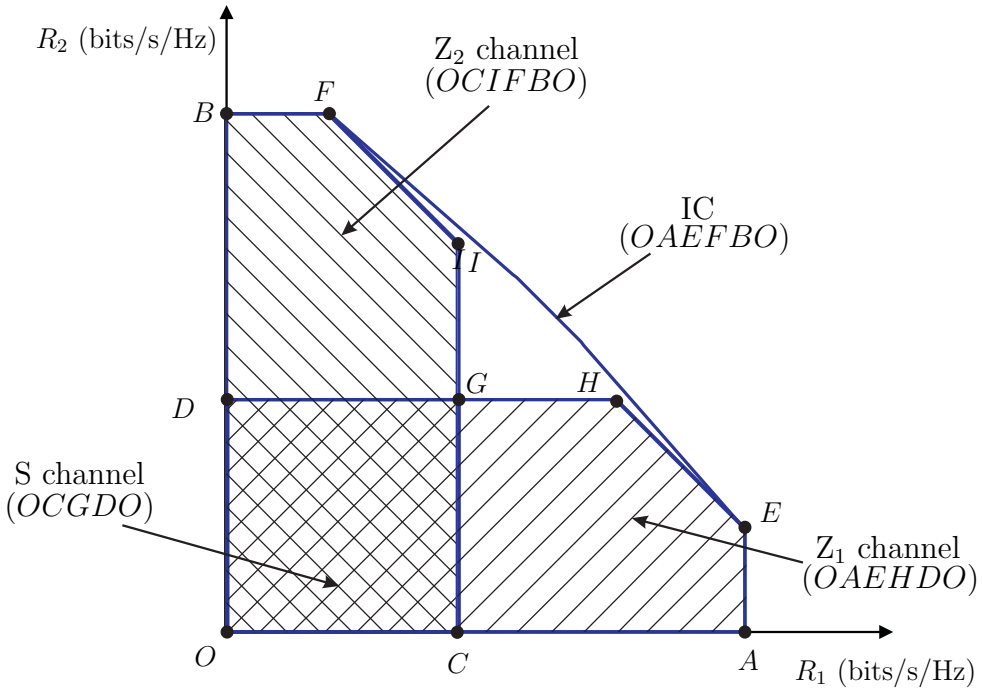

Figure 3.11. Achievable rate region for the two-user Gaussian IC in the standard form with $P_1 = P_2 = 6$ and $a_{12} = a_{21} = 0.55$ considering different levels of channel knowledge.

levels of knowledge of CSI are constrained by the following extreme points

$$A = (1.585,\ 0), \quad B = (0,\ 1.585), \quad C = (0.585,\ 0), \quad D = (0,\ 0.585),$$
$$E = (1.585,\ 1), \quad F = (1,\ 1.585), \quad G = (0.585,\ 0.585), \quad O = (0,0) \tag{3.54}$$

as shown in Figure 3.10, and

$$A = (2.807,\ 0), \quad B = (0,\ 2.807), \quad C = (1.26,\ 0), \quad D = (0,\ 1.26),$$
$$E = (2.807,\ 0.557), \quad F = (0.557,\ 2.807), \quad G = (1.26,\ 1.26),$$
$$H = (2.104,\ 1.26), \quad I = (1.26,\ 2.104), \quad O = (0,0) \tag{3.55}$$

as shown in Figure 3.11.

Considering full CSI, in both Figure 3.10 and Figure 3.11, the achievable rate region for the IC obtained by applying the Han-Kobayashi strategy is constrained by the extreme points A, E, F, B and O. As mentioned in Section 3.2.3, the capacity region of the IC with strong interference can be exactly characterized. It is shown that the Han-Kobayashi achievable rate region for the IC in Figure 3.10 coincides with the capacity region directly calculated by applying Theorem 3.2.

Considering partial knowledge of CSI in the two-user IC, the achievable rate region for the two-user IC without knowledge about a_{21} is obtained by applying the Han-Kobayashi strategy to its simplified equivalent channel, i.e., the Z_1 channel. The achievable rate region for the Z_1 channel has a rectangular shape constrained by the extreme points A, H, D and O in Figure 3.10, while it has a pentagonal shape constrained by the extreme points A, E, H, D and O in Figure 3.11. The reason for the above difference between the shapes of the achievable rate regions is as follows. Maintaining the same capacity region, the Z_1 channel can be converted to the standard form of a degraded Gaussian IC described by (3.52). The parameters in the Z_1 channel considered in Figure 3.10 fulfill the condition of very strong interference, i.e., $a_{12}(1+a_{21}P_1) \geq 1+P_1$, for its equivalent degraded Gaussian IC. The parameters in the Z_1 channel considered in Figure 3.11 fulfill the condition of strong interference, i.e., $1 \leq a_{12}(1+a_{21}P_1) \leq 1+P_1$, for its equivalent degraded Gaussian IC. The Han-Kobayashi achievable rate region for the Z_1 channel in Figure 3.10 coincides with the capacity region directly calculated by applying Theorem 3.4 for the IC with very strong interference. The Han-Kobayashi achievable rate region for the Z_1 channel in Figure 3.11 coincides with the capacity region directly calculated by applying Theorem 3.2 for the IC with strong interference. Similarly, the achievable rate region for the Z_2 channel as the simplified equivalent channel for the two-user IC without knowledge about a_{12} is shown.

The achievable rate region for the S channel as the simplified equivalent channel for the two-user IC without knowledge about a_{21} and a_{12} has a rectangular shape constrained

by the extreme points C, G, D and O in both Figure 3.10 and Figure 3.11. The achievable rate region is equal to the capacity region of the corresponding two parallel SISO channels with enhanced noise.

Now we are in the position to compare the achievable rate regions for the IC with different levels of knowledge of CSI. Taking the capacity region of the S channel corresponding to the IC with the least knowledge of CSI among the above 4 cases for reference, the performance gain due to more knowledge of CSI is clearly shown by numerical results in Figure 3.10 and Figure 3.11. The Z_i channel, $i=1,2$, has a greatly enlarged achievable rate region with respect to the corresponding increased data rate R_i as compared to the S channel. The IC with full CSI has a greatly enlarged achievable rate region with respect to the corresponding increased data rate R_j as compared to the Z_i channel, $i=1,2$, $j=1,2$, $i \neq j$. Generally, it can be concluded that the lower the data rate of one user is, the greater information-theoretic performance benefit to the other user can be achieved when more knowledge about the CSI of the crosstalk link is available. On the contrary, taking the achievable rate region for the IC with full knowledge of CSI for reference, the performance loss due to partial knowledge of CSI is also revealed from the information-theoretic point of view. Interestingly, it can be seen that partial knowledge of CSI causes only a little performance loss at some operating points of interest. From the engineering point of view, this interesting result reveals that at some operating points of interest a good system performance can be maintained considering appropriately selected significant CSI.

3.3 Multiple access channel - cooperation at receivers in the uplink

3.3.1 Equivalent channel for interference channel with cooperative receivers

As discussed above, the information-theoretic performance of the IC model corresponding to conventional cellular systems without multi-cell cooperation is severely limited by the multiuser interference. The cooperative communication concept is considered as a promising candidate for interference management. The cooperative reception in the UL is enabled by coordinated BSs which are connected by backhaul links. Taking a two-cell mobile radio cellular system as an example, the information-theoretic model for the cellular system with cooperative reception in the UL, i.e., the two-user IC with cooperative receivers, is shown in Figure 3.12.

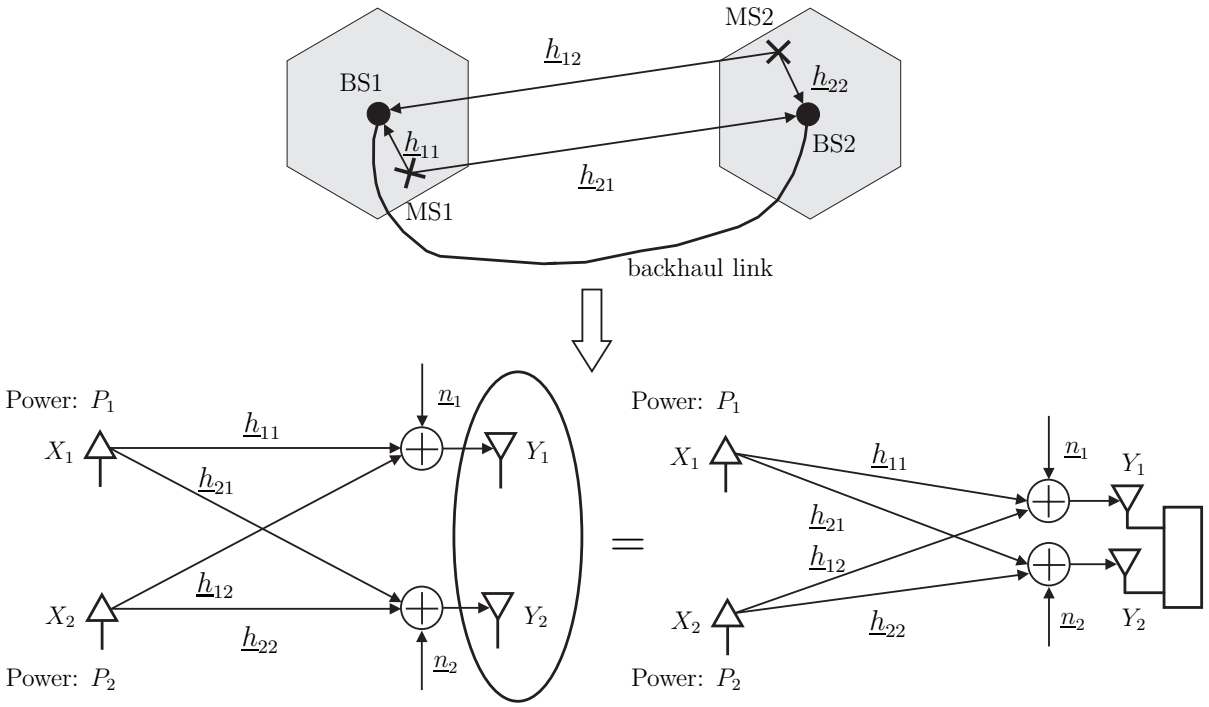

two-user IC with cooperative receivers MAC with two antennas at the common receiver

Figure 3.12. Two-cell mobile radio system with cooperative reception in the UL and its information-theoretic model: two-user IC with cooperative receivers or MAC with two antennas at the receiver.

The functionalities of the communication links in the two-user IC without cooperation and those in the two-user IC with cooperative receivers are compared as follows. In the two-user IC without cooperation, the message of every user is expected to be decoded at its corresponding receiver. The functionality of the direct link can only be the useful channel, while the functionality of the crosstalk link can only be the interfering channel. In the two-user IC with cooperative receivers, the messages of two users can be decoded through a joint signal processing at both receivers. Every direct link behaves not only as the useful channel for its corresponding user but also as the interfering channel for the other user. Every crosstalk link between transmitter i and receiver j behaves not only as the interfering channel for user j but also as the useful channel for user i, $i = 1, 2$, $j = 1, 2$, $i \neq j$. The signals carrying the same message are transmitted through two useful channels for every user. As compared to the IC without cooperative reception, the IC with cooperative receivers has a higher diversity gain.

Furthermore, from the information-theoretic point of view, the two-user IC with cooperative receivers is equivalent to the MAC with two antennas at the common receiver as shown in Figure 3.12. This equivalent channel reveals the fact that the cooperative reception makes it possible to exploit the multiple antennas at the receiver side of the IC. The application of multiple receiver antennas is often referred to as space division

multiple access (SDMA), which is a technique to increase the multiplexing gain. Since the MSs are geographically separated in two cells, distinctively different spatial signatures can be obtained with every spatial signature corresponding to a channel vector from an individual transmitter to the antenna array of both receivers. Therefore, a good condition of the channels for achieving the multiplexing gain is ensured.

In a word, the cooperative reception can increase the diversity gain and the multiplexing gain in the IC, and therefore it can enlarge the capacity region of the IC. Since the capacity region of the MAC is well understood, the capacity region of the IC with cooperative receivers is obtained straightforward.

3.3.2 Capacity region of the multiple access channel with full CSI

In this section, the capacity region of the MAC will be generally discussed. Especially, the capacity region of the MAC with two antennas at the common receiver, which is considered to be an equivalent channel for the two-user IC with cooperative receivers, is investigated in detail. In a general MAC, two or more transmitters send information to a common receiver. Taking a discrete memoryless two-user MAC consisting of three sets $\mathcal{X}_1$, $\mathcal{X}_2$ and $\mathcal{Y}$ as an example, the output variable $Y \in \mathcal{Y}$ is obtained from the two input variables $X_1 \in \mathcal{X}_1$ and $X_2 \in \mathcal{X}_2$ through the channel with conditional probabilities $\Pr\{y \mid x_1, x_2\}$. It is worth mentioning that if any transmitter or the receiver is equipped with multiple antennas, the corresponding input or output variable is a vector.

Theorem 3.8. [CT06] The capacity region of a two-user discrete memoryless MAC is the closure of the convex hull of all rate pairs (R_1, R_2) which satisfy

$$0 \leq R_1 \leq I(X_1; Y \mid X_2) \tag{3.56}$$

$$0 \leq R_2 \leq I(X_2; Y \mid X_1) \tag{3.57}$$

$$R_1 + R_2 \leq I(X_1, X_2\,; Y) \tag{3.58}$$

for some distribution of the probability $\Pr\{x_1\} \cdot \Pr\{x_2\}$ on $\mathcal{X}_1 \times \mathcal{X}_2$.

The performance gain due to the cooperative reception in the UL will be assessed in the following. As an equivalent channel for the two-user Gaussian IC with cooperative receivers, the capacity region of a two-user complex-valued Gaussian MAC with two antennas at the common receiver is investigated. In the two-user MAC as shown in Figure 3.12, let $\underline{x}_i \in \mathbb{C}$ denote the transmitted signals as input random variables X_i with individual average power constraints P_i, $i = 1, 2$. Let $\underline{y}_j \in \mathbb{C}$ denote the received

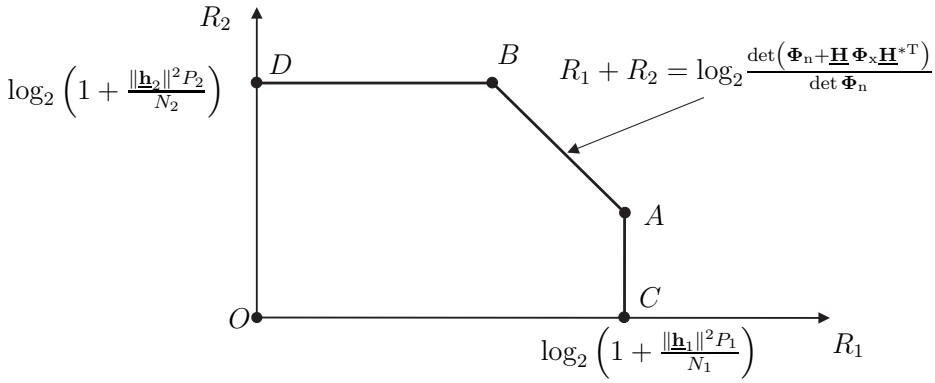

Figure 3.13. Capacity region of the two-user complex-valued Gaussian MAC, $N_1 = N_2$.

signals at individual receiver antennas as output random variables Y_j, $j=1,2$. With the channel vector $\underline{\mathbf{h}}_i = (\underline{h}_{1i}, \underline{h}_{2i})^\mathrm{T}$ corresponding to the channels between the transmitter i and the common receiver, the received vector can be obtained as

$$\underline{\mathbf{y}} = \left(\underline{y}_1, \underline{y}_2\right)^\mathrm{T} = \sum_{i=1}^{2} \underline{\mathbf{h}}_i\, \underline{x}_i + \underline{\mathbf{n}} \ . \tag{3.59}$$

The noise vector $\underline{\mathbf{n}} = (\underline{n}_1, \underline{n}_2)^\mathrm{T}$ consists of i.i.d. Gaussian noise signals $\underline{n}_1 \sim \mathcal{CN}(0, N_1)$ and $\underline{n}_2 \sim \mathcal{CN}(0, N_2)$ at the individual receiver antennas. For the Gaussian MAC, the convex hull operation in Theorem 3.8 is not required since it is sufficient to consider Gaussian inputs to achieve the capacity region [YRBC04, CV93, TV05]. Based on Theorem 3.8, the capacity region of the Gaussian MAC with a single receiver antenna and that of the Gaussian MAC with the same noise variance at different receiver antennas have been investigated in [CT06, TV05, GJJV03]. The results can be easily extended to the two-user complex-valued Gaussian MAC with individual noise variance at the two receiver antennas.

Theorem 3.9. The capacity region of a two-user complex-valued Gaussian MAC with two antennas at the receiver and a single antenna at each transmitter is the closure of all the rate pairs (R_1, R_2) satisfying:

$$0 \le R_1 \ \le \ \log_2\left(1 + P_1 \underline{\mathbf{h}}_1^{*\mathrm{T}} \mathbf{\Phi}_\mathrm{n}^{-1} \underline{\mathbf{h}}_1\right) \tag{3.60}$$

$$0 \le R_2 \ \le \ \log_2\left(1 + P_2 \underline{\mathbf{h}}_2^{*\mathrm{T}} \mathbf{\Phi}_\mathrm{n}^{-1} \underline{\mathbf{h}}_2\right) \tag{3.61}$$

$$R_1 + R_2 \ \le \ \log_2 \frac{\det\left(\mathbf{\Phi}_\mathrm{n} + \underline{\mathbf{H}}\,\mathbf{\Phi}_\mathrm{x} \underline{\mathbf{H}}^{*\mathrm{T}}\right)}{\det \mathbf{\Phi}_\mathrm{n}} \ . \tag{3.62}$$

In the above expressions, $\underline{\mathbf{H}} = (\underline{\mathbf{h}}_1, \underline{\mathbf{h}}_2)$ is the channel matrix of the system, $\mathbf{\Phi}_\mathrm{x} = \mathrm{diag}\{P_1, P_2\}$ is the covariance matrix of the input signals, and $\mathbf{\Phi}_\mathrm{n} = \mathrm{diag}\{N_1, N_2\}$ is the covariance matrix of the noise signals.

As shown in Figure 3.13, the capacity region of the investigated MAC is a pentagon with three constraints of (3.60), (3.61) and (3.62). Corresponding to (3.60) and (3.61),

at the operating points C and D the maximum rates for user 1 and for user 2 are obtained, respectively. The maximum rate for each user is calculated as the capacity of the point-to-point link between the transmitter of this user and the common receiver as if this user occupies the whole channel excluding the other user. This point-to-point link with a single antenna at each transmitter and two antennas at the common receiver is a SIMO channel. The single-user bound for each user i in its corresponding SIMO channel with Gaussian noise is achieved by receiver side maximum ratio combining which projects the received vector onto the corresponding channel vector $\underline{\mathbf{h}}_i$, $i = 1, 2$. However, in fact two users compete with each other in the MAC, and a tradeoff between the rates for the two users has to be made to perform data transmissions for two users at the same time. Therefore, the additional constraint of (3.62) is applied to limit the maximum sum-rate of the two users. The maximum sum-rate is calculated as the capacity of the point-to-point link occupied by one user, where the two transmitters are treated as one transmitter with two antennas, and the common receiver for two users is treated as the receiver for one user. Since there is no cooperation between the two transmitters in the MAC, a fixed power allocation with (P_1, P_2) for independent input signals at the two transmitter antennas is considered in the above point-to-point link for calculating the maximum sum-rate.

Considering the points on the line segments AC and BD, it is not necessary to keep the data rate for one user to be zero to achieve the maximum rate of the other user. In fact, corresponding to the point A or B, with one user transmitting at its maximum data rate, at the same time the data rate for the other user can increase to the value achieving the maximum sum-rate of two users. Taking the point A as an example, the sum-capacity-achieving rate pair (R_1, R_2) with

$$R_1 = \log_2\left(1 + P_1 \underline{\mathbf{h}}_1^{*\mathrm{T}} \mathbf{\Phi}_{\mathrm{n}}^{-1} \underline{\mathbf{h}}_1\right) \tag{3.63}$$

$$R_2 = \log_2\left(1 + P_2 \underline{\mathbf{h}}_2^{*\mathrm{T}} \left(\mathbf{\Phi}_{\mathrm{n}} + P_1 \underline{\mathbf{h}}_1 \underline{\mathbf{h}}_1^{*\mathrm{T}}\right)^{-1} \underline{\mathbf{h}}_2\right) \tag{3.64}$$

at this point is achieved by applying the MMSE-SIC receiver which is optimal from the information-theoretic point of view [TV05]. Firstly, user 2 is decoded by treating the interference from user 1 as Gaussian noise. More specifically, the Gaussian noise is a colored vector Gaussian noise since the interfering signals received at the two antennas of the common receiver from the same transmitter antenna through the SIMO channel are correlated. The decoding of user 2 suffers from the background Gaussian noise and the interfering signals from user 1. Applying the MMSE filter which is information lossless and optimal to make a compromise between maximizing SNR of the considered user and suppressing the interference from other users, the data rate for user 2 is obtained in (3.64). Once the data of user 2 is decoded, the signals from user 2 can be canceled from the received signals, and the decoding of user 1 only has to face

the background Gaussian noise. The corresponding data rate for user 1 is obtained in (3.63). Obviously, the decoding in the receiver is performed using a SIC mechanism with a MMSE filter, and hence the receiver is named as MMSE-SIC receiver. In fact, the chain rule of mutual information

$$I(X_1, X_2\,;\, Y) = I(X_2; Y) + I(X_1; Y \mid X_2) \tag{3.65}$$

is implemented at the point A to achieve the maximum sum-rate, i.e., sum-capacity in the MAC. Similarly, the sum-capacity-achieving rate pair at the point B is obtained by decoding user 1 firstly, and then the decoding of user 2 is based on the information of user 1. The rate pairs at the points on the line segment AB can be achieved by time-sharing between the decoding strategies at the operating points A and B.

In Figure 3.14, some numerical results about the capacity region of the two-user Gaussian MAC with two receiver antennas which is an equivalent channel for the two-user Gaussian IC with cooperative receivers are shown. In order to assess the performance gain due to cooperative reception as compared to no cooperation in the IC, the parameters of power constraints, noise variances, and channel gains in the corresponding MAC are assumed to be the same as in the original IC. Capacity regions of two such MACs, i.e., MAC_1 and MAC_2, which have the same channel gains but different channel coefficients are also compared. It can be seen that significant information-theoretic performance gains due to cooperative reception can be obtained when comparing the capacity regions of the MACs with the Han-Kobayashi achievable rate region for the IC. An interesting result is that the capacity region of the MAC depends on both the magnitudes and the arguments of the channel coefficients. However, the Han-Kobayashi achievable rate region for the IC only depends on the channel gains. Comparing MAC_1 and MAC_2 with the same channel gains but some different channel coefficients, their capacity regions are different. More specifically, the values of sum capacity in (3.62) for MAC_1 and MAC_2 are different.

The above discussion about the two-user MAC can be naturally extended to the K-user MAC. The capacity region of a K-user complex-valued Gaussian MAC with a single antenna at each transmitter and K antennas at the common receiver is a K dimensional polyhedron [TV05], i.e., the set of rates satisfying

$$\sum_{k\in\mathcal{S}} R_k \leq \log_2 \frac{\det\left(\mathbf{\Phi}_{\text{n}} + \underline{\mathbf{H}}\left(\sum_{k\in\mathcal{S}} \tilde{\mathbf{\Phi}}_x^{(k)}\right)\underline{\mathbf{H}}^{*\text{T}}\right)}{\det \mathbf{\Phi}_{\text{n}}} \quad \text{for } \mathcal{S} \subset \{1,\ldots,K\}, \tag{3.66}$$

where $\underline{\mathbf{H}} = (\underline{\mathbf{h}}_1, \ldots, \underline{\mathbf{h}}_K)$ is the channel matrix of the system, $\tilde{\mathbf{\Phi}}_x^{(k)} = \text{diag}\{0, \ldots, P_k, \ldots, 0\}$ is a diagonal matrix with only one non-zero element P_k in its (k,k)-th entry, and $\mathbf{\Phi}_{\text{n}} = \text{diag}\{N_1, \ldots, N_K\}$ is the covariance matrix of the noise vector. Exemplary numerical results of the capacity region of a three-user MAC are illustrated in Figure 3.15.

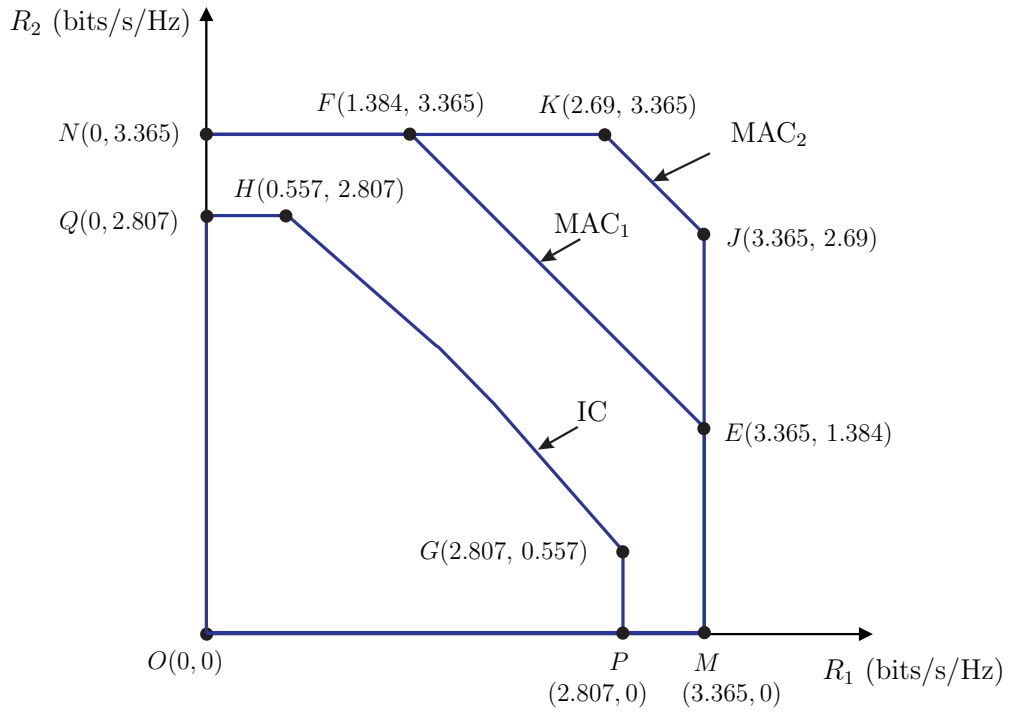

Figure 3.14. Capacity region of a two-user Gaussian MAC compared to the Han-Kobayashi achievable rate region for a two-user Gaussian IC. Common parameters: $P_1 = P_2 = 6$, $N_1 = N_2 = 1$, $a_{11} = a_{22} = 1$, $a_{12} = a_{21} = 0.55$, $h_{12} = h_{21} = \sqrt{0.55}$; Private parameters: $\underline{h}_{11} = \underline{h}_{22} = 1$ in MAC$_1$; $\underline{h}_{11} = \underline{h}_{22} = \frac{1}{\sqrt{2}}(1 + j)$ in MAC$_2$.

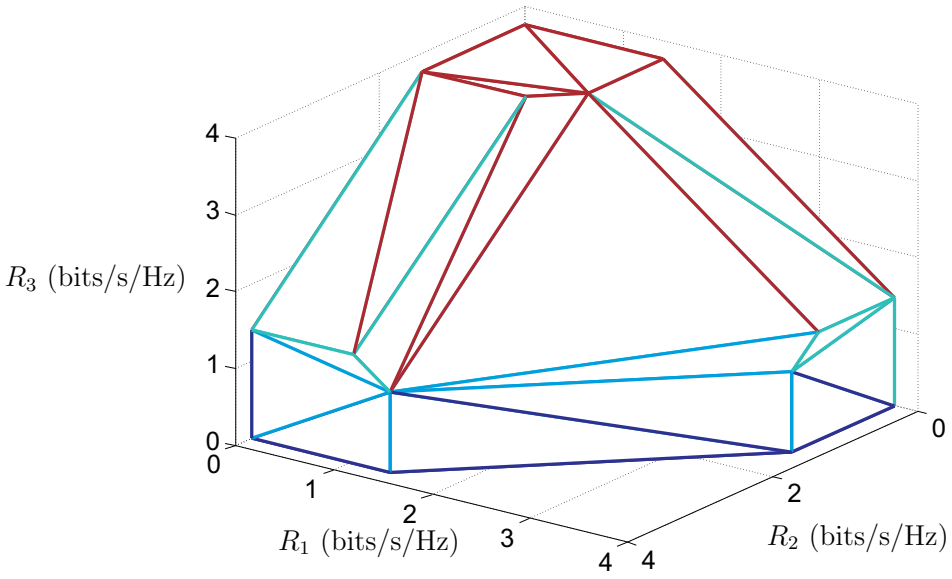

Figure 3.15. Capacity region of a three-user Gaussian MAC with $P_1 = P_2 = P_3 = 6$, $\underline{h}_{11} = \underline{h}_{22} = \underline{h}_{33} = 1$, $\underline{h}_{12} = \underline{h}_{21} = \underline{h}_{13} = \underline{h}_{31} = \underline{h}_{23} = \underline{h}_{32} = \sqrt{0.55}$, $N_1 = N_2 = N_3 = 1$.

3.3.3 Achievable rate region for the multiple access channel with partial CSI

Cooperative communication with partial CSI is the central topic of the present thesis. In the proposed UL cooperative reception scheme, simple transmitters requiring no CSI are applied in the MSs, while JD with the available knowledge of CSI is performed at the receivers in the coordinated BSs. On one side, the corresponding information-theoretic performance gain thanks to cooperative reception is investigated in the above section. On the other side, the impact of partial knowledge of CSI on the information-theoretic performance of the two-user Gaussian IC with cooperative receivers is investigated in the following. When full CSI is available, the two-user complex-valued Gaussian MAC with two antennas at the common receiver is considered as an equivalent channel for the two-user complex-valued Gaussian IC with cooperative receivers. As shown in Figure 3.13, the capacity region of the investigated MAC with full CSI is a pentagon which is basically constrained by the two corner points A and B. The chain rule for mutual information is implemented at the operating points A and B by applying the MMSE-SIC receiver. In case only partial knowledge of CSI is available, i.e., some channel coefficients are unknown, an achievable rate region for the MAC with partial CSI can be obtained by applying the same ideas as in the case of full CSI. Firstly, the rate pairs at the two corner points are obtained by utilizing the MMSE-SIC receiver which considers only partial knowledge of CSI. Then, the pentagon of the achievable rate region can be determined by the two corner points. No matter full CSI or partial CSI is considered, the intrinsic characteristics of the SIC strategy with the MMSE filter are unmodified. Assuming $\gamma_{\mathrm{F}}^{(k)}$ indicating the SINR of user k when user k is firstly decoded suffering the multiuser interference from the other user in the SIC strategy, and $\gamma_{\mathrm{S}}^{(k)}$ indicating the SINR of user k when user k is secondly decoded with the knowledge of the other decoded user in the SIC strategy, $k = 1, 2$, the data rates at the corner point A are

$$R_{1,A} = \log_2\left(1+\gamma_{\mathrm{S}}^{(1)}\right) \tag{3.67}$$

$$R_{2,A} = \log_2\left(1+\gamma_{\mathrm{F}}^{(2)}\right), \tag{3.68}$$

while the data rates at the corner point B are

$$R_{1,B} = \log_2\left(1+\gamma_{\mathrm{F}}^{(1)}\right) \tag{3.69}$$

$$R_{2,B} = \log_2\left(1+\gamma_{\mathrm{S}}^{(2)}\right). \tag{3.70}$$

However, since incomplete knowledge of CSI is considered in the MMSE-SIC receiver, the values of $\gamma_{\mathrm{F}}^{(k)}$ and $\gamma_{\mathrm{S}}^{(k)}$, $k = 1, 2$, could be reduced. Therefore, the information-theoretic performance degradation with respect to the reduced achievable rate region is inevitable.

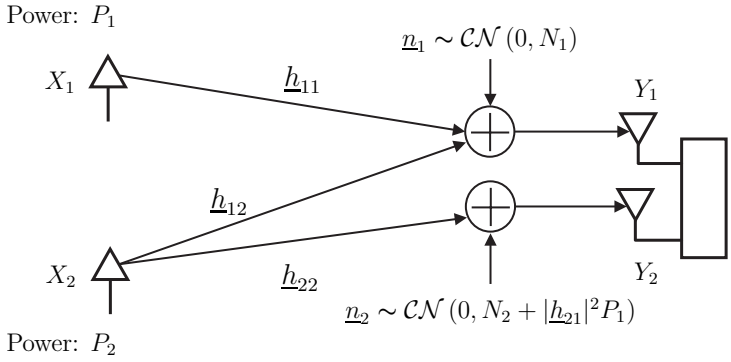

Figure 3.16. Simplified equivalent channel for the two-user Gaussian IC with cooperative receivers but without knowledge about $\underline{h}_{21}$, denoted as "Z_1-MAC".

Similar to the investigations on the two-user IC with no cooperation and with partial CSI in Section 3.2.5, the CSI of direct links is assumed to be fully known, while partial knowledge of CSI of the crosstalk links is considered in the two-user IC with cooperative receivers. The above assumptions correspond to the fact that in realistic cellular systems intracell CSI is easy to obtain while the intercell CSI is difficult to obtain. Without loss of generality, the IC with cooperative receivers but with no knowledge of $\underline{h}_{21}$ is treated as the representative channel to investigate the case where CSI of one crosstalk link is unknown. A question which naturally arises is what are the effects due to the lack of knowledge about $\underline{h}_{21}$. Firstly, the channel corresponding to $\underline{h}_{21}$ can not be considered as a useful channel for user 1 any more. Secondly, even for the case where user 1 has been decoded, the interfering signal from transmitter 1 at receiver 2 still can not be canceled in the decoding of user 2, and the remaining interference can be modeled as enhanced Gaussian noise. Last but not least, the third effect is that the correlation between the received signal components from transmitter 1 at the two receiver antennas can not be fully exploited. It is worth mentioning that the cooperative receivers in the IC corresponding to the common receiver with two antennas in the MAC make it possible to exploit the correlation between the signals from the same transmitter. However, in the IC without cooperative reception, no matter with full CSI or with partial CSI, the correlation between the signals at different receivers can not be exploited anyway, and therefore the third effect needs not to be considered. Due to the third effect, it is impractical to find a channel with full CSI as the exact equivalent channel for the two-user complex-valued Gaussian IC with cooperative receivers but without knowledge about $\underline{h}_{21}$. As a suboptimum solution, a two-user MAC in Figure 3.16 which can be described by (3.59) under the special conditions of a one-sided crosstalk link, i.e., $\underline{h}_{21}$=0, and with enhanced noise variance at one receiver antenna, i.e., $\underline{n}_2 \sim \mathcal{CN}(0, N_2 + |\underline{h}_{21}|^2 P_1)$, is considered as the simplified equivalent channel for the two-user IC with cooperative receivers but without knowledge about the $\underline{h}_{21}$. This channel is denoted as "Z_1-MAC".

The calculation of the SINR in a single-user SIMO channel applying a MMSE filter based on available knowledge of CSI is introduced now since it helps the calculation of data rates in the investigated MAC later on. In a single-user SIMO channel with the channel vector $\underline{\mathbf{h}}$ and the Gaussian distributed data symbol $\underline{x} \sim \mathcal{CN}(0, P)$, the received vector $\underline{\mathbf{y}}$ containing the received signals at the individual receiver antennas reads

$$\underline{\mathbf{y}} = \underline{\mathbf{h}}\,\underline{x} + \underline{\mathbf{z}}, \tag{3.71}$$

where the complex-valued colored Gaussian noise vector $\underline{\mathbf{z}}$ with zero-mean and the nonsingular covariance matrix $\underline{\mathbf{K}}_{\mathrm{z}}$ results from correlated noise signals with i.i.d. real and imaginary parts. Considering the SIMO channel, a matched filtering (MF) receiver dealing with the colored Gaussian noise is required to maximize the SNR. However, this receiver is often named the linear MMSE filter since it minimizes the mean square error in estimating $\underline{x}$ as shown in [TV05]. Considering the original MAC, in fact the colored noise at each receiver antenna consists of interference and noise, and the linear MMSE filter described by

$$\underline{\mathbf{c}}_{\mathrm{MMSE}} = \underline{\mathbf{K}}_{\mathrm{z}}^{-1}\underline{\mathbf{h}} \tag{3.72}$$

with full knowledge of CSI maximizes the SINR and achieves the information-theoretic optimality [TV05]. Generally, the linear MMSE filter with available CSI in the form of the estimated noise covariance matrix $\underline{\hat{\mathbf{K}}}_{\mathrm{z}}$ and the estimated channel vector $\underline{\hat{\mathbf{h}}}$ can be written as

$$\underline{\mathbf{c}} = \underline{\hat{\mathbf{K}}}_{\mathrm{z}}^{-1}\underline{\hat{\mathbf{h}}}. \tag{3.73}$$

Based on the estimated data symbol

$$\underline{\hat{x}} = \underline{\mathbf{c}}^{*\mathrm{T}}\underline{\mathbf{y}} = \underline{\mathbf{c}}^{*\mathrm{T}}\underline{\mathbf{h}}\,\underline{x} + \underline{\mathbf{c}}^{*\mathrm{T}}\underline{\mathbf{z}}, \tag{3.74}$$

the SINR can be obtained as

$$\gamma_{\mathrm{SIMO}} = \frac{P|\underline{\mathbf{c}}^{*\mathrm{T}}\underline{\mathbf{h}}|^2}{\underline{\mathbf{c}}^{*\mathrm{T}}\underline{\mathbf{K}}_{\mathrm{z}}\underline{\mathbf{c}}} = \frac{P\left|\left(\underline{\hat{\mathbf{K}}}_{\mathrm{z}}^{-1}\underline{\hat{\mathbf{h}}}\right)^{*\mathrm{T}}\underline{\mathbf{h}}\right|^2}{\left(\underline{\hat{\mathbf{K}}}_{\mathrm{z}}^{-1}\underline{\hat{\mathbf{h}}}\right)^{*\mathrm{T}}\underline{\mathbf{K}}_{\mathrm{z}}\left(\underline{\hat{\mathbf{K}}}_{\mathrm{z}}^{-1}\underline{\hat{\mathbf{h}}}\right)}\ . \tag{3.75}$$

Let us come back to the calculation of the rate pairs $(R_{1,A}, R_{2,A})$ and $(R_{1,B}, R_{2,B})$ at the corner points A and B in the pentagonal achievable rate region for the investigated MAC with two receiver antennas but without knowledge about $\underline{h}_{21}$. As indicated in (3.67)–(3.70), the SINR pairs $(\gamma_{\mathrm{S}}^{(1)}, \gamma_{\mathrm{F}}^{(2)})$ and $(\gamma_{\mathrm{F}}^{(1)}, \gamma_{\mathrm{S}}^{(2)})$ are required for the calculations of the rate pairs $(R_{1,A}, R_{2,A})$ and $(R_{1,B}, R_{2,B})$, respectively. At the operating points A and B, a SIC strategy with a MMSE filter is applied in the receiver. $\gamma_{\mathrm{F}}^{(k)}$ for user k, k=1, 2, can be calculated in the single-user SIMO channel between transmitter k and the common receiver with two antennas considering the interfering signals from the other transmitter plus the background Gaussian noise as the colored Gaussian noise. $\gamma_{\mathrm{S}}^{(k)}$ for user k, k=1, 2, can be calculated in the single-user SIMO channel between transmitter k

Table 3.1. Parameters of (3.75) for $\gamma_{\mathrm{S}}^{(1)}$ and $\gamma_{\mathrm{F}}^{(2)}$ at the operating point A.

parameters	$\gamma_{\mathrm{S}}^{(1)}$	$\gamma_{\mathrm{F}}^{(2)}$
$\underline{\mathbf{h}}$	$\hat{\underline{\mathbf{h}}}_1 = \begin{pmatrix} \underline{h}_{11} \\ 0 \end{pmatrix}$	$\underline{\mathbf{h}}_2 = \begin{pmatrix} \underline{h}_{12} \\ \underline{h}_{22} \end{pmatrix}$
$\underline{\mathbf{K}}_{\mathrm{z}}$	$\begin{pmatrix} N_1 & 0 \\ 0 & N_2 + P_1\lvert\underline{h}_{21}\rvert^2 \end{pmatrix}$	$\begin{pmatrix} N_1 & 0 \\ 0 & N_2 \end{pmatrix} + P_1\underline{\mathbf{h}}_1\underline{\mathbf{h}}_1^{*\mathrm{T}}$
$\hat{\underline{\mathbf{h}}}$	$\hat{\underline{\mathbf{h}}}_1 = \begin{pmatrix} \underline{h}_{11} \\ 0 \end{pmatrix}$	$\hat{\underline{\mathbf{h}}}_2 = \begin{pmatrix} \underline{h}_{12} \\ \underline{h}_{22} \end{pmatrix}$
$\hat{\underline{\mathbf{K}}}_{\mathrm{z}}$	$\begin{pmatrix} N_1 & 0 \\ 0 & N_2 + P_1\lvert\underline{h}_{21}\rvert^2 \end{pmatrix}$	$\begin{pmatrix} N_1 & 0 \\ 0 & N_2 + P_1\lvert\underline{h}_{21}\rvert^2 \end{pmatrix} + P_1\hat{\underline{\mathbf{h}}}_1\hat{\underline{\mathbf{h}}}_1^{*\mathrm{T}}$

Table 3.2. Parameters of (3.75) for $\gamma_{\mathrm{F}}^{(1)}$ and $\gamma_{\mathrm{S}}^{(2)}$ at the operating point B.

parameters	$\gamma_{\mathrm{F}}^{(1)}$	$\gamma_{\mathrm{S}}^{(2)}$
$\underline{\mathbf{h}}$	$\underline{\mathbf{h}}_1 = \begin{pmatrix} \underline{h}_{11} \\ \underline{h}_{21} \end{pmatrix}$	$\underline{\mathbf{h}}_2 = \begin{pmatrix} \underline{h}_{12} \\ \underline{h}_{22} \end{pmatrix}$
$\underline{\mathbf{K}}_{\mathrm{z}}$	$\begin{pmatrix} N_1 & 0 \\ 0 & N_2 \end{pmatrix} + P_2\underline{\mathbf{h}}_2\underline{\mathbf{h}}_2^{*\mathrm{T}}$	$\begin{pmatrix} N_1 & 0 \\ 0 & N_2 + P_1\lvert\underline{h}_{21}\rvert^2 \end{pmatrix}$
$\hat{\underline{\mathbf{h}}}$	$\hat{\underline{\mathbf{h}}}_1 = \begin{pmatrix} \underline{h}_{11} \\ 0 \end{pmatrix}$	$\hat{\underline{\mathbf{h}}}_2 = \begin{pmatrix} \underline{h}_{12} \\ \underline{h}_{22} \end{pmatrix}$
$\hat{\underline{\mathbf{K}}}_{\mathrm{z}}$	$\begin{pmatrix} N_1 & 0 \\ 0 & N_2 + P_1\lvert\underline{h}_{21}\rvert^2 \end{pmatrix} + P_2\hat{\underline{\mathbf{h}}}_2\hat{\underline{\mathbf{h}}}_2^{*\mathrm{T}}$	$\begin{pmatrix} N_1 & 0 \\ 0 & N_2 + P_1\lvert\underline{h}_{21}\rvert^2 \end{pmatrix}$

and the common receiver with two antennas considering the background Gaussian noise under the assumption that the other user has been decoded. Without loss of generality, $\gamma_{\mathrm{F}}^{(k)}$ and $\gamma_{\mathrm{S}}^{(k)}$, k=1, 2, can be calculated using the same equation of (3.75) with different parameters based on the available knowledge of CSI. The parameters in the equation of (3.75) to calculate the SINR pairs $(\gamma_{\mathrm{S}}^{(1)}, \gamma_{\mathrm{F}}^{(2)})$ and $(\gamma_{\mathrm{F}}^{(1)}, \gamma_{\mathrm{S}}^{(2)})$ at the operating points A and B for the investigated MAC without knowledge of $\underline{h}_{21}$ are listed in Table 3.1 and Table 3.2, respectively. These parameters are obtained based on the comparison between the exact effects due to the lack of knowledge about $\underline{h}_{21}$ and the effects due to the simplified equivalent channel Z_1-MAC in use. For the calculation of $\gamma_{\mathrm{S}}^{(1)}$ and $\gamma_{\mathrm{S}}^{(2)}$, the simplified equivalent channel Z_1-MAC is sufficient to describe the effects of the lack of knowledge about $\underline{h}_{21}$, i.e., the channel corresponding to $\underline{h}_{21}$ is not a useful channel for user 1 any more and the signal through this channel is treated as enhanced

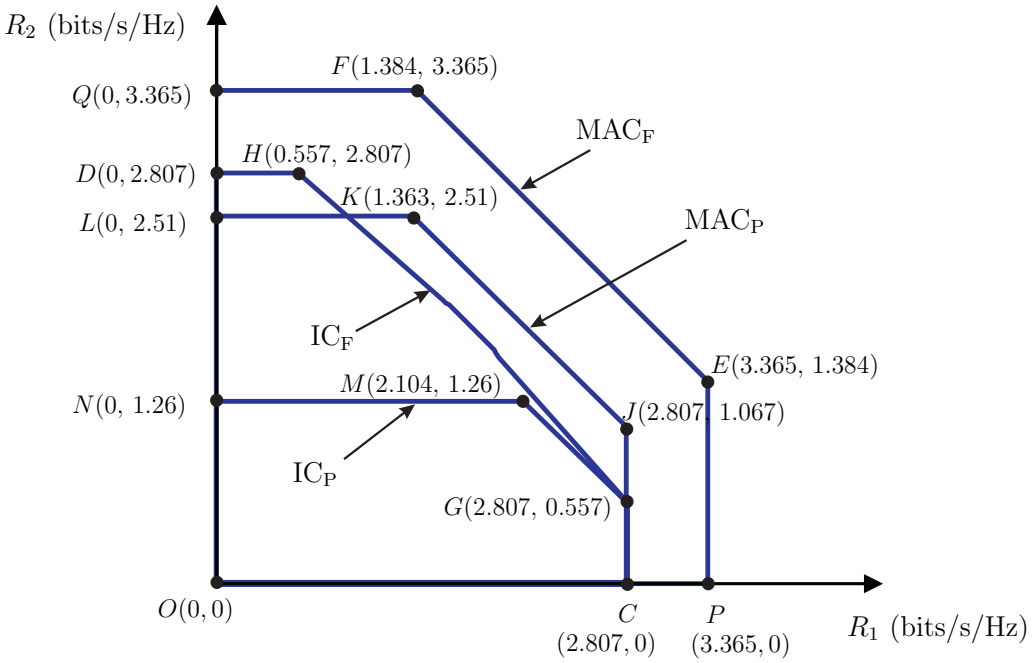

Figure 3.17. Achievable rate region for the two-user Gaussian IC with or without cooperative conception based on full CSI or partial CSI without knowledge about $\underline{h}_{21}$. Parameters: $P_1 = P_2 = 6$, $N_1 = N_2 = 1$, $\underline{h}_{11} = \underline{h}_{22} = 1$, $\underline{h}_{12} = \underline{h}_{21} = \sqrt{0.55}$.

noise at receiver antenna 2. Therefore, $\hat{\underline{\mathbf{h}}} = \underline{\mathbf{h}}$ and $\hat{\underline{\mathbf{K}}}_{\mathrm{z}} = \underline{\mathbf{K}}_{\mathrm{z}}$ are applied in the linear MMSE filter. However, for the calculation of $\gamma_{\mathrm{F}}^{(1)}$ and $\gamma_{\mathrm{F}}^{(2)}$, the simplified equivalent channel Z_1-MAC is not the exact equivalent channel for the investigated MAC missing the knowledge about $\underline{h}_{21}$. The reason is that the Z_1-MAC is not sufficient to describe the effect related to the incomplete exploitation of the correlation between the received signal components from transmitter 1 at the two receiver antennas due to the lack of knowledge about $\underline{h}_{21}$. Therefore, for the calculations of $\gamma_{\mathrm{F}}^{(1)}$ and $\gamma_{\mathrm{F}}^{(2)}$ the SIMO channel with $\underline{\mathbf{h}}$ and $\underline{\mathbf{K}}_{\mathrm{z}}$ based on the exact CSI of the investigated MAC and the linear MMSE filter with $\hat{\underline{\mathbf{h}}}_1 \neq \underline{\mathbf{h}}_1$ and $\hat{\underline{\mathbf{K}}}_{\mathrm{z}} \neq \underline{\mathbf{K}}_{\mathrm{z}}$ based on the CSI of the simplified equivalent channel Z_1-MAC are considered.

Based on the calculation results for $\gamma_{\mathrm{F}}^{(k)}$ and $\gamma_{\mathrm{S}}^{(k)}$, k=1, 2, the rate pairs $(R_{1,A}, R_{2,A})$, $(R_{1,B}, R_{2,B})$ of (3.67)–(3.70) and hence the achievable rate region for the IC with cooperative receivers but without knowledge about $\underline{h}_{21}$ can be easily obtained. Some numerical results on the information-theoretic performance of the two-user Gaussian IC with or without cooperative reception based on different levels of knowledge of CSI are shown in Figure 3.17. The Han-Kobayashi achievable rate region for the IC denoted as "$\mathrm{IC_F}$" without cooperative reception and with full knowledge of CSI, the Han-Kobayashi achievable rate region for the IC denoted as "$\mathrm{IC_P}$" without cooperative reception and without knowledge about $\underline{h}_{21}$, the capacity region of the IC denoted as "$\mathrm{MAC_F}$" with cooperative receivers and with full knowledge of CSI, and the achiev-

able rate region for the IC denoted as "$\mathrm{MAC_P}$" with cooperative receivers but without knowledge about $\underline{h}_{21}$ are compared. Referring to the achievable rate region for the $\mathrm{IC_P}$, both cooperative reception and more knowledge of CSI can improve its information-theoretic performance. Comparing the achievable rate region for the $\mathrm{IC_P}$ to that for the $\mathrm{IC_F}$, the lack of knowledge of CSI about a certain channel can cause a significant performance loss for the corresponding user. For example, the lack of knowledge about $\underline{h}_{21}$ can significantly reduce the rate region concerning R_2. Comparing the achievable rate region for the $\mathrm{MAC_P}$ to that for the $\mathrm{MAC_F}$, partial knowledge of CSI causes performance loss in the IC with cooperative reception as well. However, with the help of cooperative reception, no knowledge of $\underline{h}_{21}$ results in only a moderate degradation of the rate region concerning R_2. The reason is that cooperation between two users exploits all the channels for both users. A tradeoff between the performances of two users is made implicitly. Most importantly, cooperative reception can greatly improve the system performance even if only partial knowledge of CSI is available as can be seen when comparing the achievable rate region for the $\mathrm{MAC_P}$ to that for the $\mathrm{IC_P}$.

It is worth noting that the above achievable rate region in the case of partial CSI is obtained considering no knowledge about $\underline{h}_{21}$ at all. Therefore, enhanced noise variance and $\underline{h}_{21} = 0$ are assumed in the simplified equivalent channel. However, in realistic scenarios, the achievable rate region can be enlarged by exploiting the statistical knowledge the channel coefficient whose exact instantaneous value is unknown.

3.4 Broadcast channel - cooperation at transmitters in the downlink

3.4.1 Equivalent channel for interference channel with cooperative transmitters

In the concept of cooperative communication in cellular networks, in addition to the cooperative reception in the UL as discussed above, the cooperative transmission in the DL is investigated in this section with respect to its information-theoretic performance. Similar to the case in the UL, a two-cell mobile radio cellular system is taken as the exemplary scenario. Its information-theoretic model in the DL with cooperative transmission, i.e., the two-user complex-valued Gaussian IC with cooperative transmitters, and an equivalent channel for this IC, i.e., the two-user complex-valued Gaussian BC with two antennas at the common transmitter, are shown in Figure 3.18. Considering the reciprocity of the mobile radio channels in the investigated TDD systems, every

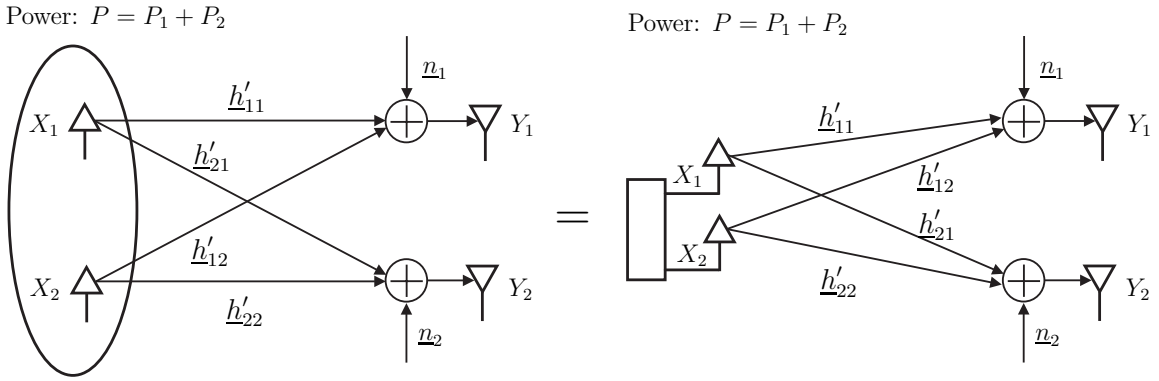

two-user IC with cooperative transmitters BC with two antennas at the common transmitter

Figure 3.18. The information-theoretic model for two-cell mobile radio cellular system applying cooperative transmission in the DL: two-user IC with cooperative transmitters or BC with two antennas at the common transmitter.

channel has the same channel coefficient in the UL and in the DL. Therefore, the relationship between the DL channel matrix $\underline{\mathbf{H}}_{\mathrm{DL}}$ of the IC which is equivalent to the channel matrix $\underline{\mathbf{H}}_{\mathrm{BC}}$ of the BC in Figure 3.18 and the UL channel matrix $\underline{\mathbf{H}}_{\mathrm{UL}}$ of the IC which is equivalent to the channel matrix $\underline{\mathbf{H}}_{\mathrm{MAC}}$ of the MAC in Figure 3.12 is

$$\underline{\mathbf{H}}_{\mathrm{UL}} = \underline{\mathbf{H}}_{\mathrm{MAC}} = \underline{\mathbf{H}}_{\mathrm{DL}}^{\mathrm{T}} = \underline{\mathbf{H}}_{\mathrm{BC}}^{\mathrm{T}} = \underline{\mathbf{H}} = \begin{pmatrix} \underline{h}_{11} & \underline{h}_{12} \\ \underline{h}_{21} & \underline{h}_{22} \end{pmatrix} = \begin{pmatrix} \underline{h}'_{11} & \underline{h}'_{21} \\ \underline{h}'_{12} & \underline{h}'_{22} \end{pmatrix}. \tag{3.76}$$

It is assumed that the noise variances at the two receivers in the BC in Figure 3.18 are equivalent to the noise variances at the two receivers in the MAC in Figure 3.12. The sum power constraint P of the transmitted signals in the BC is equal to the sum of the individual power constraints P_1 and P_2 of the transmitted signals in the MAC. Based on the above assumptions, the information-theoretic duality between the investigated MAC and the investigated BC, i.e., the equivalent channels for the IC with cooperative receivers and for the IC with cooperative transmitters, respectively, will be established.

3.4.2 Capacity region of the broadcast channel with full CSI

In a general BC, the common transmitter sends information to two or more receivers. The capacity region of the physically degraded BC was fully characterized many years ago [Cov72]. In recent years, the strategy of dirty-paper coding (DPC) which was originally proposed in [Cos83] has been found to be a very promising approach in the Gaussian MIMO BC, i.e., the vector Gaussian BC [CS03,VJG03,YC04,JVG04,WSS06]. It has been found that DPC achieves the sum-capacity [VJG03, YC04] and helps to establish the information-theoretic MAC-BC duality [VJG03,JVG04]. Recent work has shown that DPC also achieves the capacity region of the vector Gaussian BC [WSS06].

In this section, firstly the capacity region of the physically degraded BC will be briefly introduced, and the strategy to achieve the capacity region of a scalar Gaussian BC as an exemplary degraded BC will be illustrated. Then, the achievable rate region for the vector Gaussian BC with two antennas at the common transmitter and a single antenna at each receiver which is an equivalent channel for the two-user IC with cooperative transmitters will be investigated in detail.

Considering a discrete memoryless two-user BC consisting of an input set $\mathcal{X}$ and two output sets $\mathcal{Y}_1$ and $\mathcal{Y}_2$, the output variables $Y_1 \in \mathcal{Y}_1$ and $Y_2 \in \mathcal{Y}_2$ are obtained from the input variable $X \in \mathcal{X}$ through the channel with conditional probabilities $\Pr(y_1, y_2 \mid x)$. It is worth mentioning that if any receiver or the transmitter is equipped with multiple antennas, the corresponding input or output variable is a vector. Without loss of generality, a two-user BC is said to be physically degraded if [CT06]

$$\Pr\{y_1, y_2 \,|\, x\} = \Pr\{y_1 \,|\, x\} \cdot \Pr\{y_2 \mid y_1\}. \tag{3.77}$$

Theorem 3.10. [CT06] The capacity region of a two-user physically degraded BC with $X \to Y_1 \to Y_2$ is the convex hull of the closure of all rate pairs (R_1, R_2) which satisfy

$$\begin{aligned} 0 \;&\leq\; R_2 \leq I(U; Y_2) && (3.78)\\ 0 \;&\leq\; R_1 \leq I(X; Y_1 \mid U) && (3.79) \end{aligned}$$

for some distribution of the probability $\Pr\{u\} \cdot \Pr\{x \mid u\} \cdot \Pr\{y_1, y_2 \mid x\}$, where the cardinality of the auxiliary random variable U is bounded by $|\mathcal{U}| \leq \min\{|\mathcal{X}|, |\mathcal{Y}_1|, |\mathcal{Y}_2|\}$.

An exemplary degraded BC is the two-user scalar Gaussian BC with a single transmitter antenna and a single antenna per receiver. The received signals read

$$\underline{y}_k = \underline{h}_k \underline{x} + \underline{n}_k, \quad k = 1, 2, \tag{3.80}$$

with the transmitted signal x considering the average power constraint P, the channel coefficients $\underline{h}_k$, and the noise signals $\underline{n}_k \sim \mathcal{CN}(0, N_0)$, $k = 1, 2$. Without loss of generality, it is assumed that user 2 has a stronger channel, i.e., $|\underline{h}_1| \leq |\underline{h}_2|$. The transmitted signal $\underline{x} = \underline{x}_1 + \underline{x}_2$ which is simply the superposition of independent Gaussian codewords $\underline{x}_1$ for user 1 and $\underline{x}_2$ for user 2 is applied. In receiver 1, user 1 is decoded by treating the signal from user 2 as Gaussian noise. If user 1 can be decoded at receiver 1, it can also be decoded at receiver 2 where user 1 has a larger or at least the same SNR as compared to that at receiver 1. Therefore, the SIC strategy can be applied in receiver 2. Namely, receiver 2 firstly decodes user 1 by treating the signal from user 2 as Gaussian noise, and then it decodes user 2 based on the received signal from which

the signal from user 1 can be subtracted with the knowledge of the decoded user 1. Applying the above strategy, the rate pair (R_1, R_2) with

$$R_1 = \log_2\left(1 + \frac{P_1|\underline{h}_1|^2}{P_2|\underline{h}_1|^2 + N_0}\right) \tag{3.81}$$

$$R_2 = \log_2\left(1 + \frac{P_2|\underline{h}_2|^2}{N_0}\right) \tag{3.82}$$

can be achieved with the power constraints P_1 for $\underline{x}_1$ and P_2 for $\underline{x}_2$. In this BC, the strategy of superposition coding with the rate pair (R_1, R_2) in the equations of (3.81) and (3.82) combined with the SIC decoding is found to be optimal from the information-theoretic point of view [TV05, Ber74]. The capacity region of the above two-user scalar Gaussian BC is obtained from all the rate pairs calculated from (3.81) and (3.82) over all possible power allocations with the sum power constraint $P = P_1 + P_2$ lying on its boundary. This information-theoretic optimal strategy in the two-user scalar BC can be easily extended to the more general multiuser scalar Gaussian BC, where the receiver of each user can decode and subtract the codewords of the users which have smaller channel gains than that of itself.

While the SIC decoding based on superposition coding is a receiver-centric strategy, DPC is considered as a very promising transmitter-centric strategy to achieve the capacity region of the scalar Gaussian BC [Cos83, CS00]. The principle of the DPC strategy in the two-user scalar Gaussian BC is as follows. Firstly, the transmitter chooses codewords for user 1. Then, the transmitter chooses codewords for user 2 with the noncausal knowledge of the codewords for user 1 and the knowledge of CSI. In other words, the interference for user 2 is noncausally known at the transmitter. According to [CS00, YC01], the data rate R_2 for user 2 in (3.82) which can be achieved is as high as the one if no interference exists by choosing codewords for user 2 which presubtract the interference for user 2 due to the codewords for user 1. However, since the codewords for user 2 are statistically independent of the codewords for user 1, user 1 can only be reliably decoded with the data rate of (3.81) where $\underline{x}_2$ appears as Gaussian noise for user 1. It is worth noting that although the users can be encoded in any order in the DPC strategy, only when users are encoded in the order of increasing channel gains, the DPC strategy achieves the capacity region of the scalar Gaussian BC.

Now let us have a look at the achievable rate region for the IC with cooperative transmitters based on the information-theoretic results of its equivalent channel, i.e., the BC with multiple transmitter antennas. However, the BC with multiple transmitter antennas in general does not belong to the class of degraded BCs whose capacity regions have been fully characterized. Fortunately, the DPC strategy applied in the scalar Gaussian BC can be easily extended to the vector Gaussian BC, i.e., Gaussian MIMO

BC with multiple users and multiple antennas, to obtain an achievable rate region named as the DPC rate region [YC01, YRBC04]. Most recently, it has been shown that the DPC rate region coincides with the capacity region of the vector Gaussian BC [WSS06]. Thanks to the duality between the DPC rate region for the MIMO BC and the capacity region of the MIMO MAC [VJG03], the DPC rate region for the Gaussian BC with two transmitter antennas as an equivalent channel for the two-user Gaussian IC with cooperative transmitters can be easily computed. In the following, the application of the information-theoretic duality to obtain the DPC rate region for the investigated BC in Figure 3.18 considering its dual MAC in Figure 3.12 is presented.

The information-theoretic duality between the investigated BC and the investigated MAC is established based on the physical duality between their channel matrices as indicated in (3.76). The channel vectors $\underline{\mathbf{h}}_i = (\underline{h}_{1i}, \underline{h}_{2i})^{\mathrm{T}}$ of the channels from the transmitter antenna array to the receivers i, i=1, 2, are included in the channel matrix $\underline{\mathbf{H}}^{\mathrm{T}} = (\underline{\mathbf{h}}_1, \underline{\mathbf{h}}_2)^{\mathrm{T}}$ of the BC. Meanwhile, the same channel vectors $\underline{\mathbf{h}}_i$ from transmitters i to the receiver antenna array are included in the channel matrix $\underline{\mathbf{H}} = (\underline{\mathbf{h}}_1, \underline{\mathbf{h}}_2)$ of the MAC. Additionally, in order to establish the information-theoretic duality between the BC and the MAC, the same noise covariance matrix $\mathbf{\Phi}_{\mathrm{n}} = \mathrm{diag}\{N_0, N_0\}$ is assumed at the receiver side in both the BC and the dual MAC. Furthermore, the same sum power constraint P is assumed in the BC and in the dual MAC. Namely, in the BC the covariance matrices $\underline{\mathbf{Q}}_i$ of the transmitted signals for users i, i=1, 2, satisfy the sum power constraint $\mathrm{Tr}(\underline{\mathbf{Q}}_1 + \underline{\mathbf{Q}}_2) \leq P$. In the MAC with a single antenna per transmitter, the covariance matrices of the transmitted signals for users i, i=1, 2, are degraded to the scalar power constraints P_i with the sum power constraint $P_1 + P_2 \leq P$. Applying the DPC strategy in the two-user Gaussian BC, any encoding order of the users is possible. Without loss of generality, the rate pair $(R_{1,\mathrm{BC}}, R_{2,\mathrm{BC}})$ with

$$R_{1,\mathrm{BC}} = \log_2 \left(1 + \left(N_0 + \underline{\mathbf{h}}_1^{*\mathrm{T}} \underline{\mathbf{Q}}_2 \underline{\mathbf{h}}_1 \right)^{-1} \underline{\mathbf{h}}_1^{*\mathrm{T}} \underline{\mathbf{Q}}_1 \underline{\mathbf{h}}_1 \right) \tag{3.83}$$

$$R_{2,\mathrm{BC}} = \log_2 \left(1 + N_0^{-1} \underline{\mathbf{h}}_2^{*\mathrm{T}} \underline{\mathbf{Q}}_2 \underline{\mathbf{h}}_2 \right) \tag{3.84}$$

can be achieved when user 1 is firstly encoded and then user 2 is encoded [YC01, VJG03]. If the order of users for encoding is exchanged, the corresponding rate pair can be obtained using (3.83) and (3.84) with indices 1 and 2 exchanged with each other everywhere. The DPC rate region $\mathcal{R}_{\mathrm{DPC}}(P, \underline{\mathbf{H}}^{\mathrm{T}})$ is obtained as the convex hull of the closure of all rate pairs $(R_{1,\mathrm{BC}}, R_{2,\mathrm{BC}})$ calculated from (3.83) and (3.84) over all possible positive semidefinite covariance matrices $\underline{\mathbf{Q}}_1$ and $\underline{\mathbf{Q}}_2$ constrained by $\mathrm{Tr}(\underline{\mathbf{Q}}_1 + \underline{\mathbf{Q}}_2) \leq P$ and over all possible encoding orders of the users. In the investigated two-user Gaussian MAC, the MMSE-SIC receiver is applied to achieve the sum-capacity of the MAC. Without loss of generality, the rate pair $(R_{1,\mathrm{MAC}}, R_{2,\mathrm{MAC}})$ with

$$R_{1,\mathrm{MAC}} = \log_2\left(1 + P_1 \underline{\mathbf{h}}_1^{*\mathrm{T}} \left(\mathbf{\Phi}_{\mathrm{n}} + P_2 \underline{\mathbf{h}}_2 \, \underline{\mathbf{h}}_2^{*\mathrm{T}}\right)^{-1} \underline{\mathbf{h}}_1\right) \tag{3.85}$$

$$R_{2,\mathrm{MAC}} = \log_2\left(1 + P_2 \underline{\mathbf{h}}_2^{*\mathrm{T}} \mathbf{\Phi}_{\mathrm{n}}^{-1} \underline{\mathbf{h}}_2\right) \tag{3.86}$$

can be achieved when the users are decoded in the order of user 1 first and user 2 second [YRBC04, VJG03]. The capacity region of the MAC $\mathcal{R}_{\mathrm{MAC}}(P_1, P_2, \underline{\mathbf{H}})$ can be obtained using Theorem 3.9 as a pentagon considering three constraints corresponding to the sum-capacity and the individual capacities for the two users. Let

$$\mathcal{R}_{\mathrm{MAC}}^{\mathrm{union}}(P, \underline{\mathbf{H}}) \triangleq \bigcup_{P_1+P_2 \leq P} \mathcal{R}_{\mathrm{MAC}}(P_1, P_2, \underline{\mathbf{H}}) \tag{3.87}$$

denote the capacity region of the MAC with a sum power constraint instead of individual user power constraints. Referring to [VJG03], the information-theoretic duality between the investigated BC and the investigated MAC is established as follows.

Theorem 3.11. With the same sum power constraint P, the DPC rate region for the BC is equivalent to the capacity region of the dual MAC, i.e.,

$$\mathcal{R}_{\mathrm{DPC}}(P, \underline{\mathbf{H}}^{\mathrm{T}}) = \mathcal{R}_{\mathrm{MAC}}^{\mathrm{union}}(P, \underline{\mathbf{H}}) \ . \tag{3.88}$$

Theorem 3.12. The capacity region of the dual MAC with individual power constraints P_1 and P_2 for two users is the intersection of the scaled DPC rate region for the BC, which can be mathematically described as

$$\mathcal{R}_{\mathrm{MAC}}(P_1, P_2, \underline{\mathbf{H}}) = \bigcap_{\beta_i > 0,\, i=1,2} \mathcal{R}_{\mathrm{DPC}}\left(\sum_{i=1}^{2} \frac{P_i}{\beta_i}, \left(\sqrt{\beta_1}\underline{\mathbf{h}}_1, \sqrt{\beta_2}\underline{\mathbf{h}}_2\right)^{\mathrm{T}}\right). \tag{3.89}$$

Proofs of the above theorems have been presented in [VJG03] in detail for the case where $N_0 = 1$. Furthermore, the proofs can be easily extended for the case where $N_0 > 0$. An important application of the information-theoretic duality is to compute the DPC rate region in a simple way. The optimal BC covariance matrices can be obtained through a transformation of the optimal MAC covariance matrices which can be easily obtained due to the convex structure of the MAC rate equations. Especially, the covariance matrices in the investigated two-user MAC are degraded to the scalar power constraints. The DPC rate region which is difficult to be directly computed can be obtained with the help of its dual MAC whose capacity region can be easily computed.

In the following, the analytical calculation will show that every point on the boundary of the DPC rate region for the investigated two-user BC is a corner point of the capacity region achieved by the MMSE-SIC receiver for the dual MAC. For each point

corresponding to the same rate pair achieved both in the BC and in the MAC, the information-theoretic duality is established provided that the order in which the users are encoded in the DPC strategy for the BC is opposite to the order in which the users are decoded in the MMSE-SIC receiver for the MAC. Without loss of generality, a decreasing order of the users for encoding is assumed in the BC, i.e., user 2 is firstly encoded and then user 1 is encoded. Hence, an increasing order of the users for decoding has to be assumed in the MAC, i.e., user 1 is firstly decoded and then user 2 is decoded. Correspondingly, the rate pair $(R_{1,\mathrm{BC}}, R_{2,\mathrm{BC}})$ on the boundary of the DPC rate region for the BC can be obtained using (3.83) and (3.84), and the rate pair $(R_{1,\mathrm{MAC}}, R_{2,\mathrm{MAC}})$ as a corner point of the capacity region of the MAC can be obtained using (3.85) and (3.86). With

$$\underline{\mathbf{A}}_1 = N_0 \quad , \qquad \underline{\mathbf{A}}_2 = N_0 + \underline{\mathbf{h}}_2^{*\mathrm{T}} \underline{\mathbf{Q}}_1 \underline{\mathbf{h}}_2 \quad , \tag{3.90}$$

$$\underline{\mathbf{B}}_1 = \mathbf{\Phi}_{\mathrm{n}} + P_2 \underline{\mathbf{h}}_2 \, \underline{\mathbf{h}}_2^{*\mathrm{T}} \quad , \qquad \text{and} \qquad \underline{\mathbf{B}}_2 = \mathbf{\Phi}_{\mathrm{n}} \quad , \tag{3.91}$$

the above data rate equations of (3.83)–(3.86) can be rewritten as:

$$R_{i,\mathrm{BC}} = \log_2 \det \left(\mathbf{I} + \underline{\mathbf{A}}_i^{-1} \underline{\mathbf{h}}_i^{*\mathrm{T}} \underline{\mathbf{Q}}_i \underline{\mathbf{h}}_i \right) \tag{3.92}$$

$$R_{i,\mathrm{MAC}} = \log_2 \det \left(\mathbf{I} + \underline{\mathbf{B}}_i^{-1} \underline{\mathbf{h}}_i^{*\mathrm{T}} P_i \underline{\mathbf{h}}_i \right) \quad . \tag{3.93}$$

As stated in [VJG03], in order to achieve the same rate pair in the BC and in the dual MAC, i.e., $R_{i,\mathrm{BC}}$ of (3.92) being equal to $R_{i,\mathrm{MAC}}$ of (3.93), the BC covariance matrix $\underline{\mathbf{Q}}_i$ for user i is obtained as a function of the power P_i for user i in the MAC as

$$\underline{\mathbf{Q}}_i = \underline{\mathbf{B}}_i^{-1/2} \, \underline{\mathbf{F}}_i \, \underline{\mathbf{G}}_i^{*\mathrm{T}} \, \underline{\mathbf{A}}_i^{1/2} \, P_i \, \underline{\mathbf{A}}_i^{1/2} \, \underline{\mathbf{G}}_i \, \underline{\mathbf{F}}_i^{*\mathrm{T}} \, \underline{\mathbf{B}}_i^{-1/2} \quad , \tag{3.94}$$

where $\underline{\mathbf{F}}_i$ and $\underline{\mathbf{G}}_i^{*\mathrm{T}}$ are obtained from the singular value decomposition (SVD) of $\underline{\mathbf{B}}_i^{-1/2} \underline{\mathbf{h}}_i \underline{\mathbf{A}}_i^{1/2}$ as $\underline{\mathbf{B}}_i^{-1/2} \underline{\mathbf{h}}_i \underline{\mathbf{A}}_i^{1/2} = \underline{\mathbf{F}}_i \underline{\mathbf{\Lambda}}_i \underline{\mathbf{G}}_i^{*\mathrm{T}}$ with a square and diagonal matrix $\underline{\mathbf{\Lambda}}_i$. It has been proven in [VJG03] that the covariance matrices obtained from (3.94) fulfill the sum power constraint $\sum_{i=1}^{2} \mathrm{Tr}(\underline{\mathbf{Q}}_i) \leq \sum_{i=1}^{2} P_i$. Similarly, the power P_i for user i in the MAC can be obtained as a function of the BC covariance matrix $\underline{\mathbf{Q}}_i$ for user i as

$$P_i = \underline{\mathbf{A}}_i^{-1/2} \, \underline{\mathbf{F}}_i \, \underline{\mathbf{G}}_i^{*\mathrm{T}} \, \underline{\mathbf{B}}_i^{1/2} \, \underline{\mathbf{Q}}_i \, \underline{\mathbf{B}}_i^{1/2} \, \underline{\mathbf{G}}_i \, \underline{\mathbf{F}}_i^{*\mathrm{T}} \, \underline{\mathbf{A}}_i^{-1/2} \quad , \tag{3.95}$$

where $\underline{\mathbf{F}}_i$ and $\underline{\mathbf{G}}_i^{*\mathrm{T}}$ are obtained from the SVD of $\underline{\mathbf{A}}_i^{-1/2} \underline{\mathbf{h}}_i \underline{\mathbf{B}}_i^{1/2}$ as $\underline{\mathbf{A}}_i^{-1/2} \underline{\mathbf{h}}_i \underline{\mathbf{B}}_i^{1/2} = \underline{\mathbf{F}}_i \underline{\mathbf{\Lambda}}_i \underline{\mathbf{G}}_i^{*\mathrm{T}}$ with a square and diagonal matrix $\underline{\mathbf{\Lambda}}_i$. The powers derived from (3.95) fulfill the sum power constraint $\sum_{i=1}^{2} P_i \leq \sum_{i=1}^{2} \mathrm{Tr}(\underline{\mathbf{Q}}_i)$. Therefore, the MAC powers P_1, P_2 and the BC covariance matrices $\underline{\mathbf{Q}}_1$, $\underline{\mathbf{Q}}_2$ with the same sum power constraint $\sum_{i=1}^{2} P_i = \sum_{i=1}^{2} \mathrm{Tr}(\underline{\mathbf{Q}}_i) \leq P$ which lead to the same rate pair can always be found.

In order to illustrate the application of the information-theoretic duality, some numerical results are shown in the following. In the investigated two-user Gaussian IC in

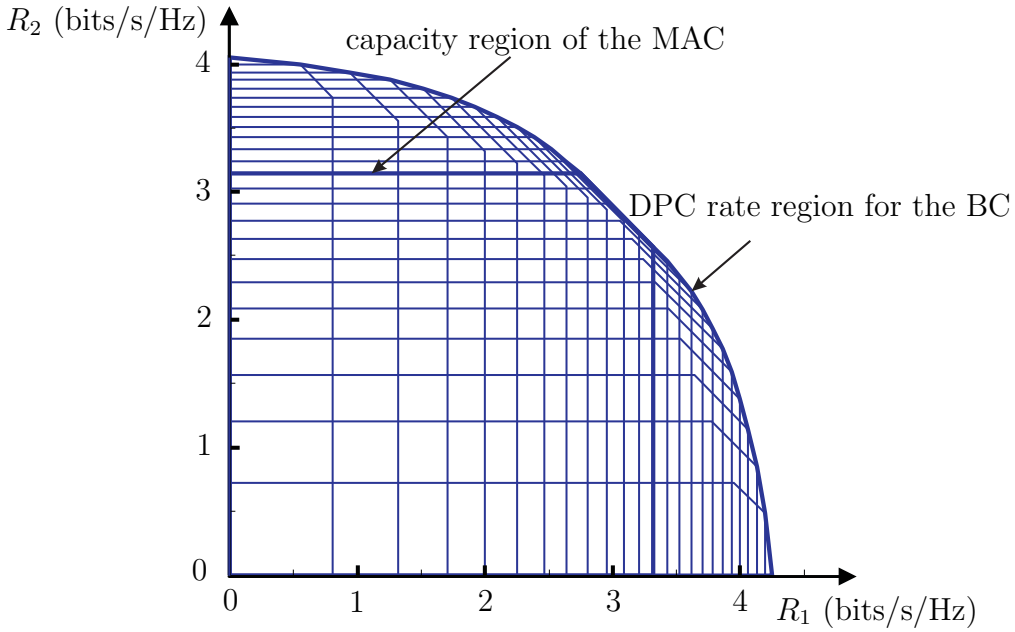

Figure 3.19. DPC rate region for the investigated two-user Gaussian BC obtained from the capacity region of its dual MAC. Parameters: $\underline{\mathbf{h}}_1 = (1, \frac{1}{\sqrt{2}}(0.5 + 0.5j))^{\mathrm{T}}$, $\underline{\mathbf{h}}_2 = (\frac{1}{\sqrt{2}}(0.3 + 0.3j), 1)^{\mathrm{T}}$, $P_1 + P_2 = P = 12$ and $N_0 = 1$.

Figure 3.12, the channel vectors $\underline{\mathbf{h}}_1 = (1, \frac{1}{\sqrt{2}}(0.5+0.5j))^{\mathrm{T}}$ and $\underline{\mathbf{h}}_2 = (\frac{1}{\sqrt{2}}(0.3+0.3j), 1)^{\mathrm{T}}$, power constraints $P_1 = 6$ and $P_2 = 6$, and noise variance $N_0 = 1$ are assumed. With cooperative transmission in the DL, the IC can be considered as the above investigated BC with two transmitter antennas. With cooperative reception in the UL, the IC can be considered as the above investigated MAC with two receiver antennas which is dual to the investigated BC. In order to achieve the same rate pair at the corner point of the capacity region of the MAC with power constraints $P_1 = 6$ and $P_2 = 6$, the corresponding optimal BC covariance matrices can be obtained from P_1 and P_2 following the equation of (3.94) as:

$$\underline{\mathbf{Q}}_1 = \begin{pmatrix} 4.4156 & -1.2273 + 1.9415j \\ -1.2273 - 1.9415j & 1.1948 \end{pmatrix} \tag{3.96}$$

$$\underline{\mathbf{Q}}_2 = \begin{pmatrix} 1.4745 & 1.9036 - 1.9036j \\ 1.9036 + 1.9036j & 4.9151 \end{pmatrix} . \tag{3.97}$$

Obviously, the sum power constraint $\mathrm{Tr}(\underline{\mathbf{Q}}_1)+\mathrm{Tr}(\underline{\mathbf{Q}}_2) = 12 = P_1+P_2$ is fulfilled. Figure 3.19 shows how the DPC rate region for the investigated two-user BC is obtained with the help of its dual MAC. Many pentagonal capacity regions of the MAC with different values of the individual user powers P_1 and P_2 satisfying the sum power constraint $P = P_1 + P_2 = 12$ are plotted. With the same sum power constraint $P = 12$, the DPC rate region for the two-user BC is obtained as a union of the pentagonal capacity regions of the dual MAC with all possible power allocations. In this way, the computational complexity to obtain the DPC rate region is significantly reduced.

3.4.3 Achievable rate region for the broadcast channel with partial CSI

In the above section, the information-theoretic duality between the BC as an equivalent channel for the two-user IC with cooperative transmitters and the MAC as an equivalent channel for the two-user IC with cooperative receivers is established. The DPC rate region as the capacity region of the BC can be computed with the help of its dual MAC. However, the duality is established based on the implicit assumption that full knowledge of CSI is available. In the case that partial knowledge of CSI is considered, the question whether the information-theoretic duality still exists is a problem which naturally arises. It has been shown that the MMSE filter is an information-theoretic optimal receiver in the MAC with the SIC strategy, and it can also be used as the optimal transmitter filter in the BC with the DPC strategy [TV05]. In this section, the information-theoretic duality between the BC applying the DPC strategy in the transmitter with the MMSE transmit signature $\underline{\mathbf{c}}_{k,\mathrm{BC}}$ for each user k and the MAC applying the SIC strategy in the receiver with the MMSE receive signature $\underline{\mathbf{c}}_{k,\mathrm{MAC}}$ for each user k, k=1, ..., K, is derived. The derivation of the information-theoretic duality in this section follows the same idea considered in the derivation of the duality between the BC and the MAC applying linear transmission and detection strategies in [TV05]. Without loss of generality, the derivation is not limited to the case of two users but is also suitable for the case of multiple users, i.e., $K \geq 2$. K antennas at the common transmitter and a single antenna at each receiver are considered in the BC, while K antennas at the common receiver and a single antenna at each transmitter are considered in the MAC. In general, different levels of knowledge of CSI can be considered in the transmit signatures $\underline{\mathbf{c}}_{k,\mathrm{BC}}$ and the receive signatures $\underline{\mathbf{c}}_{k,\mathrm{MAC}}$. When full perfect CSI is considered, the following derivation is just an alternative derivation of the information-theoretic duality presented in the above section. More interestingly, when partial knowledge of CSI is considered, the information-theoretic duality still exists when the effects of partial knowledge of CSI can be fully characterized by the suboptimum transmit signatures $\underline{\mathbf{c}}_{k,\mathrm{BC}}$ in the BC and the suboptimum receive signatures $\underline{\mathbf{c}}_{k,\mathrm{MAC}}$ in the MAC.

It is assumed that the same partial knowledge of CSI is considered in both the BC and the MAC which have dual physical channels as indicated in (3.76). Naturally, for each user k the suboptimum transmit signature $\underline{\mathbf{c}}_{k,\mathrm{BC}}$ of the MMSE filter in the BC which is equivalent to the suboptimum receive signature $\underline{\mathbf{c}}_{k,\mathrm{MAC}}$ of the MMSE filter in the MAC is applied as

$$\underline{\mathbf{c}}_k \triangleq \underline{\mathbf{c}}_{k,\mathrm{BC}} = \underline{\mathbf{c}}_{k,\mathrm{MAC}}. \tag{3.98}$$

In the Gaussian BC, the transmitted vector $\underline{\mathbf{x}}$ is obtained through the MMSE transmit filters with transmit signatures $\underline{\mathbf{c}}_k$ from data symbols $\tilde{x}_k$ with powers P'_k for individual

users k, $k=1,\ldots,K$, as

$$\underline{\mathbf{x}} = \sum_{k=1}^{K} \underline{\mathbf{c}}_k^* \tilde{\underline{x}}_k \ . \tag{3.99}$$

The normalized transmit signatures $\|\underline{\mathbf{c}}_k\|=1$ are considered to keep the powers P_k' for individual users k, $k=1,\ldots,K$, unmodified. Considering i.i.d. Gaussian noise signals $\underline{n}_k \sim \mathcal{CN}(0, N_0)$ at individual simple receivers k equipped with a single antenna, the received signal $\underline{y}_k$ for each user k is treated as this user's estimated data symbol

$$\hat{\underline{x}}_k = \underline{y}_k = \underline{\mathbf{h}}_k^{\mathrm{T}} \underline{\mathbf{c}}_k^* \tilde{\underline{x}}_k + \sum_{j<k} \underline{\mathbf{h}}_k^{\mathrm{T}} \underline{\mathbf{c}}_j^* \tilde{\underline{x}}_j + \sum_{j>k} \underline{\mathbf{h}}_k^{\mathrm{T}} \underline{\mathbf{c}}_j^* \tilde{\underline{x}}_j + \underline{n}_k \ . \tag{3.100}$$

Applying the DPC strategy, interference management is performed in the transmitter. Without loss of generality, a decreasing order of users for encoding is considered, i.e., the user k is encoded with full knowledge about the codewords of the users $k+1,\ldots,K$. With perfect knowledge of CSI, the interference $\sum_{j>k} \underline{\mathbf{h}}_k^{\mathrm{T}} \underline{\mathbf{c}}_j^* \tilde{\underline{x}}_j$ from users $k+1,\ldots,K$ can be canceled from $\underline{y}_k$ of (3.100). In the case that only partial knowledge of CSI is considered, it is assumed that the effects of partial knowledge of CSI can be fully characterized by the suboptimum transmit signatures $\underline{\mathbf{c}}_k$. In this way, the interference $\sum_{j>k} \underline{\mathbf{h}}_k^{\mathrm{T}} \underline{\mathbf{c}}_j^* \tilde{\underline{x}}_j$ is still treated as removable for user k, but the suboptimum transmit signatures with partial CSI will result in degraded SINRs and hence an information-theoretic performance degradation. The resulting SINR for each user k considering suboptimum transmit signatures reads

$$\gamma_{\mathrm{BC}}^{(k)} = \frac{P_k' |\underline{\mathbf{c}}_k^{*\mathrm{T}} \underline{\mathbf{h}}_k|^2}{N_0 + \sum_{j<k} P_j' |\underline{\mathbf{c}}_j^{*\mathrm{T}} \underline{\mathbf{h}}_k|^2} \ . \tag{3.101}$$

In the dual Gaussian MAC, from the transmitted signals $\underline{x}_k$ which are equivalent to the data symbols $\tilde{\underline{x}}_k$ with power constraints P_k for individual users k, the received vector is obtained as

$$\underline{\mathbf{y}} = \sum_{k=1}^{K} \underline{\mathbf{h}}_k \underline{x}_k + \underline{\mathbf{n}} = \sum_{k=1}^{K} \underline{\mathbf{h}}_k \tilde{\underline{x}}_k + \underline{\mathbf{n}} \ . \tag{3.102}$$

The noise vector $\underline{\mathbf{n}}$ consists of the noise signals $\underline{n}_k$ with the same statistical distributions as the noise signals in the BC. Applying the MMSE-SIC strategy in the MAC with the receive signatures $\underline{\mathbf{c}}_k$ which are equivalent to the transmit signatures in the BC, the interference management is performed in the receiver. In order to establish the information-theoretic duality, the order in which users are decoded is opposite to the order in which users are encoded in the BC. Namely, an increasing order of users for decoding is considered such that each user k is decoded with full knowledge about the transmitted signals of users $1,\ldots,k-1$. Therefore, the interference $\sum_{j<k} \underline{\mathbf{c}}_k^{*\mathrm{T}} \underline{\mathbf{h}}_j \underline{x}_j$ can be canceled from the following estimated data symbol for user k

$$\hat{\underline{x}}_k = \underline{\mathbf{c}}_k^{*\mathrm{T}} \underline{\mathbf{h}}_k \underline{x}_k + \sum_{j<k} \underline{\mathbf{c}}_k^{*\mathrm{T}} \underline{\mathbf{h}}_j \underline{x}_j + \sum_{j>k} \underline{\mathbf{c}}_k^{*\mathrm{T}} \underline{\mathbf{h}}_j \underline{x}_j + \underline{\mathbf{c}}_k^{*\mathrm{T}} \underline{\mathbf{n}} \ . \tag{3.103}$$

Similar to the case in the BC, the assumption that the effects of partial knowledge of CSI can be fully described by the suboptimum receive signatures $\underline{\mathbf{c}}_k$ is considered in the MAC. With the normalized receive signature $\|\underline{\mathbf{c}}_k\|$=1 for each user k, the resulting SINR for user k can be written as

$$\gamma_{\mathrm{MAC}}^{(k)} = \frac{P_k |\underline{\mathbf{c}}_k^{*\mathrm{T}} \underline{\mathbf{h}}_k|^2}{N_0 + \sum_{j>k} P_j |\underline{\mathbf{c}}_k^{*\mathrm{T}} \underline{\mathbf{h}}_j|^2} \ . \tag{3.104}$$

Introducing the vector $\mathbf{a} = (a_1, \ldots, a_K)^{\mathrm{T}}$ with

$$a_k = \frac{\gamma_{\mathrm{BC}}^{(k)}}{(1+\gamma_{\mathrm{BC}}^{(k)}) |\underline{\mathbf{c}}_k^{*\mathrm{T}} \underline{\mathbf{h}}_k|^2} \ , \tag{3.105}$$

the vector $\mathbf{b} = (b_1, \ldots, b_K)^{\mathrm{T}}$ with

$$b_k = \frac{\gamma_{\mathrm{MAC}}^{(k)}}{(1+\gamma_{\mathrm{MAC}}^{(k)}) |\underline{\mathbf{c}}_k^{*\mathrm{T}} \underline{\mathbf{h}}_k|^2} \ , \tag{3.106}$$

the vector $\mathbf{p}' = (P_1', \ldots, P_K')$ and the vector $\mathbf{p} = (P_1, \ldots, P_K)$, (3.101) and (3.104) can be rewritten in the matrix-vector notation as:

$$(\mathbf{I}_K - \mathrm{diag}\{a_1, \ldots, a_K\}\mathbf{A}\ )\,\mathbf{p}' = N_0 \mathbf{a} \tag{3.107}$$

$$\left(\mathbf{I}_K - \mathrm{diag}\{b_1, \ldots, b_K\}\mathbf{A}^{\mathrm{T}}\right)\mathbf{p} = N_0 \mathbf{b} \ . \tag{3.108}$$

In both (3.107) and (3.108), the same $K \times K$ lower triangular matrix $\mathbf{A}$ is considered with its (k,j)-th entry being equal to $|\underline{\mathbf{c}}_j^{*\mathrm{T}} \underline{\mathbf{h}}_k|^2$ if $j \leq k$ and equal to 0 if $j > k$. The information-theoretic duality between the BC and the MAC can be established if the BC and the MAC with the same sum power constraint can achieve the same rate sets, i.e., the same SINRs $\gamma_{\mathrm{BC}}^{(k)} = \gamma_{\mathrm{MAC}}^{(k)}$ for individual users k, k=1, ..., K. This statement can be seen by rewriting (3.107) and (3.108) as:

$$\mathbf{p}' = N_0 \left(\mathbf{I}_K - \mathrm{diag}\{a_1, \ldots, a_K\}\mathbf{A}\ \right)^{-1} \mathbf{a} = N_0 \left(\mathbf{D}_a - \mathbf{A}\ \right)^{-1} \mathbf{1}_K \tag{3.109}$$

$$\mathbf{p} = N_0 \left(\mathbf{I}_K - \mathrm{diag}\{b_1, \ldots, b_K\}\mathbf{A}^{\mathrm{T}}\right)^{-1} \mathbf{b} = N_0 \left(\mathbf{D}_b - \mathbf{A}^{\mathrm{T}}\right)^{-1} \mathbf{1}_K \ . \tag{3.110}$$

In the above expressions, $\mathbf{D}_a = \mathrm{diag}\{1/a_1, \ldots, 1/a_K\}$, $\mathbf{D}_b = \mathrm{diag}\{1/b_1, \ldots, 1/b_K\}$ and $\mathbf{1}_K$ indicating the vector with dimension K consisting of 1's are considered. Achieving the same SINRs in the BC and in the MAC, i.e., $\mathbf{a} = \mathbf{b}$, the relationship between the sum power constraint of the BC and that of the MAC is derived as

$$\begin{aligned} \sum_{k=1}^{K} P_k &= N_0 \mathbf{1}_K^{\mathrm{T}} \left(\mathbf{D}_a - \mathbf{A}\right)^{-1} \mathbf{1}_K = N_0 \mathbf{1}_K^{\mathrm{T}} \left[\left(\mathbf{D}_a - \mathbf{A}\right)^{-1}\right]^{\mathrm{T}} \mathbf{1}_K \\ &= N_0 \mathbf{1}_K^{\mathrm{T}} \left(\mathbf{D}_a - \mathbf{A}^{\mathrm{T}}\right)^{-1} \mathbf{1}_K = \sum_{k=1}^{K} P_k' \ . \end{aligned} \tag{3.111}$$

The above equation completes the derivation of the information-theoretic duality between the BC and the MAC with the same available knowledge of CSI. It is worth emphasizing that the above information-theoretic duality holds for the BC and the dual MAC under the assumption that the effects due to the partial knowledge of CSI can be fully characterized by the suboptimum transmit signatures and the suboptimum receive signatures considering partial CSI. However, this is not always the best choice to exactly assess the performance loss due to partial CSI. For example, in the case that there is no knowledge about a certain channel coefficient, the interference through the channel whose CSI is totally unknown can not be removed. In this case, the effect due to partial knowledge of CSI could be modeled by an enhanced noise variance in a simplified equivalent channel as described in Section 3.3.3 for the two-user Gaussian MAC.

Numerical results in Figure 3.20 show us how to obtain the achievable DPC rate region for the BC as an equivalent channel for the two-user Gaussian IC with cooperative transmitters where only partial knowledge of CSI is available. Considering the same sum power constraint and the same partial knowledge of CSI in both the investigated BC and its dual MAC, the DPC rate region for the BC can be obtained from the achievable rate regions for its dual MAC. The BC in Figure 3.18 with the same noise variance $N_1 = N_2 = N_0$ at different receivers is taken as the original investigated channel. The dual MAC for this BC is shown in Figure 3.12. Considering partial knowledge of CSI, the Z_1-MAC in Figure 3.16 is taken as an example of the estimated channel for the dual MAC. As mentioned in Section 3.3.3, the SINRs $\gamma_{\mathrm{F}}^{(k)}$ and $\gamma_{\mathrm{S}}^{(k)}$, k=1, 2, corresponding to the rate pairs at the corner points of the pentagonal achievable rate region for the MAC can be calculated following the equation of (3.75). The channel vector $\underline{\mathbf{h}}$ and the noise covariance matrix $\underline{\mathbf{K}}_{\mathrm{z}}$ in the SIMO channel for each user are obtained based on the dual MAC. The estimated channel vector $\hat{\underline{\mathbf{h}}}$ and the estimated noise covariance matrix $\hat{\underline{\mathbf{K}}}_{\mathrm{z}}$ are obtained based on the Z_1-MAC, and are considered in the suboptimum receive signature $\underline{\mathbf{c}} = \hat{\underline{\mathbf{K}}}_{\mathrm{z}}^{-1}\hat{\underline{\mathbf{h}}}$ for each user. These parameters $\underline{\mathbf{h}}$, $\underline{\mathbf{K}}_{\mathrm{z}}$, $\hat{\underline{\mathbf{h}}}$ and $\hat{\underline{\mathbf{K}}}_{\mathrm{z}}$ required in the calculation of $\gamma_{\mathrm{F}}^{(k)}$, $k = 1, 2$, when user k is firstly decoded in the SIC scheme can be directly found in Table 3.1 and Table 3.2. However, the calculation process of $\gamma_{\mathrm{S}}^{(k)}$, $k = 1, 2$, when user k is secondly decoded in the SIC scheme is not the same as in Section 3.3.3. In this section it is assumed that the effects due to partial knowledge of CSI can be fully characterized by the suboptimum receive signatures, and the available knowledge of CSI is sufficient to cancel the interference coming from the user which has been decoded. Correspondingly, the noise covariance matrix $\underline{\mathbf{K}}_{\mathrm{z}} = \mathrm{diag}\{N_0, N_0\}$ and the channel vector $\underline{\mathbf{h}} = (\underline{h}_{1k}, \underline{h}_{2k})^{\mathrm{T}}$ are considered in the SIMO channel for each user k, k=1, 2, while $\hat{\underline{\mathbf{h}}}$ and $\hat{\underline{\mathbf{K}}}_{\mathrm{z}}$ can be directly found in Table 3.1 and Table 3.2.

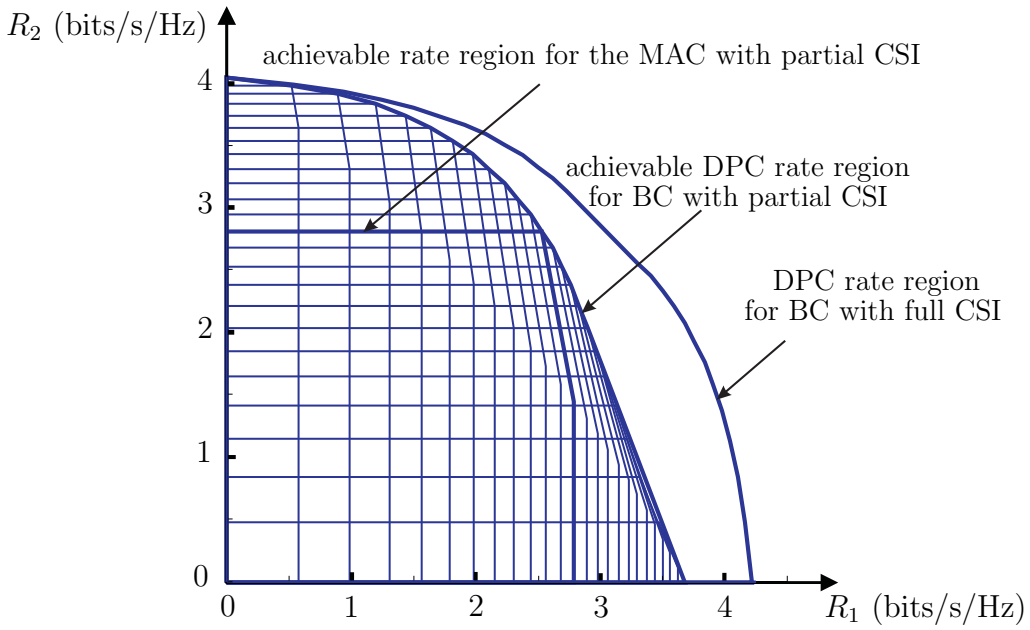

Figure 3.20. Achievable DPC rate region for the investigated two-user Gaussian BC with partial CSI obtained from the achievable rate region for its dual MAC with partial CSI. Parameters: $\underline{\mathbf{h}}_1 = (1, \frac{1}{\sqrt{2}}(0.5+0.5j))^{\mathrm{T}}$, $\underline{\mathbf{h}}_2 = (\frac{1}{\sqrt{2}}(0.3+0.3j), 1)^{\mathrm{T}}$, $P_1+P_2 = P = 12$, and $N_0 = 1$.

With different values of the individual user powers P_1 and P_2 satisfying the sum power constraint $P_1 + P_2 = 12$, many pentagonal achievable rate regions for the dual MAC with partial knowledge of CSI are computed and plotted in Figure 3.20. Similar to the case of full CSI, in the case that the same partial knowledge of CSI is considered in both the BC and the dual MAC, the achievable DPC rate region for the BC constrained by the sum power $P = 12$ can be obtained as a union of the pentagonal achievable rate regions for the dual MAC with all possible power allocations satisfying the sum power constraint $P_1 + P_2 = 12$. Comparing the achievable DPC rate region for the BC with partial CSI to the DPC rate region for the BC with full CSI, it is shown that partial knowledge of CSI can cause significant information-theoretic performance loss especially for the user whose corresponding useful channel is not fully characterized. However, at some operating points of interest, the partial knowledge of CSI causes only a little performance loss. This result encourages us to pursuit the practical cooperative transmission scheme with appropriately selected significant CSI.

3.5 Cooperative MIMO channel - full cooperation

In order to improve the system performance of conventional cellular systems without multi-cell cooperation, practical cooperative communication strategies based on coordinated BSs, i.e., cooperative reception in the UL and cooperative transmission in the

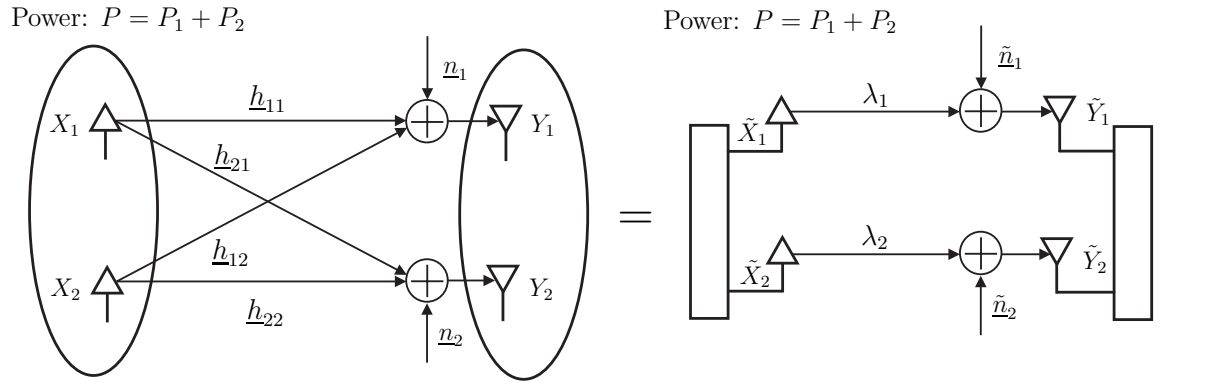

two-user IC with full cooperation — parallel channels equivalent to the MIMO channel

Figure 3.21. The information-theoretic model for the two-cell mobile radio cellular system applying fully cooperative communication scheme: MIMO channel and its equivalent channel.

DL, are proposed. Correspondingly, the information-theoretic performance gains of the investigated MAC and of the investigated BC as compared to the investigated IC are discussed in the above sections. In the present section, the cooperative communication concept in the extreme case of full cooperation where the cooperation is simultaneously performed both at the transmitters and at the receivers is investigated. In contrast to the cooperative reception scheme in the UL or the cooperative transmission scheme in the DL where the cooperation is always performed at coordinated BSs, in the fully cooperative communication scheme cooperative transmission at coordinated MSs in the UL and cooperative reception at coordinated MSs in the DL are also required besides the cooperation at BSs. Without loss of generality, the fully cooperative communication scheme will be investigated taking the two-user complex-valued Gaussian IC in Figure 3.3 corresponding to the UL channel of a two-cell mobile radio system without cooperation as the reference model. The results can be easily extended to the DL channel which is physically dual to the UL channel as indicated in (3.76).

The investigated two-user IC with fully cooperative communication scheme is depicted in Figure 3.21. Gaussian distributed input signals $\underline{x}_k \in \mathbb{C}$, $k = 1, 2$, included in the transmitted vector $\underline{\mathbf{x}} = (\underline{x}_1, \underline{x}_2)^{\mathrm{T}}$, perfect deterministic CSI at both the transmitter side and the receiver side described by the channel matrix $\underline{\mathbf{H}}$ in (3.76), and the i.i.d. Gaussian noise signals $\underline{n}_k \sim \mathcal{CN}(0, N_0)$, $k = 1, 2$, included in the noise vector $\underline{\mathbf{n}} = (\underline{n}_1, \underline{n}_2)^{\mathrm{T}}$ are assumed. The received vector $\underline{\mathbf{y}} = (\underline{y}_1, \underline{y}_2)^{\mathrm{T}}$ consisting of the received signals $\underline{y}_k \in \mathbb{C}$, $k = 1, 2$, can be written as

$$\underline{\mathbf{y}} = \underline{\mathbf{H}}\,\underline{\mathbf{x}} + \underline{\mathbf{n}} \ . \tag{3.112}$$

Applying the fully cooperative communication scheme at the transmitters and at the receivers, the sum-capacity for the investigated IC can be obtained by treating this

IC as a single-user MIMO channel. In this MIMO channel, the antennas of individual transmitters are considered as the antenna array at the transmitter side, while the antennas for individual receivers are considered as the antenna array at the receiver side. The sum power constraint $P = P_1 + P_2$ obtained from the individual user power constraints P_1 and P_2 in the investigated two-user IC is considered in the MIMO channel. Thanks to the wide spatial separation between the users in different cells of realistic cellular systems, a sufficient spatial diversity is ensured in the investigated two-user IC [GKH+07]. Therefore, it is reasonable to assume a full-rank channel matrix $\underline{\mathbf{H}}$ in the considered single-user MIMO channel corresponding to this IC. The capacity for this MIMO channel can be computed with the help of an equivalent channel, i.e., a single-user Gaussian channel with two parallel SISO subchannels as depicted in Figure 3.21 [TV05]. This equivalent channel can be obtained from the SVD of the 2×2 channel matrix $\underline{\mathbf{H}}$ with rank 2 as

$$\underline{\mathbf{H}} = \underline{\mathbf{U}}\,\mathbf{\Lambda}\,\underline{\mathbf{V}}^{*\mathrm{T}} \ , \tag{3.113}$$

where $\underline{\mathbf{U}}$ and $\underline{\mathbf{V}}$ are unitary matrices corresponding to the rotation operations in the linear data transmission. Corresponding to the scaling operation in the linear data transmission, $\mathbf{\Lambda}$ is a 2×2 square diagonal matrix with the ordered positive real-valued singular values $\lambda_1 \geq \lambda_2$ of $\underline{\mathbf{H}}$ as its diagonal elements and 0s as its off-diagonal elements. Let

$$\underline{\tilde{\mathbf{x}}} = \underline{\mathbf{V}}^{*\mathrm{T}}\underline{\mathbf{x}} \ , \qquad \underline{\tilde{\mathbf{y}}} = \underline{\mathbf{U}}^{*\mathrm{T}}\underline{\mathbf{y}} \ , \qquad \underline{\tilde{\mathbf{n}}} = \underline{\mathbf{U}}^{*\mathrm{T}}\underline{\mathbf{n}} \ , \tag{3.114}$$

(3.112) can be rewritten as

$$\underline{\tilde{\mathbf{y}}} = \underline{\mathbf{U}}^{*\mathrm{T}}\underline{\mathbf{y}} = \underline{\mathbf{U}}^{*\mathrm{T}}\underline{\mathbf{U}}\,\mathbf{\Lambda}\,\underline{\mathbf{V}}^{*\mathrm{T}}\,\underline{\mathbf{x}} + \underline{\mathbf{U}}^{*\mathrm{T}}\underline{\mathbf{n}} = \mathbf{\Lambda}\,\underline{\tilde{\mathbf{x}}} + \underline{\tilde{\mathbf{n}}} \tag{3.115}$$

with the unitary matrix $\underline{\mathbf{U}}$ satisfying $\underline{\mathbf{U}}^{*\mathrm{T}}\underline{\mathbf{U}} = \mathbf{I}$. The same sum power constraint for the signals in $\underline{\tilde{\mathbf{x}}}$ and in $\underline{\mathbf{x}}$ is ensured by

$$\underline{\tilde{\mathbf{x}}}^{*\mathrm{T}}\underline{\tilde{\mathbf{x}}} = \underline{\mathbf{x}}^{*\mathrm{T}}\underline{\mathbf{V}}\,\underline{\mathbf{V}}^{*\mathrm{T}}\underline{\mathbf{x}} = \underline{\mathbf{x}}^{*\mathrm{T}}\underline{\mathbf{x}} \tag{3.116}$$

with the unitary matrix $\underline{\mathbf{V}}$ satisfying $\underline{\mathbf{V}}\,\underline{\mathbf{V}}^{*\mathrm{T}} = \mathbf{I}$. The same statistical distribution of $\underline{\tilde{\mathbf{n}}}$ and $\underline{\mathbf{n}}$ can be ensured when $\underline{\mathbf{n}}$ is circular symmetric Gaussian random vector and $\underline{\mathbf{U}}$ is a unitary matrix [TV05]. Therefore, the channel described in (3.115) with the input vector $\underline{\tilde{\mathbf{x}}}$, the output vector $\underline{\tilde{\mathbf{y}}}$, the noise vector $\underline{\tilde{\mathbf{n}}}$, and the channel matrix $\mathbf{\Lambda}$ is equivalent to the channel described in (3.112) from the information-theoretic point of view. In the case where the transmitter of the MIMO channel has full knowledge of the CSI, the water-filling algorithm can be applied for finding the optimum power allocation which achieves the maximum capacity. The optimum transmit powers $\tilde{P}_k$ for the individual parallel subchannels with channel coefficients λ_k, $k = 1, 2$, in the equivalent channel read [TV05]

$$\tilde{P}_k = \left(P_{\mathrm{w}} - \frac{N_0}{\lambda_k^2}\right)^+ \ , \quad ([x]^+ = x, \text{ if } x \geq 0; \quad [x]^+ = 0, \text{ if } x < 0) \ , \tag{3.117}$$

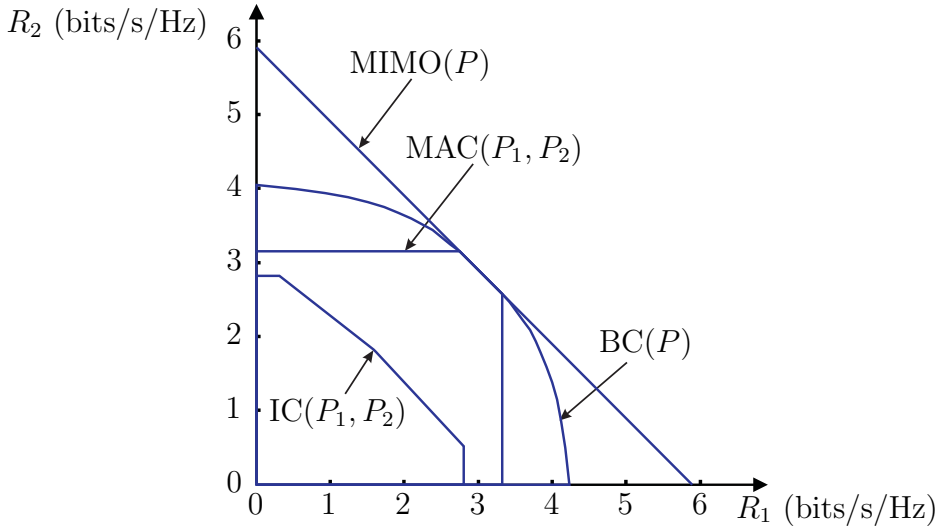

Figure 3.22. Achievable rate regions for the investigated two-user Gaussian IC with no cooperation indicated by "IC(P_1, P_2)", with only cooperative reception indicated by "MAC(P_1, P_2)", with only cooperative transmission indicated by "BC(P)", and with full cooperation indicated by "MIMO(P)". Parameters: $\underline{\mathbf{h}}_1 = (1, \frac{1}{\sqrt{2}}(0.5 + 0.5j))^{\mathrm{T}}$, $\underline{\mathbf{h}}_2 = (\frac{1}{\sqrt{2}}(0.3 + 0.3j), 1)^{\mathrm{T}}$, $P_1 = 6$, $P_2 = 6$, $P = 12$ and $N_1 = N_2 = N_0 = 1$.

where P_{w} is chosen in such a way that the power constraint $\tilde{P}_1 + \tilde{P}_2 = P$ is fulfilled. However, in the case that the transmitter of the MIMO channel has no knowledge of the CSI, the best thing to do is to allocate the power equally to parallel subchannels as

$$\tilde{P}_1 = \tilde{P}_2 = P/2 \ . \tag{3.118}$$

Considering the transmit powers $\tilde{P}_k$, $k = 1, 2$, obtained from the optimum power allocation strategy with the available channel knowledge at the transmitter side, the capacity of the equivalent channel with two parallel Gaussian SISO subchannels reads

$$C = \sum_{k=1}^{2} \log_2 \left(1 + \frac{\tilde{P}_k \lambda_k^2}{N_0} \right) \ . \tag{3.119}$$

Numerical results in Figure 3.22 give a clear view of the information-theoretic performance of the two-user Gaussian IC with different communication strategies. The following achievable rate regions are plotted and compared in Figure 3.22:

- The Han-Kobayashi achievable rate region for the two-user IC with individual user power constraints P_1 and P_2 as the information-theoretic model for the two-cell cellular system without cooperation is denoted by "IC(P_1, P_2)".
- The capacity region of the two-user MAC with individual user power constraints P_1 and P_2 as the information-theoretic model for the two-cell cellular system with cooperative reception in the UL is denoted by "MAC(P_1, P_2)".

- The DPC rate region for the two-user BC with the sum power constraint P as the information-theoretic model for the two-cell cellular system with cooperative transmission in the DL is denoted by "BC(P)".
- The achievable rate region for the full cooperative two-user IC with the sum power constraint P as the information-theoretic model for the two-cell cellular system with cooperative transmitters and cooperative receivers is denoted by "MIMO(P)".

It is worth noting that the last achievable rate region is obtained with respect to the sum-capacity which is equivalent to the capacity of the MIMO channel corresponding to this IC. It can be seen that the cooperative communication scheme can significantly improve the system performance from the fact that the "MAC(P_1, P_2)" and the "BC(P)" outperform the "IC(P_1, P_2)". The "BC(P)" is obtained by exploiting the information-theoretic duality between the BC and the MAC as a union of the capacity regions "MAC(P_1, P_2)" over all possible power allocation P_1 and P_2 satisfying $P_1 + P_2 = P$. Therefore, the capacity region "MAC($P_1 = 6, P_2 = 6$)" is contained in the DPC rate region "BC($P = 12$)". Obviously, the "MIMO(P)" considering both transmitter cooperation and receiver cooperation outperforms the "MAC(P_1, P_2)" and the "BC(P)".

Corresponding to the boundary of the achievable rate region "MIMO(P)", the sum-capacity of the full cooperative IC which is equivalent to the capacity of the MIMO channel for this IC is an upper bound of the sum-capacity of the BC [VJG03]. Although in Figure 3.22 the boundary of the DPC rate region for the BC is quite close to the boundary of the achievable rate region for the full cooperative IC in a segment, the upper bound on the sum-capacity for the BC derived from the capacity of the MIMO channel is in general not tight. A tighter upper bound can be derived by introducing noise correlations at different receivers which affect the capacity of the MIMO channel but have no influence on the capacity region of the BC without receiver cooperation. As a much tighter upper bound of the sum-capacity of the BC, the Sato bound is obtained from the capacity of the MIMO channel with worst-case noise [Sat78b, VJG03, YC04]. From the mathematical point of view, this is a min-max problem of the capacity considering the input covariance matrix and the noise covariance matrix simultaneously [JB04]. Additionally, an iterative water-filling algorithm has been proposed to obtain the optimum input covariance matrices for maximum sum-capacity in the Gaussian vector MAC [YRBC04]. A similar iterative algorithm considering the sum power constraint has been proposed for power allocation aiming at sum-rate maximization in the IC [DWA09].

Chapter 4

Cooperative reception in the uplink

4.1 Preliminary remarks

As one part of the cooperative communication concept, cooperative reception in the UL is discussed in this chapter from the following two points of view. Firstly, typical multiuser detection strategies which could theoretically be used as candidates for the joint signal processing in cooperative reception are reviewed. Especially, some novel advanced multiuser detection techniques based on statistical signal processing are proposed. Secondly, a practical cooperative reception scheme, i.e., decentralized iterative JD with significant CSI at the coordinated BSs, is proposed. Practical issues in realistic cellular systems such as the implementation complexity and the limited ability to track CSI are taken into consideration in this scheme.

According to the multiuser OFDM-MIMO system model of a K-cell mobile radio cellular system presented in Chapter 2, one BS and one active MS per cell are considered at each time slot in each OFDM subcarrier. In the UL with the channel matrix $\underline{\mathbf{H}}_{\mathrm{UL}}$ of dimensions $K_{\mathrm{A}} \times K_{\mathrm{M}}$ assuming $K_{\mathrm{A}} \geq K_{\mathrm{M}} = K$, the received vector $\underline{\mathbf{e}}$ reads

$$\underline{\mathbf{e}} = (\underline{e}^{(1)}, \ldots, \underline{e}^{(K_{\mathrm{A}})})^{\mathrm{T}} = \underline{\mathbf{H}}_{\mathrm{UL}} \cdot \underline{\mathbf{s}} + \underline{\mathbf{n}} = \underline{\mathbf{H}}_{\mathrm{UL}} \cdot \underline{\mathbf{d}} + \underline{\mathbf{n}} \ . \tag{4.1}$$

The transmitted vector $\underline{\mathbf{s}} = (\underline{s}^{(1)}, \ldots, \underline{s}^{(K)})^{\mathrm{T}}$ is equivalent to the data vector $\underline{\mathbf{d}} = (\underline{d}^{(1)}, \ldots, \underline{d}^{(K)})^{\mathrm{T}}$ if simple OFDM transmitters without any pre-processing or cooperation are applied at the MSs. The transmit power per data symbol is denoted by P_{d}. Based on the observation of the received vector $\underline{\mathbf{e}}$, multiuser detection is performed for cooperative reception at the coordinated BSs which jointly serve the MSs.

4.2 Multiuser detection strategies

4.2.1 Optimum detection

Section 4.2 starts with a review of conventional multiuser detection strategies as potential candidates for the cooperative reception scheme [Web03].

Aiming at minimum detection error probability, the optimum multiuser receiver has been proposed in [Ver86, Ver98]. Let $\mathbb{D}$ denote the data symbol alphabet with $\underline{d}^{(k)} \in \mathbb{D}$,

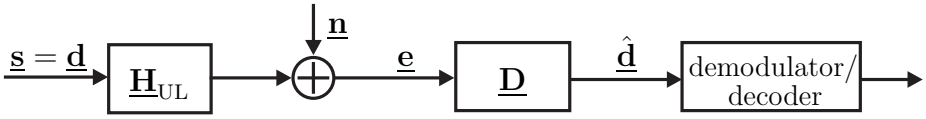

Figure 4.1. UL system model with a linear multiuser receiver.

and let $\mathbb{D}^K$ denote the data vector alphabet with $\underline{\mathbf{d}} \in \mathbb{D}^K$. Following the maximum-a-posteriori (MAP) criterion, the estimated data vector $\hat{\underline{\mathbf{d}}}$ can be obtained as

$$\hat{\underline{\mathbf{d}}} = \underset{\underline{\mathbf{d}} \in \mathbb{D}^K}{\operatorname{argmax}} \left\{ \Pr\left\{ \underline{\mathbf{d}} | \underline{\mathbf{e}} \right\} \right\} \quad . \tag{4.2}$$

If equal a priori probabilities $\Pr\{\underline{\mathbf{d}}\}$ are considered or the probabilities $\Pr\{\underline{\mathbf{d}}\}$ are unknown to the receiver, the maximum-likelihood (ML) detector described by

$$\hat{\underline{\mathbf{d}}} = \underset{\underline{\mathbf{d}} \in \mathbb{D}^K}{\operatorname{argmax}} \left\{ \mathrm{p}\left(\underline{\mathbf{e}} | \underline{\mathbf{d}} \right) \right\} \tag{4.3}$$

can be derived from the MAP detector described by (4.2) according to the Bayes's rule. Considering the system model of (4.1) with the assumed i.i.d. Gaussian noise signals, i.e., $\underline{\mathbf{n}} \sim \mathcal{CN}\left(0, \sigma^2 \mathbf{I}^{K_\mathrm{A} \times K_\mathrm{A}}\right)$, the ML detector of (4.3) can be rewritten as

$$\hat{\underline{\mathbf{d}}} = \underset{\underline{\mathbf{d}} \in \mathbb{D}^K}{\operatorname{argmax}} \left\{ \mathrm{p}\left(\underline{\mathbf{n}} = \underline{\mathbf{e}} - \underline{\mathbf{H}}_{\mathrm{UL}} \underline{\mathbf{d}} \right) \right\} = \underset{\underline{\mathbf{d}} \in \mathbb{D}^K}{\operatorname{argmax}} \left\{ \frac{\exp\left(-\frac{\| \underline{\mathbf{e}} - \underline{\mathbf{H}}_{\mathrm{UL}} \underline{\mathbf{d}} \|^2}{\sigma^2} \right)}{(\pi \sigma^2)^{K_\mathrm{A}}} \right\} = \underset{\underline{\mathbf{d}} \in \mathbb{D}^K}{\operatorname{argmin}} \left\{ \| \underline{\mathbf{e}} - \underline{\mathbf{H}}_{\mathrm{UL}} \underline{\mathbf{d}} \|^2 \right\} \quad . \tag{4.4}$$

An exhaustive search is required in both the MAP detector and the ML detector. Even a moderate number K of users can already result in extremely high computational complexity. Therefore, efficient suboptimum multiuser detectors which make a tradeoff between performance and complexity are of more interest in practice.

4.2.2 Linear multiuser detection

Concerning suboptimum multiuser detection with moderate computational complexity, the conventional linear multiuser receivers are firstly discussed. As described in Figure 4.1, the estimated data vector in a general linear multiuser receiver can be written as

$$\hat{\underline{\mathbf{d}}} = \underline{\mathbf{D}} \cdot \underline{\mathbf{e}} = \underline{\mathbf{D}}\, \underline{\mathbf{H}}_{\mathrm{UL}} \cdot \underline{\mathbf{d}} + \underline{\mathbf{D}} \cdot \underline{\mathbf{n}} \ , \tag{4.5}$$

where $\underline{\mathbf{D}}$ is the considered linear demodulator matrix. Through the linear operation on the received signals, one can obtain continuous-valued data estimates ignoring the constraint of the discrete data symbol alphabet. Quantization techniques can be afterwards applied if necessary. Various linear multiuser receivers with respect to different performance criteria have been studied [BFKM93, KKB96, Mos96, Ver98, TH99, Web03, Küh06]. In the following, the principles of two typical linear multiuser receivers are discussed.

Matched filtering (MF) receiver

As a simple but classic linear multiuser receiver, the MF receiver fights against the background noise to maximize the output SNR. Following the principle of maximal-ratio combining (MRC), the MF receiver for user k projects the received vector $\underline{\mathbf{e}}$ onto the direction along $\underline{\mathbf{h}}_k = [\underline{\mathbf{H}}_{\mathrm{UL}}]_k$ corresponding to the useful channels of user k. The matrix operator $[\cdot]_k$ returns the k-th column of its argument as a column vector. Consequently, the MF demodulator matrix is obtained as

$$\underline{\mathbf{D}}_{\mathrm{MF}} = \underline{\mathbf{H}}_{\mathrm{UL}}^{*\mathrm{T}} \ . \tag{4.6}$$

Considering i.i.d. complex-valued Gaussian noise signals with the variance σ^2, the resulting output SNR for each user k is

$$\gamma_{\mathrm{MF}}^{(k)} = \frac{\|\underline{\mathbf{h}}_k\|^2 \, \mathrm{E}\left\{|\underline{d}^{(k)}|^2\right\}}{\sigma^2} = \frac{\|\underline{\mathbf{h}}_k\|^2 P_{\mathrm{d}}}{\sigma^2} \ . \tag{4.7}$$

Zero forcing (ZF) receiver

The ZF multiuser receiver fights against the multiuser interference to achieve interference-free communications. In fact, the multiuser ZF receiver is a decorrelator which combines the MF and the linear projection operation for interference nulling. For each user k the decorrelator projects the received vector $\underline{\mathbf{e}}$ onto the direction within the subspace orthogonal to all the vectors $\underline{\mathbf{h}}_1, \ldots, \underline{\mathbf{h}}_{k-1}, \underline{\mathbf{h}}_{k+1}, \ldots, \underline{\mathbf{h}}_K$ and closest to $\underline{\mathbf{h}}_k$. Assuming that the column vectors of the channel matrix $\underline{\mathbf{H}}_{\mathrm{UL}}$ of dimensions $K_{\mathrm{A}} \times K$ are linearly independent and $K_{\mathrm{A}} \geq K$, the ZF demodulator matrix $\underline{\mathbf{D}}_{\mathrm{ZF}}$ is derived as the left Moore-Penrose pseudo-inverse of $\underline{\mathbf{H}}_{\mathrm{UL}}$ [KKB96, TV05], i.e.,

$$\underline{\mathbf{D}}_{\mathrm{ZF}} = \left(\underline{\mathbf{H}}_{\mathrm{UL}}^{*\mathrm{T}} \underline{\mathbf{H}}_{\mathrm{UL}}\right)^{-1} \underline{\mathbf{H}}_{\mathrm{UL}}^{*\mathrm{T}} \ . \tag{4.8}$$

Applying $\underline{\mathbf{D}}_{\mathrm{ZF}}$ in (4.5), the estimated data vector is obtained as

$$\hat{\underline{\mathbf{d}}} = \left(\underline{\mathbf{H}}_{\mathrm{UL}}^{*\mathrm{T}} \underline{\mathbf{H}}_{\mathrm{UL}}\right)^{-1} \underline{\mathbf{H}}_{\mathrm{UL}}^{*\mathrm{T}} \cdot \underline{\mathbf{e}} = \underline{\mathbf{d}} + \left(\underline{\mathbf{H}}_{\mathrm{UL}}^{*\mathrm{T}} \underline{\mathbf{H}}_{\mathrm{UL}}\right)^{-1} \underline{\mathbf{H}}_{\mathrm{UL}}^{*\mathrm{T}} \cdot \underline{\mathbf{n}} \ . \tag{4.9}$$

The resulting output SNR can be obtained as

$$\gamma_{\mathrm{ZF}}^{(k)} = \frac{P_{\mathrm{d}}}{\sigma^2 \left[\left(\underline{\mathbf{H}}_{\mathrm{UL}}^{*\mathrm{T}} \underline{\mathbf{H}}_{\mathrm{UL}}\right)^{-1}\right]_{k,k}} \leq \gamma_{\mathrm{MF}}^{(k)} = \frac{P_{\mathrm{d}} \left[\underline{\mathbf{H}}_{\mathrm{UL}}^{*\mathrm{T}} \underline{\mathbf{H}}_{\mathrm{UL}}\right]_{k,k}}{\sigma^2} \ , \tag{4.10}$$

where the matrix operator $[\cdot]_{k,k}$ returns the (k,k)-th element of its argument. The ZF receiver totally removes all the multiuser interference paying the price of the amplified noise. Therefore, the ZF multiuser receiver is a suitable choice for the interference-limited cellular systems with weak background noise.

Additionally, the MMSE multiuser receiver which makes a compromise between the noise enhancement and the interference cancellation has been studied in [Fis02, KKB96, Web03, Küh06].

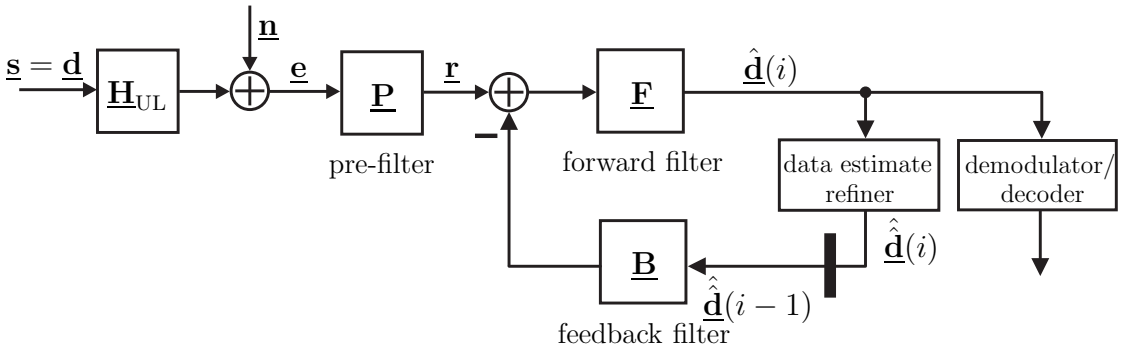

Figure 4.2. General structure of iterative interference cancellation multiuser receiver.

4.2.3 Iterative interference cancellation

In this section, iterative interference cancellation techniques as an attractive subclass of multiuser detection strategies are discussed. The basic principle of iterative interference cancellation is to iteratively use the estimated data symbols obtained from the previous iteration as the feedback to reconstruct and cancel the interference in the current iteration [And05, Kha08]. The general structure of the interference cancellation multiuser receiver is depicted in Figure 4.2. With the pre-filter matrix $\underline{\mathbf{P}}$, the forward filter matrix $\underline{\mathbf{F}}$ and the feedback filter matrix $\underline{\mathbf{B}}$, the estimated data vector $\hat{\underline{\mathbf{d}}}(i)$ in the i-th iteration is obtained from the received vector $\underline{\mathbf{e}}$ based on the refined estimated data vector $\hat{\underline{\mathbf{d}}}(i-1)$ from the $(i-1)$-th iteration as

$$\hat{\underline{\mathbf{d}}}(i) = \underline{\mathbf{F}} \left(\underline{\mathbf{P}} \cdot \underline{\mathbf{e}} - \underline{\mathbf{B}} \cdot \hat{\underline{\mathbf{d}}}(i-1) \right) \quad . \tag{4.11}$$

The structures of the filter matrices $\underline{\mathbf{P}}$, $\underline{\mathbf{F}}$ and $\underline{\mathbf{B}}$ vary according to the applied iterative interference cancellation algorithm, e.g., PIC or SIC. A linear iterative multiuser receiver is obtained if a simple transparent data estimate refinement is applied, i.e., $\hat{\underline{\mathbf{d}}}(i) = \hat{\underline{\mathbf{d}}}(i)$. A nonlinear iterative multiuser receiver is obtained if hard or soft quantization techniques are applied for the data estimate refinement. A suitable data estimate refiner could improve the system performance. After the iterative interference cancellation, the data estimates will be forwarded to the demodulator and decoder. Two main iterative interference cancellation techniques, i.e., PIC and SIC, are discussed in the following.

Parallel interference cancellation (PIC)

The basic principle of PIC follows the idea of the Jacobi algorithm in linear algebra which calculates the solution of a system of linear equations in an iterative way instead

1. $g^{(k)} = \sum_{k_\mathrm{A}} \underline{H}_{\mathrm{UL}}^{(k_\mathrm{A},k)^*} \underline{H}_{\mathrm{UL}}^{(k_\mathrm{A},k)}$, $\forall k$
2. $\hat{\underline{d}}^{(k)}(0) = 0$, $\forall k$
3. $\underline{r}^{(k)} = \sum_{k_\mathrm{A}} \underline{H}_{\mathrm{UL}}^{(k_\mathrm{A},k)^*} \cdot \underline{e}^{(k_\mathrm{A})}$, $\forall k$
4. **for** $i = 1, \ldots, L$ **do**
5. $\quad \hat{\underline{d}}^{(k)}(i) = \frac{1}{g^{(k)}} \cdot \left(\underline{r}^{(k)} - \sum_{k' \neq k} \sum_{k_\mathrm{A}} \underline{H}_{\mathrm{UL}}^{(k_\mathrm{A},k)^*} \underline{H}_{\mathrm{UL}}^{(k_\mathrm{A},k')} \cdot \hat{\underline{d}}^{(k')}(i-1) \right)$, $\forall k$
6. $\quad \hat{\underline{d}}^{(k)}(i) = \mathcal{Q}_{\mathrm{HD}} \left(\hat{\underline{d}}^{(k)}(i) \right)$, $\forall k$
7. **end for** // parallel computation for all $k = 1, \ldots, K$ in every iteration i

Figure 4.3. PIC algorithm in the iterative multiuser receiver.

of performing matrix inversion [HJ85, GvL96]. The matrix-vector notation of the PIC algorithm aiming at the ZF solution can be described by

$$\hat{\underline{\mathbf{d}}}(i) = \left(\mathrm{diag}\left(\underline{\mathbf{H}}_{\mathrm{UL}}^{*\mathrm{T}} \underline{\mathbf{H}}_{\mathrm{UL}}\right)\right)^{-1} \left(\underline{\mathbf{H}}_{\mathrm{UL}}^{*\mathrm{T}} \cdot \underline{\mathbf{e}} - \overline{\mathrm{diag}}\left(\underline{\mathbf{H}}_{\mathrm{UL}}^{*\mathrm{T}} \underline{\mathbf{H}}_{\mathrm{UL}}\right) \hat{\underline{\mathbf{d}}}(i-1) \right) \quad , \tag{4.12}$$

where $\overline{\mathrm{diag}}(\cdot)$ returns a matrix containing the offdiagonal elements of its argument. Corresponding to the general structure of the iterative multiuser receiver in Figure 4.2, the pre-filter matrix $\underline{\mathbf{P}}$, the forward filter matrix $\underline{\mathbf{F}}$ and the feedback filter matrix $\underline{\mathbf{B}}$ are:

$$\underline{\mathbf{P}} = \underline{\mathbf{H}}_{\mathrm{UL}}^{*\mathrm{T}} \tag{4.13}$$

$$\underline{\mathbf{F}} = \left(\mathrm{diag}\left(\underline{\mathbf{H}}_{\mathrm{UL}}^{*\mathrm{T}} \underline{\mathbf{H}}_{\mathrm{UL}}\right)\right)^{-1} \tag{4.14}$$

$$\underline{\mathbf{B}} = \overline{\mathrm{diag}}\left(\underline{\mathbf{H}}_{\mathrm{UL}}^{*\mathrm{T}} \underline{\mathbf{H}}_{\mathrm{UL}}\right) \quad . \tag{4.15}$$

At the end of each iteration, the data estimates $\hat{\underline{d}}^{(k)}$ included in the estimated data vector $\hat{\underline{\mathbf{d}}}(i)$ go through the data estimate refiner to obtain the refined data estimates $\hat{\hat{\underline{d}}}^{(k)}$ included in the refined estimated data vector $\hat{\hat{\underline{\mathbf{d}}}}(i)$. In practice, hard quantization exploiting the knowledge of the data symbol alphabet $\mathbb{D}$ as described by

$$\hat{\hat{\underline{d}}}^{(k)} = \mathcal{Q}_{\mathrm{HD}}(\hat{\underline{d}}^{(k)}) = \underset{\underline{d}^{(k)} \in \mathbb{D}}{\mathrm{argmin}} \left\{ \| \hat{\underline{d}}^{(k)} - \underline{d}^{(k)} \|^2 \right\}, \quad k = 1, \ldots, K, \tag{4.16}$$

is frequently used for the data estimate refinement. When BPSK modulation is applied, the hard quantization function is simplified to the sign function, i.e., $\mathcal{Q}_{\mathrm{HD}}(\hat{\underline{d}}^{(k)}) = \mathrm{sgn}(\hat{\underline{d}}^{(k)})$. In Figure 4.3, a nonlinear PIC receiver with hard quantization is shown. When transparent data estimate refinement $\hat{\hat{\underline{\mathbf{d}}}}(i) = \hat{\underline{\mathbf{d}}}(i)$ is applied, (4.12) describes the iterative version of the linear ZF algorithm described by (4.9). If this PIC algorithm converges, the limiting values of the data estimates are equivalent to the data estimates directly obtained from the ZF algorithm. Considering a channel matrix of size $K \times K$, the linear ZF algorithm requiring the matrix inversion has a computational complexity

order $\mathcal{O}(K^3)$. The corresponding PIC algorithm with L iterations has a computational complexity order $\mathcal{O}(K^2 \cdot L)$. For typical realistic cellular systems with a large number of users, K is much larger than L, and therefore the PIC algorithm is of more interest. A practical cooperative reception scheme based on the PIC algorithm will be proposed in Section 4.3.

Successive interference cancellation (SIC)

Unlike the PIC technique which performs interference cancellation for users simultaneously, the SIC technique performs interference cancellation for users successively. Interestingly, SIC is a capacity-achieving strategy in many basic information-theoretic models [TV05, CT06, GJJV03].

The SIC technique investigated in this section is based on the QR decomposition following the idea of the Gram-Schmidt algorithm [GvL96, WBR+, WRB+02]. Similar to the above PIC algorithm, the QR-SIC algorithm discussed in the following is also designed aiming at the ZF solution for interference-limited cellular systems. The matrix $\underline{\mathbf{H}}_{\mathrm{UL}}$ of dimensions $K_{\mathrm{A}} \times K$ can be decomposed into a unitary matrix $\underline{\mathbf{Q}}$ of dimensions $K_{\mathrm{A}} \times K$ and an upper triangular matrix $\underline{\mathbf{R}}$ of dimensions $K \times K$ as [GvL96]

$$\underline{\mathbf{H}}_{\mathrm{UL}} = (\underline{\mathbf{h}}_1, \ldots, \underline{\mathbf{h}}_K) = \underline{\mathbf{Q}} \cdot \underline{\mathbf{R}} = \left(\underline{\mathbf{q}}_1, \ldots, \underline{\mathbf{q}}_K\right) \cdot \begin{pmatrix} \underline{R}^{(1,1)} & \ldots & \underline{R}^{(1,K)} \\ & \ddots & \vdots \\ 0 & & \underline{R}^{(K,K)} \end{pmatrix} \quad , \tag{4.17}$$

where $\underline{\mathbf{h}}_k = [\underline{\mathbf{H}}_{\mathrm{UL}}]_k$ and $\underline{\mathbf{q}}_k = \left[\ \underline{\mathbf{Q}}\ \right]_k$ with the matrix operator $[\cdot]_k$ returning the k-th column of its argument as a column vector. Since the matrix $\underline{\mathbf{Q}}$ is unitary,

$$\underline{\mathbf{Q}}^{*\mathrm{T}} \cdot \underline{\mathbf{e}} = \underline{\mathbf{Q}}^{*\mathrm{T}} \cdot (\underline{\mathbf{H}}_{\mathrm{UL}} \cdot \underline{\mathbf{d}} + \underline{\mathbf{n}}) = (\underline{\mathbf{Q}}^{*\mathrm{T}} \cdot \underline{\mathbf{Q}}) \cdot \underline{\mathbf{R}} \cdot \underline{\mathbf{d}} + \underline{\mathbf{Q}}^{*\mathrm{T}} \cdot \underline{\mathbf{n}} = \underline{\mathbf{R}} \cdot \underline{\mathbf{d}} + \tilde{\underline{\mathbf{n}}} \tag{4.18}$$

holds considering the received vector $\underline{\mathbf{e}}$ of (4.1) and the modified noise vector $\tilde{\underline{\mathbf{n}}} = \underline{\mathbf{Q}}^{*\mathrm{T}} \cdot \underline{\mathbf{n}}$ with the same statistics as the noise vector $\underline{\mathbf{n}}$. Motivated by the equation of (4.18), an iterative interference cancellation algorithm aiming at the ZF solution is derived as

$$\hat{\underline{\mathbf{d}}}(i) = \left(\mathrm{diag}\left(\underline{\mathbf{R}}\right)\right)^{-1} \left(\underline{\mathbf{Q}}^{*\mathrm{T}} \cdot \underline{\mathbf{e}} - \overline{\mathrm{diag}}\left(\underline{\mathbf{R}}\right) \cdot \hat{\underline{\mathbf{d}}}(i-1)\right) \quad . \tag{4.19}$$

Corresponding to the general iterative multiuser receiver in Figure 4.2, the pre-filter matrix $\underline{\mathbf{P}}$, the forward filter matrix $\underline{\mathbf{F}}$ and the feedback filter matrix $\underline{\mathbf{B}}$ are:

$$\underline{\mathbf{P}} = \underline{\mathbf{Q}}^{*\mathrm{T}} \tag{4.20}$$

$$\underline{\mathbf{F}} = \left(\mathrm{diag}\left(\underline{\mathbf{R}}\right)\right)^{-1} \tag{4.21}$$

$$\underline{\mathbf{B}} = \overline{\mathrm{diag}}\left(\underline{\mathbf{R}}\right) \quad . \tag{4.22}$$

1. $\underline{\mathbf{H}}_{\mathrm{UL}} = \underline{\mathbf{Q}} \cdot \underline{\mathbf{R}}$ applying sorted QR decomposition (SQRD)
2. **for** $k = K, \ldots, 1$ **do**
3. $\quad \underline{y}^{(k)} = \frac{1}{\underline{R}^{(k,k)}} \sum_{k_\mathrm{A}} \underline{Q}^{(k_\mathrm{A},k)^*} \underline{e}^{(k_\mathrm{A})}$
4. $\quad \hat{\underline{d}}^{(k)} = \underline{y}^{(k)} - \frac{1}{\underline{R}^{(k,k)}} \sum_{k'=k+1}^{K} \underline{R}^{(k,k')} \hat{\underline{d}}^{(k')}$
5. $\quad \hat{\underline{d}}^{(k)} = \mathcal{Q}_{\mathrm{HD}} \left(\hat{\underline{d}}^{(k)} \right)$
6. **end for** // successive computation from $k = K$ to $k = 1$
7. reordering of refined data estimates $\hat{\underline{d}}^{(k)}$ included in $\hat{\underline{\mathbf{d}}}^{(k)}$ according to SQRD

Figure 4.4. The SQRD-based SIC algorithm.

With the upper triangular matrix $\underline{\mathbf{R}}$, the data estimate for user $k = 1, \ldots, K$

$$\hat{\underline{d}}^{(k)}(i) = \frac{1}{\underline{R}^{(k,k)}} \cdot \left(\underline{R}^{(k,k)} \cdot \underline{d}^{(k)} + \tilde{\underline{n}}^{(k)} + \sum_{k'=k+1}^{K} \underline{R}^{(k,k')} \cdot \underline{d}^{(k')} - \sum_{k'=k+1}^{K} \underline{R}^{(k,k')} \cdot \hat{\underline{d}}^{(k')}(i-1) \right) \tag{4.23}$$

can be obtained. Obviously, it is not necessary to perform data estimation for any user k before the required data estimates $\hat{\underline{d}}^{(k')}$, $k' = k+1, \ldots, K$ for interference cancellation of this user k have already been reliably obtained. Therefore, the interference cancellation is performed successively in the order from user $k = K$ to user $k = 1$. Only the data symbol of one user is estimated per iteration, and altogether $L = K$ iterations are required to complete the data estimation for all users. Corresponding to the equation of (4.19), $\hat{\underline{\mathbf{d}}}(i-1) = (0, \ldots, \hat{\underline{d}}^{(k+1)}, \ldots, \hat{\underline{d}}^{(K)})^{\mathrm{T}}$ including previously obtained data estimates is considered in the iteration $i = K-k+1$ for user k to obtain its data estimate $\hat{\underline{d}}^{(k)}$ included in the estimated data vector $\hat{\underline{\mathbf{d}}}(i) = (0, \ldots, 0, \hat{\underline{d}}^{(k)}, \ldots, \hat{\underline{d}}^{(K)})^{\mathrm{T}}$. The very nice thing is that in the first iteration the interference-free data estimate of user $k = K$ can be directly obtained. In the following in iteration i, the interference-free data estimate of user $k = K - i + 1$ can be obtained based on the correctly refined data estimates $\hat{\underline{d}}^{(k')}$, $k' = k+1, \ldots, K$. For the data estimate refinement, hard quantization $\mathcal{Q}_{\mathrm{HD}}(\cdot)$ described in (4.16) can be applied. In general, the interference-free data estimates of the SIC receiver can be written as

$$\hat{\underline{d}}^{(k)} = \underline{d}^{(k)} + \frac{1}{\underline{R}^{(k,k)}} \cdot \tilde{\underline{n}}^{(k)}, \; k = 1, \ldots, K \; . \tag{4.24}$$

The SNR of each user k obtained from (4.24) is proportional to $\underline{R}^{(k,k)}$. Different permutations of the column vectors in the channel matrix $\underline{\mathbf{H}}_{\mathrm{UL}}$ result in different matrices $\underline{\mathbf{R}}$ and consequently different system performance [Küh06]. In order to reduce the error propagation effect of hard decision, the sorted QR decomposition (SQRD) algorithm

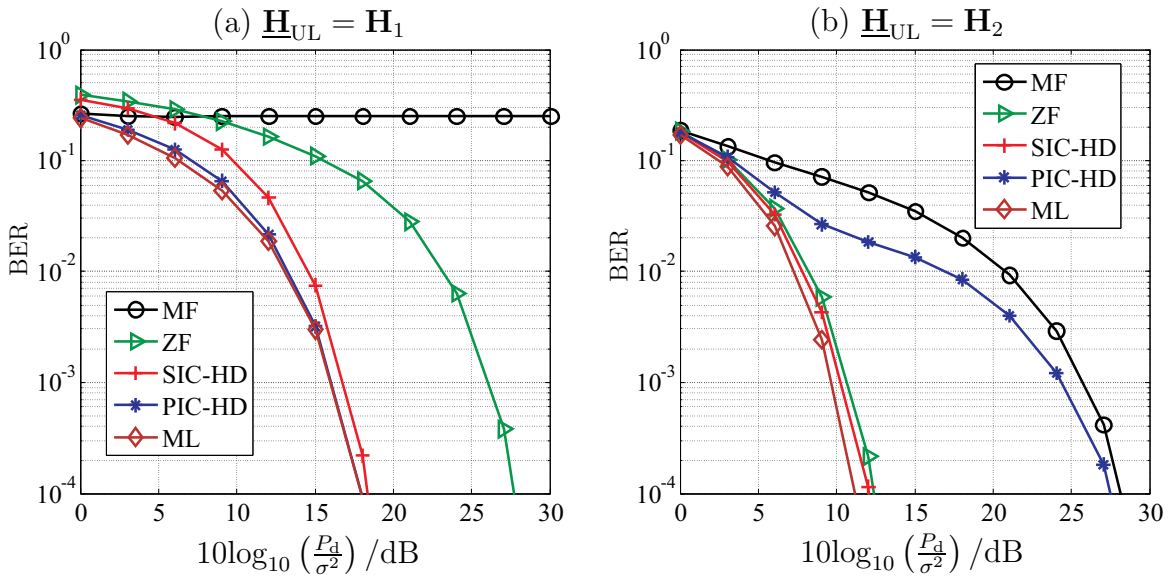

Figure 4.5. BERs for different multiuser receivers considering two exemplary channel matrices $\mathbf{H}_1 = (0.4, 1; 0.2, 1)$ and $\mathbf{H}_2 = (1, 0.2, 0.2; 0.1, 1, 0.2; 0.4, 0.1, 1)$.

which intends to maximize $\underline{R}^{(k,k)}$ in every detecting step can be applied in the SIC receiver [FGVW99, WBR+, WRB+02]. In Figure 4.4, the SQRD-based SIC algorithm is described.

Assuming QPSK modulation, numerical results in Figure 4.5 illustrate the system performance of the above multiuser receivers. It is shown that the channel structure of the multiuser MIMO system, i.e., the relationship between the channel coefficients, has a significant influence on the system performance of the iterative interference cancellation receivers. The channel structure determines whether the PIC algorithm converges or not. In case of convergence, the BER curve of the PIC receiver without quantization is equivalent to that of the ZF receiver, which is also equivalent to the BER curve of the SIC receiver without quantization. Additionally, the BER curve based on the limiting values of the PIC receiver with hard quantization denoted by "PIC–HD", and the BER curve of the SIC receiver with hard quantization denoted by "SIC–HD" are plotted. Considering the channel matrix $\mathbf{H}_1$, the PIC receiver with hard quantization has a better performance than the ZF receiver. However, this result is not always true due to the error propagation of hard decision as illustrated by the BER curves considering the channel matrix $\mathbf{H}_2$. If the column vectors of the channel matrix have distinctively different Euclidean norms, the SIC receiver can benefit much from the sorting and the quantization to achieve much better system performance than the ZF receiver. Generally, there is no simple answer to the question whether the PIC receiver or the SIC receiver has a better performance. Different scenarios with different MIMO channel structures have their own favourite iterative receivers [VA90, PH94, GW96, And05].

As for the implementation issues, the PIC receiver considering K users and L iterations has the computational complexity order $\mathcal{O}(L \cdot K^2)$ and the iteration latency order $\mathcal{O}(L)$. The SIC receiver based on the QR decomposition with K iterations has the computational complexity order $\mathcal{O}(K^3)$ and the iteration latency order $\mathcal{O}(K)$. In realistic cellular networks with a large value of K, the PIC receiver is a more practical choice as compared to the SIC receiver if only a small number L of iterations is sufficient.

4.2.4 Advanced multiuser detection based on statistical signal processing

Following the principles of statistical signal processing [Kay93, Kay98], two advanced multiuser detection schemes exploiting soft information are proposed in this section. The soft information is extracted from the statistical knowledge of random system parameters in the form of probability density functions (PDFs).

The multiuser detection schemes in the above sections are designed based on known system parameters, e.g., noise variances and channel coefficients. In practice, these parameters have to be previously estimated, and then could be treated as known deterministic parameters in multiuser detection. However, in most realistic scenarios many parameters are not constants but random variables with certain statistical distributions. Although it may be difficult to exactly track the instantaneous values of these parameters at each time slot, in most scenarios it is easy to obtain a statistical knowledge of these parameters based on measured or empirical data. In communication systems where the computational complexity is not a key issue but high system performance is required, it is worth pursuing the optimum data detection scheme exploiting the soft information extracted from a statistical knowledge of the random parameters. At least, the optimum data detection scheme can provide an upper-bound of the system performance to evaluate different suboptimum data detection schemes. In the following, the first advanced multiuser detection scheme exploits the statistical knowledge of random noise variances in different subcarriers of an OFDM system [WW08, WWKK08]. The second advanced multiuser detection scheme exploits the statistical knowledge of imperfect CSI, i.e., the PDF of the channel coefficients and the PDF of the channel errors, in a two-user communication channel with cooperative receivers.

Optimum nonlinear MMSE detection with random noise variances

In a lot of research work on data detection in mobile radio systems, the noise for each user is simply assumed to be Gaussian distributed with known variance [MW03,

INF01]. However, in many realistic scenarios of interest the noise variance is changing as a random variable, and consequently the noise is not strictly Gaussian distributed [WC00, EODD02]. In practice, a suboptimum solution was proposed which firstly performs a separate estimation of the instantaneous noise variance at each time slot and then makes use of this estimate for data detection [WM02, ZLW01]. However, an insufficient number of received signals in realistic systems limits the performance of the noise variance estimation and hence the data detection. Fortunately, the approximate distribution of the noise variance can be easily obtained in most realistic scenarios. Exploiting the data symbol alphabet and the statistical knowledge of the noise signals concerning the PDF of the noise variance, an optimum nonlinear MMSE detector is proposed in the following. For the sake of simplicity, this proposal is firstly considered in a simple exemplary scenario, i.e., a real-valued OFDM system. This is not a strong restriction as any complex-valued system can be equivalently modeled as a real-valued system with double number of dimensions.

In the considered multiuser OFDM system, the data symbols d_k of the individual users k, $k=1,\ldots,K$, are transmitted over individual subcarriers k with channel coefficients h_k. The system model can be described by

$$\mathbf{e} = \mathbf{H} \cdot \mathbf{d} + \mathbf{n} \ , \tag{4.25}$$

with the transmitted vector which is equal to the data vector $\mathbf{d}=(d_1,\ldots,d_K)^{\mathrm{T}}$ when applying the simple OFDM transmitter, the received vector $\mathbf{e}=(e_1,\ldots,e_K)^{\mathrm{T}}$, the noise vector $\mathbf{n}=(n_1,\ldots,n_K)^{\mathrm{T}}$ and the channel matrix $\mathbf{H}=\mathrm{diag}\{h_1,\ldots,h_K\}$. Let $y_k=h_k d_k$ denote the received useful signal in each subcarrier k. Without any intra-subcarrier or inter-subcarrier interference, the received signal e_k in each subcarrier

$$e_k = h_k \cdot d_k + n_k = y_k + n_k \tag{4.26}$$

contains the received useful signal y_k and the noise signal n_k. Applying the BPSK modulation with $d_k \in \{-1;+1\}$, $k=1,\ldots,K$, the symbol alphabet of the received useful signal y_k in each subcarrier k can be obtained as

$$\mathbb{V}_{y_k} = \{v_1, v_2\} = \{-h_k, h_k\} \subset \mathbb{R} \ . \tag{4.27}$$

Concerning the model of the noise statistics in the considered OFDM system, the noise signals n_k are assumed to be independently Gaussian distributed if the values of the individual noise variances σ_k^2, $k=1,\ldots,K$, are known. The conditional joint PDF of the noise vector can be written as

$$\mathrm{p}(\mathbf{n}|\sigma_1^2,\ldots,\sigma_K^2) = \frac{e^{-\frac{1}{2}\left(n_1^2/\sigma_1^2+\cdots+n_K^2/\sigma_K^2\right)}}{(\sqrt{2\pi})^K \cdot \sigma_1 \cdots \sigma_K} \ . \tag{4.28}$$

The PDF of the noise variance is derived from a realistic noise model as follows:

- There are N noise or interference sources which are generally considered as N noise sources with the same given unit power. The noise signal at the receiver in each subcarrier results from the superposition of N noise signal components from individual noise sources through N individual fading channels. Therefore, with unit power at different noise sources, the noise variance at each receiver, i.e., the power of the received noise signal, is the sum of the gains of the fading channels.
- The fading channels in each subcarrier corresponding to different noise sources are independent. Their channel coefficients are identically Gaussian distributed with mean 0 and variance Ω in the real-valued system. Therefore, the noise variance at each receiver is Chi-square distributed.
- The fading channels from the same noise source to receivers in different subcarriers are correlated. Therefore, the noise variances σ_k^2 at different receivers are correlated multivariate Chi-square distributed with N degrees of freedom.
- In most scenarios of multi-channel reception, the correlation between pairs of noise variances at two receivers decays as the spacing between the receivers increases. Considering this fact, the exponential correlation coefficient of the noise variances σ_i^2 and σ_j^2 at two receivers is assumed as $\rho_{i,j} = \mathrm{cov}(\sigma_i^2, \sigma_j^2)/\sqrt{\mathrm{var}(\sigma_i^2)\mathrm{var}(\sigma_j^2)} = \rho^{|i-j|}$ with $0<\rho<1$ based on previous studies on correlated fading channels [KZK03, AP05].

According to the above statement, the joint PDF of the exponentially correlated multivariate Chi-square distributed noise variances can be derived using [KZK03] as

$$\mathrm{p}\left(\sigma_1^2,\ldots,\sigma_K^2\right) = \frac{(\sigma_1\sigma_K)^{(\frac{N}{2}-1)} e^{-\frac{\sigma_1^2+\sigma_K^2+(1+\rho^2)\sum_{k=2}^{K-1}\sigma_k^2}{2\Omega(1-\rho^2)}}}{(2\Omega)^{(K+\frac{N}{2}-1)}\Gamma(\frac{N}{2})(1-\rho^2)^{\frac{N(K-1)}{2}}} \cdot \prod_{k=1}^{K-1} (\frac{\rho}{1-\rho^2})^{\frac{2-N}{2}} I_{(\frac{N}{2}-1)}\big(\frac{\rho}{\Omega(1-\rho^2)}\sigma_k\sigma_{k+1}\big), \tag{4.29}$$

where $\Gamma(x)$ indicates the Gamma function, and $I_\kappa\big(x\big)$ indicates the modified Bessel function of the first kind with the order κ. The PDF of the noise vector $\mathbf{n}$ is calculated as the marginal PDF from the conditional joint PDF of the noise vector $\mathrm{p}(\mathbf{n}|\sigma_1^2,\ldots,\sigma_K^2)$ in (4.28) using (4.29), i.e.,

$$\mathrm{p}(\mathbf{n}) = \int_0^{+\infty} \cdots \int_0^{+\infty} \mathrm{p}(\mathbf{n}|\sigma_1^2,\ldots,\sigma_K^2) \cdot \mathrm{p}\left(\sigma_1^2,\ldots,\sigma_K^2\right) \mathrm{d}\sigma_1^2 \cdots \mathrm{d}\sigma_K^2 \ , \tag{4.30}$$

which can also be considered as the inverse Gaussian transform of $\mathrm{p}\left(\sigma_1^2,\ldots,\sigma_K^2\right)$ [AVP06, NK07]. With

$$\varphi(a,b,c) = 2c^{\frac{a+1}{2}} b^{-\frac{a+1}{2}} K_{(a+1)}(2\sqrt{bc}) \ , \tag{4.31}$$

where $K_\kappa(x)$ indicates the modified Bessel function of the second kind with the order κ, $\mathrm{p}(\mathbf{n})$ is obtained as

$$\mathrm{p}(\mathbf{n})=\frac{(2\Omega(1-\rho^2))^{\frac{N(1-K)}{2}}}{(\sqrt{2\pi})^K(2\Omega)^{\frac{N}{2}}\Gamma(\frac{N}{2})}\cdot\sum_{i_1,\ldots,i_{K-1}=0}^{\infty}\left(\prod_{j=1}^{K-1}\frac{1}{i_j!}\cdot\frac{\left(\frac{\rho}{2\Omega(1-\rho^2)}\right)^{2i_j}}{\Gamma(i_j+\frac{N}{2})}\cdot\varphi\left(\frac{N-3}{2}+i_1,\frac{1}{2\Omega(1-\rho^2)},\frac{n_1^2}{2}\right)\right.$$
$$\left.\cdots\varphi\left(\frac{N-3}{2}+i_{k-2}+i_{k-1},\frac{1+\rho^2}{2\Omega(1-\rho^2)},\frac{n_{k-1}^2}{2}\right)\cdots\varphi\left(\frac{N-3}{2}+i_{K-1},\frac{1}{2\Omega(1-\rho^2)},\frac{n_K^2}{2}\right)\right). \tag{4.32}$$

Based on the received signal as described by (4.26), the estimated data symbol $\hat{d}_k$ can be obtained through a suitable data detection technique at the receiver. Considering the scaling factor, i.e., the channel coefficient h_k in each subcarrier k, the estimated received useful signal is denoted by $\hat{y}_k=h_k\hat{d}_k$. The SNRs at the output of the receiver read

$$\gamma_{\mathrm{out}}^{(k)}=\frac{y_k^2}{\mathrm{E}\{(\hat{y}_k-y_k)^2\}}=\frac{h_k^2\cdot d_k^2}{h_k^2\cdot\mathrm{E}\{(\hat{d}_k-d_k)^2\}}=\frac{d_k^2}{\mathrm{E}\{(\hat{d}_k-d_k)^2\}},\quad k=1,\ldots,K, \tag{4.33}$$

and the above output SNRs are used for the performance assessment of different data detection techniques. Obviously, the multiuser detector which minimizes the mean square error as described by

$$\hat{d}_k=\underset{\hat{d}_k}{\mathrm{argmin}}\left\{\mathrm{E}\left\{(\hat{d}_k-d_k)^2|\mathbf{e}\right\}\right\} \tag{4.34}$$

maximizes the output SNR. Considering the scaling factor h_k, the data symbol estimate is rewritten as

$$\hat{d}_k=\underset{\hat{d}_k}{\mathrm{argmin}}\left\{\mathrm{E}\left\{(\underbrace{h_k\cdot\hat{d}_k}_{\hat{y}_k}-\underbrace{h_k\cdot d_k}_{y_k})^2|\mathbf{e}\right\}\right\}=\frac{\hat{y}_k}{h_k}=\frac{1}{h_k}\cdot\underset{\hat{y}_k}{\mathrm{argmin}}\left\{\mathrm{E}\left\{(\hat{y}_k-y_k)^2|\mathbf{e}\right\}\right\}\quad. \tag{4.35}$$

In other words, the nonlinear MMSE detection of the data symbol d_k can be converted to the nonlinear MMSE detection of the received useful signal y_k considering a scaling factor. The estimated received useful signal can be obtained by minimizing

$$\mathrm{E}\left\{(\hat{y}_k-y_k)^2\middle|\mathbf{e}\right\}=(\hat{y}_k-\mathrm{E}\{y_k|\mathbf{e}\})^2+\mathrm{var}\{y_k|\mathbf{e}\}\quad, \tag{4.36}$$

i.e., by choosing

$$\hat{y}_k=\mathrm{E}\{y_k|\mathbf{e}\}\quad. \tag{4.37}$$

With respect to different levels of knowledge of the noise variance, alternative nonlinear MMSE detectors can be implemented in various ways. In the best case where the noise

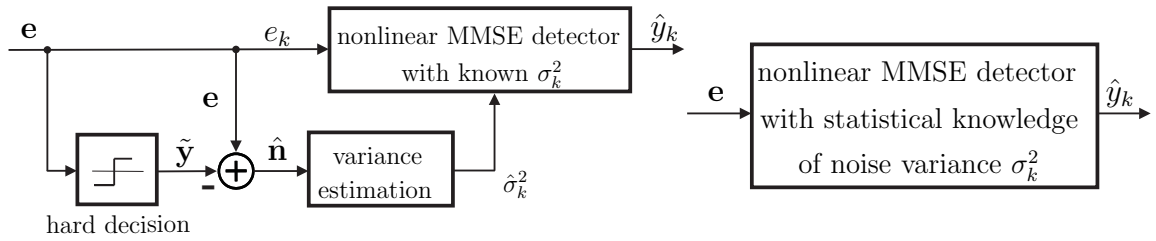

conventional nonlinear MMSE detector optimum nonlinear MMSE detector

Figure 4.6. Nonlinear MMSE detectors with separately estimated noise variance or with the statistical knowledge of noise variance σ_k^2.

variances σ_k^2 in the subcarriers $k, k = 1, \ldots, K$, are perfectly known by the nonlinear MMSE detector, the noise signals n_k in different subcarriers are independently Gaussian distributed. Therefore, the estimated received useful signal $\hat{y}_k$ of each user k depends only on the received signal e_k in its own subcarrier, and (4.37) is simplified to

$$\hat{y}_k = \mathrm{E}\{y_k|e_k\} = \frac{\sum\limits_{m=1}^{2} v_m \, \mathrm{p}(e_k|y_k = v_m) \Pr\{v_m\}}{\sum\limits_{m=1}^{2} \mathrm{p}(e_k|y_k = v_m) \Pr\{v_m\}} = \frac{\sum\limits_{m=1}^{2} v_m \, e^{-\frac{(e_k - v_m)^2}{2\sigma_k^2}}}{\sum\limits_{m=1}^{2} e^{-\frac{(e_k - v_m)^2}{2\sigma_k^2}}} \quad . \tag{4.38}$$

In (4.38), equal a-priori probabilities $\Pr\{v_m\}$ are assumed for all possible symbols $v_m \in \mathbb{V}_{y_k}$ described by (4.27), and $\mathrm{p}(e_k|y_k{=}v_m) = \mathrm{p}(n_k)$ can be calculated from the PDF of the Gaussian distributed noise signal with the known noise variance. However, in most realistic mobile communication systems, the value of the noise variance is not a-priori known by the receiver. Many state of the art data detectors have a separate noise variance estimator. For simplicity, it is assumed that all subcarriers have the same noise variance σ^2, and consequently a nonlinear MMSE detector with a separate noise variance estimator is implemented as shown in Figure 4.6. The noise variance is estimated by exploiting the estimated noise vector $\hat{\mathbf{n}}$ in K subcarriers as

$$\hat{\sigma}_k^2 = (\hat{\mathbf{n}}^{\mathrm{T}} \cdot \hat{\mathbf{n}})/K = ((\mathbf{e} - \tilde{\mathbf{y}})^{\mathrm{T}} \cdot (\mathbf{e} - \tilde{\mathbf{y}}))/K \quad , \tag{4.39}$$

where the initially estimated received useful vector $\tilde{\mathbf{y}}$ is obtained by hard decision.

In realistic communication systems, the statistical knowledge of the noise variance instead of the exact value of the instantaneous noise variance is much easier to be obtained. In order to avoid the separate variance estimation and to obtain better system performance, one promising optimum nonlinear MMSE detector as shown in Figure 4.6 which makes full use of the limited knowledge of noise is applied as follows. With the received useful vector alphabet

$$\mathbb{U}_{\mathbf{y}} = \{\mathbf{u}_1, \ldots, \mathbf{u}_M\}, \quad \mathbf{u}_m = (u_{m,1} \ldots u_{m,K})^{\mathrm{T}} \tag{4.40}$$

of cardinality $M{=}2^K$ with $u_{m,k} \in \mathbb{V}_{y_k},\ m = 1, \ldots, M,\ k = 1, \ldots, K$, the received useful signal estimate at each receiver following the rationale of (4.37) can be obtained as

$$\hat{y}_k = \frac{\sum\limits_{m=1}^{M=2^K} u_{m,k}\, \mathrm{p}(\mathbf{e}|\mathbf{y} = \mathbf{u}_m) \Pr\{\mathbf{u}_m\}}{\sum\limits_{m=1}^{M=2^K} \mathrm{p}(\mathbf{e}|\mathbf{y} = \mathbf{u}_m) \Pr\{\mathbf{u}_m\}} = \frac{\sum\limits_{m=1}^{M=2^K} u_{m,k}\, \mathrm{p}(\mathbf{e} - \mathbf{u}_m)}{\sum\limits_{m=1}^{M=2^K} \mathrm{p}(\mathbf{e} - \mathbf{u}_m)} \ , \tag{4.41}$$

where equal a-priori probabilities $\Pr\{\mathbf{u}_m\}$ are assumed. The required PDF

$$\mathrm{p}(\mathbf{e}|\mathbf{y} = \mathbf{u}_m) = \mathrm{p}(\mathbf{e} - \mathbf{u}_m) = \mathrm{p}(\mathbf{n}) \tag{4.42}$$

in (4.41) can be calculated from (4.32) which is derived from the realistic noise statistic model with the exponentially correlated multivariate Chi-square distributed noise variances. In this way, the optimum nonlinear MMSE detector exploiting the knowledge of the given alphabet of the received useful vector and the statistical knowledge of noise is implemented to minimize the mean square error, i.e., to maximize the output SNR.

The performance of the proposed optimum nonlinear MMSE detector with statistical knowledge of noise variance is assessed with the help of some numerical results. Data transmission applying BPSK modulation in a two-user OFDM system allocating a single subcarrier to each user with noise coming from two noise sources is considered, i.e., $K = 2$ and $N = 2$ are assumed in (4.32) for the PDF of the noise vector. In order to obtain numerical results, a truncation of the infinite series in (4.32) is made to the first I terms. It can be verified that the error Δ_I resulting from the truncation can meet any desired accuracy when I is large enough [WWKK08]. The PDF of the noise vector is shown in Figure 4.7 considering the first $I = 60$ terms of the infinite series in (4.32). Exploiting the obtained PDF of the noise and the data alphabet of the useful signal in the proposed optimum nonlinear MMSE detector, the received useful signal estimate $\hat{y}_1$ as a function of the received signals e_1 and e_2 which is described by (4.41) is plotted in Figure 4.8. Since the noise signals in different subcarriers are correlated with each other as a result of their exponentially correlated noise variances, the estimate $\hat{y}_1$ of the useful signal in subcarrier 1 depends not only on the received signal e_1 in subcarrier 1, but also on the received signal e_2 in subcarrier 2. As one special case of correlated noise variances, the case of the same noise variance in all the subcarriers, i.e., $\sigma_k^2 = \sigma^2$, is considered in Figure 4.9. The numerical results with respect to the cumulative distribution functions (CDFs) of the SNR $\gamma_{\mathrm{out}}^{(1)}$ are shown in Figure 4.9. It can be seen that the proposed detector exploiting the PDF of the noise variance clearly outperforms the conventional detector with separately estimated noise variance.

The above optimum nonlinear MMSE detection can be easily extended to other applications in the field of multiuser detection. Especially, the principle of this proposal can

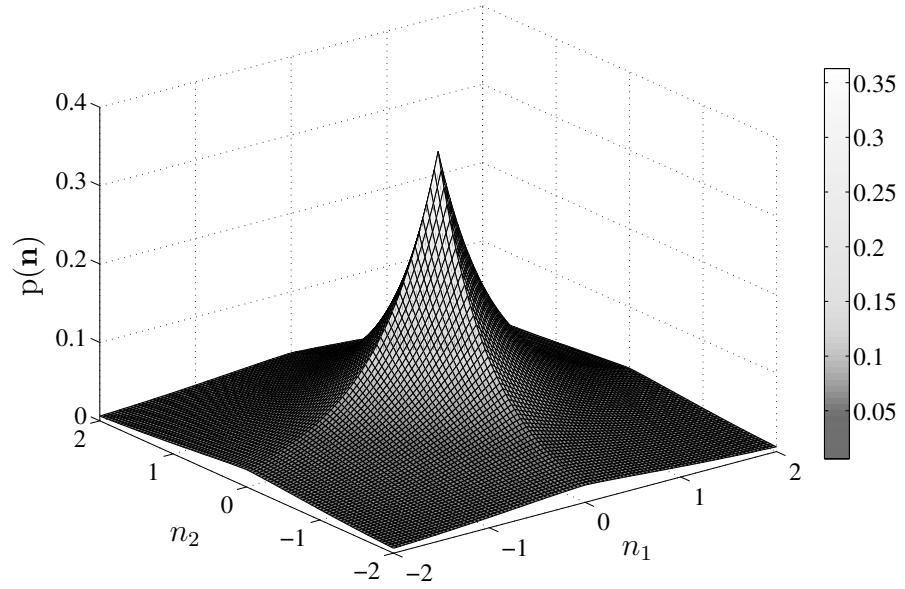

Figure 4.7. PDF of the noise with exponentially correlated noise variance with multivariate Chi-square distribution with $N = 2$ degrees of freedom, $\rho = 0.9$, $I = 60$.

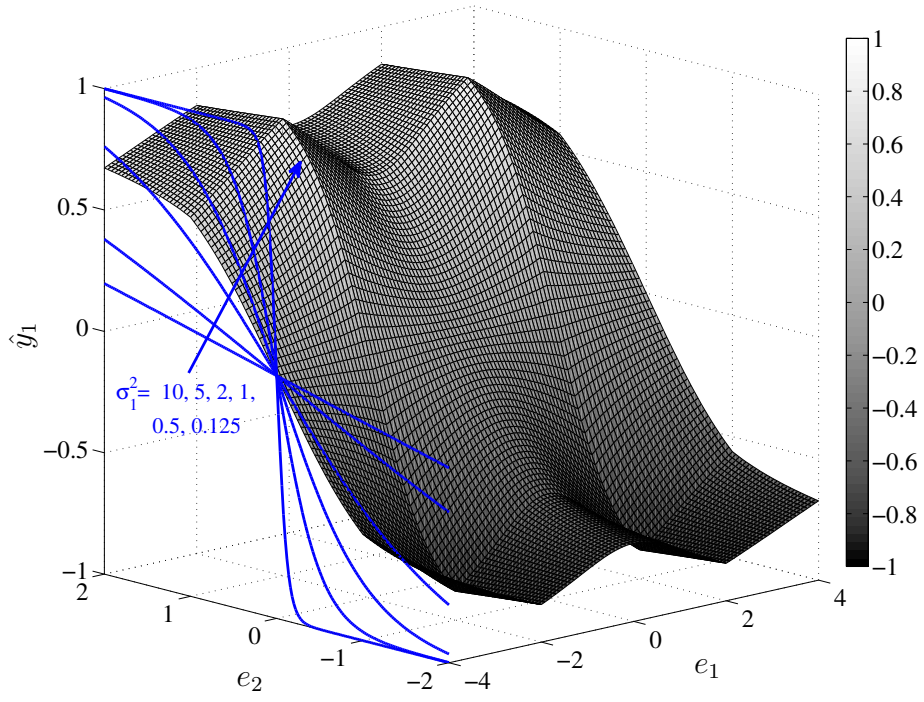

Figure 4.8. The received useful signal estimate $\hat{y}_1$ as a function of the received signals e_1 and e_2 with the known PDF $\mathrm{p}(\sigma_1^2, \sigma_2^2)$ with parameters $\Omega = 1$, $N = 2$, $K = 2$, $h_1 = 1$, $h_2 = 2$, $\rho = 0.9$, $I = 60$ and that with known noise variance $\sigma_1^2 = 10, 5, 2, 1, 0.5, 0.125$.

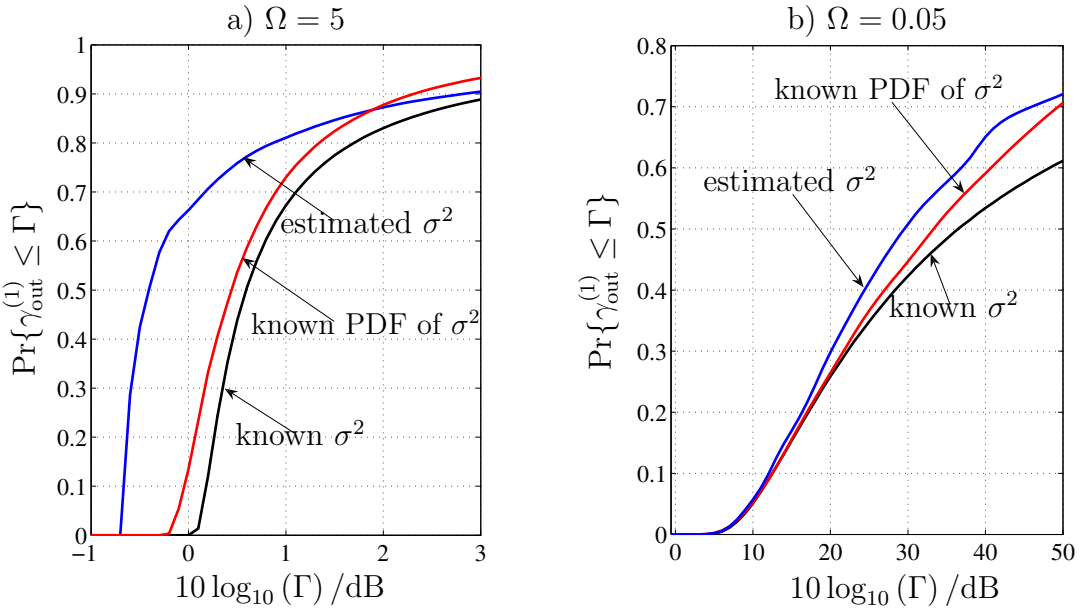

Figure 4.9. CDFs of $\gamma_{\text{out}}^{(1)}$ for the nonlinear MMSE detector with known σ^2, the conventional nonlinear MMSE detector with separately estimated σ^2, and the nonlinear MMSE detector with known PDF of σ^2. Parameters: $K = 2$, $N = 2$, $h_1 = 1, h_2 = 2$.

be applied in the data estimate refinement for the iterative multiuser receiver. In the data estimate refinement, instead of the hard quantization technique, the soft quantization technique which exploits the soft information could significantly reduce the risk of error propagation and improve the system performance.

Optimum ML multiuser detection in IC with cooperative receivers exploiting statistical knowledge of imperfect CSI

Conventional multiuser detection techniques are designed under the assumption that perfect deterministic CSI is available [Ver98, TV05]. However, this assumption is quite unrealistic considering the limited ability to track the CSI in realistic systems. In recent years, researchers have paid more and more attention to the influence of imperfect CSI on data detection in MIMO systems. Some improved suboptimum detection techniques taking channel errors into consideration have been proposed [DKZ08, WSM06, FF08, Tar07, Cho08]. In order to improve the system performance with limited knowledge of CSI, an optimum multiuser detection following the ML rationale exploiting the statistical knowledge of the imperfect CSI, i.e., the PDF of the channel coefficients and the PDF of the channel errors, is proposed in the following. The benefits of this proposal are also demonstrated.

For the sake of simplicity, a two-user real-valued IC with cooperative receivers is taken

as an exemplary system model for investigation. Applying BPSK modulation, uniformly distributed transmitted signals $s_k \in \mathbb{S} = \{-1; +1\}$, $k = 1, 2$ are considered in the transmitted vector $\mathbf{s} = (s_1, s_2)^{\mathrm{T}}$. Gaussian distributed noise signals, i.e., $n_k \sim \mathcal{N}(0, \sigma_{\mathrm{n}}^2)$, $k = 1, 2$, are assumed in the noise vector $\mathbf{n} = (n_1, n_2)^{\mathrm{T}}$. As for the channel model, two types of fading channels are investigated. In the channel model of type I, the channel coefficients $h_{ij} \sim \mathcal{N}(0, \sigma_{h_{ij}}^2)$, i=1, 2, j=1, 2, with the same zero mean and individual variances are considered. In the channel model of type II, the channel coefficients $h_{ij} \sim \mathcal{N}(\mu_{ij}, \sigma_h^2)$, i=1, 2, j=1, 2, with individual non-zero means and the same variance are considered. Let $\mathbf{h} = (h_{11}, h_{21}, h_{12}, h_{22})^{\mathrm{T}}$ denote the channel vector. Without loss of generality, the PDF of the CSI corresponding to the above mentioned two types of fading channels can be written as

$$\mathrm{p}(\mathbf{h}) = \prod_{i,j} \mathrm{p}(h_{ij}) = \frac{\exp\left(-\frac{1}{2}\sum\limits_{i,j}\frac{(h_{ij}-\mu_{ij})^2}{\sigma_{h_{ij}}^2}\right)}{(2\pi)^2 \prod\limits_{i,j}\sigma_{h_{ij}}}, \; i = 1, 2; \; j = 1, 2 \; . \tag{4.43}$$

Let

$$\underline{\mathbf{H}} = \begin{pmatrix} h_{11} & h_{12} \\ h_{21} & h_{22} \end{pmatrix} \tag{4.44}$$

denote the channel matrix. The received vector $\mathbf{e} = (e_1, e_2)^{\mathrm{T}}$ is given by

$$\mathbf{e} = \mathbf{H} \cdot \mathbf{s} + \mathbf{n} \; . \tag{4.45}$$

At the receiver with different levels of knowledge of the CSI, different data detection techniques can be applied. When perfect deterministic instantaneous CSI is available to the cooperative receivers in the considered two-user IC, the optimum multiuser detector with respect to the bit error rate (BER) is obtained following the ML rationale as

$$\hat{\mathbf{s}} = \underset{\mathbf{s} \in \mathbb{S}^2}{\operatorname{argmax}} \left\{ \mathrm{p}(\mathbf{e}|\mathbf{s}, \mathbf{h}) \right\} \tag{4.46}$$

exploiting the given alphabet $\mathbb{S}^2$ of the transmitted vector with $\mathbb{S} = \{-1; +1\}$ and the PDF

$$\mathrm{p}(\mathbf{e}|\mathbf{s}, \mathbf{h}) = \frac{\exp\left(-\frac{1}{2\sigma_{\mathrm{n}}^2}\left[(e_1 - h_{11}s_1 - h_{12}s_2)^2 + (e_2 - h_{21}s_1 - h_{22}s_2)^2\right]\right)}{\left(\sqrt{2\pi\sigma^2}\right)^2} \; . \tag{4.47}$$

However, in most realistic systems only imperfect instantaneous CSI is available to the receivers, and the above detection technique directly applying the estimated channel vector $\hat{\mathbf{h}}$ instead of the perfect channel vector $\mathbf{h}$ will be degraded to a suboptimum solution. Fortunately, although the perfect knowledge of instantaneous CSI is difficult to be obtained in realistic systems, the statistical knowledge of imperfect CSI

can be easily obtained by the receiver with moderate effort. Based on the measured and empirical data, it is reasonable to assume that the channel errors are identically independent Gaussian distributed, i.e., $\delta_{h_{ij}} = (\hat{h}_{ij} - h_{ij}) \sim \mathcal{N}(0, \sigma_\Delta^2)$, i=1, 2; j=1, 2. Therefore, the PDF of the imperfect CSI conditioned on the perfect CSI is obtained from the distribution of the channel errors as

$$\mathrm{p}(\hat{\mathbf{h}}|\mathbf{h}) = \prod_{i,j} \mathrm{p}(\hat{h}_{ij} - h_{ij}) = \frac{\exp\left(-\frac{1}{2}\sum\limits_{i,j}\frac{(\hat{h}_{ij}-h_{ij})^2}{\sigma_\Delta^2}\right)}{\left(\sqrt{2\pi\sigma_\Delta^2}\right)^4}, \; i = 1, 2; \; j = 1, 2 \; . \tag{4.48}$$

An optimum detection scheme exploiting the limited statistical knowledge of imperfect CSI is proposed for realistic systems as

$$\hat{\mathbf{s}} = \underset{\mathbf{s}\in\mathbb{S}}{\operatorname{argmax}} \left\{ \mathrm{p}\left(\mathbf{e}|\mathbf{s}, \hat{\mathbf{h}}\right) \right\} \quad , \tag{4.49}$$

where $\mathrm{p}\left(\mathbf{e}|\mathbf{s}, \hat{\mathbf{h}}\right)$ is calculated as the marginal PDF of $\mathrm{p}\left(\mathbf{e}, \mathbf{h}|\mathbf{s}, \hat{\mathbf{h}}\right)$ using (4.47) as

$$\mathrm{p}\left(\mathbf{e}|\mathbf{s}, \hat{\mathbf{h}}\right) = \int \mathrm{p}\left(\mathbf{e}, \mathbf{h}|\mathbf{s}, \hat{\mathbf{h}}\right) \mathrm{d}\mathbf{h} = \int \mathrm{p}\left(\mathbf{e}|\mathbf{s}, \mathbf{h}\right) \mathrm{p}(\mathbf{h}|\hat{\mathbf{h}}) \mathrm{d}\mathbf{h} \; . \tag{4.50}$$

The required PDF $\mathrm{p}(\mathbf{h}|\hat{\mathbf{h}})$ in (4.50) can be calculated according to the Bayes' theorem using (4.43) and (4.48) as

$$\mathrm{p}(\mathbf{h}|\hat{\mathbf{h}}) = \frac{\mathrm{p}(\hat{\mathbf{h}}|\mathbf{h})\mathrm{p}(\mathbf{h})}{\int \mathrm{p}(\hat{\mathbf{h}}|\mathbf{h})\mathrm{p}(\mathbf{h})\mathrm{d}\mathbf{h}} \; . \tag{4.51}$$

The system performance is assessed based on numerical simulation results taking the BER as the performance criterion. The simulation results in Figure 4.10 correspond to the fading channel model of type I with the same zero-mean $\mu = 0$ but different variances $\sigma_{h_{ij}}^2$, i.e., $h_{11} \sim \mathcal{N}(0, 1000)$, $h_{21} \sim \mathcal{N}(0, 0.1)$, $h_{12} \sim \mathcal{N}(0, 0.0001)$, $h_{22} \sim \mathcal{N}(0, 100000)$. The simulation results in Figure 4.11 correspond to the fading channel model of type II with the same variance $\sigma_h^2 = 0.1$ but different nonzero-mean values μ_{ij}, i.e., $h_{11} \sim \mathcal{N}(1, 0.1)$, $h_{21} \sim \mathcal{N}(0.001, 0.1)$, $h_{12} \sim \mathcal{N}(0.001, 0.1)$, $h_{22} \sim \mathcal{N}(1, 0.1)$. In Figure 4.10 and Figure 4.11, the system performance of ZF, i.e., $\hat{\mathbf{s}} = \mathrm{sign}\left\{ \left(\hat{\mathbf{H}}^{\mathrm{T}}\hat{\mathbf{H}}\right)^{-1}\hat{\mathbf{H}}^{\mathrm{T}} \cdot \mathbf{e} \right\}$ applying the estimated channel matrix $\hat{\mathbf{H}}$, the suboptimum detection following the ML rationale in (4.46) but applying the estimated channel vector $\hat{\mathbf{h}}$ instead of $\mathbf{h}$, and the optimum detection described by (4.49) exploiting the statistical knowledge of imperfect CSI in (4.50) are compared. Numerical results clearly indicate how much the optimum data detection scheme outperforms other data detection schemes as a function of the extent of perfectness of CSI indicated by $10\log_{10}(1/\sigma_\Delta^2)$ and the pseudo-signal-to-noise-ratio (PSNR) indicated by $10\log_{10}(1/\sigma^2)$.

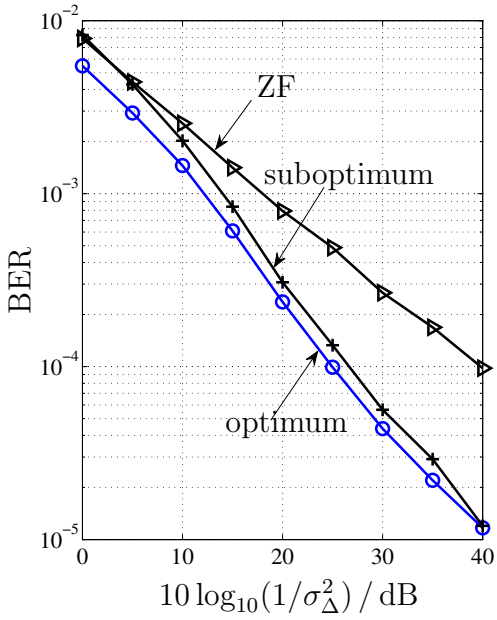

(a) BER as a function of the extent of the perfectness of CSI, parameter: $10\log_{10}(1/\sigma^2) = 40\,\text{dB}$

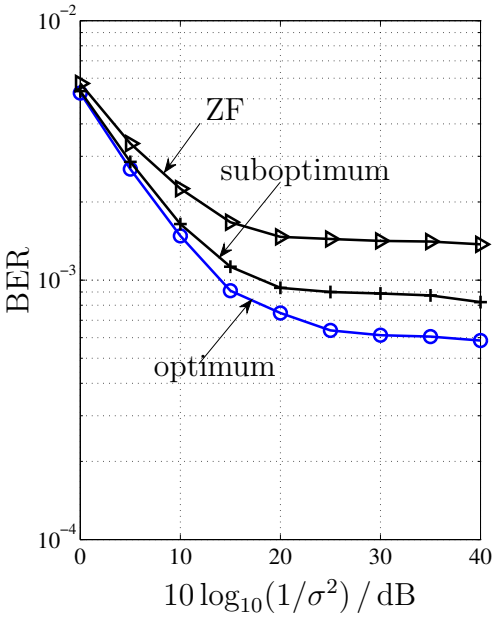

(b) BER as a function of PSNR, parameter: $10\log_{10}(1/\sigma_\Delta^2) = 15\,\text{dB}$

Figure 4.10. BER versus the extent of the perfectness of CSI and PSNR in the fading channel model of type I applying different data detection techniques.

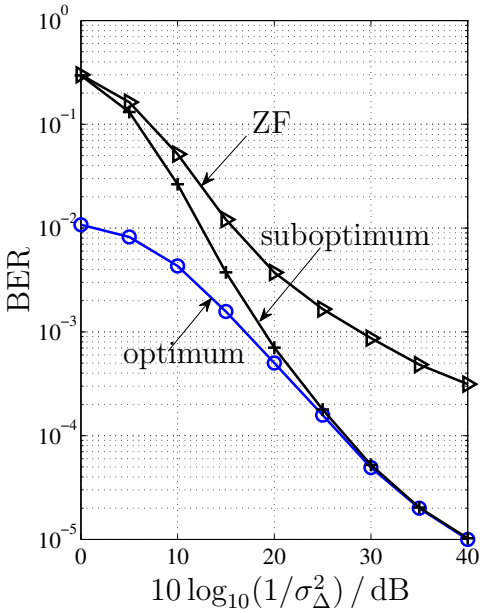

(a) BER as a function of the extent of the perfectness of CSI, parameter: $10\log_{10}(1/\sigma^2) = 40\,\text{dB}$

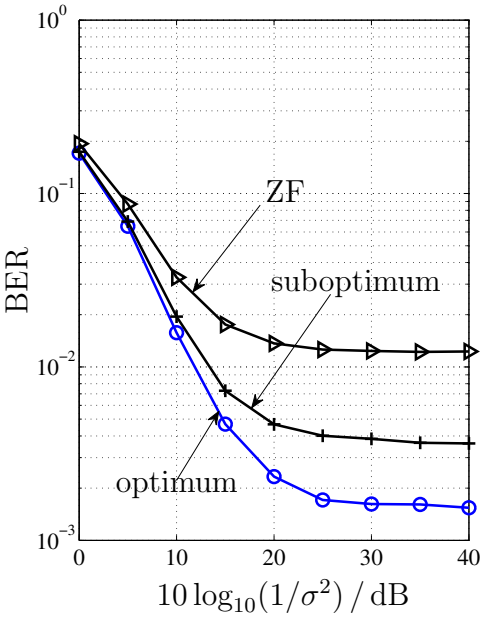

(b) BER as a function of PSNR, parameter: $10\log_{10}(1/\sigma_\Delta^2) = 15\,\text{dB}$

Figure 4.11. BER versus the extent of the perfectness of CSI and PSNR in the fading channel model of type II applying different data detection techniques.

4.3 Practical cooperative reception scheme

4.3.1 Design guidelines and framework

Now let us turn to the topic of high interest about the practical realization of cooperative communication in future mobile radio cellular systems. According to the above theoretical investigations in the present thesis, some design guidelines are derived taking the practical constraints in realistic systems such as the implementation complexity and the ability to track CSI into consideration. Without loss of generality, the following design guidelines are suitable for both the cooperative reception scheme in the UL and the cooperative transmission scheme in the DL.

- Information-theoretic results in Chapter 3 show that the cooperative communication scheme can significantly enlarge the achievable rate region as compared to the scheme with no cooperation. At some operating points of interest, the cooperative communication scheme considering appropriately selected partial CSI still achieves good system performance with little capacity loss. These information-theoretic results encourage us to perform the multi-cell cooperative signal processing for interference management in realistic cellular systems. The practical cooperative communication scheme should make a good compromise between system performance and implementation complexity. In practice, JD with significant CSI is applied in the UL to implement cooperative reception, and JT with significant CSI is applied in the DL to implement cooperative transmission.

- The significant CSI corresponding to the selected significant channels is considered in JD/JT. Different from various state of the art significant channel selection strategies as mentioned in Section 1.3, a practical dynamic MS-oriented significant channel selection strategy is proposed. Exploiting a limited amount of CSI for each MS, the channels which really play a significant role in the system performance are selected as the significant channels for this MS. In most realistic scenarios, for each MS the significant channels which are not necessarily limited in a fixed structure-oriented small subsystem still exist in this MS's own cell and adjacent cells around it. Therefore, in practice for each MS a MS-oriented subsystem with a moderate size can be firstly defined. Then, the dynamic MS-oriented significant channel selection scheme proposed in [WWAD07, WWWS09] can be performed in every MS-oriented subsystem.

- Concerning multiuser detection algorithms for JD and multiuser transmission algorithms for JT, only the ones which are able to achieve the required system performance with moderate implementation complexity in an interference-limited

cellular system are suitable choices. Generally, JD/JT can be implemented in a centralized or decentralized way. In the centralized scheme, joint signal processing is performed in a CU which coordinates all the BSs connected to it via backhaul links. In the decentralized scheme, distributed cooperative signal processing without a CU is performed at the coordinated BSs. The neighboring cooperative BSs are directly connected with each other via backhaul links. The backhaul links could be high-speed optical fibers or directed point-to-point radio links. An efficient JD/JT scheme based on a suitable implementation architecture which can make full use the MS-oriented significant CSI is expected.

- The system performance of the cooperative communication scheme varies with different smart BS-antenna-layouts introduced in Chapter 2. Furthermore, the system performance could be significantly influenced by the imperfectness of CSI due to the limited ability to track the CSI in reality. In a word, a systematic design of a practical cooperative communication should jointly take the signal processing algorithm, the significant channel selection strategy, the implementation architecture, the BS-antenna-layout, and the impact of imperfect channel knowledge into consideration.

Based on the above design guidelines, the flow of the CSI in the general framework of a practical cooperative communication scheme gradually shows up in Figure 4.12. The functionalities of the main steps in the CSI flow and the corresponding CSI to be obtained or that to be applied in every step are described as follows:

(1) Step 1: System initialization is performed. Namely, the cooperative multiuser OFDM-MIMO system in every single subcarrier is established from the following main aspects:

- Applying the OFDM transmission technique, all the intracell interference can be avoided, and only intercell interference is left to be dealt with.
- It is sufficient to investigate a single subcarrier with one active MS per cell at each time slot. The active MS can be selected through random scheduling or adaptive scheduling techniques according to different criteria.
- The BSs can be designed with smart BS-antenna-layouts such as the omni-DAS, the sector-DAS I, and the sector-DAS II as introduced in Section 2.3.
- The infrastructure of coordinated BSs is established by connecting neighboring BSs through backhaul links. In practice, a certain protocol for backhaul communications has to be considered.

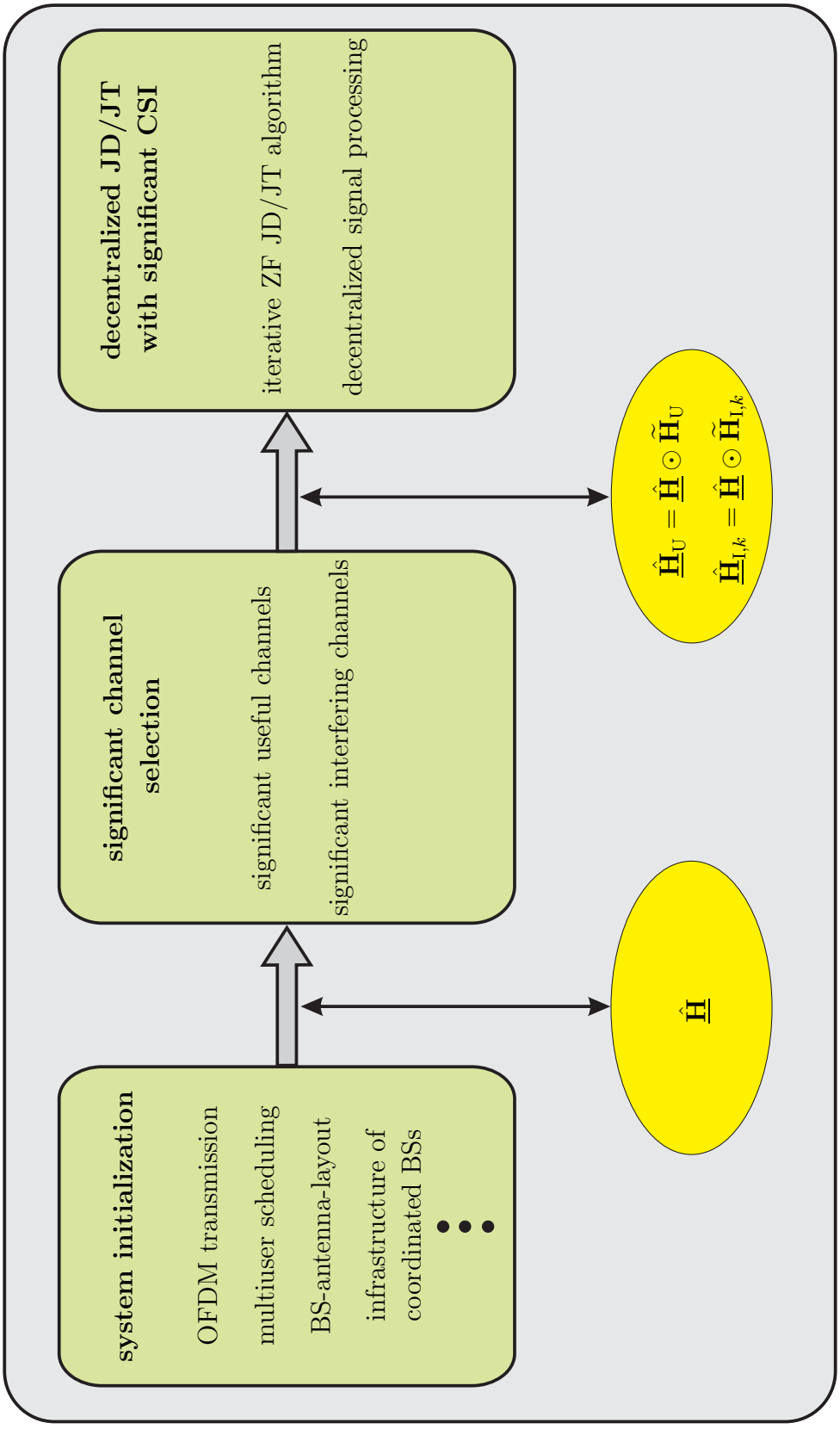

Figure 4.12. The CSI flow in the general framework of cooperative communication.

From the point of view of the channel knowledge, the goal of this step is to obtain the estimated full channel matrix $\underline{\hat{\mathbf{H}}}$ for the considered active MSs in the investigated single subcarrier based on various system setup decisions.

(2) Step 2: Significant channels with respect to the significant useful channels and the significant interfering channels for each MS are selected. Without loss of generality, this selection is performed in one single subcarrier of a K-cell cellular system. As a result, the selection can be mathematically represented by the significant useful channel indicator matrix $\widetilde{\mathbf{H}}_{\mathrm{U}}$ for all the MSs and the MS-specific significant interfering channel indicator matrices $\widetilde{\mathbf{H}}_{\mathrm{I},k}$ for individual MSs k, $k = 1, \ldots, K$.

From the point of view of the channel knowledge, the goal of this step is to obtain the estimated significant useful channel matrix $\underline{\hat{\mathbf{H}}}_{\mathrm{U}}$ for all the MSs and the estimated MS-specific significant interfering channel matrices $\underline{\hat{\mathbf{H}}}_{\mathrm{I},k}$ for individual MSs k from the estimated full channel matrix $\underline{\hat{\mathbf{H}}}$ as:

$$\underline{\hat{\mathbf{H}}}_{\mathrm{U}} = \underline{\hat{\mathbf{H}}} \odot \widetilde{\mathbf{H}}_{\mathrm{U}} \tag{4.52}$$

$$\underline{\hat{\mathbf{H}}}_{\mathrm{I},k} = \underline{\hat{\mathbf{H}}} \odot \widetilde{\mathbf{H}}_{\mathrm{I},k} \ . \tag{4.53}$$

The operator $\odot$ denotes the element-wise multiplication of two matrices.

(3) Step 3: The decentralized cooperative signal processing considering the estimated CSI of the significant channels is performed at the coordinated BSs.

- Theoretically, the iterative ZF JD algorithm with partial CSI focusing on interference cancellation is applied for cooperative reception in the UL. The iterative ZF JT algorithm with partial CSI focusing on interference presubstraction is applied for cooperative transmission in the DL.
- In practice, the signal processing following the above algorithms is implemented in a decentralized way based on the infrastructure of coordinated BSs. The signal processing for all MSs is simultaneously performed at the involved BSs corresponding to the significant channels. Intermediate results are exchanged between those BSs during the signal processing.

From the point of view of the channel knowledge, this step applies the estimated significant CSI included in the partial channel matrices $\underline{\hat{\mathbf{H}}}_{\mathrm{U}}$ and $\underline{\hat{\mathbf{H}}}_{\mathrm{I},k}$ in the signal processing.

Paying attention to the practical issues in realistic cellular systems, the present thesis reconsiders the concept of cooperative communication from a point of view of partial CSI, i.e., significant CSI and imperfect CSI. As the key contributions in the proposed

practical cooperative communication scheme, the significant channel selection in Step 2 will be discussed in detail for the UL in Section 4.3.2 and for the DL in Section 5.3.2. The decentralized signal processing with significant CSI in Step 3 will be discussed in detail for the UL in Section 4.3.3 and for the DL in Section 5.3.3. The system performance of the proposed cooperative communication scheme will be assessed in Chapter 6, where the impact of the imperfectness of CSI will also be evaluated. Additionally, diversity techniques which are beyond the scope of the present thesis can be applied when no knowledge of CSI is available.

4.3.2 Significant channel selection

Without loss of generality, the following significant channel selection is performed in a K-cell cellular system. This investigated system could also be a subsystem in a very large cellular system. Based on the system model of Chapter 2, one BS with N_{A} antennas and one MS with a single antenna are considered in each cell. Altogether $K_{\mathrm{A}} = N_{\mathrm{A}} \cdot K$ antennas at the BS side and K antennas at the MS side are considered. The UL channel matrix $\underline{\mathbf{H}}_{\mathrm{UL}} = \underline{\mathbf{H}}$ of this K-cell system is of dimensions $K_{\mathrm{A}} \times K$.

Following the design guidelines in Section 4.3.1, the MS-oriented significant CSI is considered in the cooperative signal processing in order to maintain good system performance with reduced implementation complexity. The MS-oriented significant CSI is defined as the CSI of the significant channels which play a significant role in the system performance of each MS. The signal processing algorithm which has an influence on the system performance shall be taken into consideration in the design of the significant channel selection scheme. In the iterative ZF JD algorithm which will be described in Section 4.3.3 in detail, the matched filtering estimate for each MS is computed, and then the interfering signals are iteratively cancelled from this estimate. According to the functionality of the physical mobile radio channels in the UL data transmission, two types of significant channels for one MS can be distinguished from each other as follows:

- Significant useful channels for one MS in the UL are the channels over which we get significant useful contributions when we estimate the data symbols transmitted from this MS.

- Significant interfering channels for one MS in the UL are the channels over which we get significant interfering signals from other MSs when we receive the data symbols from this MS.

The useful channels for each MS k are the channels between this MS and all the BSs corresponding to the k-th column vector of the channel matrix $\underline{\mathbf{H}}$. In the formalism of the $K_{\mathrm{A}} \times K$ significant useful channel indicator matrix $\widetilde{\mathbf{H}}_{\mathrm{U}}$, "1"s are assigned to the positions corresponding to the selected significant useful channels for each MS k in the k-th column of $\widetilde{\mathbf{H}}_{\mathrm{U}}$. The left positions in each column k are occupied by "0"s indicating insignificant useful channels for MS k. Obviously, a single matrix $\widetilde{\mathbf{H}}_{\mathrm{U}}$ is sufficient to represent all the significant useful channels for all the MSs.

The interfering channels for each MS k are the channels between other MSs and all the BSs corresponding to the channel coefficients in the channel matrix $\underline{\mathbf{H}}$ exclusive of the k-th column. A significant interfering channel for one MS could be considered as an insignificant interfering channel for another MS. Therefore, it is reasonable to separately represent the significant interfering channels for individual MSs k by individual matrices $\widetilde{\mathbf{H}}_{\mathrm{I},k}$ of dimensions $K_{\mathrm{A}} \times K$ named as the MS-specific significant interfering channel indicator matrices. Furthermore, for each MS there are some channels irrelevant to the interference considered in the proposed cooperative communication scheme. Corresponding to these channels, there are two kinds of "don't care" elements in each $\widetilde{\mathbf{H}}_{\mathrm{I},k}$. One kind of the "don't care" elements are the elements in the k-th column of $\widetilde{\mathbf{H}}_{\mathrm{I},k}$ denoting the useful channels for MS k. The other kind of "don't care" elements are the elements in the rows corresponding to the insignificant useful channels for this MS k in $\widetilde{\mathbf{H}}_{\mathrm{I},k}$. At the BS antennas corresponding to the insignificant useful channels for one MS k, the received signals will not be considered for this MS k in the proposed JD scheme with significant CSI. Therefore, it is not necessary to consider the interfering channels linked to these BS antennas for MS k. Excluding the "don't care" elements, the CSI of the left channels is exploited to determine the significant interfering channels. In the MS specific significant interfering channel indicator matrix $\widetilde{\mathbf{H}}_{\mathrm{I},k}$, "1"s are assigned to the positions corresponding to the selected significant interfering channels for MS k. "0"s are assigned to the positions corresponding to the insignificant interfering channels for MS k. It doesn't matter which values are assigned into the positions of the "don't care" elements.

Two mathematical criteria for the significant channel selection, i.e., Criterion-I and Criterion-II, are considered. Taking the channel group including all the channels between all the antennas of one BS and one MS as the selection unit, Criterion-I is described as follows. Let $\mathbb{S}_{k_{\mathrm{B}}}$ denote the set of indices of the antennas k_{A} which belong to the BS k_{B}. For each MS k, a channel with the channel coefficient $\underline{H}^{(k_{\mathrm{A}},k)}$ is selected as a significant useful channel if the channel group gain $\sum_{\forall k_{\mathrm{A}} \in \mathbb{S}_{k_{\mathrm{B}}}} |\underline{H}^{(k_{\mathrm{A}},k)}|^2$ covers a significant portion of the sum of all useful channel energies for this MS $\sum_{k_{\mathrm{B}}} \sum_{\forall k_{\mathrm{A}} \in \mathbb{S}_{k_{\mathrm{B}}}} |\underline{H}^{(k_{\mathrm{A}},k)}|^2$. Let $\mathbb{B}_k$ denote the set of indices of BSs k_{B} corresponding to the selected significant useful channel groups for each MS k. For each MS k,

Algorithm-I to obtain $\widetilde{\mathbf{H}}_{\mathrm{U}}$

1. $\widetilde{\mathbf{H}}_{\mathrm{U}} = \mathbf{0}^{K_{\mathrm{A}} \times K}$, $\mathbf{u} = \mathbf{0}^{K_{\mathrm{B}} \times 1}$
2. **for** $k = 1, \ldots, K$ **do**
3. $\quad \mathbb{B}_k = \emptyset$, $\mathbb{K}_{\mathrm{B}} = \{1, \ldots, K_{\mathrm{B}}\}$
4. $\quad$ **for** $k_{\mathrm{B}} = 1, \ldots, K_{\mathrm{B}}$ **do**
5. $\quad\quad u^{(k_{\mathrm{B}})} = \sum_{\forall k_{\mathrm{A}} \in \mathbb{S}_{k_{\mathrm{B}}}} \left| \underline{\hat{H}}^{(k_{\mathrm{A}},k)} \right|^2$
6. $\quad$ **end for**
7. $\quad$ **for** $b = 1, \ldots, N_{\mathrm{UG}}$ **do**
8. $\quad\quad k_{\mathrm{B}} = \underset{c \in \mathbb{K}_{\mathrm{B}}}{\operatorname{argmax}}\ u^{(c)}$
9. $\quad\quad$ **for** $\forall\, k_{\mathrm{A}} \in \mathbb{S}_{k_{\mathrm{B}}}$ **do**
10. $\quad\quad\quad \widetilde{H}_{\mathrm{U}}^{(k_{\mathrm{A}},k)} = 1$
11. $\quad\quad$ **end for**
12. $\quad\quad \mathbb{K}_{\mathrm{B}} \leftarrow \mathbb{K}_{\mathrm{B}} - \{k_{\mathrm{B}}\}$
13. $\quad\quad \mathbb{B}_k \leftarrow \mathbb{B}_k + \{k_{\mathrm{B}}\}$
14. $\quad$ **end for**
15. **end for**

Algorithm-I to obtain $\widetilde{\mathbf{H}}_{\mathrm{I},k}$

1. $\widetilde{\mathbf{H}}_{\mathrm{I},k} = \mathbf{0}^{K_{\mathrm{A}} \times K}$, $\mathbf{U} = \mathbf{0}^{K_{\mathrm{B}} \times K}$, $\mathbb{K}_{\mathrm{I}} = \emptyset$, $\mathbb{K}_{\bar{k}} = \{1, \ldots, (k-1), (k+1), \ldots, K\}$
2. **for** $\forall\, k' \in \mathbb{K}_{\bar{k}}$ **do**
3. $\quad$ **for** $\forall\, k_{\mathrm{B}} \in \mathbb{B}_k$ **do**
4. $\quad\quad U^{(k_{\mathrm{B}},k')} = \sum_{\forall k_{\mathrm{A}} \in \mathbb{S}_{k_{\mathrm{B}}}} \left| \underline{\hat{H}}^{(k_{\mathrm{A}},k)^*} \cdot \underline{\hat{H}}^{(k_{\mathrm{A}},k')} \right|$
5. $\quad\quad \mathbb{K}_{\mathrm{I}} \leftarrow \mathbb{K}_{\mathrm{I}} + \{(k_{\mathrm{B}}, k')\}$
6. $\quad$ **end for**
7. **end for**
8. **for** $b = 1, \ldots, N_{\mathrm{IG}}$ **do**
9. $\quad (k_{\mathrm{B}}, k') = \underset{(c_{\mathrm{B}},c') \in \mathbb{K}_{\mathrm{I}}}{\operatorname{argmax}}\ U^{(c_{\mathrm{B}},c')}$
10. $\quad$ **for** $\forall\, k_{\mathrm{A}} \in \mathbb{S}_{k_{\mathrm{B}}}$ **do**
11. $\quad\quad \widetilde{H}_{\mathrm{I},k}^{(k_{\mathrm{A}},k')} = 1$
12. $\quad$ **end for**
13. $\quad \mathbb{K}_{\mathrm{I}} \leftarrow \mathbb{K}_{\mathrm{I}} - \{(k_{\mathrm{B}}, k')\}$
14. **end for**

Figure 4.13. Algorithm-I according to Criterion-I for the significant channel selection.

a channel with the channel coefficient $\underline{H}^{(k_{\mathrm{A}},k')}$ is selected as a significant interfering channel if the channel group weighting factor magnitude $\sum_{\forall k_{\mathrm{A}} \in \mathbb{S}_{k_{\mathrm{B}}}} \left| \underline{H}^{(k_{\mathrm{A}},k)^*} \underline{H}^{(k_{\mathrm{A}},k')} \right|$ corresponding to the scaling of the interference in the matched filtering estimate covers a significant portion of the sum of the channel group weighting factor magnitudes $\sum_{k' \in \mathbb{K}_{\bar{k}}} \sum_{k_{\mathrm{B}} \in \mathbb{B}_k} \sum_{\forall k_{\mathrm{A}} \in \mathbb{S}_{k_{\mathrm{B}}}} \left| \underline{H}^{(k_{\mathrm{A}},k)^*} \underline{H}^{(k_{\mathrm{A}},k')} \right|$ for all the interferences to MS k, where $\mathbb{K}_{\bar{k}} = \{1, \ldots, k-1, k+1, \ldots, K\}$.

Taking the single channel between one BS antenna and one MS as the selection unit, Criterion-II is described as follows. Let $\mathbb{A}_k$ denote the set of indices of the BS antennas k_{A} corresponding to the selected significant useful channels for each MS k. For each MS k, a channel with the channel coefficient $\underline{H}^{(k_{\mathrm{A}},k)}$ is selected as a significant useful channel if the channel gain $|\underline{H}^{(k_{\mathrm{A}},k)}|^2$ covers a significant portion of the sum of all useful channel energies for this MS $\sum_{k_{\mathrm{A}}} |\underline{H}^{(k_{\mathrm{A}},k)}|^2$. For each MS k, a channel with the channel coefficient $\underline{H}^{(k_{\mathrm{A}},k')}$ is selected as a significant interfering channel if the channel weighting factor magnitude $\left| \underline{H}^{(k_{\mathrm{A}},k)^*} \underline{H}^{(k_{\mathrm{A}},k')} \right|$ corresponding to the scaling of the interference in the matched filtering estimate covers a significant portion of the sum of the channel weighting factor magnitudes $\sum_{k' \in \mathbb{K}_{\bar{k}}} \sum_{k_{\mathrm{A}} \in \mathbb{A}_k} \left| \underline{H}^{(k_{\mathrm{A}},k)^*} \underline{H}^{(k_{\mathrm{A}},k')} \right|$ for all the interferences to MS k, where $\mathbb{K}_{\bar{k}} = \{1, \ldots, k-1, k+1, \ldots, K\}$.

In reality, the available knowledge of CSI in the estimated channel matrix $\underline{\hat{\mathbf{H}}}$ is exploited to select the significant channels. Following the above criteria, only the channel magnitudes play a role in the significant channel selection. In practice, two efficient

Algorithm-II to obtain $\widetilde{\mathbf{H}}_{\mathrm{U}}$

1. $\widetilde{\mathbf{H}}_{\mathrm{U}} = \mathbf{0}^{K_{\mathrm{A}} \times K}$, $\mathbf{u} = \mathbf{0}^{K_{\mathrm{A}} \times 1}$
2. **for** $k = 1, \ldots, K$ **do**
3. $\quad \mathbb{A}_k = \emptyset$, $\mathbb{K}_{\mathrm{A}} = \{1, \ldots, K_{\mathrm{A}}\}$
4. $\quad$ **for** $k_{\mathrm{A}} = 1, \ldots, K_{\mathrm{A}}$ **do**
5. $\quad\quad u^{(k_{\mathrm{A}})} = \left| \underline{\hat{H}}^{(k_{\mathrm{A}},k)} \right|^2$
6. $\quad$ **end for**
7. $\quad$ **for** $a = 1, \ldots, N_{\mathrm{U}}$ **do**
8. $\quad\quad k_{\mathrm{A}} = \underset{c \in \mathbb{K}_{\mathrm{A}}}{\operatorname{argmax}}\ u^{(c)}$
9. $\quad\quad \widetilde{H}_{\mathrm{U}}^{(k_{\mathrm{A}},k)} = 1$
10. $\quad\quad \mathbb{K}_{\mathrm{A}} \leftarrow \mathbb{K}_{\mathrm{A}} - \{k_{\mathrm{A}}\}$
11. $\quad\quad \mathbb{A}_k \leftarrow \mathbb{A}_k + \{k_{\mathrm{A}}\}$
12. $\quad$ **end for**
13. **end for**

Algorithm-II to obtain $\widetilde{\mathbf{H}}_{\mathrm{I},k}$

1. $\widetilde{\mathbf{H}}_{\mathrm{I},k} = \mathbf{0}^{K_{\mathrm{A}} \times K}$, $\mathbf{U} = \mathbf{0}^{K_{\mathrm{A}} \times K}$, $\mathbb{K}_{\mathrm{I}} = \emptyset$, $\mathbb{K}_{\bar{k}} = \{1, \ldots, (k-1), (k+1), \ldots, K\}$
2. **for** $\forall\, k' \in \mathbb{K}_{\bar{k}}$ **do**
3. $\quad$ **for** $\forall\, k_{\mathrm{A}} \in \mathbb{A}_k$ **do**
4. $\quad\quad U^{(k_{\mathrm{A}},k')} = \left| \underline{\hat{H}}^{(k_{\mathrm{A}},k)^*} \cdot \underline{\hat{H}}^{(k_{\mathrm{A}},k')} \right|$
5. $\quad\quad \mathbb{K}_{\mathrm{I}} \leftarrow \mathbb{K}_{\mathrm{I}} + \{(k_{\mathrm{A}}, k')\}$
6. $\quad$ **end for**
7. **end for**
8. **for** $b = 1, \ldots, N_{\mathrm{I}}$ **do**
9. $\quad (k_{\mathrm{A}}, k') = \underset{(c_{\mathrm{A}},c') \in \mathbb{K}_{\mathrm{I}}}{\operatorname{argmax}}\ U^{(c_{\mathrm{A}},c')}$
10. $\quad \widetilde{H}_{\mathrm{I},k}^{(k_{\mathrm{A}},k')} = 1$
11. $\quad \mathbb{K}_{\mathrm{I}} \leftarrow \mathbb{K}_{\mathrm{I}} - \{(k_{\mathrm{A}}, k')\}$
12. **end for**

Figure 4.14. Algorithm-II according to Criterion-II for the significant channel selection.

algorithms, i.e., Algorithm-I according to Criterion-I and Algorithm-II according to Criterion-II, are proposed in Figure 4.13 and Figure 4.14, respectively. In Algorithm-I, the significant useful channel selection is performed by choosing N_{UG} significant useful channel groups with the maximum channel group energies for every MS. Excluding the "don't care" elements, the significant interfering channel selection is performed by choosing N_{IG} significant interfering channel groups with the maximum channel group weighting factor magnitudes of the interferences to every MS. In Algorithm-II, the significant useful channel selection is performed by choosing N_{U} significant useful channels with the maximum channel energies for every MS. Excluding the "don't care" elements, the significant interfering channel selection is performed by choosing N_{I} significant interfering channels with the maximum channel weighting factor magnitudes of the interferences to every MS. Suitable numbers N_{UG}, N_{IG}, N_{U} and N_{I} can be found based on some trial tests in different realistic scenarios.

Two MSs have compatible significant interfering channels if all the significant interfering channels selected for one MS will never be considered as insignificant interfering channels for the other MS. If all the MSs have compatible significant interfering channels, all the individual MS-specific significant interfering channel indicator matrices $\widetilde{\mathbf{H}}_{\mathrm{I},k}$ can be represented by one combined significant interfering channel indicator matrix $\widetilde{\mathbf{H}}_{\mathrm{I}}$. Details of the rules for this combination can be found in Table 4.1 with "1" indicating a significant channel, "0" indicating an insignificant channel, "$*$" indicating a "don't care" element and "incomp."(i.e., incompatible) indicating the case that two matrices are incompatible.

Table 4.1. Rules to determine the elements in $\widetilde{\mathbf{H}}_{\mathrm{I}}$ as the combination of $\widetilde{\mathbf{H}}_{\mathrm{I},k'}$ and $\widetilde{\mathbf{H}}_{\mathrm{I},k''}$.

$\widetilde{H}_{\mathrm{I},k''}^{(k_{\mathrm{A}},k)}$ \ $\widetilde{H}_{\mathrm{I},k'}^{(k_{\mathrm{A}},k)}$	$*$	0	1
$*$	$*$	0	1
0	0	0	incomp.
1	1	incomp.	1

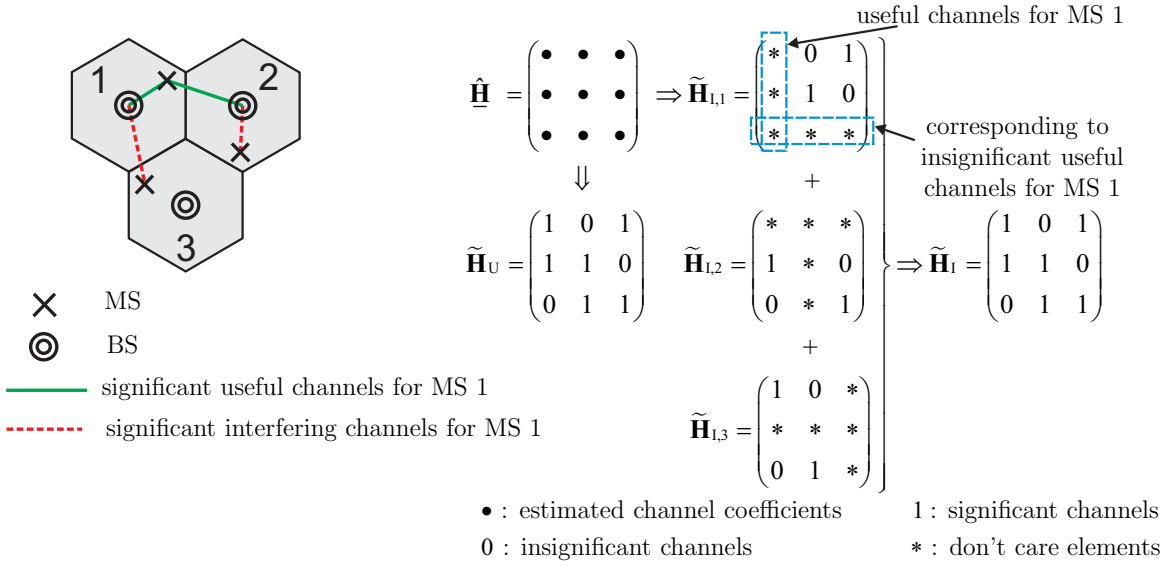

Figure 4.15. Example for the significant channel selection and the indicator matrix formalism.

In Figure 4.15, the proposed significant channel selection scheme and the corresponding significant channel indicator matrix formalism are visualized. For the sake of simplicity, a 3-cell omni-DAS with one antenna at each BS is used as an exemplary scenario. It is assumed that the relation between the channel magnitudes strongly depends on the corresponding distances between the MSs and the BSs. With one antenna per BS, Algorithm-I and Algorithm-II lead to the same selection results. Figure 4.15 can also be considered as an exemplary application of Algorithm-I with each position inside the matrices corresponding to one channel group. Depending on the number of antennas per BS, each group may contain one or several elements.

In practice, the effort to estimate and to collect the CSI in the above significant channel selection scheme can be maintained in a permissible level. On one side, only the roughly estimated channel magnitudes instead of the accurately estimated channel coefficients are required in the above selection. On the other side, it is not necessary to perform

the significant channel selection at every signal processing time slot. According to the characteristics of the time-variant mobile channels in the investigated scenario, in a certain time interval the cooperative signal processing could be performed based on the same significant channel selection result. A concrete working procedure of a practical cooperative reception scheme with the significant channel selection and the JD is proposed as follows:

1. **At every time interval ΔT:**
   Every BS roughly estimates the magnitudes of channels directly linked to it. After collecting the roughly estimated channel magnitudes from other BSs, the above described significant channel selection for every MS is presented.

2. **At every data transmission time slot $\Delta\tau$ inside the time interval ΔT:**
   Every BS precisely estimates the instantaneous CSI of the selected significant channels directly linked to it.

3. **At every signal processing time slot Δt inside the time slot $\Delta\tau$:**
   BSs cooperate with each other to perform JD with the estimated significant CSI.

4.3.3 Decentralized iterative ZF joint detection with partial CSI

In this section, the JD scheme is investigated from the aspects of the channel knowledge, the signal processing algorithm and the decentralized implementation architecture.

Concerning the channel knowledge, partial CSI with respect to the imperfect significant CSI is considered in JD. In reality the estimated CSI is applied in both the significant channel selection and the JD scheme. Knowing that the imperfectness of CSI may have an influence on the significant channel selection result, the present section focuses on the JD with partial CSI based on a given result of the significant channel selection. On one side, the significant CSI is extracted out of the full CSI according to the significant channel indicator matrices $\widetilde{\mathbf{H}}_{\mathrm{U}}$, $\widetilde{\mathbf{H}}_{\mathrm{I},k}$ and $\widetilde{\mathbf{H}}_{\mathrm{I}}$. On the other side, the CSI considered in JD is a part of the estimated channel coefficients included in the estimated channel matrix $\underline{\hat{\mathbf{H}}}$ consisting of the channel matrix $\underline{\mathbf{H}}$ and the channel error matrix $\underline{\boldsymbol{\Delta}}$ as described in (2.26). Consequently, the imperfect significant CSI considered in JD is obtained as follows. The estimated significant useful channel matrix in the UL is given by

$$\underline{\hat{\mathbf{H}}}_{\mathrm{UL,U}} = \underline{\hat{\mathbf{H}}}_{\mathrm{U}} = \underline{\hat{\mathbf{H}}} \odot \widetilde{\mathbf{H}}_{\mathrm{U}} = \underline{\mathbf{H}} \odot \widetilde{\mathbf{H}}_{\mathrm{U}} + \underline{\boldsymbol{\Delta}} \odot \widetilde{\mathbf{H}}_{\mathrm{U}} = \underline{\mathbf{H}}_{\mathrm{U}} + \underline{\boldsymbol{\Delta}}_{\mathrm{U}} \tag{4.54}$$

consisting of the significant useful channel matrix $\underline{\mathbf{H}}_{\mathrm{U}}$ and the significant useful channel error matrix $\underline{\boldsymbol{\Delta}}_{\mathrm{U}}$. The estimated MS-specific significant interfering channel matrices in the UL are given by

$$\hat{\underline{\mathbf{H}}}_{\mathrm{UL,I},k} = \hat{\underline{\mathbf{H}}}_{\mathrm{I},k} = \hat{\underline{\mathbf{H}}} \odot \widetilde{\mathbf{H}}_{\mathrm{I},k} = \underline{\mathbf{H}} \odot \widetilde{\mathbf{H}}_{\mathrm{I},k} + \underline{\boldsymbol{\Delta}} \odot \widetilde{\mathbf{H}}_{\mathrm{I},k} = \underline{\mathbf{H}}_{\mathrm{I},k} + \underline{\boldsymbol{\Delta}}_{\mathrm{I},k} \tag{4.55}$$

consisting of the MS-specific significant interfering channel matrices $\underline{\mathbf{H}}_{\mathrm{I},k}$ and the MS-specific significant interfering channel error matrices $\underline{\boldsymbol{\Delta}}_{\mathrm{I},k}$. The estimated combined significant interfering channel matrix in the UL is given by

$$\hat{\underline{\mathbf{H}}}_{\mathrm{UL,I}} = \hat{\underline{\mathbf{H}}}_{\mathrm{I}} = \hat{\underline{\mathbf{H}}} \odot \widetilde{\mathbf{H}}_{\mathrm{I}} = \underline{\mathbf{H}} \odot \widetilde{\mathbf{H}}_{\mathrm{I}} + \underline{\boldsymbol{\Delta}} \odot \widetilde{\mathbf{H}}_{\mathrm{I}} = \underline{\mathbf{H}}_{\mathrm{I}} + \underline{\boldsymbol{\Delta}}_{\mathrm{I}} \tag{4.56}$$

consisting of the combined significant interfering channel matrix $\underline{\mathbf{H}}_{\mathrm{I}}$ and the combined significant interfering channel error matrix $\underline{\boldsymbol{\Delta}}_{\mathrm{I}}$. The significant channel matrices $\underline{\mathbf{H}}_{\mathrm{U}}$, $\underline{\mathbf{H}}_{\mathrm{I},k}$ and $\underline{\mathbf{H}}_{\mathrm{I}}$ contain perfect channel coefficients of the significant channels from the perfect channel matrix $\underline{\mathbf{H}}$, "0"s corresponding to the insignificant channels, and the "don't care" elements. The significant channel error matrices $\underline{\boldsymbol{\Delta}}_{\mathrm{U}}$, $\underline{\boldsymbol{\Delta}}_{\mathrm{I},k}$ and $\underline{\boldsymbol{\Delta}}_{\mathrm{I}}$ contain the non-zero channel estimation errors of the significant channels from $\underline{\boldsymbol{\Delta}}$, "0"s corresponding to the insignificant channels, and the "don't care" elements.

Concerning the signal processing algorithm, the iterative ZF JD algorithm focusing on interference cancellation with partial CSI is proposed in the UL. This algorithm follows the idea of the PIC algorithm with full CSI as described in Section 4.2.3 but considers the estimated significant CSI in practice. The reasons why this algorithm is chosen for the practical cooperative reception scheme are as follows:

- As one practical multiuser detection strategy, the parallel iterative ZF algorithm has a moderate computational complexity as mentioned in Section 4.2.3.
- This algorithm follows the principle of interference cancellation, and therefore has a good performance in realistic interference-limited cellular systems.
- The parallel signal processing with MS-oriented significant CSI is suitable for a decentralized implementation based on the infrastructure of coordinated BSs.

Applying the significant CSI described by $\hat{\underline{\mathbf{H}}}_{\mathrm{UL,U}}$ given in (4.54) and by $\hat{\underline{\mathbf{H}}}_{\mathrm{UL,I},k}$ given in (4.55) in the PIC algorithm described by (4.12), the iterative partial ZF JD algorithm can be derived in the form of matrix-vector-notation as

$$\hat{\underline{\mathbf{d}}}(i) = \hat{\mathbf{G}}_{\mathrm{UL}}^{-1} \left(\hat{\underline{\mathbf{H}}}_{\mathrm{UL,U}}^{*\mathrm{T}} \cdot \underline{\mathbf{e}} - \overline{\mathrm{diag}} \left(\hat{\underline{\mathbf{R}}}_{\mathrm{UL}} \right) \cdot \hat{\underline{\tilde{\mathbf{d}}}}(i-1) \right) \quad . \tag{4.57}$$

In the above equation, the estimated channel gain scaling matrix $\hat{\mathbf{G}}_{\mathrm{UL}}$ is given as

$$\hat{\mathbf{G}}_{\mathrm{UL}} = \mathrm{diag} \left(\hat{\underline{\mathbf{H}}}_{\mathrm{UL,U}}^{*\mathrm{T}} \hat{\underline{\mathbf{H}}}_{\mathrm{UL,U}} \right) = \mathrm{diag} \left(\hat{\underline{\mathbf{H}}}_{\mathrm{U}}^{*\mathrm{T}} \hat{\underline{\mathbf{H}}}_{\mathrm{U}} \right) \quad , \tag{4.58}$$

and the estimated channel correlation matrix $\hat{\underline{\mathbf{R}}}_{\mathrm{UL}}$ is given as

$$\hat{\underline{\mathbf{R}}}_{\mathrm{UL}} = \begin{pmatrix} \left[\hat{\underline{\mathbf{H}}}_{\mathrm{UL,U}}\right]_1^{*\mathrm{T}} \hat{\underline{\mathbf{H}}}_{\mathrm{UL,I},1} \\ \vdots \\ \left[\hat{\underline{\mathbf{H}}}_{\mathrm{UL,U}}\right]_K^{*\mathrm{T}} \hat{\underline{\mathbf{H}}}_{\mathrm{UL,I},K} \end{pmatrix} = \begin{pmatrix} \left[\hat{\underline{\mathbf{H}}}_{\mathrm{U}}\right]_1^{*\mathrm{T}} \hat{\underline{\mathbf{H}}}_{\mathrm{I},1} \\ \vdots \\ \left[\hat{\underline{\mathbf{H}}}_{\mathrm{U}}\right]_K^{*\mathrm{T}} \hat{\underline{\mathbf{H}}}_{\mathrm{I},K} \end{pmatrix} , \tag{4.59}$$

where the matrix operator $[\cdot]_k$ returns the k-th column vector of its argument. The cooperative receivers applying the iterative JD algorithm described by (4.57) can be considered as a special case of the general iterative multiuser receiver in Figure 4.2. Correspondingly, the pre-filter matrix $\underline{\mathbf{P}}$, the forward filter matrix $\underline{\mathbf{F}}$ and the feedback filter matrix $\underline{\mathbf{B}}$ are:

$$\underline{\mathbf{P}} = \hat{\underline{\mathbf{H}}}_{\mathrm{UL,U}}^{*\mathrm{T}} = \hat{\underline{\mathbf{H}}}_{\mathrm{U}}^{*\mathrm{T}} \tag{4.60}$$

$$\underline{\mathbf{F}} = \hat{\mathbf{G}}_{\mathrm{UL}}^{-1} \tag{4.61}$$

$$\underline{\mathbf{B}} = \overline{\mathrm{diag}}\left(\hat{\underline{\mathbf{R}}}_{\mathrm{UL}}\right) . \tag{4.62}$$

Furthermore, in each iteration i various data estimate refinement techniques can be applied to obtain the refined estimated data vector $\hat{\hat{\underline{\mathbf{d}}}}(i)$ from the estimated data vector $\hat{\underline{\mathbf{d}}}(i)$. Knowing that a suitable data estimate refinement can further improve the system performance, firstly the iterative algorithm with the transparent data estimate refinement considering $\hat{\hat{\underline{\mathbf{d}}}}(i) = \hat{\underline{\mathbf{d}}}(i)$ is investigated. Without loss of generality, it can be treated as a benchmark for this iterative algorithm with different kinds of data estimate refinement techniques. In the case that the linear iterative algorithm of (4.57) with $\hat{\hat{\underline{\mathbf{d}}}}(i) = \hat{\underline{\mathbf{d}}}(i)$ converges and the matrix $\left(\hat{\mathbf{G}}_{\mathrm{UL}} + \overline{\mathrm{diag}}\left(\hat{\underline{\mathbf{R}}}_{\mathrm{UL}}\right)\right)$ has full rank, the formula for calculating the limiting value of the iterative partial ZF JD algorithm can be generally written as

$$\hat{\underline{\mathbf{d}}}(\infty) = \left(\hat{\mathbf{G}}_{\mathrm{UL}} + \overline{\mathrm{diag}}\left(\hat{\underline{\mathbf{R}}}_{\mathrm{UL}}\right)\right)^{-1} \hat{\underline{\mathbf{H}}}_{\mathrm{UL,U}}^{*\mathrm{T}} \cdot \underline{\mathbf{e}} . \tag{4.63}$$

Under special conditions, this formula can be simplified step by step in different cases as shown in the following:

- In the case that all the individual MS specific matrices $\hat{\underline{\mathbf{H}}}_{\mathrm{UL,I},k}$ can be combined to one channel matrix $\hat{\underline{\mathbf{H}}}_{\mathrm{UL,I}}$, one obtains

$$\hat{\underline{\mathbf{R}}}_{\mathrm{UL}} = \hat{\underline{\mathbf{H}}}_{\mathrm{UL,U}}^{*\mathrm{T}} \hat{\underline{\mathbf{H}}}_{\mathrm{UL,I}} = \hat{\underline{\mathbf{H}}}_{\mathrm{U}}^{*\mathrm{T}} \hat{\underline{\mathbf{H}}}_{\mathrm{I}} , \tag{4.64}$$

  and the limiting value of the iterative partial ZF JD algorithm is described by

$$\hat{\underline{\mathbf{d}}}(\infty) = \left(\hat{\mathbf{G}}_{\mathrm{UL}} + \overline{\mathrm{diag}}\left(\hat{\underline{\mathbf{H}}}_{\mathrm{U}}^{*\mathrm{T}} \hat{\underline{\mathbf{H}}}_{\mathrm{I}}\right)\right)^{-1} \hat{\underline{\mathbf{H}}}_{\mathrm{U}}^{*\mathrm{T}} \cdot \underline{\mathbf{e}}. \tag{4.65}$$

- In the above case, if the estimated significant interfering channel matrix $\hat{\underline{\mathbf{H}}}_{\mathrm{UL,I}}$ covers all the non-zero elements of the estimated significant useful channel matrix $\hat{\underline{\mathbf{H}}}_{\mathrm{UL,U}}$, one obtains

$$\hat{\mathbf{G}}_{\mathrm{UL}} = \mathrm{diag}\left(\hat{\underline{\mathbf{H}}}_{\mathrm{UL,U}}^{*\mathrm{T}}\hat{\underline{\mathbf{H}}}_{\mathrm{UL,U}}\right) = \mathrm{diag}\left(\hat{\underline{\mathbf{H}}}_{\mathrm{UL,U}}^{*\mathrm{T}}\hat{\underline{\mathbf{H}}}_{\mathrm{UL,I}}\right) = \mathrm{diag}\left(\hat{\underline{\mathbf{H}}}_{\mathrm{U}}^{*\mathrm{T}}\hat{\underline{\mathbf{H}}}_{\mathrm{I}}\right) \quad , \tag{4.66}$$

  and the limiting value of this iterative JD algorithm can be represented by

$$\hat{\underline{\mathbf{d}}}(\infty) = \left(\hat{\underline{\mathbf{H}}}_{\mathrm{U}}^{*\mathrm{T}}\hat{\underline{\mathbf{H}}}_{\mathrm{I}}\right)^{-1}\hat{\underline{\mathbf{H}}}_{\mathrm{U}}^{*\mathrm{T}} \cdot \underline{\mathbf{e}} \ . \tag{4.67}$$

- One special case is the iterative JD with estimated full CSI, for which

$$\hat{\underline{\mathbf{H}}}_{\mathrm{UL,U}} = \hat{\underline{\mathbf{H}}}_{\mathrm{UL,I}} = \hat{\underline{\mathbf{H}}}_{\mathrm{UL}} = \hat{\underline{\mathbf{H}}} \tag{4.68}$$

  holds, and the limiting value of this iterative JD algorithm is

$$\hat{\underline{\mathbf{d}}}(\infty) = \left(\hat{\underline{\mathbf{H}}}_{\mathrm{UL}}^{*\mathrm{T}}\hat{\underline{\mathbf{H}}}_{\mathrm{UL}}\right)^{-1}\hat{\underline{\mathbf{H}}}_{\mathrm{UL}}^{*\mathrm{T}} \cdot \underline{\mathbf{e}} = \left(\hat{\underline{\mathbf{H}}}^{*\mathrm{T}}\hat{\underline{\mathbf{H}}}\right)^{-1}\hat{\underline{\mathbf{H}}}^{*\mathrm{T}} \cdot \underline{\mathbf{e}} \ . \tag{4.69}$$

Concerning the signal processing architecture, a decentralized scheme instead of a centralized scheme is applied. The reasons for this choice are as follows:

- From the network operator's point of view, the change to the current architecture of cellular networks is expected as little as possible. Based on the existing networks, the proposed decentralized scheme requires only some extra backhaul links between the neighboring BSs will not cause much change.

- The decentralized implementation architecture can make full use of the proposed iterative ZF JD/JT algorithm. The joint signal processing of all the MSs can be distributed to a parallel cooperative signal processing of individual MSs at the coordinated BSs. The computational load is shared by the coordinated BSs to avoid the CU which has to make huge signaling efforts.

- As compared to the centralized scheme with every fixed CU being responsible for one fixed cooperative cluster, the flexible decentralized scheme can more efficiently make full use of the dynamically selected MS-oriented significant CSI. Although the significant channels for one MS are not necessarily limited to a static structure-oriented geographical area, but in most realistic scenarios they still exist in this MS's own cell and adjacent cells. Since only local significant CSI is considered at each BS in the decentralized scheme, only backhaul links connecting adjacent BSs and only the synchronization in the local area are required.

1. Initialization for the iterative signal processing of individual MSs k, $k=1,\ldots,K$, at their corresponding BSs $k_{\mathrm{B}}=k$ in parallel:
   a. Assign the channel gain scaling factor
   $$\hat{g}^{(k)} = \sum_{k_{\mathrm{A}}} \underline{\hat{H}}_{\mathrm{U}}^{(k_{\mathrm{A}},k)^*} \underline{\hat{H}}_{\mathrm{U}}^{(k_{\mathrm{A}},k)} = \sum_{k_{\mathrm{A}}} \left| \underline{\hat{H}}_{\mathrm{U}}^{(k_{\mathrm{A}},k)} \right|^2$$
   for every MS k at BS $k_{\mathrm{B}}=k$. $\hat{g}^{(k)}$ can be previously estimated in practice.
   b. Assign the initial value of the estimated data symbol for every MS k at BS $k_{\mathrm{B}}=k$
   $$\underline{\hat{d}}^{(k)}(0) = 0 \ .$$
2. Matched filtering for every MS k, $k=1,\ldots,K$, in parallel:
   a. Compute the matched filtering estimate components
   $$\underline{r}^{(k_{\mathrm{A}},k)} = \underline{\hat{H}}_{\mathrm{U}}^{(k_{\mathrm{A}},k)^*} \cdot \underline{e}^{(k_{\mathrm{A}})}$$
   for every MS k at the BSs corresponding to its significant useful channels.
   b. Collect $\underline{r}^{(k_{\mathrm{A}},k)}$ from coordinated BSs through the backhaul links, and sum them up together at BS $k_{\mathrm{B}}=k$ to obtain the matched filtering estimate for each MS k as
   $$\underline{r}^{(k)} = \sum_{k_{\mathrm{A}}} \underline{r}^{(k_{\mathrm{A}},k)} = \sum_{k_{\mathrm{A}}} \underline{\hat{H}}_{\mathrm{U}}^{(k_{\mathrm{A}},k)^*} \cdot \underline{e}^{(k_{\mathrm{A}})} \ .$$
3. Iterative interference cancellation for every MS k, $k=1,\ldots,K$, in parallel:
   for $i=1,\ldots,L$ **do**
   a. Compute the reconstructed interfering signals
   $$\underline{\hat{w}}_k^{(k_{\mathrm{A}},k')} = \underline{\hat{H}}_{\mathrm{U}}^{(k_{\mathrm{A}},k)^*} \underline{\hat{H}}_{\mathrm{I},k}^{(k_{\mathrm{A}},k')} \cdot \underline{\hat{d}}^{(k')}(i-1)$$
   from different MSs $k' \neq k$ to MS k at the BSs with antennas k_{A} corresponding to the significant interfering channels for every MS k.
   b. Collect the reconstructed interfering signals $\underline{\hat{w}}_k^{(k_{\mathrm{A}},k')}$ from coordinated BSs through the backhaul links, and subtract them from $\underline{r}^{(k)}$ at BS $k_{\mathrm{B}}=k$ to obtain the estimated data symbol for every MS k as
   $$\underline{\hat{d}}^{(k)}(i) = \frac{\left(\underline{r}^{(k)} - \sum\limits_{k'\neq k} \sum\limits_{k_{\mathrm{A}}} \underline{\hat{w}}_k^{(k_{\mathrm{A}},k')}\right)}{\hat{g}^{(k)}} = \frac{1}{\hat{g}^{(k)}} \cdot \left(\underline{r}^{(k)} - \sum_{k'\neq k} \sum_{k_{\mathrm{A}}} \underline{\hat{H}}_{\mathrm{U}}^{(k_{\mathrm{A}},k)^*} \underline{\hat{H}}_{\mathrm{I},k}^{(k_{\mathrm{A}},k')} \cdot \underline{\hat{d}}^{(k')}(i-1) \right) .$$
   c. Forward the estimated data symbols $\underline{\hat{d}}^{(k)}(i)$ which are required at other BSs in the next iteration to compute the reconstructed interfering signals in Step **3.a**.
   end for

Figure 4.16. Decentralized signal processing scheme for JD with partial CSI.

The decentralized cooperative signal processing scheme for JD to estimate the data symbols $\underline{\hat{d}}^{(k)}$ for individual MSs k, $k=1,\ldots,K$, is described in Figure 4.16. It is worth noting that only the significant CSI is considered in the signal processing. In the part of matched filtering, only the CSI from $\underline{\hat{\mathbf{H}}}_{\mathrm{U}}$ corresponding to the significant useful channels for every MS is considered. In the part of iterative interference cancellation, at the BSs corresponding to the significant useful channels for each MS k, only the

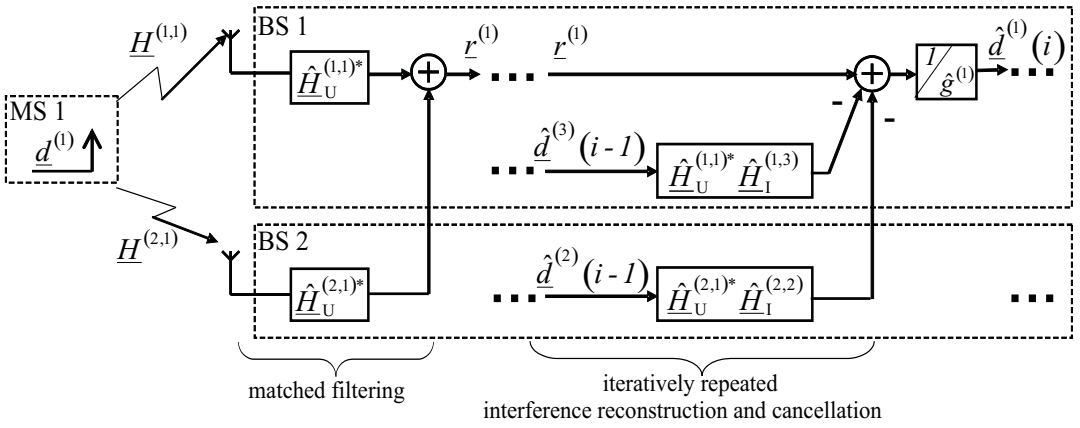

Figure 4.17. Signal processing for MS 1 in a 3-cell DAS applying the decentralized JD with partial CSI.

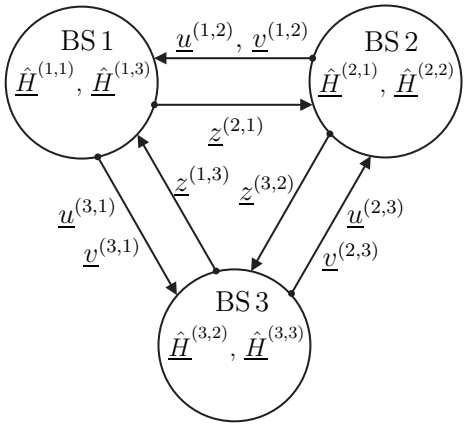

between two BSs	$\underline{u}^{(m,n)}$ from BS n to BS m	$\underline{z}^{(m,n)}$ from BS n to BS m	$\underline{v}^{(m,n)}$ from BS n to BS m
1 and 2	$\underline{u}^{(1,2)} = \hat{\underline{H}}_{\mathrm{U}}^{(2,1)^*} \cdot \underline{e}^{(2)}$	$\underline{z}^{(2,1)} = \hat{\underline{d}}^{(1)}(i-1)$	$\underline{v}^{(1,2)} = \hat{\underline{H}}_{\mathrm{U}}^{(2,1)^*} \hat{\underline{H}}_{\mathrm{I}}^{(2,2)} \cdot \hat{\underline{d}}^{(2)}(i-1)$
2 and 3	$\underline{u}^{(2,3)} = \hat{\underline{H}}_{\mathrm{U}}^{(3,2)^*} \cdot \underline{e}^{(3)}$	$\underline{z}^{(3,2)} = \hat{\underline{d}}^{(2)}(i-1)$	$\underline{v}^{(2,3)} = \hat{\underline{H}}_{\mathrm{U}}^{(3,2)^*} \hat{\underline{H}}_{\mathrm{I}}^{(3,3)} \cdot \hat{\underline{d}}^{(3)}(i-1)$
3 and 1	$\underline{u}^{(3,1)} = \hat{\underline{H}}_{\mathrm{U}}^{(1,3)^*} \cdot \underline{e}^{(1)}$	$\underline{z}^{(1,3)} = \hat{\underline{d}}^{(3)}(i-1)$	$\underline{v}^{(3,1)} = \hat{\underline{H}}_{\mathrm{U}}^{(1,3)^*} \hat{\underline{H}}_{\mathrm{I}}^{(1,1)} \cdot \hat{\underline{d}}^{(1)}(i-1)$

Figure 4.18. Backhaul communications for JD with partial CSI in a 3-cell DAS.

CSI from $\hat{\underline{\mathbf{H}}}_{\mathrm{I},k}$ corresponding to the significant interfering channels for this MS k is considered. For the sake of simplicity, the 3-cell DAS with a single antenna at each BS in Figure 4.15 is taken as the exemplary scenario to visualize the implementation of JD with significant CSI in Figure 4.17. Significant CSI according to the significant channel selection results in Figure 4.15 is applied in JD. In Figure 4.17, the signal processing for MS 1 is shown as an example. Two significant useful channels for MS 1 corresponding to its neighboring BS 1 and BS 2 are considered to obtain the matched filtering data estimate $\underline{r}^{(1)}$. Only one significant interfering channel at each involved BS is considered for interference reconstruction and cancellation.

Additionally, the backhaul communications between coordinated BSs in the above exemplary 3-cell DAS applying the proposed decentralized JD scheme are demonstrated in Figure 4.18. For the computation of the data estimates $\hat{\underline{d}}^{(k)}(i)$ of MSs k, $k=1,\ldots,K$,

at their corresponding BSs $k_{\mathrm{B}} = k$, three kinds of information have to be exchanged between the coordinated BSs as follows:

- "$\underline{u}^{(m,n)}$" denotes the matched filtering data estimate which has to be forwarded from BS n to BS m.
- "$\underline{z}^{(m,n)}$" denotes the preliminary estimated data symbol in the previous iteration which has to be forwarded from BS n to BS m.
- "$\underline{v}^{(m,n)}$" denotes the weighted interfering signal which has to be forwarded from BS n to BS m.

In the cooperative reception scheme applying JD with full CSI, for each MS k all $\underline{u}^{(m,n)}$, $\underline{v}^{(m,n)}$ and $\underline{z}^{(m,n)}$ from BSs $k_{\mathrm{B}} = n = 1, \ldots, k-1, k+1, \ldots, K$ have be to forwarded to BS $k_{\mathrm{B}} = m = k$. In the proposed cooperative reception scheme applying JD with significant CSI, the backhaul communication load can be significantly reduced. This merit is shown in Figure 4.18 where a few intermediate results are exchanged between BSs.

Chapter 5

Cooperative transmission in the downlink

5.1 Preliminary remarks

The cooperative transmission scheme in the DL as the counterpart to the cooperative reception scheme in the UL is discussed in this chapter. While the cooperative reception scheme with multiuser detection strategies in the UL is considered as a transmitter-oriented processing, the cooperative transmission scheme with multiuser transmission strategies in the DL is considered as a receiver-oriented processing [MWQ04, Irm05, JUN05]. That is to say, in the cooperative reception scheme the transmitters are a-priori given and the receivers are a-posteriori adapted to the known transmitters. On the contrary, in the cooperative transmission scheme the receivers are a-priori given and the transmitters are a-posteriori adapted to the known receivers. However, the above two cooperative schemes with different philosophies with respect to the signal processing strategy have shared values in common with respect to the practical implementation. Namely, both schemes make full use of the coordinated BSs connected by high speed backhaul links for the multicell cooperative signal processing and make the MSs as simple as possible.

In this chapter, cooperative transmission is discussed from two points of view. Concerning the signal processing algorithm, several multiuser transmission strategies which can theoretically be applied for JT in the cooperative transmission scheme are studied in Section 5.2. Concerning the practical cooperative transmission scheme, a decentralized iterative JT scheme with significant CSI based on the infrastructure of the coordinated BSs is proposed in Section 5.3 taking practical constraints into consideration.

The discussion in this chapter is based on the multiuser OFDM-MIMO system model of the K-cell cellular system introduced in Chapter 2. The reciprocity between the UL channel and the DL channel as indicated in (2.24) is considered in the investigated TDD systems. With the DL channel matrix $\underline{\mathbf{H}}_{\mathrm{DL}}$ of dimensions $K_{\mathrm{M}} \times K_{\mathrm{A}}$ assuming $K_{\mathrm{A}} \geq K_{\mathrm{M}} = K$, the received vector $\underline{\mathbf{e}} = (\underline{e}^{(1)} \dots \underline{e}^{(K)})^{\mathrm{T}}$ can be written as

$$\underline{\mathbf{e}} = \underline{\mathbf{H}}_{\mathrm{DL}} \cdot \underline{\mathbf{s}} + \underline{\mathbf{n}} = \hat{\underline{\mathbf{d}}} \ . \tag{5.1}$$

The estimated data vector $\hat{\underline{\mathbf{d}}} = (\hat{\underline{d}}^{(1)} \dots \hat{\underline{d}}^{(K)})^{\mathrm{T}}$ is equivalent to the received vector $\underline{\mathbf{e}}$ if simple OFDM receivers without any post-processing or cooperation are applied. The transmitted vector $\underline{\mathbf{s}}$ is obtained through JT at the cooperative transmitters from the data vector $\underline{\mathbf{d}}$ with the covariance matrix $\mathbf{\Phi}_{\mathrm{d}} = \mathrm{E}\{\underline{\mathbf{d}}\,\underline{\mathbf{d}}^{*\mathrm{T}}\} = P_{\mathrm{d}}\mathbf{I}^{K \times K}$.

5.2 Multiuser transmission strategies

5.2.1 Principle of the capacity-achieving dirty-paper coding

The multiuser transmission strategies are generally referred to as precoding for multiuser MIMO systems [Fis02, SPSH04]. As discussed in Chapter 3, the multiuser Gaussian MIMO BC is considered as the information-theoretic model for the DL cellular system with cooperative transmission. In such a vector Gaussian BC, DPC is considered as an information-theoretic optimal precoding strategy [CS03, VJG03, YC04, WSS06].

Briefly speaking, the principle of the DPC strategy is that for each single user if its interference is a-priori noncausally known to the transmitter, the channel capacity for this user is the same as if the interference is not present [Cos83, YC01, CS03, YC04]. In [TV05], a plausibility argument was given to show that the appropriate DPC can completely cancel the impact of the interference and achieve the AWGN capacity in a vector channel. In this argument, high-dimensional coding based on high-dimensional codewords which are uniformly distributed in a sphere with a given radius is considered. Noteworthy, in the multiuser Gaussian MIMO BC the interference for one user comes from other users. Therefore, the principle of the DPC strategy shall be adapted to the multiuser channel. Namely, the users are successively encoded in such a way that the codewords of previously encoded users are known to the encoders of the following users to be encoded. Taking the known codewords of the other users and the channel knowledge into consideration, the encoders choose codewords for their users which presubtract the impact of the interference from the previously encoded users [YC01, VJG03, YC04, WSS06].

5.2.2 Linear multiuser precoding

Since the above information-theoretic optimal DPC strategy has very high computational complexity, the practical precoding schemes with low complexity are of more interest in realistic mobile radio cellular systems. As the counterpart to the conventional transmitter-oriented linear multiuser receivers discussed in Section 4.2.2, the most common receiver-oriented linear multiuser transmitters are reviewed in this section. The DL system model with a general linear multiuser transmitter and simple single-user receivers without any post-processing is shown in Figure 5.1. The received vector $\underline{\mathbf{e}}$ is taken as the estimated data vector $\hat{\underline{\mathbf{d}}}$ as

$$\hat{\underline{\mathbf{d}}} = \underline{\mathbf{e}} = \underline{\mathbf{H}}_{\mathrm{DL}} \cdot \underline{\mathbf{s}} + \underline{\mathbf{n}} = \underline{\mathbf{H}}_{\mathrm{DL}} \underbrace{\underline{\mathbf{M}} \cdot \underline{\mathbf{d}}}_{\underline{\mathbf{s}}} + \underline{\mathbf{n}} \ , \tag{5.2}$$

where the transmitted vector $\underline{\mathbf{s}}$ is obtained from the data vector $\underline{\mathbf{d}}$ through a linear modulator with the modulator matrix $\underline{\mathbf{M}}$.

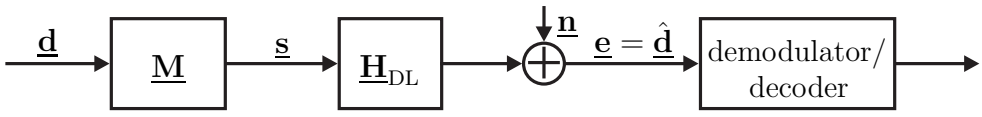

Figure 5.1. DL system model with a linear multiuser transmitter.

Matched filtering (MF) transmitter

Similar to the MF multiuser receiver, the MF multiuser transmitter is also designed to maximize the output SNR. From (5.2), the output SNR is calculated as

$$\gamma^{(k)} = \frac{\mathrm{E}\left\{|\underline{\mathbf{h}}_k^{\mathrm{T}}\,\underline{\mathbf{M}}_k\,\underline{d}^{(k)}|^2\right\}}{\mathrm{E}\left\{|\underline{n}^{(k)}|^2\right\}} = \frac{|\underline{\mathbf{h}}_k^{\mathrm{T}}\,\underline{\mathbf{M}}_k|^2\,P_{\mathrm{d}}}{\sigma^2} \quad , \tag{5.3}$$

with $\underline{\mathbf{M}}_k = [\underline{\mathbf{M}}]_k$ and $\underline{\mathbf{h}}_k = \left[\underline{\mathbf{H}}_{\mathrm{DL}}^{\mathrm{T}}\right]_k$. The matrix operator $[\cdot]_k$ returns the k-th column of its argument as a column vector. The rationale of MRC leads to the MF modulator matrix $\underline{\mathbf{M}}_{\mathrm{MF}}$ with $[\underline{\mathbf{M}}_{\mathrm{MF}}]_k = \underline{\mathbf{h}}_k^*$ as [MBQ04]

$$\underline{\mathbf{M}}_{\mathrm{MF}} = \underline{\mathbf{H}}_{\mathrm{DL}}^{*\mathrm{T}} \quad . \tag{5.4}$$

Zero forcing (ZF) transmitter

With the a-priori knowledge of the receiver and the CSI of the system, the ZF multiuser transmitter looks for the solution leading to interference-free data estimation. Intuitively, interference-free data estimation at the receiver can be achieved if the condition

$$\underline{\mathbf{d}} = \underline{\mathbf{H}}_{\mathrm{DL}}\underline{\mathbf{M}}_{\mathrm{ZF}} \cdot \underline{\mathbf{d}} \quad \Longrightarrow \quad \underline{\mathbf{H}}_{\mathrm{DL}}\underline{\mathbf{M}}_{\mathrm{ZF}} = \mathbf{I}^{K\times K} \tag{5.5}$$

for the ZF modulator matrix $\underline{\mathbf{M}}_{\mathrm{ZF}}$ is fulfilled. Minimizing the transmit power $\mathrm{E}\{\|\underline{\mathbf{s}}\|^2\}$ under the side condition of (5.5), the ZF modulator matrix $\underline{\mathbf{M}}_{\mathrm{ZF}}$ can be obtained as

$$\underline{\mathbf{M}}_{\mathrm{ZF}} = \underline{\mathbf{H}}_{\mathrm{DL}}^{*\mathrm{T}}\left(\underline{\mathbf{H}}_{\mathrm{DL}}\underline{\mathbf{H}}_{\mathrm{DL}}^{*\mathrm{T}}\right)^{-1} \quad , \tag{5.6}$$

which is the right Moore-Penrose pseudo-inverse of the channel matrix $\underline{\mathbf{H}}_{\mathrm{DL}}$ [MBW+00].

For a fair comparison of different linear transmitters, the transmit power for every data symbol carried by the transmitted vector $\underline{\mathbf{s}}$ could be kept the same as $P_{\mathrm{s}}^{(k)} = P_{\mathrm{d}}$. Namely, the norm of each column of the modulator matrix $\underline{\mathbf{M}}$ is kept to be 1 as

$$\left[\underline{\mathbf{M}}^{*\mathrm{T}}\underline{\mathbf{M}}\right]_{k,k} = 1 \quad , \tag{5.7}$$

where the matrix operator $[\cdot]_{k,k}$ returns the (k,k)-th element of its argument. Correspondingly, the above MF modulator matrix under the condition of (5.7) is obtained with the scaling matrix Γ_{MF} as

$$\underline{\mathbf{M}}_{\mathrm{MF}} = \underline{\mathbf{H}}_{\mathrm{DL}}^{*\mathrm{T}}\Gamma_{\mathrm{MF}} = \underline{\mathbf{H}}_{\mathrm{DL}}^{*\mathrm{T}}\underbrace{\left(\mathrm{diag}\left(\underline{\mathbf{H}}_{\mathrm{DL}}\underline{\mathbf{H}}_{\mathrm{DL}}^{*\mathrm{T}}\right)\right)^{-\frac{1}{2}}}_{\Gamma_{\mathrm{MF}}} \quad . \tag{5.8}$$

The above ZF modulator matrix under the condition of (5.7) is obtained with the scaling matrix Γ_{ZF} as

$$\underline{\mathbf{M}}_{\mathrm{ZF}} = \underline{\mathbf{H}}_{\mathrm{DL}}^{*\mathrm{T}} \left(\underline{\mathbf{H}}_{\mathrm{DL}} \underline{\mathbf{H}}_{\mathrm{DL}}^{*\mathrm{T}}\right)^{-1} \Gamma_{\mathrm{ZF}} = \underline{\mathbf{H}}_{\mathrm{DL}}^{*\mathrm{T}} \left(\underline{\mathbf{H}}_{\mathrm{DL}} \underline{\mathbf{H}}_{\mathrm{DL}}^{*\mathrm{T}}\right)^{-1} \underbrace{\left(\mathrm{diag}\left(\left(\underline{\mathbf{H}}_{\mathrm{DL}} \underline{\mathbf{H}}_{\mathrm{DL}}^{*\mathrm{T}}\right)^{-1}\right)\right)^{-\frac{1}{2}}}_{\Gamma_{\mathrm{ZF}}} \quad . \tag{5.9}$$

The output SNRs resulting from the above linear multiuser transmitters read

$$\gamma_{\mathrm{ZF}}^{(k)} = \frac{P_{\mathrm{d}}}{\sigma^2 \left[\left(\underline{\mathbf{H}}_{\mathrm{DL}} \underline{\mathbf{H}}_{\mathrm{DL}}^{*\mathrm{T}}\right)^{-1}\right]_{k,k}} \leq \gamma_{\mathrm{MF}}^{(k)} = \frac{P_{\mathrm{d}} \left[\underline{\mathbf{H}}_{\mathrm{DL}} \underline{\mathbf{H}}_{\mathrm{DL}}^{*\mathrm{T}}\right]_{k,k}}{\sigma^2} \quad . \tag{5.10}$$

Generally, the MF multiuser transmitter can be applied in cellular systems with strong noise, while the ZF multiuser transmitter is a suitable choice for the interference-limited cellular systems with weak noise. Additionally, the MMSE multiuser transmitter considering both the transmit power constraint and the relationship between the transmit power and the noise power makes a good compromise between the interference presubstraction and the transmit power increment [JUN05, Irm05].

5.2.3 Iterative interference presubstraction

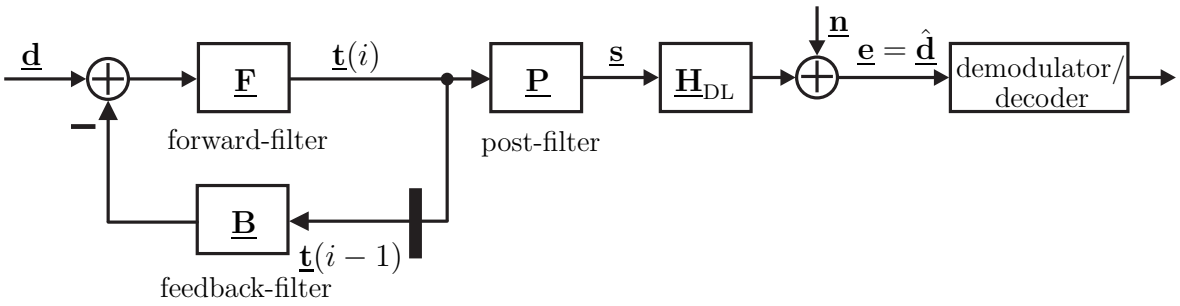

Figure 5.2. General structure of an iterative interference presubstraction multiuser transmitter.

As the counterpart to the iterative interference cancellation technique for multiuser detection in Section 4.2.3, the iterative interference presubstraction technique for multiuser transmission is studied in the present section. The principle of this precoding technique is to iteratively subtract the predicted interference in the transmitter to obtain the received signals with reduced interference or no interference. A general structure of the multiuser transmitter applying the iterative interference presubstraction technique in the DL is shown in Figure 5.2. With the forward-filter matrix $\underline{\mathbf{F}}$ and the feedback-filter matrix $\underline{\mathbf{B}}$, the predistorted vector $\underline{\mathbf{t}}(i)$ in the i-the iteration can be obtained from the data vector $\underline{\mathbf{d}}$ and the predistorted vector $\underline{\mathbf{t}}(i-1)$ in the $(i-1)$-th iteration as

$$\underline{\mathbf{t}}(i) = \underline{\mathbf{F}} \left(\underline{\mathbf{d}} - \underline{\mathbf{B}} \cdot \underline{\mathbf{t}}(i-1)\right) \quad . \tag{5.11}$$

After a sufficient number of iterations, the transmitted vector $\underline{\mathbf{s}}$ can be obtained from the predistorted vector $\underline{\mathbf{t}}$ through the post-filter matrix $\underline{\mathbf{P}}$ as

$$\underline{\mathbf{s}} = \underline{\mathbf{P}} \cdot \underline{\mathbf{t}} \ . \tag{5.12}$$

In contrast to its counterpart for multiuser detection, the iterative interference presubstraction technique for multiuser transmission with previously known data symbols at transmitters neither requires immediate decisions nor causes error propagation. In the following, two typical iterative interference presubstraction techniques are studied.

Parallel interference presubstraction

Similar to the PIC technique for multiuser detection in Section 4.2.3, the parallel interference presubstraction technique for multiuser transmission follows the idea of the Jacobi algorithm as well [HJ85]. Implementing the linear ZF multiuser modulator described by (5.6) in its iterative version, the parallel interference presubstraction technique is obtained with the predistorted vector in the i-th iteration as

$$\underline{\mathbf{t}}(i) = \left(\mathrm{diag}\left(\underline{\mathbf{H}}_{\mathrm{DL}}\underline{\mathbf{H}}_{\mathrm{DL}}^{*\mathrm{T}}\right)\right)^{-1}\left(\underline{\mathbf{d}} - \overline{\mathrm{diag}}\left(\underline{\mathbf{H}}_{\mathrm{DL}}\underline{\mathbf{H}}_{\mathrm{DL}}^{*\mathrm{T}}\right) \cdot \underline{\mathbf{t}}(i-1)\right) \ , \tag{5.13}$$

and the transmitted vector as

$$\underline{\mathbf{s}} = \underline{\mathbf{H}}_{\mathrm{DL}}^{*\mathrm{T}} \cdot \underline{\mathbf{t}} \ . \tag{5.14}$$

Corresponding to the general structure of the iterative multiuser transmitter in Figure 5.2, the forward-filter matrix $\mathbf{F}$, the feedback-filter matrix $\underline{\mathbf{B}}$ and the post-filter matrix $\underline{\mathbf{P}}$ are chosen to be:

$$\mathbf{F} = \left(\mathrm{diag}\left(\underline{\mathbf{H}}_{\mathrm{DL}}\underline{\mathbf{H}}_{\mathrm{DL}}^{*\mathrm{T}}\right)\right)^{-1} \tag{5.15}$$

$$\underline{\mathbf{B}} = \overline{\mathrm{diag}}\left(\underline{\mathbf{H}}_{\mathrm{DL}}\underline{\mathbf{H}}_{\mathrm{DL}}^{*\mathrm{T}}\right) \tag{5.16}$$

$$\underline{\mathbf{P}} = \underline{\mathbf{H}}_{\mathrm{DL}}^{*\mathrm{T}} \ . \tag{5.17}$$

Concerning the computational complexity, the following conclusion similar to that in Section 4.2.3 can be derived. In realistic cellular systems with a large number of users, the parallel interference presubstraction algorithm with a limited number of iterations generally has less computational complexity as compared to its corresponding fully-linear algorithm requiring pseudo-inverse of the channel matrix.

According to the matrix-vector notation of the iterative ZF transmitter of (5.13) and (5.14), the parallel interference presubstraction algorithm which generates individual transmitted signals aiming at interference-free data transmission is described in Figure 5.3. Following this algorithm, a decentralized iterative ZF JT scheme with significant CSI is proposed in Section 5.3 for cooperative transmission in practice. For a fair system performance comparison, a transmit power scaling matrix can be considered as shown in Chapter 6.

1. $g^{(k)} = \sum_{k_\mathrm{A}} \underline{H}_{\mathrm{DL}}^{(k,k_\mathrm{A})} \underline{H}_{\mathrm{DL}}^{(k,k_\mathrm{A})^*}$, $\forall k$
2. $\underline{t}^{(k)}(0) = 0$, $\forall k$
3. **for** $i = 1, \ldots, L$ **do**
4. $\quad \underline{t}^{(k)}(i) = \frac{1}{g^{(k)}} \cdot \Big(\underline{d}^{(k)} - \sum_{k' \neq k} \sum_{k_\mathrm{A}} \underline{H}_{\mathrm{DL}}^{(k,k_\mathrm{A})} \underline{H}_{\mathrm{DL}}{}^{(k',k_\mathrm{A})^*} \cdot \underline{t}^{(k')}(i-1) \Big)$, $\forall k$
5. **end for** // parallel computation for all $k = 1, \ldots, K$ in every iteration i
6. $\underline{s}^{(k_\mathrm{A})} = \sum_k \underline{H}_{\mathrm{DL}}^{(k,k_\mathrm{A})^*} \cdot \underline{t}^{(k)}$

Figure 5.3. Parallel interference presubstraction algorithm for multiuser transmission.

Tomlinson-Harashima precoding (THP)

THP is a nonlinear successive interference presubstraction technique [Tom71, HM72], and it has been successfully extended from temporal preequalization in SISO channels to spatial preequalization in MIMO channels [Fis02, WFVH04]. It is worth noting that the THP technique is a scalar implementation of the principle of the DPC strategy. Additional shaping gain can be achieved by applying complicated high-dimensional precoding techniques [WFH04a, HPS05, ESZ05].

Applying QR decomposition to $\underline{\mathbf{H}}_{\mathrm{DL}}^{*\mathrm{T}}$, a lower triangular matrix $\underline{\mathbf{R}}^{*\mathrm{T}}$ with real-valued diagonal elements and a unitary matrix $\underline{\mathbf{Q}}^{*\mathrm{T}}$ can be obtained from $\underline{\mathbf{H}}_{\mathrm{DL}} = \underline{\mathbf{R}}^{*\mathrm{T}} \underline{\mathbf{Q}}^{*\mathrm{T}}$. Intuitively, the successive interference presubstraction technique can be designed based on the QR decomposition aiming at the receiver-oriented ZF solution described by

$$\underline{\mathbf{e}} = \underline{\mathbf{H}}_{\mathrm{DL}} \underbrace{\underline{\mathbf{M}}_{\mathrm{QR-ZF}} \cdot \underline{\mathbf{d}}}_{\underline{\mathbf{s}}} + \underline{\mathbf{n}} = \underbrace{\underline{\mathbf{R}}^{*\mathrm{T}} \underline{\mathbf{Q}}^{*\mathrm{T}}}_{\underline{\mathbf{H}}_{\mathrm{DL}}} \underbrace{\underline{\mathbf{Q}} \left(\underline{\mathbf{R}}^{*\mathrm{T}} \right)^{-1}}_{\underline{\mathbf{M}}_{\mathrm{QR-ZF}}} \cdot \underline{\mathbf{d}} + \underline{\mathbf{n}} = \underline{\mathbf{d}} + \underline{\mathbf{n}} \ . \tag{5.18}$$

The iterative version of the ZF solution described in (5.18) can be written as:

$$\begin{aligned} \underline{\mathbf{t}}(i) &= \left(\mathrm{diag} \left(\underline{\mathbf{R}}^{*\mathrm{T}} \right) \right)^{-1} \left(\underline{\mathbf{d}} - \overline{\mathrm{diag}} \left(\underline{\mathbf{R}}^{*\mathrm{T}} \right) \underline{\mathbf{t}}(i-1) \right) \\ \underline{\mathbf{s}} &= \underline{\mathbf{Q}} \cdot \underline{\mathbf{t}} \ . \end{aligned} \tag{5.19}$$

Corresponding to the general structure of the iterative multiuser transmitter in Figure 5.2, the forward-filter matrix $\mathbf{F}$, the feedback-filter matrix $\underline{\mathbf{B}}$ and the post-filter matrix $\underline{\mathbf{P}}$ are taken as:

$$\mathbf{F} = \left(\mathrm{diag} \left(\underline{\mathbf{R}}^{*\mathrm{T}} \right) \right)^{-1} \tag{5.20}$$

$$\underline{\mathbf{B}} = \overline{\mathrm{diag}} \left(\underline{\mathbf{R}}^{*\mathrm{T}} \right) \tag{5.21}$$

$$\underline{\mathbf{P}} = \underline{\mathbf{Q}} \ . \tag{5.22}$$

Successively starting from user $k=1$ and ending with user $k=K$, in every iteration $i =$

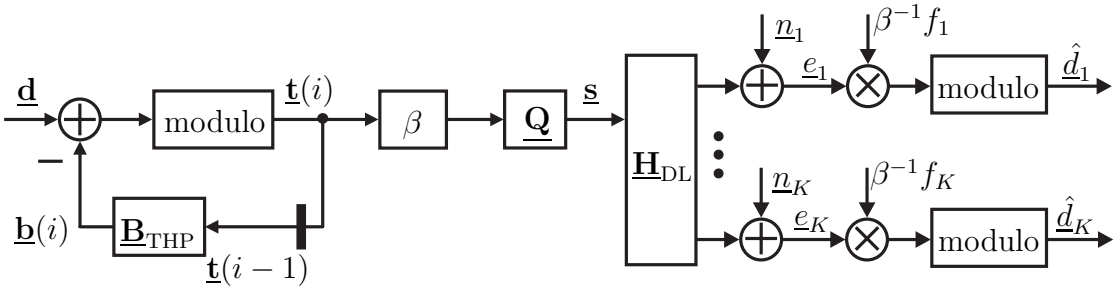

Figure 5.4. THP multiuser transmitter in the DL.

1. $\underline{\mathbf{H}}_{\mathrm{DL}}^{*\mathrm{T}} = \underline{\mathbf{Q}} \cdot \underline{\mathbf{R}}$ applying sorted QR decomposition (SQRD)
2. **for** $k = 1, \ldots, K$ **do**
3. $\quad \underline{b}^{(k)} = 0$
4. $\quad$ **for** $k' = 1, \ldots, k-1$ **do**
5. $\quad\quad \underline{b}^{(k)} = \underline{b}^{(k)} + \left(\underline{R}^{(k',k)^*} / \underline{R}^{(k,k)^*} \right) \cdot \underline{t}^{(k')}$
6. $\quad$ **end for**
7. $\quad \underline{q}^{(k)} = \underset{\text{representative } \underline{q}^{(k)} \text{for } \underline{d}^{(k)}}{\operatorname{argmin}} \left\{ | \underline{q}^{(k)} - \underline{b}^{(k)} | \right\}$
8. $\quad \underline{t}^{(k)} = \underline{q}^{(k)} - \underline{b}^{(k)}$
9. **end for**
10. $\underline{\mathbf{s}} = \beta \underline{\mathbf{Q}} \cdot \underline{\mathbf{t}}$

Figure 5.5. THP algorithm for multiuser transmission.

k, only one predistorted data symbol $\underline{t}^{(k)}$ is computed from the previous predistorted data vector $\underline{\mathbf{t}}(i-1) = (\underline{t}^{(1)}, \ldots, \underline{t}^{(k-1)}, 0, \ldots, 0)^{\mathrm{T}}$ to obtain the predistorted data vector $\underline{\mathbf{t}}(i) = (\underline{t}^{(1)}, \ldots, \underline{t}^{(k)}, 0, \ldots, 0)^{\mathrm{T}}$. Obviously, $L = K$ iterations are required to complete this successive iterative process. A practical structure of the THP transmitter for multiuser transmission is shown in Figure 5.4, and the corresponding THP algorithm is described in Figure 5.5. The forward-filter matrix $\mathbf{F}$ is implemented by taking its diagonal elements f_k, k=1,...,K, as the scaling factors at receivers. Correspondingly, the feedback matrix $\underline{\mathbf{B}}_{\mathrm{THP}}$ in Figure 5.4 is adapted to be

$$\underline{\mathbf{B}}_{\mathrm{THP}} = \mathbf{F}\underline{\mathbf{B}} = \left(\operatorname{diag}\left(\underline{\mathbf{R}}^{*\mathrm{T}} \right) \right)^{-1} \overline{\operatorname{diag}} \left(\underline{\mathbf{R}}^{*\mathrm{T}} \right) \quad . \tag{5.23}$$

Additionally, the modulo operation is applied in the THP transmitter to avoid significant increments of the transmit power [WFVH04, HZZW07], while its counterpart is applied at the receiver side. Assuming the square M-ary QAM constellation $\mathbb{D} = \{ d_{\mathrm{I}} + j * d_{\mathrm{Q}} \mid d_{\mathrm{I}}, d_{\mathrm{Q}} \in \{ \pm 1, \pm 3, \ldots, \pm(\sqrt{M} - 1) \}$ as the data symbol alphabet, the modulo device chooses the effective data symbol $\underline{q}^{(k)}$ closest to the feedback-filter output $\underline{b}^{(k)}$ from the periodically extended constellation of $\mathbb{D}$ [WFH04b]. The predistorted data symbols $\underline{t}^{(k)}$ after the modulo operation are approximately uniformly distributed in the bounded square region of width $2\sqrt{M}$. In order to keep the transmit power approximately unmodified for each data symbol, the scaling factor β is considered

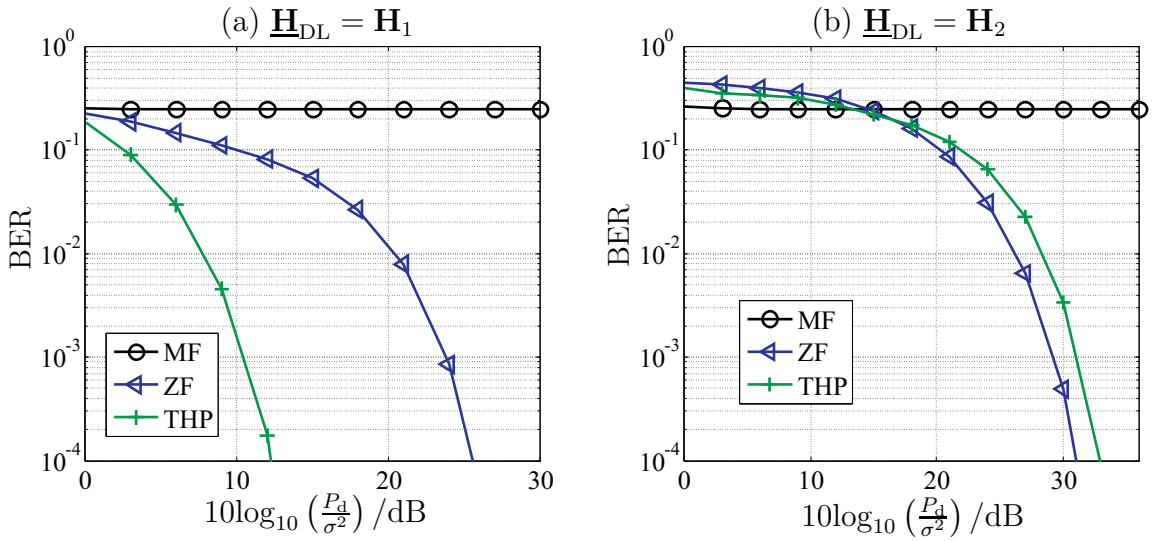

Figure 5.6. BERs of different multiuser transmitters considering two exemplary channel matrices, i.e., $\mathbf{H}_1$=(10, 10, 10; 1, 2, 5; 0.1, 0.1, 1) and $\mathbf{H}_2$=(1, 1, 1; 0.8, 1, 0.8; 0.8, 0.8, 1).

as [Fis02]

$$\beta = \sqrt{M/(M-1)} \ . \tag{5.24}$$

Generally, the QR decomposition based on a permutation which results in a larger $\min_k\{|R^{(k,k)}|\}$ leads to a better system performance of the THP transmitter. In practice, the SQRD algorithm introduced in Section 4.2.3 can be applied.

Assuming QPSK modulation, numerical results with respect to BER versus the pseudo-SNRs are shown in Figure 5.6 to illustrate the system performance of the above transmitters. If the algorithm converges, the BER curve of the limiting values of the iterative ZF transmitter applying the parallel interference presubstraction technique is equivalent to that of the ZF transmitter. Therefore, the system performance of this iterative transmitter can be directly evaluated with respect to the BER curve of the ZF transmitter. It is shown that the channel structure of the multiuser MIMO system, i.e., the relationship between the channel coefficients, has a great influence on the system performance of the iterative transmitters. Especially, higher system performance can be obtained from the THP transmitter in the case where the row vectors of the channel matrix have distinctively different Euclidean norms. The reason is that in this case THP can benefit more from the sorted QR decomposition to reduce the scaling factor magnitudes for noise signals. Generally, there is no simple answer to the question which iterative precoding technique, i.e., parallel interference presubstraction or THP, results in a better system performance. The MIMO channel structures, the pseudo-SNR conditions, and power control strategies have a great influence on the performance of the precoding techniques [WFH04b].

5.3 Practical cooperative transmission scheme

5.3.1 Design guidelines

As the counterpart to the practical cooperative reception scheme in Section 4.3, a practical cooperative transmission scheme is proposed in the present section. In TDD mobile radio cellular systems, the channel reciprocity between the UL and the DL leads to the dual estimated channel matrices $\underline{\hat{\mathbf{H}}}_{\mathrm{UL}}$ in the UL and $\underline{\hat{\mathbf{H}}}_{\mathrm{DL}}$ in the DL known by the BSs in practice. Namely, the relationship

$$\underline{\hat{\mathbf{H}}}_{\mathrm{DL}} = \underline{\hat{\mathbf{H}}}_{\mathrm{UL}}^{\mathrm{T}} = \underline{\hat{\mathbf{H}}}^{\mathrm{T}} \tag{5.25}$$

holds with the general estimated channel matrix $\underline{\hat{\mathbf{H}}}$ of the whole system. In Chapter 4, the design guidelines and the framework for the general cooperative communication scheme have been discussed. Some additional design guidelines for the cooperative transmission scheme in the DL are stressed as follows:

- Due to the channel reciprocity and the duality of the estimated channel matrices in the UL and in the DL as described in (5.25), it is reasonable to apply the same mathematical criterion in the significant channel selection for both the UL and the DL. Based on one general estimated channel matrix $\underline{\hat{\mathbf{H}}}$, the same significant channels should be selected for both the UL and the DL.
- An efficient signal processing algorithm is required for JT in practice. Namely, the signal processing algorithm is expected to be good at dealing with interference in interference-limited cellular systems. Meanwhile, it should be implementable with low computational complexity. Following the similar idea in JD, an iterative algorithm aiming at the ZF solution with significant CSI is proposed for JT in the DL. However, in contrast to JD at the receivers in the UL, JT in the DL is applied at the transmitters following the receiver-oriented precoding strategy.
- A very nice thing is that cooperative reception in the UL and cooperative transmission in the DL could be performed based on the same infrastructure of coordinated BSs without requiring any extra hardware. The idea behind this infrastructure is to shift the computational load to the BSs and to make the MSs as simple as possible. Similar to the decentralized JD in the UL, a multi-cell cooperative signal processing for JT in the DL is implemented in a decentralized way based on coordinated BSs connected by high-speed backhaul links.

Under the general framework of the cooperative communication scheme in Figure 4.12, a practical cooperative transmission scheme is designed with the significant channel selection and the decentralized JT.

5.3.2 Significant channel selection

In the proposed practical cooperative communication scheme, only the MS-oriented significant CSI is considered in the cooperative signal processing. The significant CSI corresponds to the significant channels which play a significant role for the system performance of each MS. Obviously, the system performance depends on the signal processing algorithm for JT. The procedure of the iterative ZF algorithm with significant CSI for JT which is described in Section 5.3.3 in detail is generally stated as follows. Firstly, the interference caused by every MS corresponding to the significant interfering channels of this MS is predicted and predistorted. Then, the transmitted signals are obtained from the predistorted data symbols through matched filtering corresponding to the significant useful channels of the involved MSs. According to the functionality of the mobile radio channels in the DL data transmission, two types of significant channels for a MS can be distinguished from each other as follows:

- Significant useful channels for a MS in the DL are the channels over which we generate significant useful contributions to the received signals for this MS.
- Significant interfering channels for a MS in the DL are the channels over which we cause significant interferences to other MSs when we transmit the data symbol for this MS.

In fact, the receiver-oriented iterative ZF interference presubstraction algorithm applied for JT is dual to the transmitter-oriented iterative ZF interference cancellation algorithm applied for JD with respect to the data transmission schemes in the UL and in the DL. Applying the dual signal processing algorithms for JD and for JT based on the dual UL and DL estimated channel matrices in (5.25), it is reasonable to select the same significant channels for both the UL and the DL. From a mathematical point of view, for both the UL and the DL the significant channel selection algorithm is performed based on the same estimated channel coefficients contained in the general estimated channel matrix $\underline{\hat{\mathbf{H}}}$. As a result of this selection, the significant useful channels for all MSs can be indicated by the significant useful channel indicator matrices $\widetilde{\mathbf{H}}_{\mathrm{DL,U}}$ for the DL, $\widetilde{\mathbf{H}}_{\mathrm{UL,U}}$ for the UL, and $\widetilde{\mathbf{H}}_{\mathrm{U}}$ for the general system fulfilling the relationship

$$\widetilde{\mathbf{H}}_{\mathrm{DL,U}} = \widetilde{\mathbf{H}}^{\mathrm{T}}_{\mathrm{UL,U}} = \widetilde{\mathbf{H}}^{\mathrm{T}}_{\mathrm{U}} \ . \tag{5.26}$$

The significant interfering channels for individual MSs k can be indicated by the MS specific significant interfering channel indicator matrices $\widetilde{\mathbf{H}}_{\mathrm{DL,I},k}$ for the DL, $\widetilde{\mathbf{H}}_{\mathrm{UL,I},k}$ for the UL, and $\widetilde{\mathbf{H}}_{\mathrm{I},k}$ for the general system fulfilling the relationship

$$\widetilde{\mathbf{H}}_{\mathrm{DL,I},k} = \widetilde{\mathbf{H}}^{\mathrm{T}}_{\mathrm{UL,I},k} = \widetilde{\mathbf{H}}^{\mathrm{T}}_{\mathrm{I},k} \ . \tag{5.27}$$

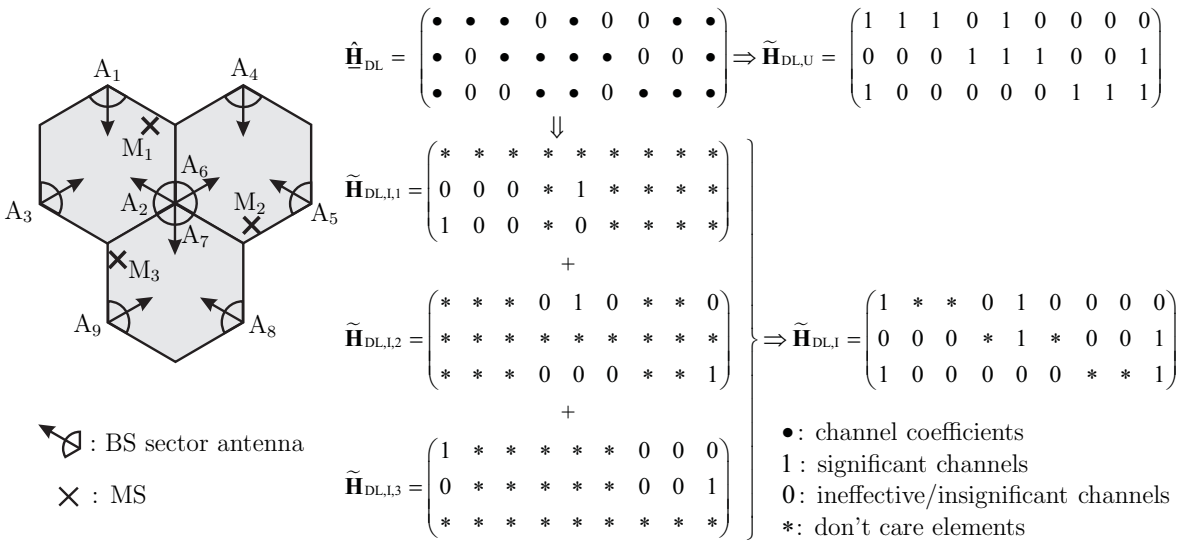

Figure 5.7. Example for channel selection and indicator matrix formalism in a 3-cell sector-DAS.

As mentioned in Chapter 4, all MS-specific indicator matrices $\widetilde{\mathbf{H}}_{\mathrm{I},k}$ can be represented by a single combined significant interfering channel indicator matrix $\widetilde{\mathbf{H}}_{\mathrm{I}}$ if they are compatible with each other. Correspondingly, the relationship between the DL and the UL combined significant interfering channel indicator matrices holds as

$$\widetilde{\mathbf{H}}_{\mathrm{DL,I}} = \widetilde{\mathbf{H}}_{\mathrm{UL,I}}^{\mathrm{T}} = \widetilde{\mathbf{H}}_{\mathrm{I}}^{\mathrm{T}} \ . \tag{5.28}$$

Details of the significant channel selection scheme based on the general estimated channel matrix $\underline{\hat{\mathbf{H}}}$ are discussed in Section 4.3.2. One example of the significant channel selection in a 3-cell omni-DAS is shown in Figure 4.15. Considering the smart BS-antenna-layout, one more example of the significant channel selection in a 3-cell sector-DAS with 3 distributed 120 degree sector antennas in 3 vertices of each cell is given in Figure 5.7. For simplicity, it is assumed that the relationship between the channel magnitudes strongly depends on the corresponding distances between the MSs and the BS antennas. Especially, in such a sector-DAS one should pay attention to the fact that there are some ineffective channels corresponding to the ineffective antennas for each MS. It is not necessary to estimate the channel coefficients of these ineffective channels or to consider them during the significant channel selection. One can simply assign "0"s to the corresponding positions of these ineffective channels in the estimated channel matrix and the significant channel indicator matrices. In Figure 5.7, according to the distances between the MSs and the BS antennas denoted by M_k, $k = 1, 2, 3$, and $\mathrm{A}_{k_\mathrm{A}}$, $k_\mathrm{A} = 1, \ldots, 9$, respectively, the significant channel selection is performed. 4 significant useful channels and 2 significant interfering channels for each MS are selected. The corresponding significant channel indicator matrix formalism is shown.

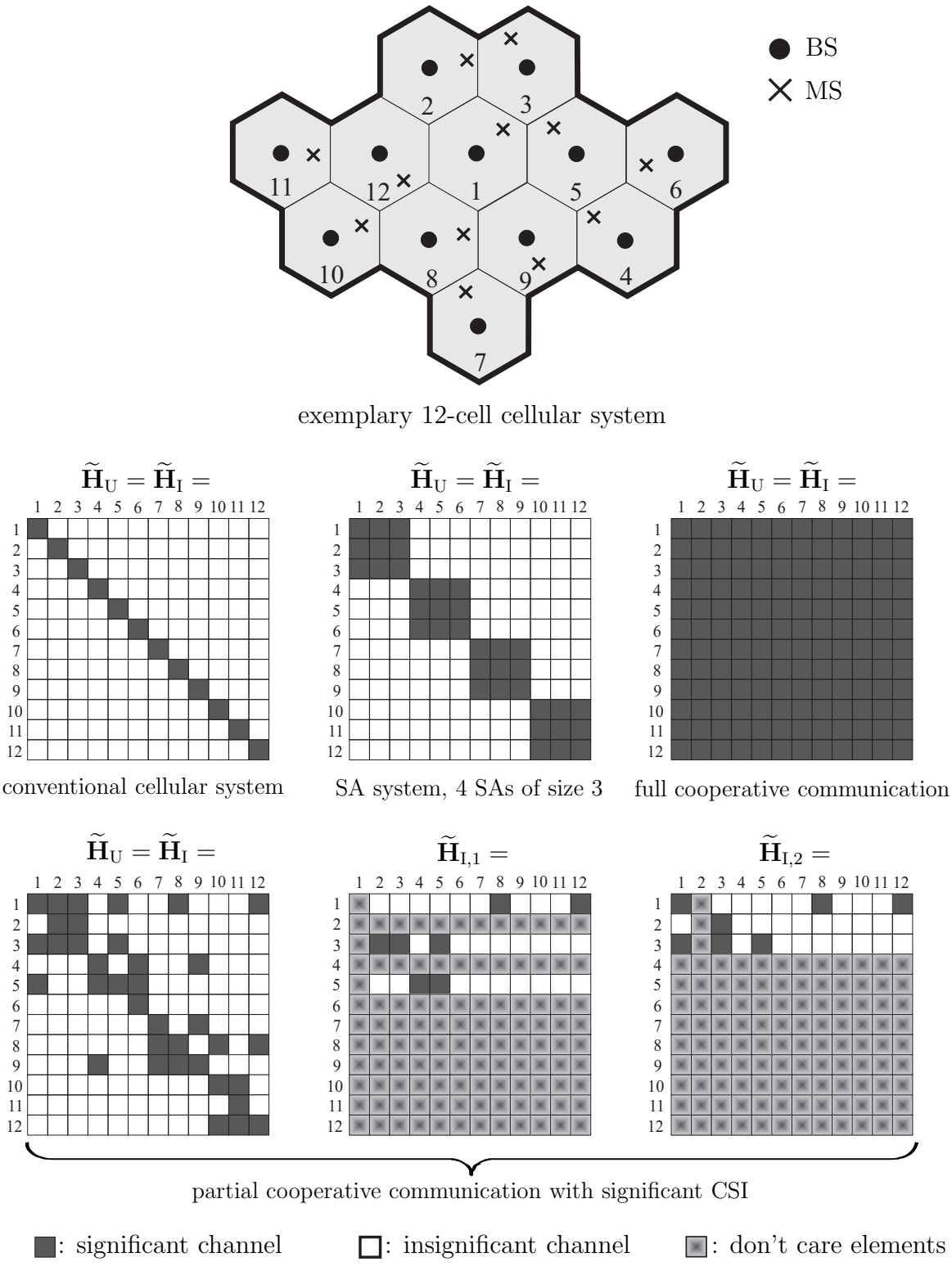

Figure 5.8. Significant channels considered in different communication schemes.

Furthermore, in Figure 5.8, a 12-cell omni-DAS with a single antenna per BS is taken as an exemplary scenario to illustrate several cooperative communication schemes considering different significant channel selection strategies. Interestingly, all the illustrated

communication schemes can be considered as special cases of the general cooperative communication scheme with partial CSI. Concerning the conventional cellular system without multi-cell cooperation, the signal processing for each MS considers only the useful channels between this MS and the BS in the same cell ignoring the intercell interfering channels. Corresponding to the intra-cell useful channels, a diagonal matrix is taken as the significant useful channel indicator matrix $\widetilde{\mathbf{H}}_{\mathrm{U}}$. The significant interfering channel indicator matrix can be represented by $\widetilde{\mathbf{H}}_{\mathrm{I}} = \widetilde{\mathbf{H}}_{\mathrm{U}}$ since all its non-zero diagonal elements are "don't care" elements for all MSs. Concerning the state of the art SA systems or group-cell systems [WMSL02, LWZ04, ZTZ+05, TXX+05], cooperative signal processing is performed in each structure-oriented fixed geographical area, e.g., a SA. The 12-cell system for example can be considered as 4 SAs with 3 cells in each SA. A block diagonal matrix with every block corresponding to one SA is taken as $\widetilde{\mathbf{H}}_{\mathrm{U}}$ which is equivalent to $\widetilde{\mathbf{H}}_{\mathrm{I}}$. Concerning the full cooperative communication scheme in the whole system, all useful channels and all interfering channels for every MS are considered in its signal processing. Correspondingly, a matrix with all elements being "1"s is taken as $\widetilde{\mathbf{H}}_{\mathrm{U}}$ and $\widetilde{\mathbf{H}}_{\mathrm{I}}$. Finally, concerning the proposed cooperative communication scheme with significant CSI, the dynamically selected MS-oriented significant channels are considered in the signal processing for every MS. Corresponding to the distances between the MSs and the BSs in the snapshot of the 12-cell scenario in Figure 5.8, $\widetilde{\mathbf{H}}_{\mathrm{U}}$ for all MSs, $\widetilde{\mathbf{H}}_{\mathrm{I},1}$ and $\widetilde{\mathbf{H}}_{\mathrm{I},2}$ for MS 1 and MS 2, respectively, are shown. It is shown that the significant channels corresponding to "1"s in the significant channel indicator matrices are dynamically selected without the constraint of the structure-oriented geographical area. In this example, considering the "don't care" elements, the MS specific matrices $\widetilde{\mathbf{H}}_{\mathrm{I},1}$ and $\widetilde{\mathbf{H}}_{\mathrm{I},2}$ can even be represented by a single combined matrix $\widetilde{\mathbf{H}}_{\mathrm{I}} = \widetilde{\mathbf{H}}_{\mathrm{U}}$.

5.3.3 Decentralized iterative ZF joint transmission with partial CSI

Referring to the CSI flow of the cooperative reception scheme in Section 4.3, the proposed cooperative transmission scheme works in a similar way. Firstly, significant channels are selected based on the roughly estimated channel magnitudes. Then, the instantaneous CSI of the selected significant channels is precisely estimated and applied in JT. In this section, the JT scheme is investigated from the aspects of the channel knowledge, the signal processing algorithm and the implementation architecture.

Concerning the channel knowledge, the same estimated significant CSI is considered for JD in the UL as for JT in the DL. According to the dual UL and DL estimated channel matrices in (5.25) and the dual UL and DL significant channel indicator matrices in

(5.26), (5.27) and (5.28), the following dual UL and DL estimated significant channel matrices can be easily derived as:

$$\underline{\hat{\mathbf{H}}}_{\mathrm{DL,U}} = \underline{\hat{\mathbf{H}}}_{\mathrm{DL}} \odot \widetilde{\mathbf{H}}_{\mathrm{DL,U}} = \underline{\hat{\mathbf{H}}}^{\mathrm{T}} \odot \widetilde{\mathbf{H}}_{\mathrm{U}}^{\mathrm{T}} = \underline{\hat{\mathbf{H}}}_{\mathrm{U}}^{\mathrm{T}} = \underline{\hat{\mathbf{H}}}_{\mathrm{UL,U}}^{\mathrm{T}} \tag{5.29}$$

$$\underline{\hat{\mathbf{H}}}_{\mathrm{DL,I},k} = \underline{\hat{\mathbf{H}}}_{\mathrm{DL}} \odot \widetilde{\mathbf{H}}_{\mathrm{DL,I},k} = \underline{\hat{\mathbf{H}}}^{\mathrm{T}} \odot \widetilde{\mathbf{H}}_{\mathrm{I},k}^{\mathrm{T}} = \underline{\hat{\mathbf{H}}}_{\mathrm{I},k}^{\mathrm{T}} = \underline{\hat{\mathbf{H}}}_{\mathrm{UL,I},k}^{\mathrm{T}} \tag{5.30}$$

$$\underline{\hat{\mathbf{H}}}_{\mathrm{DL,I}} = \underline{\hat{\mathbf{H}}}_{\mathrm{DL}} \odot \widetilde{\mathbf{H}}_{\mathrm{DL,I}} = \underline{\hat{\mathbf{H}}}^{\mathrm{T}} \odot \widetilde{\mathbf{H}}_{\mathrm{I}}^{\mathrm{T}} = \underline{\hat{\mathbf{H}}}_{\mathrm{I}}^{\mathrm{T}} = \underline{\hat{\mathbf{H}}}_{\mathrm{UL,I}}^{\mathrm{T}} \ . \tag{5.31}$$

The operator $\odot$ denotes the element-wise multiplication of two matrices. $\underline{\hat{\mathbf{H}}}_{\mathrm{DL,U}}$, $\underline{\hat{\mathbf{H}}}_{\mathrm{DL,I},k}$ and $\underline{\hat{\mathbf{H}}}_{\mathrm{DL,I}}$ are the DL estimated significant useful channel matrix, MS specific estimated significant interfering channel matrices, and combined significant interfering channel matrix, respectively. The corresponding UL matrices $\underline{\hat{\mathbf{H}}}_{\mathrm{UL,U}}$, $\underline{\hat{\mathbf{H}}}_{\mathrm{UL,I},k}$, $\underline{\hat{\mathbf{H}}}_{\mathrm{UL,I}}$ and the corresponding general matrices $\underline{\hat{\mathbf{H}}}_{\mathrm{U}}$, $\underline{\hat{\mathbf{H}}}_{\mathrm{I},k}$, $\underline{\hat{\mathbf{H}}}_{\mathrm{I}}$ are introduced in Section 4.3.

Concerning the signal processing algorithm, the iterative ZF interference presubstraction algorithm with partial CSI is proposed for the decentralized JT to implement cooperative transmission in the DL. The reasons for this choice are similar to those for the choice of the iterative ZF interference cancellation algorithm for JD in the UL. Briefly speaking, this iterative partial ZF JT algorithm is good at dealing with interference with moderate computational complexity. Applying the MS-oriented significant CSI described by $\underline{\hat{\mathbf{H}}}_{\mathrm{DL,U}}$ in (5.29) and $\underline{\hat{\mathbf{H}}}_{\mathrm{DL,I},k}$ in (5.30) instead of full CSI in the iterative ZF interference presubstraction algorithm described by (5.13) and (5.14), the practical iterative partial ZF JT algorithm can directly be derived. This algorithm can be described in the form of the matrix-vector-notation as

$$\underline{\mathbf{t}}(i) = \hat{\mathbf{G}}_{\mathrm{DL}}^{-1} \cdot \left(\underline{\mathbf{d}} - \overline{\mathrm{diag}} \left(\underline{\hat{\mathbf{R}}}_{\mathrm{DL}} \right) \cdot \underline{\mathbf{t}}(i-1) \right) \tag{5.32}$$

to obtain the predistorted vector $\underline{\mathbf{t}}(i)$ in the i-th iteration under the assumption of $\underline{\mathbf{t}}(0) = 0$. After a sufficient number of iterations, the transmitted vector is obtained as

$$\underline{\mathbf{s}} = \underline{\hat{\mathbf{H}}}_{\mathrm{DL,U}}^{*\mathrm{T}} \cdot \underline{\mathbf{t}} \ . \tag{5.33}$$

The DL estimated channel gain scaling matrix $\hat{\mathbf{G}}_{\mathrm{DL}}$ of (5.32) is given as

$$\hat{\mathbf{G}}_{\mathrm{DL}} = \mathrm{diag} \left(\underline{\hat{\mathbf{H}}}_{\mathrm{DL,U}} \underline{\hat{\mathbf{H}}}_{\mathrm{DL,U}}^{*\mathrm{T}} \right) \ . \tag{5.34}$$

According to (5.29) and (4.58), the following relationship

$$\hat{\mathbf{G}}_{\mathrm{DL}} = \hat{\mathbf{G}}_{\mathrm{UL}} = \hat{\mathbf{G}} = \mathrm{diag} \left(\underline{\hat{\mathbf{H}}}_{\mathrm{U}}^{*\mathrm{T}} \underline{\hat{\mathbf{H}}}_{\mathrm{U}} \right) \tag{5.35}$$

holds with $\hat{\mathbf{G}}$ defined as the general estimated channel gain scaling matrix of the system. The DL estimated channel correlation matrix of (5.32) is given as

$$\underline{\hat{\mathbf{R}}}_{\mathrm{DL}} = \left(\underline{\hat{\mathbf{H}}}_{\mathrm{DL,I},1} \left[\underline{\hat{\mathbf{H}}}_{\mathrm{DL,U}}^{*\mathrm{T}} \right]_1 , \ldots , \underline{\hat{\mathbf{H}}}_{\mathrm{DL,I},K} \left[\underline{\hat{\mathbf{H}}}_{\mathrm{DL,U}}^{*\mathrm{T}} \right]_K \right) \ . \tag{5.36}$$

According to (5.29), (5.30) and (4.59), the following relationship

$$\underline{\hat{\mathbf{R}}}_{\mathrm{DL}} = \underline{\hat{\mathbf{R}}}_{\mathrm{UL}}^{\mathrm{T}} = \underline{\hat{\mathbf{R}}}^{\mathrm{T}} = \left(\underline{\hat{\mathbf{H}}}_{\mathrm{I},1}^{\mathrm{T}} \left[\underline{\hat{\mathbf{H}}}_{\mathrm{U}}^{*}\right]_{1}, \ldots, \underline{\hat{\mathbf{H}}}_{\mathrm{I},K}^{\mathrm{T}} \left[\underline{\hat{\mathbf{H}}}_{\mathrm{U}}^{*}\right]_{K}\right) \tag{5.37}$$

can be derived with $\underline{\hat{\mathbf{R}}}$ defined as the general channel correlation matrix of the system, see Appendix A.2. The cooperative transmitters applying the above iterative JT algorithm can be considered as a special case of the general iterative multiuser transmitter in Figure 5.2. Correspondingly, the forward-filter matrix $\mathbf{F}$, the feedback-filter matrix $\underline{\mathbf{B}}$ and the post-filter matrix $\underline{\mathbf{P}}$ are taken as:

$$\mathbf{F} = \hat{\mathbf{G}}_{\mathrm{DL}}^{-1} = \hat{\mathbf{G}}^{-1} \tag{5.38}$$

$$\underline{\mathbf{B}} = \overline{\mathrm{diag}}\left(\underline{\hat{\mathbf{R}}}_{\mathrm{DL}}\right) = \overline{\mathrm{diag}}\left(\underline{\hat{\mathbf{R}}}^{\mathrm{T}}\right) \tag{5.39}$$

$$\underline{\mathbf{P}} = \underline{\hat{\mathbf{H}}}_{\mathrm{DL,U}}^{*\mathrm{T}} = \underline{\hat{\mathbf{H}}}_{\mathrm{U}}^{*} \ . \tag{5.40}$$

Furthermore, if the above iterative algorithm converges and the matrix $\left(\hat{\mathbf{G}}_{\mathrm{DL}} + \overline{\mathrm{diag}}\left(\underline{\hat{\mathbf{R}}}_{\mathrm{DL}}\right)\right)$ has full rank, one can obtain the formula for calculating the limiting value of this iterative partial ZF JT algorithm as

$$\underline{\mathbf{s}}(\infty) = \underline{\hat{\mathbf{H}}}_{\mathrm{DL,U}}^{*\mathrm{T}} \cdot \underline{\mathbf{t}}(\infty) = \underline{\hat{\mathbf{H}}}_{\mathrm{DL,U}}^{*\mathrm{T}} \left(\hat{\mathbf{G}}_{\mathrm{DL}} + \overline{\mathrm{diag}}\left(\underline{\hat{\mathbf{R}}}_{\mathrm{DL}}\right)\right)^{-1} \cdot \underline{\mathbf{d}} = \underline{\hat{\mathbf{H}}}_{\mathrm{U}}^{*} \left(\hat{\mathbf{G}} + \overline{\mathrm{diag}}\left(\underline{\hat{\mathbf{R}}}^{\mathrm{T}}\right)\right)^{-1} \cdot \underline{\mathbf{d}}. \tag{5.41}$$

Under different special conditions, the above formula for calculating the limiting values in the general case can be simplified step by step as shown in the following:

- In the case that all the individual MS specific matrices $\underline{\hat{\mathbf{H}}}_{\mathrm{DL,I},k}$ can be combined to one channel matrix $\underline{\hat{\mathbf{H}}}_{\mathrm{DL,I}}$, one obtains

  $$\underline{\hat{\mathbf{R}}}_{\mathrm{DL}} = \underline{\hat{\mathbf{H}}}_{\mathrm{DL,I}} \underline{\hat{\mathbf{H}}}_{\mathrm{DL,U}}^{*\mathrm{T}} = \underline{\hat{\mathbf{H}}}_{\mathrm{I}}^{\mathrm{T}} \underline{\hat{\mathbf{H}}}_{\mathrm{U}}^{*} \ , \tag{5.42}$$

  and the limiting value of the iterative partial ZF JT algorithm is described by

  $$\underline{\mathbf{s}}(\infty) = \underline{\hat{\mathbf{H}}}_{\mathrm{DL,U}}^{*\mathrm{T}} \cdot \left(\hat{\mathbf{G}}_{\mathrm{DL}} + \overline{\mathrm{diag}}\left(\underline{\hat{\mathbf{H}}}_{\mathrm{DL,I}} \underline{\hat{\mathbf{H}}}_{\mathrm{DL,U}}^{*\mathrm{T}}\right)\right)^{-1} \cdot \underline{\mathbf{d}} = \underline{\hat{\mathbf{H}}}_{\mathrm{U}}^{*} \cdot \left(\hat{\mathbf{G}} + \overline{\mathrm{diag}}\left(\underline{\hat{\mathbf{H}}}_{\mathrm{I}}^{\mathrm{T}} \underline{\hat{\mathbf{H}}}_{\mathrm{U}}^{*}\right)\right)^{-1} \cdot \underline{\mathbf{d}}. \tag{5.43}$$

- In the above case, if the estimated significant interfering channel matrix $\underline{\hat{\mathbf{H}}}_{\mathrm{DL,I}}$ covers all the non-zero elements of the estimated significant useful channel matrix $\underline{\hat{\mathbf{H}}}_{\mathrm{DL,U}}$, one obtains

  $$\hat{\mathbf{G}}_{\mathrm{DL}} = \mathrm{diag}\left(\underline{\hat{\mathbf{H}}}_{\mathrm{DL,U}} \underline{\hat{\mathbf{H}}}_{\mathrm{DL,U}}^{*\mathrm{T}}\right) = \mathrm{diag}\left(\underline{\hat{\mathbf{H}}}_{\mathrm{DL,I}} \underline{\hat{\mathbf{H}}}_{\mathrm{DL,U}}^{*\mathrm{T}}\right) = \mathrm{diag}\left(\underline{\hat{\mathbf{H}}}_{\mathrm{I}}^{\mathrm{T}} \underline{\hat{\mathbf{H}}}_{\mathrm{U}}^{*}\right), \tag{5.44}$$

  and the limiting value of this iterative JT algorithm can be represented by

  $$\underline{\mathbf{s}}(\infty) = \underline{\hat{\mathbf{H}}}_{\mathrm{DL,U}}^{*\mathrm{T}} \cdot \left(\underline{\hat{\mathbf{H}}}_{\mathrm{DL,I}} \underline{\hat{\mathbf{H}}}_{\mathrm{DL,U}}^{*\mathrm{T}}\right)^{-1} \cdot \underline{\mathbf{d}} = \underline{\hat{\mathbf{H}}}_{\mathrm{U}}^{*} \cdot \left(\underline{\hat{\mathbf{H}}}_{\mathrm{I}}^{\mathrm{T}} \underline{\hat{\mathbf{H}}}_{\mathrm{U}}^{*}\right)^{-1} \cdot \underline{\mathbf{d}} \ . \tag{5.45}$$

- One special case is the iterative ZF JT with estimated full CSI, for which

$$\underline{\hat{\mathbf{H}}}_{\mathrm{DL,U}} = \underline{\hat{\mathbf{H}}}_{\mathrm{DL,I}} = \underline{\hat{\mathbf{H}}}_{\mathrm{DL}} = \underline{\hat{\mathbf{H}}}^{\mathrm{T}} \tag{5.46}$$

  holds, and the limiting value of this iterative JT algorithm is

$$\underline{\mathbf{s}}(\infty) = \underline{\hat{\mathbf{H}}}_{\mathrm{DL}}^{*\mathrm{T}} \cdot \left(\underline{\hat{\mathbf{H}}}_{\mathrm{DL}} \underline{\hat{\mathbf{H}}}_{\mathrm{DL}}^{*\mathrm{T}} \right)^{-1} \cdot \underline{\mathbf{d}} = \underline{\hat{\mathbf{H}}}^{*} \cdot \left(\underline{\hat{\mathbf{H}}}^{\mathrm{T}} \underline{\hat{\mathbf{H}}}^{*} \right)^{-1} \cdot \underline{\mathbf{d}} \ . \tag{5.47}$$

Concerning the signal processing architecture, the above iterative partial ZF JT algorithm is performed in a decentralized way. The reasons for the choice of a decentralized implementation instead of a centralized implementation are the same as mentioned in Chapter 4 for the decentralized JD scheme. Briefly speaking, the decentralized implementation can distribute the computational load to individual BSs and avoid the complicated CU. The flexible decentralized implementation of the proposed parallel iterative algorithm can make full use of the dynamically selected significant CSI. Only local significant CSI is required at the involved coordinated BSs for each MS to achieve good system performance.

In Figure 5.9, a decentralized cooperative signal processing architecture for JT at coordinated BSs is proposed. It is noteworthy that only significant CSI is considered in the signal processing. In the part of iterative interference prediction and presubstraction to obtain the predistorted data symbol $\underline{t}^{(k)}$ for each MS k, the CSI in $\underline{\hat{\mathbf{H}}}_{\mathrm{I},k'}$ corresponding to the significant interfering channels for other MSs k' to this MS k is required. The CSI in $\underline{\hat{\mathbf{H}}}_{\mathrm{U}}$ corresponding to the significant useful channels for other MSs k' from the BS antennas where the above considered significant interfering channels are generated is also required. In the part of the transmit matched filtering to obtain the transmitted signal $\underline{s}^{(k_{\mathrm{A}})}$ at BS antenna k_{A} from its related predistorted data symbols $\underline{t}^{(k)}$, the CSI in $\underline{\hat{\mathbf{H}}}_{\mathrm{U}}$ corresponding to the MSs' significant useful channels related to this BS antenna k_{A} is required. Taking the 3-cell DAS with a single antenna at each BS in Figure 4.15 as an exemplary scenario, the above decentralized signal processing for JT with significant CSI is visualized in Figure 5.10. The significant CSI considered in the signal processing corresponds to the significant channel selection results indicated in Figure 4.15. The part of signal processing for MS 1 is shown in Figure 5.10 as an example. The signal processing for MS 1 is performed at its neighboring BS 1 and BS 2 corresponding to its two significant useful channels. In the interference prediction and presubstraction part in order to obtain the predistorted data symbol $\underline{t}^{(1)}$ for MS 1, one significant interfering channel from other MSs at each involved BS for MS 1 is considered. The predistorted data symbol $\underline{t}^{(1)}$ is considered in the transmit matched filtering part to obtain the transmitted signals $\underline{s}^{(1)}$ at BS 1 and $\underline{s}^{(2)}$ at BS 2 corresponding to the significant useful channels for MS 1.

1. Initialization of the iterative signal processing of individual MSs k, $k=1,\ldots,K$, at their corresponding BSs $k_{\mathrm{B}}=k$ in parallel:

   a. Assign the channel gain scaling factor

   $$\hat{g}^{(k)}=\sum_{k_{\mathrm{A}}}\underline{\hat{H}}_{\mathrm{U}}^{(k_{\mathrm{A}},k)}\underline{\hat{H}}_{\mathrm{U}}^{(k_{\mathrm{A}},k)^{*}}=\sum_{k_{\mathrm{A}}}\left|\underline{\hat{H}}_{\mathrm{U}}^{(k_{\mathrm{A}},k)}\right|^{2}$$

   for every MS k at BS $k_{\mathrm{B}}=k$. $\hat{g}^{(k)}$ can be previously estimated in practice.

   b. Assign the initial value of the predistorted data symbol

   $$\underline{t}^{(k)}(0)=0$$

   for every MS k at BS $k_{\mathrm{B}}=k$.

2. Iterative interference presubstraction for every MS k, $k=1,\ldots,K$, in parallel:

   for $i=1,\ldots,L$ **do**

   a. Compute the predicted interfering signals

   $$\underline{\hat{w}}_{k}^{(k_{\mathrm{A}},k')}=\underline{\hat{H}}_{\mathrm{I},k'}^{(k_{\mathrm{A}},k)}\underline{\hat{H}}_{\mathrm{U}}^{(k_{\mathrm{A}},k')^{*}}\cdot\underline{t}^{(k')}(i-1)$$

   from different MSs $k'\neq k$ to MS k at the BSs with antennas k_{A} corresponding to the significant interfering channels of MSs k'.

   b. Collect the predicted interfering signals $\underline{\hat{w}}_{k}^{(k_{\mathrm{A}},k')}$ from coordinated BSs through the backhaul links, and subtract them from the data symbol $\underline{d}^{(k)}$ at BS $k_{\mathrm{B}}=k$ to obtain the predistorted data symbol for every MS k as

   $$\underline{t}^{(k)}(i)=\frac{\left(\underline{d}^{(k)}-\sum\limits_{k'\neq k}\sum\limits_{k_{\mathrm{A}}}\underline{\hat{w}}_{k}^{(k_{\mathrm{A}},k')}\right)}{\hat{g}^{(k)}}=\frac{1}{\hat{g}^{(k)}}\cdot\left(\underline{d}^{(k)}-\sum_{k'\neq k}\sum_{k_{\mathrm{A}}}\underline{\hat{H}}_{\mathrm{I},k'}^{(k_{\mathrm{A}},k)}\underline{\hat{H}}_{\mathrm{U}}^{(k_{\mathrm{A}},k')^{*}}\cdot\underline{t}^{(k')}(i-1)\right).$$

   c. Forward the predistorted data symbols $\underline{t}^{(k)}(i)$ which are required at other BSs in the next iteration to compute the predicted interfering signals in Step **2.a**.

   end for

3. Matched filtering to obtain the transmitted signals $\underline{s}^{(k_{\mathrm{A}})}$, $k_{\mathrm{A}}=1,\ldots,K_{\mathrm{A}}$, in parallel:

   a. Forward the predistorted data symbols $\underline{t}^{(k)}$ to the BSs corresponding to the significant useful channels for MSs k, $k=1,\ldots,K$, and compute

   $$\underline{s}^{(k_{\mathrm{A}},k)}=\underline{\hat{H}}_{\mathrm{U}}^{(k_{\mathrm{A}},k)^{*}}\cdot\underline{t}^{(k)}$$

   as the transmit matched filtering components for every MS k at the involved BSs.

   b. Sum up $\underline{s}^{(k_{\mathrm{A}},k)}$ together for every antenna at the corresponding BS to obtain the transmitted signal at each BS antenna k_{A} as

   $$\underline{s}^{(k_{\mathrm{A}})}=\sum_{k}\underline{s}^{(k_{\mathrm{A}},k)}=\sum_{k}\underline{\hat{H}}_{\mathrm{U}}^{(k_{\mathrm{A}},k)^{*}}\cdot\underline{t}^{(k)}\ .$$

Figure 5.9. Decentralized signal processing scheme for JT with partial CSI.

Additionally, required backhaul communications between the coordinated BSs in the above exemplary DAS with $K=3$ cells are demonstrated in Figure 5.11. Generally, the following three kinds of information have to be exchanged between the coordinated BSs:

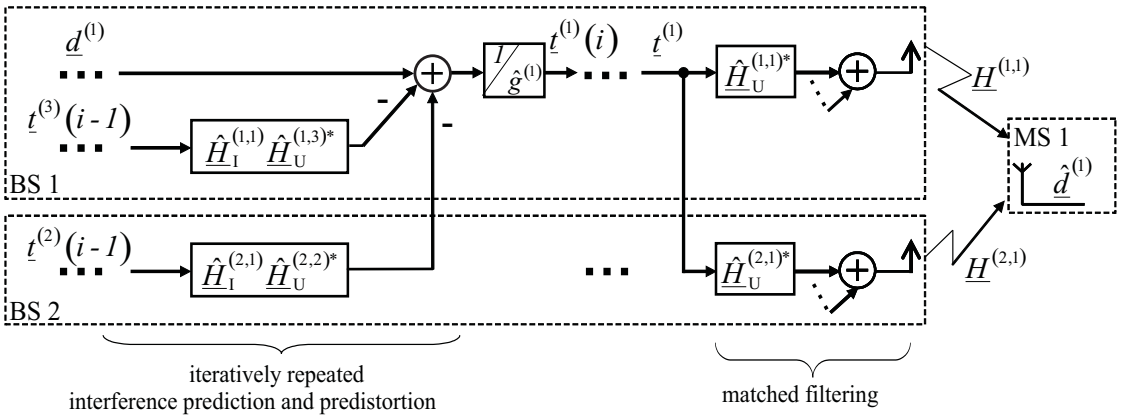

Figure 5.10. Signal processing for MS 1 in a 3-cell DAS applying the decentralized JT with partial CSI.

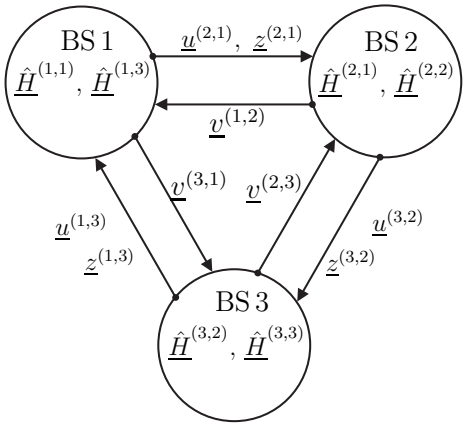

between two BSs	$\underline{z}^{(m,n)}$ from BS n to BS m	$\underline{v}^{(m,n)}$ from BS n to BS m	$\underline{u}^{(m,n)}$ from BS n to BS m
1 and 2	$\underline{z}^{(2,1)} = \underline{t}^{(1)}(i-1)$	$\underline{v}^{(1,2)} = \hat{\underline{H}}_{\mathrm{I}}^{(2,1)} \hat{\underline{H}}_{\mathrm{U}}^{(2,2)^*} \cdot \underline{t}^{(2)}(i-1)$	$\underline{u}^{(2,1)} = \underline{t}^{(1)}$
2 and 3	$\underline{z}^{(3,2)} = \underline{t}^{(2)}(i-1)$	$\underline{v}^{(2,3)} = \hat{\underline{H}}_{\mathrm{I}}^{(3,2)} \hat{\underline{H}}_{\mathrm{U}}^{(3,3)^*} \cdot \underline{t}^{(3)}(i-1)$	$\underline{u}^{(3,2)} = \underline{t}^{(2)}$
3 and 1	$\underline{z}^{(1,3)} = \underline{t}^{(3)}(i-1)$	$\underline{v}^{(3,1)} = \hat{\underline{H}}_{\mathrm{I}}^{(1,3)} \hat{\underline{H}}_{\mathrm{U}}^{(1,1)^*} \cdot \underline{t}^{(1)}(i-1)$	$\underline{u}^{(1,3)} = \underline{t}^{(3)}$

Figure 5.11. Backhaul communications for JT with partial CSI in a 3-cell DAS.

- "$\underline{z}^{(m,n)}$" denotes the preliminary predistorted data symbol in the previous iteration which has to be forwarded from BS n to BS m.
- "$\underline{v}^{(m,n)}$" denotes the weighted predicted interfering signal which has to be forwarded from BS n to BS m.
- "$\underline{u}^{(m,n)}$" denotes the final predistorted data symbol after the iterative process for matched filtering which has to be forwarded from BS n to BS m.

In the cooperative transmission scheme with full CSI, for each MS k all $\underline{z}^{(m,n)}$, $\underline{v}^{(m,n)}$ and $\underline{u}^{(m,n)}$ have be to forwarded from BS $k_{\mathrm{B}} = n = k$ to BSs $k_{\mathrm{B}} = m = 1, \ldots, k-1, k+1, \ldots, K$. Fortunately, the backhaul communication load can be significantly reduced when considering only the significant CSI. Corresponding to the significant channel selection results in Figure 4.15, the required variables to be exchanged between coordinated BSs are given in Figure 5.11.

Chapter 6

Implementation complexity and system performance

6.1 Evaluation of implementation complexity

In Chapter 6, the implementation complexity and the system performance of the proposed cooperative communication scheme are assessed. In the present section, the implementation complexity with respect to the computational load and the backhaul communication load is evaluated taking the UL as an example.

Based on the system model in Chapter 2, the JD scheme proposed in Chapter 4 is applied in a cellular system with K cells. It is assumed that N_{U} significant useful channels and N_{I} significant interfering channels for every MS are considered in the iterative ZF JD algorithm with L iterations. The interfering channels considered for each MS in JD can only be selected from the channels between other MSs and the BS antennas corresponding to the significant useful channels of this MS. Therefore, the relation $N_{\mathrm{I}} \leq (K-1) \cdot N_{\mathrm{U}}$ holds.

The computational load of the proposed JD scheme is evaluated in terms of the number N_{CL} of multiplications in the signal processing algorithm to estimate one data vector. Corresponding to the two steps in the signal processing, i.e., matched filtering and iterative interference cancellation, the computational load of the whole system consists of two parts as described by

$$N_{\mathrm{CL}} = \underbrace{N_{\mathrm{U}} \cdot K}_{\text{matched filtering}} + \underbrace{N_{\mathrm{I}} \cdot L \cdot K}_{\text{interference cancellation}} . \tag{6.1}$$

Obviously, the computational load is linear in the numbers of considered significant useful and interfering channels, i.e., N_{U} and N_{I}.

The backhaul communication load of the proposed JD scheme is evaluated in terms of the number N_{BL} of intermediate signal processing results which have to be exchanged between the BSs to estimate one data vector. For the sake of simplicity, a single antenna per BS is considered. The significant channels are selected according to the MS-oriented dynamic significant channel selection strategy proposed in Section 4.3.2. Although the significant channels for one MS are not necessarily constrained in a fixed

structure-oriented geographical area, in most realistic scenarios they will be in the MS's own cell and adjacent cells around it. Therefore, in the decentralized JD scheme without the complicated CU, only local CSI is required at each BS, and only local intermediate signal processing results need to be delivered through the backhaul links between neighboring BSs. In the proposed JD scheme, the data estimate for each MS is finally obtained at its corresponding BS in the same cell after the iterative signal processing. The channel between the MS and the BS in the same cell is almost always selected as a significant useful channel for this MS. As mentioned in Chapter 4, the backhaul communication load results from three kinds of intermediate signal processing results, i.e., the weighted useful contributions in the matched filtering part, the weighted interfering signals and the preliminary estimated data symbols required in the interference cancellation part. It is found that even with the same number of significant interfering channels, the backhaul communication load varies with different choices of significant interfering channels. The upper bound of the backhaul communication load of the whole system can be derived as

$$N_{\mathrm{BL}} = \underbrace{(N_{\mathrm{U}}-1)\cdot K}_{\text{matched filtering}} + \underbrace{\begin{cases} 2\cdot N_{\mathrm{I}}\cdot L\cdot K, & \text{for } 1 \le N_{\mathrm{I}} < (K-1) \\ 2\cdot (K-1)\cdot L\cdot K, & \text{for } (K-1) \le N_{\mathrm{I}} \le (K-1)\cdot N_{\mathrm{U}} \end{cases}}_{\text{interference cancellation}} . \tag{6.2}$$

The backhaul communication load is greatly reduced if small numbers of significant channels, i.e., N_{U} and N_{I}, are considered as compared to that of the JD scheme with full CSI. The above evaluations show that the proposed cooperative communication scheme considering MS-oriented significant CSI has moderate implementation complexity.

6.2 Analytical calculations for performance assessment

6.2.1 Dualities between the uplink and the downlink

Considering the channel reciprocity between the UL and the DL in the investigated TDD system, the corresponding dual matrices for the UL and for the DL in the proposed cooperative communication scheme are summarized as follows:

- estimated full and significant channel matrices

$$\underline{\hat{\mathbf{H}}}_{\mathrm{UL}} = \underline{\hat{\mathbf{H}}}_{\mathrm{DL}}^{\mathrm{T}} = \underline{\hat{\mathbf{H}}} \tag{6.3}$$

$$\underline{\hat{\mathbf{H}}}_{\mathrm{UL,U}} = \underline{\hat{\mathbf{H}}}_{\mathrm{DL,U}}^{\mathrm{T}} = \underline{\hat{\mathbf{H}}}_{\mathrm{U}} \tag{6.4}$$

$$\underline{\hat{\mathbf{H}}}_{\mathrm{UL,I},k} = \underline{\hat{\mathbf{H}}}_{\mathrm{DL,I},k}^{\mathrm{T}} = \underline{\hat{\mathbf{H}}}_{\mathrm{I},k} \ , \tag{6.5}$$

- estimated channel energy scaling matrix

$$\hat{\mathbf{G}}_{\mathrm{UL}} = \hat{\mathbf{G}}_{\mathrm{DL}} = \hat{\mathbf{G}} = \mathrm{diag}\left(\underline{\hat{\mathbf{H}}}_{\mathrm{U}}^{*\mathrm{T}}\underline{\hat{\mathbf{H}}}_{\mathrm{U}}\right) \quad , \tag{6.6}$$

  and

- estimated channel correlation matrix

$$\underline{\hat{\mathbf{R}}}_{\mathrm{UL}} = \underline{\hat{\mathbf{R}}}_{\mathrm{DL}}^{\mathrm{T}} = \underline{\hat{\mathbf{R}}} = \begin{pmatrix} \left[\underline{\hat{\mathbf{H}}}_{\mathrm{U}}\right]_1^{*\mathrm{T}} \underline{\hat{\mathbf{H}}}_{\mathrm{I},1} \\ \vdots \\ \left[\underline{\hat{\mathbf{H}}}_{\mathrm{U}}\right]_K^{*\mathrm{T}} \underline{\hat{\mathbf{H}}}_{\mathrm{I},K} \end{pmatrix} \quad . \tag{6.7}$$

Additionally, as one prerequisite for a fair system performance assessment of JD in the UL and JT in the DL, the same transmit power for every MS in the UL and in the DL has to be used. To ensure this, the estimated transmit power scaling matrix

$$\hat{\mathbf{\Gamma}} = \left(\mathrm{diag}\left(\left(\hat{\mathbf{G}} + \overline{\mathrm{diag}}\left(\underline{\hat{\mathbf{R}}}\right)\right)^{-1}\underline{\hat{\mathbf{H}}}_{\mathrm{U}}^{*\mathrm{T}}\underline{\hat{\mathbf{H}}}_{\mathrm{U}}\left(\hat{\mathbf{G}} + \overline{\mathrm{diag}}\left(\underline{\hat{\mathbf{R}}}^{*\mathrm{T}}\right)\right)^{-1}\right)\right)^{-\frac{1}{2}} \tag{6.8}$$

is applied in the DL, see Appendix A.3. It is worth noting that this estimated transmit power scaling matrix is also used to keep the transmit power for every data symbol unmodified in the JT scheme considering different partial CSI.

6.2.2 Limiting values of data estimates

The system performance of the proposed cooperative communication scheme is investigated based on the limiting values of the iterative partial ZF JD and JT algorithms in the UL and in the DL, respectively.

The limiting value of the estimated data vector applying the iterative partial JD described by (4.57) with transparent data estimate refinement reads

$$\underline{\hat{\mathbf{d}}}_{\mathrm{UL}} = \left(\hat{\mathbf{G}} + \overline{\mathrm{diag}}\left(\underline{\hat{\mathbf{R}}}\right)\right)^{-1}\underline{\hat{\mathbf{H}}}_{\mathrm{U}}^{*\mathrm{T}} \cdot \underline{\mathbf{e}} = \left(\hat{\mathbf{G}} + \overline{\mathrm{diag}}\left(\underline{\hat{\mathbf{R}}}\right)\right)^{-1}\underline{\hat{\mathbf{H}}}_{\mathrm{U}}^{*\mathrm{T}}\underline{\mathbf{H}} \cdot \underline{\mathbf{d}} + \left(\hat{\mathbf{G}} + \overline{\mathrm{diag}}\left(\underline{\hat{\mathbf{R}}}\right)\right)^{-1}\underline{\hat{\mathbf{H}}}_{\mathrm{U}}^{*\mathrm{T}} \cdot \underline{\mathbf{n}}. \tag{6.9}$$

The limiting value of the estimated data vector applying the iterative partial JT described by (5.32) and (5.33) considering the scaling matrix $\hat{\mathbf{\Gamma}}$ from (6.8) reads

$$\underline{\hat{\mathbf{d}}}_{\mathrm{DL}} = \hat{\mathbf{\Gamma}}^{-1}\left(\underline{\mathbf{H}}^{\mathrm{T}} \cdot \underline{\mathbf{s}} + \underline{\mathbf{n}}\right) = \hat{\mathbf{\Gamma}}^{-1}\underline{\mathbf{H}}^{\mathrm{T}}\underline{\hat{\mathbf{H}}}_{\mathrm{U}}^{*}\left(\hat{\mathbf{G}} + \overline{\mathrm{diag}}\left(\underline{\hat{\mathbf{R}}}^{\mathrm{T}}\right)\right)^{-1}\hat{\mathbf{\Gamma}} \cdot \underline{\mathbf{d}} + \hat{\mathbf{\Gamma}}^{-1} \cdot \underline{\mathbf{n}} \ . \tag{6.10}$$

As can be seen from the above equations, the limiting values of the estimated data vectors applying the iterative partial JD in the UL and the iterative partial JT in the DL are in general different.

6.2.3 Convergence behaviour

The convergence behaviour needs to be analyzed for the iterative ZF JD/JT algorithm with significant CSI. The loop matrix

$$\underline{\mathbf{L}}_{\mathrm{UL}} = \hat{\mathbf{G}}^{-1}\overline{\mathrm{diag}}\left(\hat{\underline{\mathbf{R}}}\right) \tag{6.11}$$

of the iterative partial ZF JD algorithm described by (4.57) and the loop matrix

$$\underline{\mathbf{L}}_{\mathrm{DL}} = \hat{\mathbf{G}}^{-1}\overline{\mathrm{diag}}\left(\hat{\underline{\mathbf{R}}}^{\mathrm{T}}\right) \tag{6.12}$$

of the iterative partial ZF JT algorithm described by (5.32) have the same spectral radius, see Appendix A.4. So we can conclude that the iterative partial ZF JD algorithm in the UL and the iterative partial ZF JT algorithm in the DL have the same speed of convergence.

6.2.4 Signal-to-interference-plus-noise ratio

Based on the limiting values of the iterative JD/JT algorithm, the SINR can be calculated as an important performance criterion. Furthermore, the system performance in every channel snapshot can be analytically assessed in terms of the bit error rate (BER) and the capacity with the help of the SINR. In the following the SINR based on one channel snapshot is calculated. It is assumed that the modulation scheme used here can ensure the same average transmitted power P_{d} per data symbol, and the noise is white Gaussian distributed with a variance of $\sigma^2/2$ for both the real and imaginary part. The data vector $\underline{\mathbf{d}}$ and the noise vector $\underline{\mathbf{n}}$ are statistically independent. Since only partial CSI instead of full CSI is applied in the cooperative signal processing, the data estimates may contain slightly rotated and scaled useful contributions. However, such a rotation or scaling can be easily estimated and compensated at the receiver.

In the UL, the limiting value of the estimated data vector of (6.9) can be rewritten as

$$\begin{aligned}\hat{\underline{\mathbf{d}}}_{\mathrm{UL}} = {} & \underbrace{\mathrm{diag}\left(\left(\hat{\mathbf{G}}+\overline{\mathrm{diag}}\left(\hat{\underline{\mathbf{R}}}\right)\right)^{-1}\hat{\underline{\mathbf{H}}}_{\mathrm{U}}^{*\mathrm{T}}\underline{\mathbf{H}}\right)\cdot\underline{\mathbf{d}}}_{\text{useful contribution}} + \underbrace{\overline{\mathrm{diag}}\left(\left(\hat{\mathbf{G}}+\overline{\mathrm{diag}}\left(\hat{\underline{\mathbf{R}}}\right)\right)^{-1}\hat{\underline{\mathbf{H}}}_{\mathrm{U}}^{*\mathrm{T}}\underline{\mathbf{H}}\right)\cdot\underline{\mathbf{d}}}_{\text{interference}} \\ & + \underbrace{\left(\hat{\mathbf{G}}+\overline{\mathrm{diag}}\left(\hat{\underline{\mathbf{R}}}\right)\right)^{-1}\hat{\underline{\mathbf{H}}}_{\mathrm{U}}^{*\mathrm{T}}\cdot\underline{\mathbf{n}}}_{\text{noise}} \ . \end{aligned} \tag{6.13}$$

The SINR of the data estimate $\hat{\underline{d}}^{(k)}$ for MS k in the UL reads

$$\gamma_{\mathrm{JD}}^{(k)} = \frac{S_{\mathrm{JD}}^{(k)}}{I_{\mathrm{JD}}^{(k)} + N_{\mathrm{JD}}^{(k)}}, \tag{6.14}$$

where

$$S_{\mathrm{JD}}^{(k)} = P_{\mathrm{d}} \left[\mathrm{diag}\left(\left(\hat{\mathbf{G}} + \overline{\mathrm{diag}}\left(\underline{\hat{\mathbf{R}}} \right) \right)^{-1} \underline{\hat{\mathbf{H}}}_{\mathrm{U}}^{*\mathrm{T}} \underline{\mathbf{H}} \right) \mathrm{diag}\left(\underline{\mathbf{H}}^{*\mathrm{T}} \underline{\hat{\mathbf{H}}}_{\mathrm{U}} \left(\hat{\mathbf{G}} + \overline{\mathrm{diag}}\left(\underline{\hat{\mathbf{R}}}^{*\mathrm{T}} \right) \right)^{-1} \right) \right]_{k,k}, \tag{6.15}$$

$$I_{\mathrm{JD}}^{(k)} = P_{\mathrm{d}} \left[\overline{\mathrm{diag}}\left(\left(\hat{\mathbf{G}} + \overline{\mathrm{diag}}\left(\underline{\hat{\mathbf{R}}} \right) \right)^{-1} \underline{\hat{\mathbf{H}}}_{\mathrm{U}}^{*\mathrm{T}} \underline{\mathbf{H}} \right) \overline{\mathrm{diag}}\left(\underline{\mathbf{H}}^{*\mathrm{T}} \underline{\hat{\mathbf{H}}}_{\mathrm{U}} \left(\hat{\mathbf{G}} + \overline{\mathrm{diag}}\left(\underline{\hat{\mathbf{R}}}^{*\mathrm{T}} \right) \right)^{-1} \right) \right]_{k,k}, \tag{6.16}$$

and

$$N_{\mathrm{JD}}^{(k)} = \sigma^2 \left[\left(\hat{\mathbf{G}} + \overline{\mathrm{diag}}\left(\underline{\hat{\mathbf{R}}} \right) \right)^{-1} \underline{\hat{\mathbf{H}}}_{\mathrm{U}}^{*\mathrm{T}} \underline{\hat{\mathbf{H}}}_{\mathrm{U}} \left(\hat{\mathbf{G}} + \overline{\mathrm{diag}}\left(\underline{\hat{\mathbf{R}}}^{*\mathrm{T}} \right) \right)^{-1} \right]_{k,k} \tag{6.17}$$

can be calculated from (6.13).

In the DL, the limiting value of the estimated data vector of (6.10) can be rewritten as

$$\begin{aligned} \underline{\hat{\mathbf{d}}} \;=\; & \underbrace{\mathrm{diag}\left(\hat{\mathbf{\Gamma}}^{-1} \underline{\mathbf{H}}^{\mathrm{T}} \underline{\hat{\mathbf{H}}}_{\mathrm{U}}^{*} \left(\hat{\mathbf{G}} + \overline{\mathrm{diag}}\left(\underline{\hat{\mathbf{R}}}^{\mathrm{T}} \right) \right)^{-1} \hat{\mathbf{\Gamma}} \right) \cdot \underline{\mathbf{d}}}_{\text{useful contribution}} \\ & + \underbrace{\overline{\mathrm{diag}}\left(\hat{\mathbf{\Gamma}}^{-1} \underline{\mathbf{H}}^{\mathrm{T}} \underline{\hat{\mathbf{H}}}_{\mathrm{U}}^{*} \left(\hat{\mathbf{G}} + \overline{\mathrm{diag}}\left(\underline{\hat{\mathbf{R}}}^{\mathrm{T}} \right) \right)^{-1} \hat{\mathbf{\Gamma}} \right) \cdot \underline{\mathbf{d}}}_{\text{interference}} + \underbrace{\hat{\mathbf{\Gamma}}^{-1} \cdot \underline{\mathbf{n}}}_{\text{noise}} \; . \end{aligned} \tag{6.18}$$

The SINR of the data estimate $\underline{\hat{d}}^{(k)}$ for MS k in the DL reads

$$\gamma_{\mathrm{JT}}^{(k)} = \frac{S_{\mathrm{JT}}^{(k)}}{I_{\mathrm{JT}}^{(k)} + N_{\mathrm{JT}}^{(k)}}, \tag{6.19}$$

where

$$\begin{aligned} S_{\mathrm{JT}}^{(k)} &= P_{\mathrm{d}} \left[\mathrm{diag}\left(\hat{\mathbf{\Gamma}}^{-1} \underline{\mathbf{H}}^{\mathrm{T}} \underline{\hat{\mathbf{H}}}_{\mathrm{U}}^{*} \left(\hat{\mathbf{G}} + \overline{\mathrm{diag}}(\underline{\hat{\mathbf{R}}}^{\mathrm{T}}) \right)^{-1} \hat{\mathbf{\Gamma}} \right) \mathrm{diag}\left(\hat{\mathbf{\Gamma}} \left(\hat{\mathbf{G}} + \overline{\mathrm{diag}}(\underline{\hat{\mathbf{R}}}^{*}) \right)^{-1} \underline{\hat{\mathbf{H}}}_{\mathrm{U}}^{\mathrm{T}} \underline{\mathbf{H}}^{*} \hat{\mathbf{\Gamma}}^{-1} \right) \right]_{k,k} \\ &= P_{\mathrm{d}} \left[\mathrm{diag}\left(\underline{\mathbf{H}}^{\mathrm{T}} \underline{\hat{\mathbf{H}}}_{\mathrm{U}}^{*} \left(\hat{\mathbf{G}} + \overline{\mathrm{diag}}(\underline{\hat{\mathbf{R}}}^{\mathrm{T}}) \right)^{-1} \right) \mathrm{diag}\left(\left(\hat{\mathbf{G}} + \overline{\mathrm{diag}}(\underline{\hat{\mathbf{R}}}^{*}) \right)^{-1} \underline{\hat{\mathbf{H}}}_{\mathrm{U}}^{\mathrm{T}} \underline{\mathbf{H}}^{*} \right) \right]_{k,k}, \end{aligned} \tag{6.20}$$

$$I_{\mathrm{JT}}^{(k)} = P_{\mathrm{d}} \left[\overline{\mathrm{diag}}\left(\hat{\mathbf{\Gamma}}^{-1} \underline{\mathbf{H}}^{\mathrm{T}} \underline{\hat{\mathbf{H}}}_{\mathrm{U}}^{*} \left(\hat{\mathbf{G}} + \overline{\mathrm{diag}}(\underline{\hat{\mathbf{R}}}^{\mathrm{T}}) \right)^{-1} \hat{\mathbf{\Gamma}} \right) \overline{\mathrm{diag}}\left(\hat{\mathbf{\Gamma}} \left(\hat{\mathbf{G}} + \overline{\mathrm{diag}}(\underline{\hat{\mathbf{R}}}^{*}) \right)^{-1} \underline{\hat{\mathbf{H}}}_{\mathrm{U}}^{\mathrm{T}} \underline{\mathbf{H}}^{*} \hat{\mathbf{\Gamma}}^{-1} \right) \right]_{k,k}, \tag{6.21}$$

and

$$N_{\mathrm{JT}}^{(k)} = \sigma^2 \left[\left(\hat{\mathbf{G}} + \overline{\mathrm{diag}}\left(\underline{\hat{\mathbf{R}}} \right) \right)^{-1} \underline{\hat{\mathbf{H}}}_{\mathrm{U}}^{*\mathrm{T}} \underline{\hat{\mathbf{H}}}_{\mathrm{U}} \left(\hat{\mathbf{G}} + \overline{\mathrm{diag}}\left(\underline{\hat{\mathbf{R}}}^{*\mathrm{T}} \right) \right)^{-1} \right]_{k,k} \tag{6.22}$$

can be calculated from (6.18).

Given the same average transmit power per data symbol P_{d} and the same noise variance σ^2, the data estimates in the UL and in the DL will contain the same average useful signal power and the same average noise power. However, in general, with the same partial CSI, the average interference power in the UL applying JD is different from that in the DL applying JT.

6.3 Numerical results for performance assessment

6.3.1 Preliminary remarks

In this section, the system performance of the proposed cooperative communication scheme is assessed with respect to numerical simulation results in both the UL and the DL. The numerical results concerning the iterative JD/JT algorithm are obtained based on the limiting values. The system performance of the proposed scheme is compared to the one of conventional and state of the art communication schemes.

A realistic cellular system including 21 cells with the cluster size $r = 1$ is taken as the reference scenario as shown in Figure 6.1. Concerning the channel model and the BS-antenna-layout considered in this scenario, details are discussed in Chapter 2. Here, some key preassumptions for the simulations are listed as follows:

- Rayleigh fading and a path loss with attenuation exponent $\alpha = 3$ with respect to the distance are considered.
- Applying the OFDM transmission technique, in every cell one BS with 3 antennas and one active MS with a single antenna in every time slot and subcarrier are considered. The candidate BS-antenna-layouts are those introduced in Section 2.3, i.e., omni-DAS, sector-DAS I, and sector-DAS II.
- QPSK modulation with the transmit power P_{d} per data symbol is applied. The background noise is assumed to be white and Gaussian distributed with a variance of $\sigma^2/2$ for both the real and imaginary parts.

Some terms and parameters considered in the following discussions are introduced here.

- **bad vertex:** Applying any one of the three BS-antenna-layouts in Figure 6.1, a vertex of the hexagonal cell 1 which is far away from the BS antennas of cell 1 is denoted as "bad vertex".
- **RxMF-cell/TxMF-cell:** In conventional cellular systems, the MF technique considering only the intra-cell useful channels for each MS is applied in individual cells. At the receiver side in the UL and at the transmitter side in the DL, they are denoted as "RxMF-cell" and "TxMF-cell", respectively.
- **JD-SA/JT-SA:** Applying the state of the art structure-oriented static significant channel selection strategy for JD/JT [WMSL02], the 21-cell cellular system is divided into 7 SAs. Specifically, cells $3n-2$, $3n-1$, and $3n$ are contained in SA n, $n = 1, \ldots, 7$. The intra-SA JD scheme in the UL and the intra-SA JT scheme in the DL are denoted as "JD-SA" and "JT-SA", respectively.

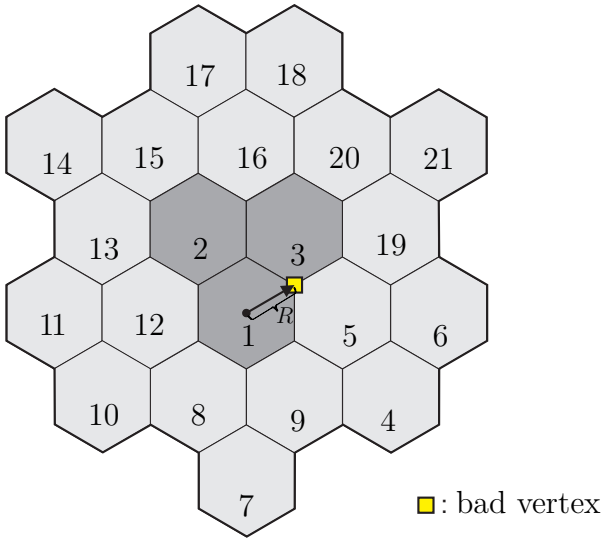

Figure 6.1. Reference scenario of a 21-cell cellular system in simulations.

- **JD-**$(N_{\mathrm{U}}, N_{\mathrm{I}})$**/JT-**$(N_{\mathrm{U}}, N_{\mathrm{I}})$**/JD-**$(N_{\mathrm{UG}}, N_{\mathrm{IG}})$**/JT-**$(N_{\mathrm{UG}}, N_{\mathrm{IG}})$**:** Applying the proposed two dynamic MS-oriented significant channel selection algorithms, N_{U} significant useful channels and N_{I} significant interfering channels for each MS, or N_{UG} significant useful channel groups and N_{IG} significant interfering channel groups for each MS can be selected. The proposed JD scheme in the UL and JT scheme in the DL considering the significant channels selected following the two algorithms are denoted as "JD-$(N_{\mathrm{U}}, N_{\mathrm{I}})$", "JT-$(N_{\mathrm{U}}, N_{\mathrm{I}})$", "JD-$(N_{\mathrm{UG}}, N_{\mathrm{IG}})$" and "JT-$(N_{\mathrm{UG}}, N_{\mathrm{IG}})$", respectively.

- $\boldsymbol{\Upsilon_{\mathrm{N}}}$**:** This parameter is used to indicate the ratio of the average receive signal power to the noise power in the reference scenario. Assuming MS 1 is located at the "bad vertex", the MF receive power for MS 1 considering all BS antennas in the 21-cell system can be calculated as a constant parameter based on one channel snapshot. With the unit transmit power per data symbol $P_{\mathrm{d}} = 1$, the average receive power for the MS at the "bad vertex" over sufficient channel snapshots is $P_{\mathrm{B}} = \mathrm{E}\{\sum_{k_{\mathrm{A}}} \underline{H}^{(k_{\mathrm{A}},1)} \underline{H}^{(k_{\mathrm{A}},1)^*}\}$. The relative noise condition in the reference scenario can be fully characterized by the parameter $\Upsilon_{\mathrm{N}}(\mathrm{dB}) = 10\log_{10}\big(P_{\mathrm{B}}/\sigma^2\big)$.

- $\boldsymbol{\Upsilon_{\Delta}}$**:** The relative accuracy of CSI in the reference scenario can be characterized by the ratio $\Upsilon_{\Delta}(\mathrm{dB}) = 10\log_{10}\big(P_{\mathrm{B}}/\sigma_{\Delta}^2\big)$, where P_{B} is the average MF receive power of the MS at the "bad vertex" and σ_{Δ}^2 is the variance of channel estimation error.

In the following, the influence of the significant channel selection, the influence of the smart BS-antenna-layout and the influence of the imperfectness of CSI on the proposed cooperative communication scheme are analyzed by Monte Carlo simulations.

6.3.2 Influence of the significant channel selection

In this section, the influence of the significant channel selection scheme on system performance of the cooperative communication in the UL and in the DL is investigated. In this part of the performance assessment, perfect CSI is assumed to be available. Considering the reciprocity of the mobile radio channels in the investigated TDD system, the same significant channels are selected in both the UL and the DL. The following aspects concerning the influence of the significant channel selection are investigated.

- One important issue of an iterative algorithm is its convergence behaviour. The convergence behaviour of the proposed iterative JD/JT algorithm considering different numbers of significant channels is assessed.
- System performances of various communication schemes considering different significant channels are compared in terms of the complementary cumulative distribution function (CCDF) of the BER. The BER of the cooperative communication scheme applying the iterative JD/JT algorithm is calculated based on its limiting values.
- Applying the proposed MS-oriented dynamic significant channel selection strategy, the influence of different numbers of significant useful/interfering channels considered in JD/JT is investigated with respect to outage capacity.
- The proposed practical significant channel selection scheme is compared with an optimum channel selection scheme achieving the maximum reliability information of data detection. The corresponding performance loss is given in an exemplary scenario.

Firstly, let us have a look at the convergence behaviour of the proposed iterative JD/JT algorithm. In Figure 6.2, the convergence behaviour is assessed with respect to the spectral radius of the loop matrices in the UL and in the DL with the help of the CCDF. Based on the 21-cell reference scenario, the case of full cooperation considering all the channels and two exemplary partial cooperation cases, i.e., JD/JT-$(N_{\mathrm{UG}}, N_{\mathrm{IG}})$ considering $N_{\mathrm{UG}} = 3$ significant useful channel groups and $N_{\mathrm{IG}} = 6$ or $N_{\mathrm{IG}} = 20$ significant interfering channel groups, are investigated. The most important results derived from Figure 6.2 are the following:

- The same spectral radius distribution in the UL and the DL indicating the same convergence speed of the iterative partial JD algorithm and the iterative partial JT algorithm is obtained. This numerical results coincide with the analytical assessment in Section 6.2.

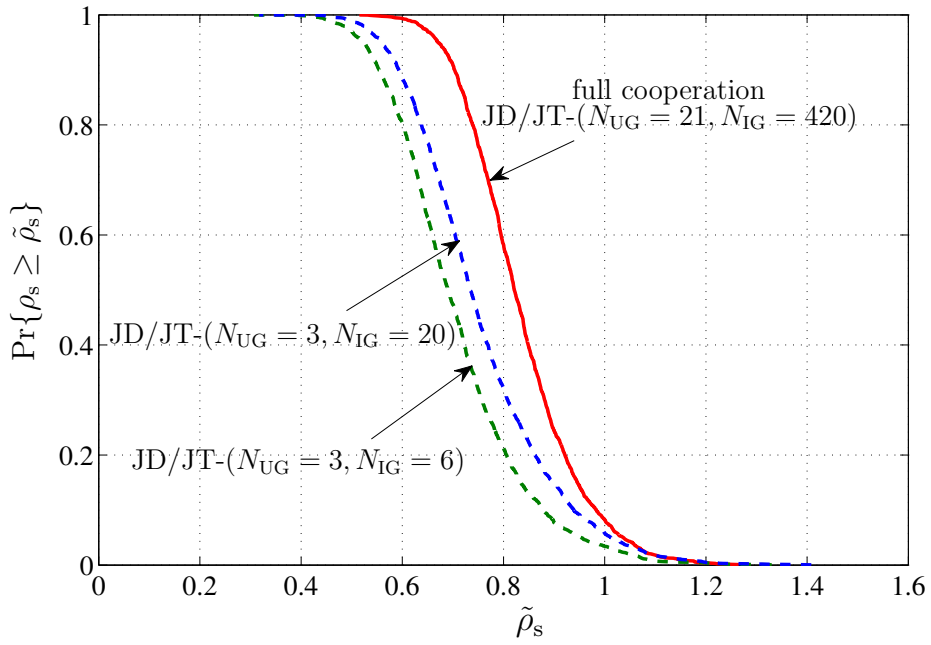

Figure 6.2. CCDF of spectral radius ρ_{s} of iterative algorithm loop matrix in the UL/DL.

- Since most of the spectral radiuses are smaller than 1 in JD/JT with full CSI or with partial CSI, convergence is ensured in most cases. Partial JD/JT can even converge faster than full JD/JT. Generally, considering significant CSI in the iterative algorithm, the convergence behaviour will not be destroyed.

Secondly, the BER performance of various communication schemes considering different significant channels is assessed with the help of the CCDF in Figure 6.3 for the UL and in Figure 6.4 for the DL. As mentioned before, the reference scenario in Figure 6.1 can be considered 7 SAs including 3 cells in each SA. SA 1 is in the center and 6 SAs are around SA 1. The investigated 21-cell cellular system can be considered as a subsystem in a realistic large cellular system. Namely, in a large cellular system extended from this 21-cell reference scenario, every SA is surrounded by 6 SAs. Without loss of generality, the average BER performance of the MSs which are physically located in the central SA 1 including cells 1, 2, and 3 is assessed to compare different significant channel selection strategies in this 21-cell reference scenario. As shown in Section 5.3.2, different communication schemes consider different channels in the signal processing. Interestingly, the conventional cellular communication scheme and the SA communication scheme can be considered as special cases of the general cooperative communication scheme considering different significant channel selection strategies. The most important results derived from Figure 6.3 and Figure 6.4 are the following:

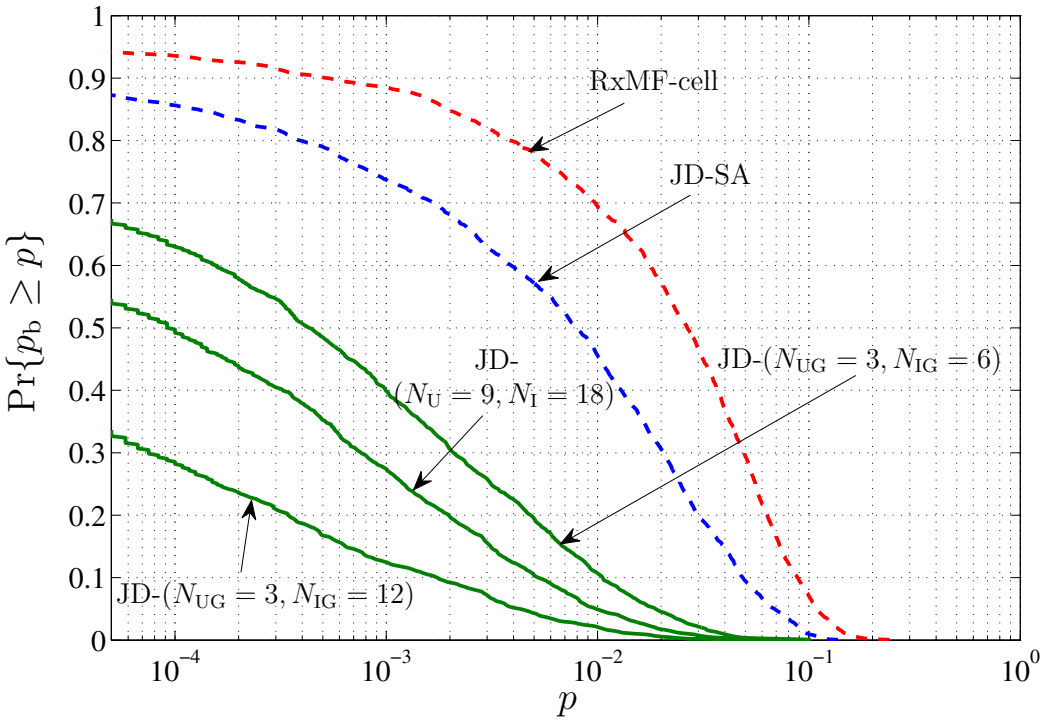

Figure 6.3. CCDF of the average BER in SA 1 including cells 1, 2, and 3 in the UL with $\Upsilon_{\mathrm{N}} = 40\,\mathrm{dB}$ (interference-limited cellular system).

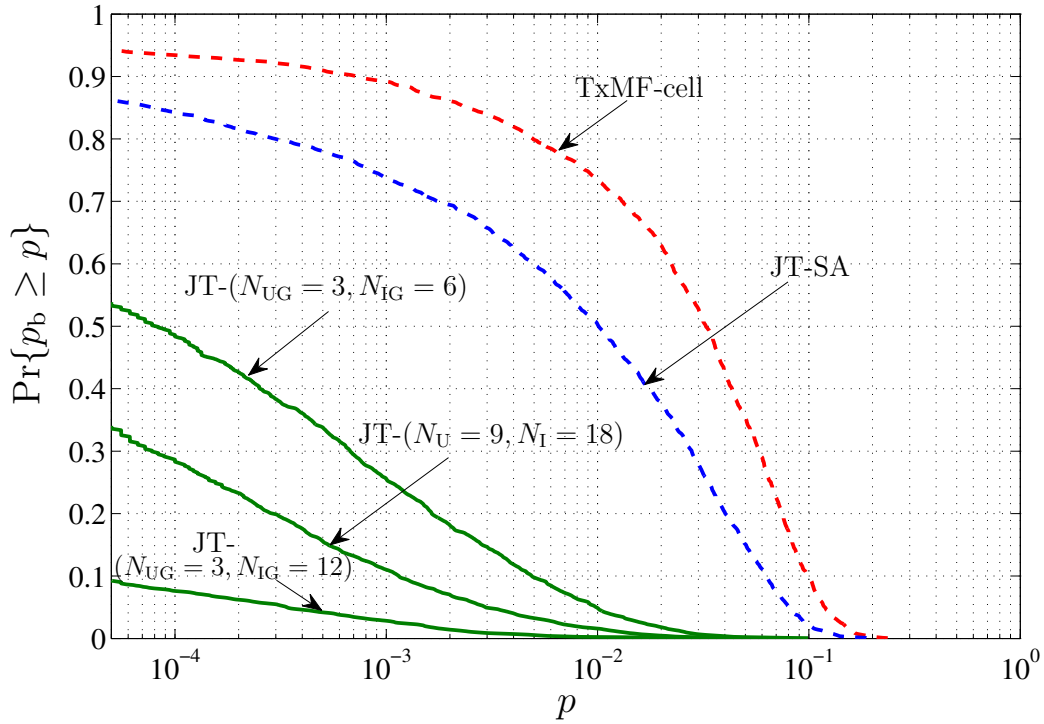

Figure 6.4. CCDF of the average BER in SA 1 including cells 1, 2, and 3 in the DL with $\Upsilon_{\mathrm{N}} = 40\,\mathrm{dB}$ (interference-limited cellular system).

- The conventional cellular communication scheme applying intra-cell MF denoted by "RxMF-cell" and "TxMF-cell" in the UL and in the DL, respectively, gives the worst performance among all the investigated schemes. The reason is that this scheme considers only intra-cell useful channels but no inter-cell interfering channels in the signal processing. The system performance is strongly limited by inter-cell interference.

- The SA communication scheme applying intra-SA JD/JT denoted by "JD-SA" and "JT-SA" in the UL and in the DL, respectively, outperforms the conventional cellular communication scheme. The reason is that all the intra-SA channels are considered as significant channels for each MS, and the inter-cell interference is significantly reduced.

- For the cooperative communication scheme, the two MS-oriented dynamic significant channel selection algorithms introduced as Algorithm-I and Algorithm-II in Section 4.3.2 are considered here. For a fair system performance comparison, the same number of significant useful channels and the same number of significant interfering channels for each MS as considered in the SA-based JD/JT for each MS are selected. Corresponding to Algorithm-I, the BER curves of the cooperative communication scheme applying JD/JT considering 3 significant useful channel groups and 6 significant interfering channel groups for every MS denoted by "JD-($N_{\mathrm{UG}} = 3, N_{\mathrm{IG}} = 6$)" and "JT-($N_{\mathrm{UG}} = 3, N_{\mathrm{IG}} = 6$)" in the UL and in the DL, respectively, are plotted. Corresponding to Algorithm-II, the BER curves of the cooperative communication scheme applying JD/JT considering 9 significant useful channels and 18 significant interfering channels denoted by "JD-($N_{\mathrm{U}} = 9, N_{\mathrm{I}} = 18$)" and "JT-($N_{\mathrm{U}} = 9, N_{\mathrm{I}} = 18$)" in the UL and in the DL, respectively, are plotted. Obviously, in both the UL and the DL, "JD/JT-($N_{\mathrm{UG}} = 3, N_{\mathrm{IG}} = 6$)" outperforms the corresponding "JD/JT-SA". Furthermore, "JD/JT-($N_{\mathrm{U}} = 9, N_{\mathrm{I}} = 18$)" outperforms "JD/JT-($N_{\mathrm{UG}} = 3, N_{\mathrm{IG}} = 6$)". The reason is that the channels which really play a significant role in the system performance for each MS have a higher chance to be selected by the dynamic MS-oriented selection strategy. Algorithm-II directly selecting individual significant channels can further break the constraint in Algorithm-I that the channels between one MS and all antennas of one BS have to be selected together.

- As illustrated by the BER curves denoted by "JD-($N_{\mathrm{UG}} = 3, N_{\mathrm{IG}} = 12$)" and "JT-($N_{\mathrm{UG}} = 3, N_{\mathrm{IG}} = 12$)" in the UL and in the DL, respectively, the system performance of the cooperative communication scheme can be further improved by considering some more significant channel groups. Generally, applying JD/JT with a few appropriately selected significant channels, both the UL and the DL can achieve very low BERs, although they don't have the same BER distribution.

Thirdly, the influence of different amount of considered significant CSI corresponding to different numbers of selected significant channels on system performance of the proposed cooperative communication scheme is investigated. Similar to the above investigations, the system performance of the representative MSs in SA 1 including cells 1, 2, and 3 is assessed in the 21-cell reference scenario. Applying the MS-oriented dynamic significant channel selection strategy considering different numbers N_{UG} of significant useful channel groups and different numbers N_{IG} of significant interfering channel groups, the outage capacity of MSs in the three central cells is calculated and shown in Figure 6.5 for the UL and in Figure 6.6 for the DL. The calculations are based on the assumption that the remaining interfering signals and the noise signals after partial JD/JT are uncorrelated and Gaussian distributed. With $\gamma^{(k)}$ indicating the SINR for MS k which can be derived from the analytical assessment of the SINR in Section 6.2.4, the corresponding instantaneous capacity is calculated as

$$C_{\mathrm{int}}^{(k)} = \log_2\left(1+\gamma^{(k)}\right) \quad . \tag{6.23}$$

Based on a sufficient number of channel snapshots, the outage capacity C_{out} in SA 1 is defined with respect to its outage probability p_{out} as

$$p_{\mathrm{out}} = \Pr\left\{C_{\mathrm{int}}^{(k)} < C_{\mathrm{out}}\right\}, \quad k = 1,2,3 \ , \tag{6.24}$$

where p_{out} describes the probability that the instantaneous capacity $C_{\mathrm{int}}^{(k)}$ of one MS in SA 1 is smaller than the outage capacity C_{out}. For every pair of $(N_{\mathrm{UG}}, N_{\mathrm{IG}})$, an outage capacity C_{out} can be calculated based on a given p_{out}. The most important results derived from Figure 6.5 and Figure 6.6 concerning the influence of the numbers of selected significant useful/interfering channels are the following:

- Generally, the more significant channels are considered in the proposed cooperative communication scheme, the better system performance can be achieved in the interference-limited cellular system. Considering N_{UG} significant useful channel groups for each MS in JD/JT,

  $$\eta = \frac{N_{\mathrm{IG}}}{N_{\mathrm{UG}} \cdot (K-1)} \tag{6.25}$$

  indicates the ratio of the number of significant interfering channel groups N_{IG} considered for each MS in JD/JT to the number of interfering channel groups $N_{\mathrm{UG}} \cdot (K-1)$ connected to all the involved BSs for each MS. Interestingly, it is shown that the outage capacity increases with the number N_{UG} and the ratio η rather than directly with the number N_{IG}.

- Concerning the number of significant useful channels, the more significant useful channels are considered, the more noise can be suppressed. However, the more

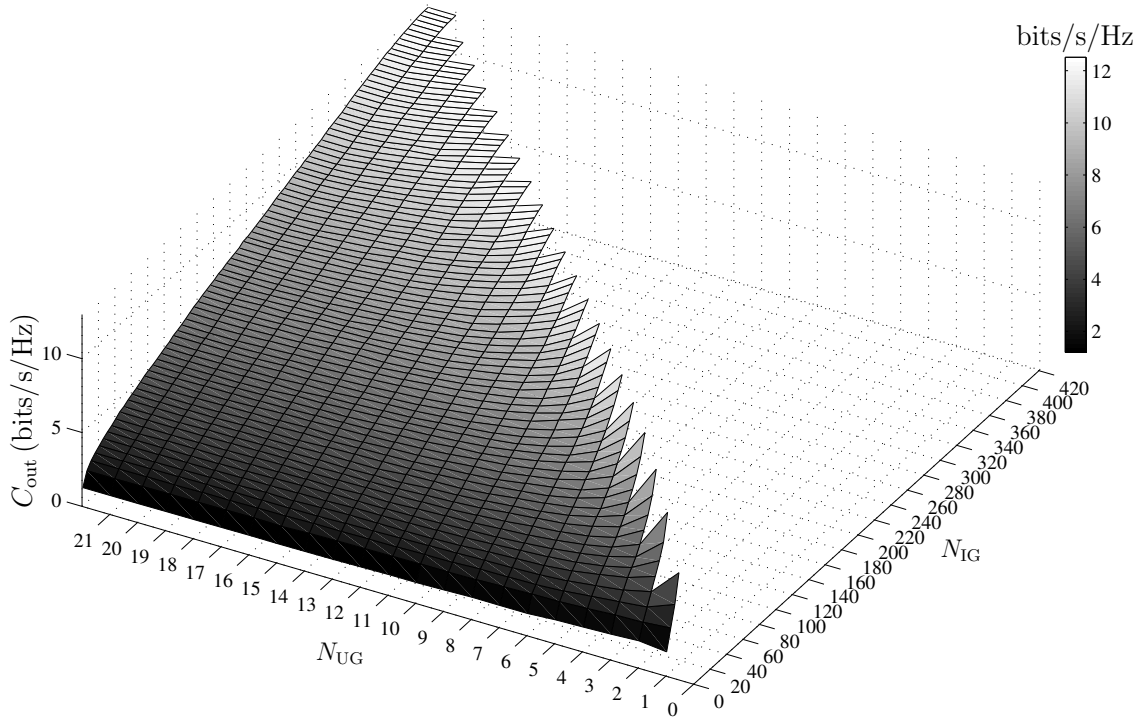

Figure 6.5. Outage capacity of MSs in SA 1 including cells 1, 2, and 3 applying JD in the UL considering different numbers of significant channel groups, $p_{\text{out}} = 0.1$, $\Upsilon_{\text{N}} = 40\,\text{dB}$ (interference-limited cellular system).

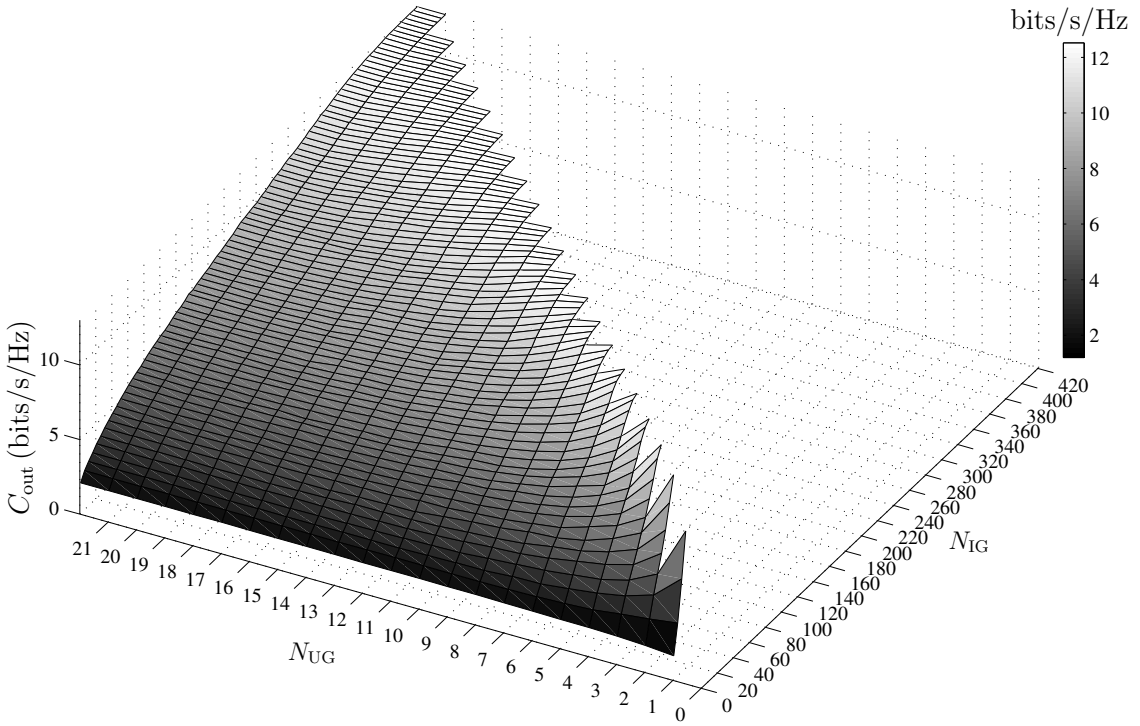

Figure 6.6. Outage capacity of MSs in SA 1 including cells 1, 2, and 3 applying JT in the DL considering different numbers of significant channel groups, $p_{\text{out}} = 0.1$, $\Upsilon_{\text{N}} = 40\,\text{dB}$ (interference-limited cellular system).

BSs corresponding to the significant useful channels for each MS are involved in JD/JT, the more interference is included in the matched filtering data estimate for each MS. Therefore, in realistic interference-limited cellular systems, it is not always true that a larger number of significant useful channels considered in JD/JT can lead to a better system performance.

- Concerning the number of the significant interfering channels, generally the more interfering channels are considered, the more interference can be eliminated or avoided, but the larger the noise enhancement will be. In interference-limited cellular systems with weak noise, the system performance of the proposed cooperative communication scheme, i.e., "JD/JT-($N_{\mathrm{UG}}, N_{\mathrm{IG}}$)", is mainly limited by the remaining $(N_{\mathrm{UG}} \cdot (K-1) - N_{\mathrm{IG}})$ interfering channel groups which are not taken into consideration in JD/JT. However, in cellular systems with very strong noise and weak interference, it is not necessary to consider too many interfering channels in JD/JT. Considering all the $N_{\mathrm{IG}} = N_{\mathrm{UG}} \cdot (K-1)$ interfering channel groups corresponding to N_{UG} significant useful channel groups in JD and in JT, the same outage capacity is obtained in the UL and in the DL. Considering the same number $N_{\mathrm{IG}} < N_{\mathrm{UG}} \cdot (K-1)$ of interfering channel groups, the UL and the DL have different outage capacities in general. This result implies that considering the same number of significant channels the UL and the DL have the same output SNRs but different output SINRs. The reason is that the data estimates in the UL and those in the DL generally contain different interference powers.

- The outage capacity of the 21-cell cellular system with the cluster size $r = 1$ applying the intra-SA JD/JT with 3 cells per SA has been calculated for reasons of comparison. $C_{\mathrm{out}} = 1.8$ bits/s/Hz holds for the UL applying "JD-SA", and $C_{\mathrm{out}} = 1.6$ bits/s/Hz holds for the DL applying "JT-SA". For a fair comparison, the same number of useful channel groups and the same number of interfering channel groups as considered in the intra-SA JD/JT are considered in the JD/JT based on the MS-oriented dynamic significant channel selection strategy. $C_{\mathrm{out}} = 2.75$ bits/s/Hz holds for the UL applying "JD-($N_{\mathrm{UG}} = 3, N_{\mathrm{IG}} = 6$)", and $C_{\mathrm{out}} = 3.068$ bits/s/Hz holds for the DL applying "JT-($N_{\mathrm{UG}} = 3, N_{\mathrm{IG}} = 6$)". Obviously, the JD/JT scheme with dynamically selected MS-oriented significant channels outperforms the JD/JT scheme with structure-oriented fixed significant channels.

The proposed practical significant channel selection strategy is based on channel gains and weighting factor magnitudes of the interference. In most scenarios, the channels selected following this strategy play a significant role in the system performance. However, it is worth pointing out that from the point of view of system performance this practical proposal is not the optimum solution. For example, the significant channels can be selected in a way to obtain the maximum SINR indicating the maximum

throughput of data transmission, or to obtain the maximum average magnitude of LLRs indicating the maximum reliability information of data detection. In the following, the idea of an advanced significant channel selection scheme aiming at optimum system performance in terms of the reliability information is illustrated in an exemplary scenario.

For the sake of simplicity, a real-valued two-user communication channel with a 2×2 channel matrix $\mathbf{H}$ including i.i.d. channel coefficients $h_{ij} \sim \mathcal{N}(0,1)$, $i, j{=}1,2$ is taken as an exemplary scenario. Applying BPSK modulation, i.i.d. data symbols are included in the transmitted data vector $\mathbf{d} = (d_1, d_2)^{\mathrm{T}}$. The noise vector $\mathbf{n} = (n_1, n_2)^{\mathrm{T}}$ contains the Gaussian distributed noise signals, i.e., $n_k \sim \mathcal{N}(0, \sigma^2)$, $k{=}1,2, \sigma^2 = 0.1$. The received vector $\mathbf{y} = (y_1, y_2)^{\mathrm{T}}$ is obtained as $\mathbf{y} = \mathbf{H} \cdot \mathbf{d} + \mathbf{n}$. For a snapshot of the channel matrix $\mathbf{H}$, the average magnitude of LLRs is obtained as

$$\overline{\left|LLR(\mathbf{H})\right|} = \underset{\{\mathbf{d},\mathbf{n}\}}{\mathrm{E}} \{(\left|L\left(d_1|\mathbf{y}\right)\right| + |L\left(d_2|\mathbf{y}\right)|)/2\} \ , \tag{6.26}$$

where $L\left(d_{\mathrm{i}}|\mathbf{y}\right)$ with $i{=}1,2$ can be calculated as

$$L\left(d_{\mathrm{i}}|\mathbf{y}\right) {=} \ln\left(\frac{P(d_{\mathrm{i}}=+1|\mathbf{y})}{P(d_{\mathrm{i}}=-1|\mathbf{y})}\right) = \ln\left(\frac{P(\mathbf{y}|d_{\mathrm{i}}=+1,d_{\mathrm{j}}=+1)+P(\mathbf{y}|d_{\mathrm{i}}=+1,d_{\mathrm{j}}=-1)}{P(\mathbf{y}|d_{\mathrm{i}}=-1,d_{\mathrm{j}}=+1)+P(\mathbf{y}|d_{\mathrm{i}}=-1,d_{\mathrm{j}}=-1)}\right) \tag{6.27}$$

with $j{=}1,2, j \neq i$. Two significant channel selection schemes are compared. Scheme I as a simplified version of the proposed practical channel selection strategy selects 3 out of 4 channel coefficients with the largest channel gains. Scheme II aiming at the maximum reliability information selects 3 out of 4 channel coefficients to achieve the largest average magnitude of LLRs over random data symbols and random noise signals. In the calculation, the exact channel coefficients of the 3 selected significant channels and the statistical channel knowledge of the other insignificant channel are considered. If h_{12} is treated as the insignificant channel,

$$\begin{aligned} P(\mathbf{y}|d_1,d_2) &= \int \frac{\exp\left(-\frac{(y_1-h_{11}d_1-\hat{h}_{12}d_2)^2}{2\sigma^2}\right)}{\sqrt{2\pi\sigma^2}} \cdot \frac{\exp\left(-\frac{(\hat{h}_{12})^2}{2}\right)}{\sqrt{2\pi}} \mathrm{d}\hat{h}_{12} \cdot \frac{\exp\left(-\frac{(y_2-h_{21}d_1-h_{22}d_2)^2}{2\sigma^2}\right)}{\sqrt{2\pi\sigma^2}} \\ &= \frac{\exp\left(-\frac{(y_1-h_{11}d_1)^2}{2(d_2^2+\sigma^2)} - \frac{(y_2-h_{21}d_1-h_{22}d_2)^2}{2\sigma^2}\right)}{2\pi\sqrt{(d_2^2+\sigma^2)\sigma^2}} \end{aligned} \tag{6.28}$$

is applied in (6.27). Without loss of generality, (6.28) can be easily modified to the case that any other channel is treated as the insignificant one. According to the selection results of the applied significant channel selection scheme, $\overline{\left|LLR(\mathbf{H})\right|}$ for each snapshot of the channel matrix $\mathbf{H}$ is obtained. Based on a sufficient number of snapshots of the channel matrix, the expectation $\overline{\left|LLR\right|} = \underset{\{\mathbf{H}\}}{\mathrm{E}} \{\overline{\left|LLR(\mathbf{H})\right|}\}$ can be calculated. The reliability information loss of Scheme I as compared to Scheme II in this example can be measured by $(\overline{\left|LLR\right|}^{(\mathrm{II})} - \overline{\left|LLR\right|}^{(\mathrm{I})}) \approx 22.7 - 18.7 = 4$.

6.3.3 Influence of the smart BS-antenna-layout

In this section, the influence of the smart BS-antenna-layout on the system performance of the proposed cooperative communication scheme in both the UL and the DL is investigated. Some preliminary remarks concerning the investigations in the present section are firstly made as follows:

- In a reference scenario with a finite size, in general the inter-cell interference for the MS in a cell close to the scenario boundary is smaller than that for the MS in a cell close to the scenario center. However, as mentioned before, the 21-cell reference scenario could be a subsystem of a realistic large cellular system, and every cell is surrounded by many other cells in reality. Without loss of generality, the system performance of the MS in cell 1 of the 21-cell reference scenario is investigated in this section ignoring the boundary effect.
- The influence of the smart BS-antenna-layout is investigated by comparing system performances under different combinations of signal processing techniques and BS-antenna-layouts. More precisely, the conventional intra-cell MF and the proposed multi-cell JD/JT with significant CSI are considered as the candidate signal processing techniques. The omni-DAS, the sector-DAS I, and the sector-DAS II which are introduced in Section 2.3 are considered as candidate BS-antenna-layouts.
- This section focuses on purely interference-limited cellular systems without noise, where the SINR of (6.14) and (6.19) can be simplified to the signal-to-interference ratio (SIR). The system performance is assessed in terms of the outage probability of the SIR calculated with respect to 10 dB.

In Figure 6.7 and Figure 6.8, the system performance of the MS in cell 1 moving from the cell center to the "bad vertex" in the direction of the arrow as indicated in Figure 6.1 is investigated for the UL and for the DL, respectively. For every BS-antenna-layout candidate, 3 intra-cell useful channels are considered in the conventional intra-cell RxMF/TxMF. For a fair comparison, the same number of useful channels $N_{\mathrm{U}} = 3$ is selected as significant useful channels and considered in the proposed JD/JT scheme. Additionally, $N_{\mathrm{I}} = 6$ significant interfering channels are taken into consideration in the proposed JD/JT scheme for inter-cell interference management. At every investigated position from the cell center to the "bad vertex", the outage probability of the SIR is calculated. In order to keep the continuity of system performance, for all BS-antenna-layouts it is assumed that the position of the "bad vertex" is served by the same antennas which serve the positions very close to the "bad vertex" inside cell 1.

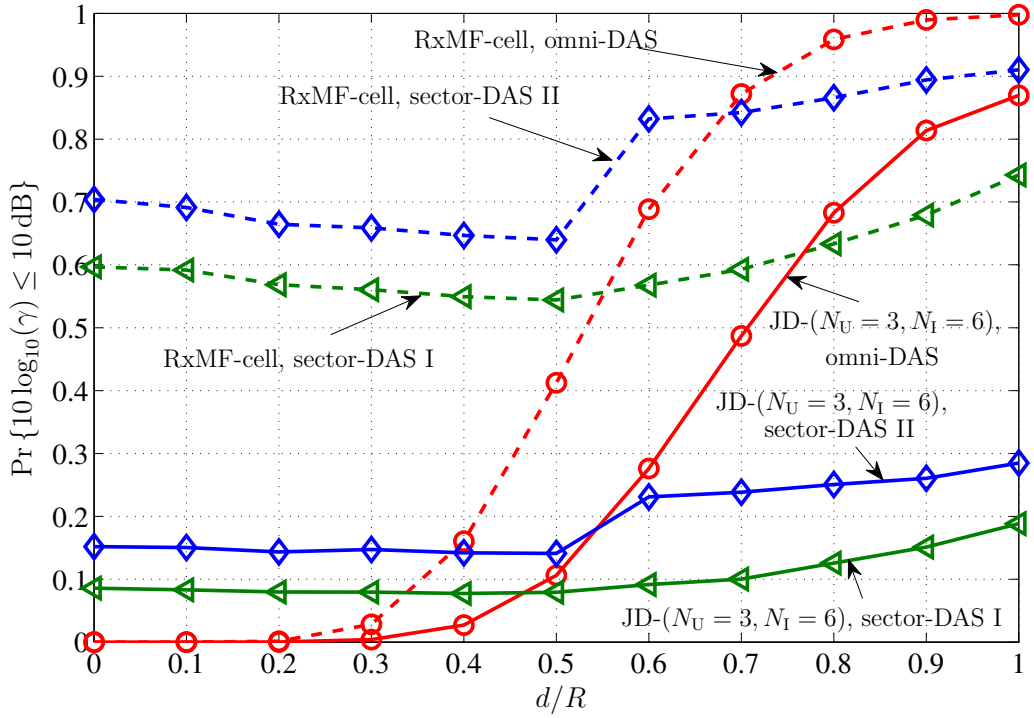

Figure 6.7. Outage probability of SIR for MS moving from cell center to the "bad vertex" in cell 1 in the UL with d/R indicating the ratio of the distance d between the MS and the cell center to the cell radius R.

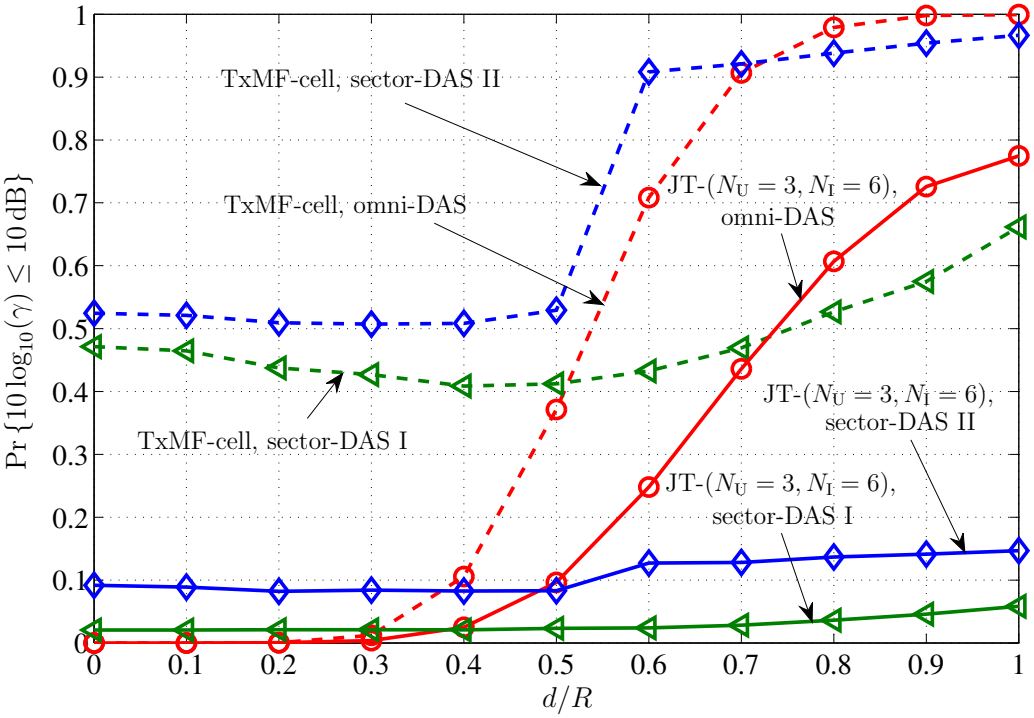

Figure 6.8. Outage probability of SIR for MS moving from cell center to the "bad vertex" in cell 1 in the DL with d/R indicating the ratio of the distance d between the MS and the cell center to the cell radius R.

In Figure 6.9, the system performance difference between different combinations of signal processing techniques and BS-antenna-layouts is more clearly shown with the help of contour plots. Sector-DAS I as a representative BS-antenna-layout with directional antennas is compared with omni-DAS as a representative BS-antenna-layout with omnidirectional antennas. The contours of the following ratios with respect to the outage probability of SIR are plotted for the whole area of cell 1. For comparing the performances of the sector-DAS I and the omni-DAS applying the intra-cell MF,

$$\Upsilon_{\mathrm{RxMF-cell}} = 10\log_{10}\left(\frac{\Pr\{10\log_{10}\left(\gamma_{\mathrm{sector,RxMF-cell}}\right) \leq 10\mathrm{dB}\}}{\Pr\{10\log_{10}\left(\gamma_{\mathrm{omni,RxMF-cell}}\right) \leq 10\mathrm{dB}\}}\right)\mathrm{dB} \tag{6.29}$$

and

$$\Upsilon_{\mathrm{TxMF-cell}} = 10\log_{10}\left(\frac{\Pr\{10\log_{10}\left(\gamma_{\mathrm{sector,TxMF-cell}}\right) \leq 10\mathrm{dB}\}}{\Pr\{10\log_{10}\left(\gamma_{\mathrm{omni,TxMF-cell}}\right) \leq 10\mathrm{dB}\}}\right)\mathrm{dB} \tag{6.30}$$

are considered for the UL and the DL, respectively. For comparing the performances of the sector-DAS I and the omni-DAS applying the iterative ZF JD/JT with significant CSI,

$$\Upsilon_{\mathrm{JD}-(N_{\mathrm{U}},N_{\mathrm{I}})} = 10\log_{10}\left(\frac{\Pr\{10\log_{10}\left(\gamma_{\mathrm{sector,JD}-(N_{\mathrm{U}},N_{\mathrm{I}})}\right) \leq 10\mathrm{dB}\}}{\Pr\{10\log_{10}\left(\gamma_{\mathrm{omni,JD}-(N_{\mathrm{U}},N_{\mathrm{I}})}\right) \leq 10\mathrm{dB}\}}\right)\mathrm{dB} \tag{6.31}$$

and

$$\Upsilon_{\mathrm{JT}-(N_{\mathrm{U}},N_{\mathrm{I}})} = 10\log_{10}\left(\frac{\Pr\{10\log_{10}\left(\gamma_{\mathrm{sector,JT}-(N_{\mathrm{U}},N_{\mathrm{I}})}\right) \leq 10\mathrm{dB}\}}{\Pr\{10\log_{10}\left(\gamma_{\mathrm{omni,JT}-(N_{\mathrm{U}},N_{\mathrm{I}})}\right) \leq 10\mathrm{dB}\}}\right)\mathrm{dB} \tag{6.32}$$

are considered for the UL and the DL, respectively. Similar to Figure 6.7 and Figure 6.8, $N_{\mathrm{U}} = 3$ significant useful channels and $N_{\mathrm{I}} = 6$ significant interfering channels are considered in the proposed JD/JT scheme in Figure 6.9.

Concerning the influence of the smart BS-antenna-layout on the system performance, the most important results drawn from Figure 6.7, Figure 6.8, and Figure 6.9 are as follows:

- When applying the same signal processing technique for the MS at positions close to the cell center, the omni-DAS with omnidirectional BS-antennas in the cell center outperforms the considered two sector-DASs with directional BS-antennas at cell vertices. On the contrary, the considered two sector-DASs outperform the omni-DAS at positions close to the cell boundary. These results hold both in the UL and in the DL. The main reason for these results is that the useful signal is much stronger at the positions close to the BS-antennas than the positions far away from the BS-antennas.

- Figure 6.7 and Figure 6.8 show that the sector-DAS I outperforms the sector-DAS II at all the investigated positions from the cell center to the "bad vertex". This phenomenon is mainly due to the fact that the BS-antennas in sector-DAS I have

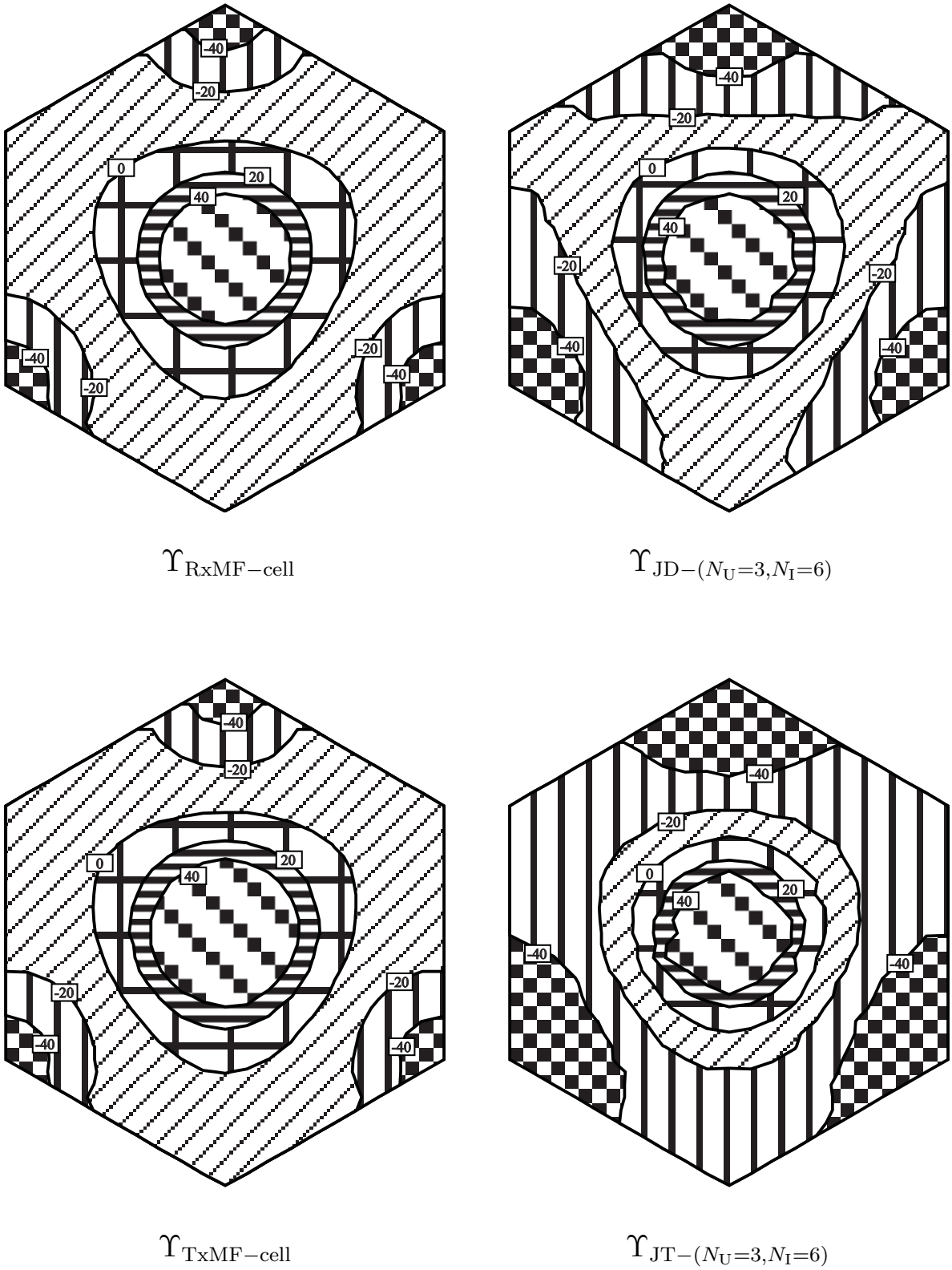

Figure 6.9. Contours with respect to the ratios of the outage probability of SIR for the MS in cell 1 described in dB.

more favourable directions than those in sector-DAS II to avoid inter-cell interference. Namely, as compared to sector-DAS I, in sector-DAS II the BS-antennas considered for MS in cell 1 are more likely to receive inter-cell interference from other MSs in the UL, and the BS-antennas considered for other MSs are more likely to cause inter-cell interference to MS in cell 1 in the DL.

- In Figure 6.7 and Figure 6.8, the outage probability curves corresponding to the same signal processing technique have some intersection points. These points indicate the threshold points where one sector-DAS begins to outperform omni-DAS when the MS is moving from the cell center to the "bad vertex". There is no point of intersection between the curves corresponding to the two sector DASs. The threshold point is closer to the cell center when applying "JD/JT-($N_{\mathrm{U}} = 3, N_{\mathrm{I}} = 6$)" as compared to that applying "RxMF/TxMF-cell". This result implies that the area where sector-DAS outperforms omni-DAS when applying the iterative ZF JD/JT with significant CSI is larger than that when applying the conventional intra-cell MF.

- Based on the above results, sector-DAS I as a better choice of the two sector BS-antenna-layouts is further compared to the conventional omni-DAS in Figure 6.9. In an explicit manner, the contour plots of the ratios in (6.29), (6.30), (6.31) and (6.32) described in dB clearly show the areas in cell 1 where the communication quality of the sector-DAS I is better than that of the omni-DAS, and vice versa. The corresponding extent of performance gain on the contour lines are indicated. The following results can be seen when comparing the contour plot for "RxMF/TxMF-cell" and for "JD/JT-($N_{\mathrm{U}} = 3, N_{\mathrm{I}} = 6$)". When the proposed iterative ZF JD/JT with significant CSI is applied, the area where sector-DAS I outperforms omni-DAS is larger and with a higher extent of performance gain than that when the conventional intra-cell MF is applied. This phenomenon is more obvious in the DL than in the UL.

- In a word, additional performance gain can be achieved by the smart BS-antenna-layout in the proposed cooperative communication scheme with an intelligent signal processing technique. Furthermore, one can even benefit more from the smart sector BS-antenna-layout when applying the JD/JT with significant CSI which is good at inter-cell interference management as compared to applying the conventional intra-cell MF.

Therefore, a good combination of an intelligent signal processing technique and a smart BS-antenna-layout shall be taken into consideration in the design of a practical cooperative communication scheme. The smart BS-antenna-layout is expected to take the most of the advantages of the signal processing technique.

6.3.4 Influence of the imperfectness of CSI

The above investigations are based on the ideal assumption that perfect channel knowledge is available. However, this is not the case in reality due to the limited ability to track CSI in realistic cellular systems. In this section, the influence of the imperfectness of CSI on the cooperative communication scheme is studied.

Firstly, the sensitivity of some typical multiuser detection/transmission algorithms to the imperfectness of CSI is checked in Figure 6.10 and Figure 6.11 for the UL and the DL, respectively. Two exemplary real-valued channel matrices $\mathbf{H}_1 = (10, 1, 0.1; 10, 2, 0.1; 10, 5, 1)$ and $\mathbf{H}_2 = (1, 0.8, 0.8; 1, 1, 0.8; 1, 0.8, 1)$ of small dimensions are considered for the first investigations. Correspondingly, i.i.d. real-valued Gaussian channel-errors with a variance of σ_Δ^2 are assumed. The extent of the imperfectness of CSI can be indicated by the variance described in dB, i.e., $10\log_{10}(\sigma_\Delta^2)$. In the simulation, QPSK modulation with the symbol alphabet $\mathbb{D} = \{d_\mathrm{I} + j * d_\mathrm{Q} \mid d_\mathrm{I}, d_\mathrm{Q} \in \{\pm 1\}\}$ is applied. In Figure 6.10 with different levels of the imperfectness of CSI, the performances of the ZF detection algorithm as the limiting version of the linear iterative PIC algorithm, the nonlinear SIC algorithm as introduced in Section 4.2.3, and the ML detection algorithm as discussed in Section 4.2.1 are reviewed. Additionally, the optimum MF bound denoted by "Opt. MF" is given as the best achievable lower bound of the BER of any data detector. This optimum MF bound is obtained by applying the MF considering all useful channels under the ideal assumption of no multiuser interference. Similarly, in Figure 6.11, the performances of the ZF transmission algorithm as the limiting version of the linear iterative parallel interference presubstraction algorithm and the nonlinear THP algorithm as introduced in Section 5.2.3 are reviewed. In addition, the optimum MF bound denoted by "Opt. MF" under the ideal assumption of no interference is given as the best achievable lower bound of the BER of any data transmitter. The most important results derived from Figure 6.10 and Figure 6.11 are as follows:

- The input SNRs for individual signal processing algorithms are adjusted in such a way that the resulting BER values are always around 10^{-3} under perfect CSI. With the increment of the channel-error variance, the sensitivity of different signal processing algorithms to the imperfectness of CSI can be reviewed with respect to the starting point and the speed of the BER performance degradation.

- Both in the UL and in the DL, with the increment of the extent of imperfectness of CSI, the BERs of the linear/nonlinear interference cancellation/presubstraction algorithms start to significantly increase earlier than the BERs of the optimum detection/transmission algorithms and the optimum MF bound. However,

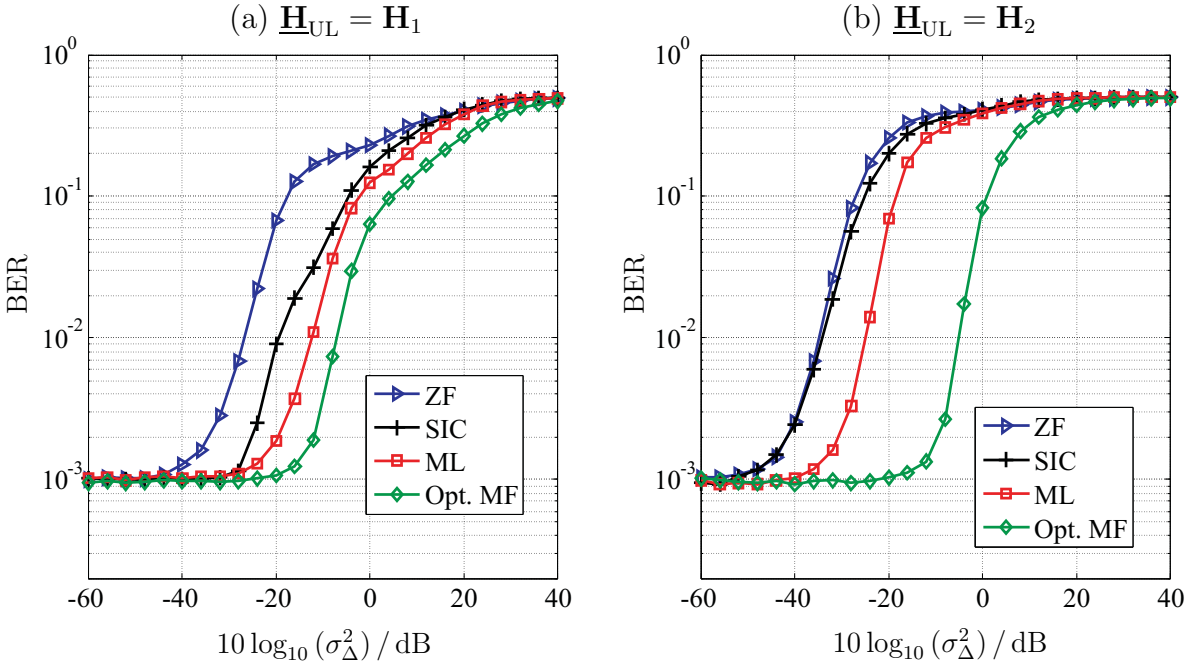

Figure 6.10. BER as a function of the extent of the imperfectness of CSI in the UL applying different multiuser detection algorithms considering channel matrices $\mathbf{H}_1 = (10, 1, 0.1; 10, 2, 0.1; 10, 5, 1)$ and $\mathbf{H}_2 = (1, 0.8, 0.8; 1, 1, 0.8; 1, 0.8, 1)$.

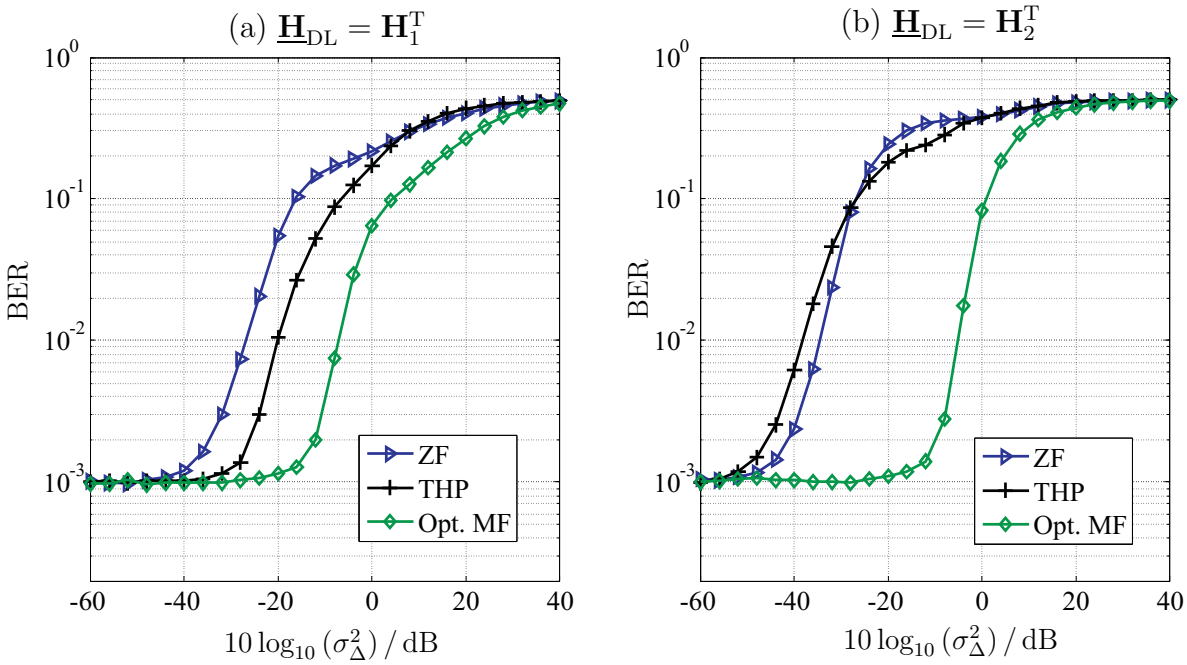

Figure 6.11. BER as a function of the extent of the imperfectness of CSI in the DL applying different multiuser transmission algorithms considering channel matrices $\mathbf{H}_1$=$(10, 1, 0.1; 10, 2, 0.1; 10, 5, 1)$ and $\mathbf{H}_2 = (1, 0.8, 0.8; 1, 1, 0.8; 1, 0.8, 1)$.

the linear/nonlinear interference cancellation/presubstraction algorithms have a lower speed of BER performance degradation as compared to the optimum detection/transmission algorithms and the optimum MF bound.

- The sensitivity of the linear ZF detection algorithm and that of the nonlinear SIC algorithm to the imperfectness of CSI can be compared in Figure 6.10. The sensitivity of the linear ZF transmission algorithm and that of the nonlinear THP algorithm to the imperfectness of CSI can be compared in Figure 6.11. Generally, the answer to the question whether the linear or the nonlinear algorithm dealing with multiuser interference is more sensitive to the imperfectness of CSI depends on the structure of the channel matrix. Especially, the following result can be derived when the channel vectors corresponding to different data symbols have distinctively different Euclidean norms. As the level of the imperfectness of CSI increases, the BER performance of the nonlinear algorithm starts to degrade later but then degrades with a higher speed than that of the linear algorithm.

In the following, the influence of the imperfectness of CSI on the proposed practical cooperative communication scheme is investigated in the 21-cell reference scenario. The system performance is assessed in both the UL and the DL considering alternative BS-antenna-layouts, i.e., omni-DAS and sector-DAS I. Applying the OFDM transmission technique, MSs suffer from only the inter-cell interference and the background Gaussian noise in the reference scenario. The system performance of the cooperative communication scheme dealing with interference and noise is limited by the imperfect knowledge of CSI. In realistic large cellular systems, each cell is surrounded by many cells. Without loss of generality, the following investigations focus on the performance of the MS in cell 1, i.e., MS $k = 1$, which is close to the center of the reference scenario. It is assumed that MS 1 is located at the fixed position of "bad vertex" as shown in Figure 6.1, while other MSs are randomly distributed in other cells. If a good system performance of MS 1 at this "bad vertex" can be obtained when applying the practical cooperative communication scheme, even a better system performance for MS 1 can be expected in the general case that this MS is randomly distributed in cell 1. As mentioned in Section 6.3.1, the parameter Υ_{N} is used to indicate the noise condition in the system. The parameter Υ_{Δ} is used to indicate the relative accuracy of CSI, which implicitly indicates the extent of imperfectness of CSI. Roughly speaking, the smaller the value of Υ_{N} is, the stronger the background noise is. The smaller the value of Υ_{Δ} is, the worse extent the imperfectness of the channel knowledge has.

The impact of imperfect CSI in individual steps of the cooperative communication scheme is investigated in Figure 6.12 and Figure 6.13 for the UL and for the DL,

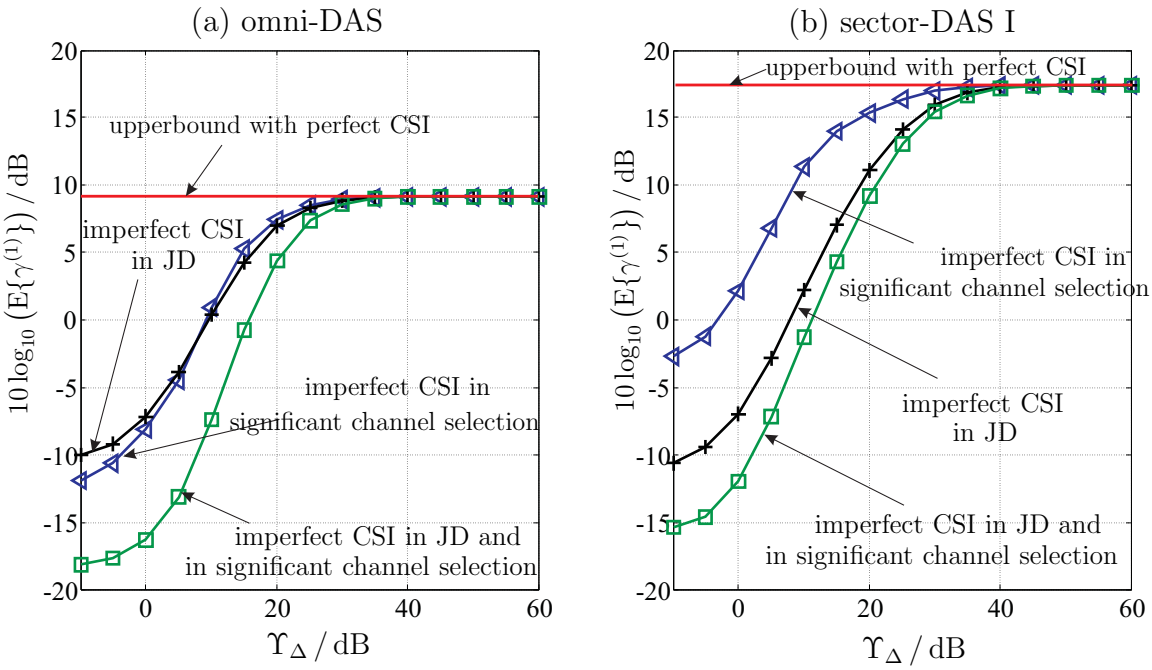

Figure 6.12. Average SINR $\mathrm{E}\{\gamma^{(1)}\}$ as a function of Υ_Δ for investigations on the impact of imperfect CSI in different steps of the cooperative reception scheme applying "JD-($N_\mathrm{U} = 4, N_\mathrm{I} = 10$)" in the UL with $\Upsilon_\mathrm{N} = 40\,\mathrm{dB}$ (interference-limited cellular system).

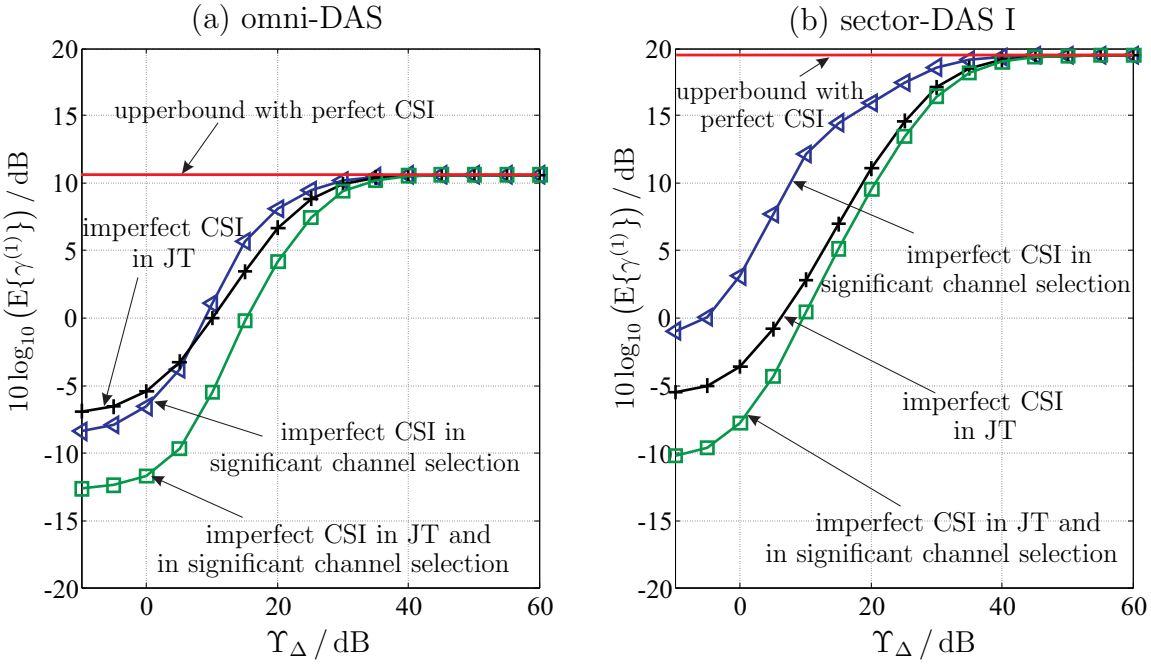

Figure 6.13. Average SINR $\mathrm{E}\{\gamma^{(1)}\}$ as a function of Υ_Δ for investigations on the impact of imperfect CSI in different steps of the cooperative transmission scheme applying "JT-($N_\mathrm{U} = 4, N_\mathrm{I} = 10$)" in the DL with $\Upsilon_\mathrm{N} = 40\,\mathrm{dB}$ (interference-limited cellular system).

respectively. With different levels of the imperfectness of CSI, the system performance of MS 1 is assessed with respect to the average SINR. In the 21-cell reference scenario applying the practical cooperative communication scheme, 4 significant useful channels and 10 significant interfering channels are considered. The most important results derived from the above two figures are as follows:

- The influence of imperfect CSI on the system performance is assessed in the following three cases. In the first case, imperfect CSI is applied in the significant channel selection. Based on the imperfect selection results of significant channels, perfect CSI is applied in the JD/JT. In the second case, perfect CSI is applied in the significant channel selection. Based on the perfect selection results, imperfect CSI of the significant channels is applied in JD/JT. In the third case, the imperfect CSI is applied in the whole cooperative communication scheme including both the significant channel selection and the JD/JT. Taking the system performance upper bound obtained by applying perfect CSI in the whole cooperative communication scheme as the reference, the performance degradation caused by the imperfectness of the CSI in different steps of the cooperative communication scheme is clearly shown.

- Obviously, the accuracy of the CSI, or the imperfectness of the CSI from another view, applied in JD/JT has a significant influence on the system performance. Furthermore, it is interesting to see that imperfect CSI applied in the significant channel selection can also cause serious performance degradation. With increasing imperfectness of the CSI, insignificant channels in reality can be selected as significant channels, and it has a great impact on the cooperative communication scheme designed for appropriate selected significant CSI. It tells us from another point of view how important it is to select suitable significant channels in order to achieve a good performance of the cooperative communication scheme.

- It is shown that in both the UL and the DL of the omni-DAS, the imperfect CSI in the significant channel selection and that in the JD/JT cause comparable performance degradations. In both the UL and the DL of the sector-DAS I, the imperfect CSI in the significant channel selection causes generally much less performance degradation than that caused by the imperfect CSI in the JD/JT. The reason is that with the smart BS-antenna-layout in the sector-DAS I, the mobile radio channels corresponding to the distributed BS-antennas have distinctively different channel coefficients. The significant channel selection in the sector-DAS I is more robust against the imperfectness of CSI as compared to that in the omni-DAS.

The question about how much CSI should be considered in JD/JT as a function of the extent of imperfectness of the CSI in order to achieve optimum system performance is exemplarily answered by the numerical results in Figure 6.14 and Figure 6.15 for the UL and for the DL, respectively. With different levels of the imperfectness of CSI applied in JD/JT, the system performance of MS 1 at the "bad vertex" in the 21-cell reference scenario considering different numbers of significant channels in JD/JT is assessed with respect to the average SINR. The most important results derived from Figure 6.14 and Figure 6.15 are as follows:

- With a high accuracy of the CSI, i.e., with a large value of the ratio Υ_{Δ}, generally the more significant useful channels and their corresponding significant interfering channels are considered in JD/JT, the better system performance can be obtained. The "full JD/JT" considers all $N_{\mathrm{U}} = 63$ useful channels and all $N_{\mathrm{I}} = N_{\mathrm{U}} \cdot (K-1) = 1260$ interfering channels for every MS in the omni-DAS and all the channels except the ineffective channels due to the sector antennas for every MS in the sector-DAS I. This JD/JT scheme with full CSI achieves the best system performance among all the investigated JD/JT schemes.

- With increasing imperfectness of the CSI, the JD/JT with full CSI which is more sensitive to the channel knowledge condition as compared to the other investigated JD/JT schemes considering less CSI is not always the best choice any more. The intra-cell MF denoted by "RxMF/TxMF-cell" can be considered as a special case of "JD/JT-($N_{\mathrm{U}} = 3, N_{\mathrm{I}} = 0$)" in which intra-cell useful channels are selected as significant useful channels and no interfering channels are considered. With a high level of the imperfectness of the CSI, i.e., with a small value of the ratio Υ_{Δ}, the simple intra-cell MF which is more robust against bad knowledge of CSI can even offer us a better system performance than the other JD/JT schemes with partial CSI. With different levels of the imperfectness of CSI, every investigated JD/JT scheme with certain numbers of significant useful channels and significant interfering channels, e.g., "JD/JT-($N_{\mathrm{U}} = 4, N_{\mathrm{I}} = 10$)" and "JD/JT-($N_{\mathrm{U}} = 4, N_{\mathrm{I}} = 2$)", has the chance to achieve the best system performance among all the investigated JD/JT schemes.

- From the above exemplary numerical results, it can be derived that in realistic cellular systems the amount of CSI which shall be considered in JD/JT to obtain optimum system performance is a function of the imperfectness of CSI. Generally, the larger the imperfectness of the CSI is, the less amount of CSI should be considered. In a word, the proposed cooperative communication scheme considering partial CSI can achieve optimum system performance with reduced implementation complexity and alleviated sensitivity to the imperfectness of the CSI.

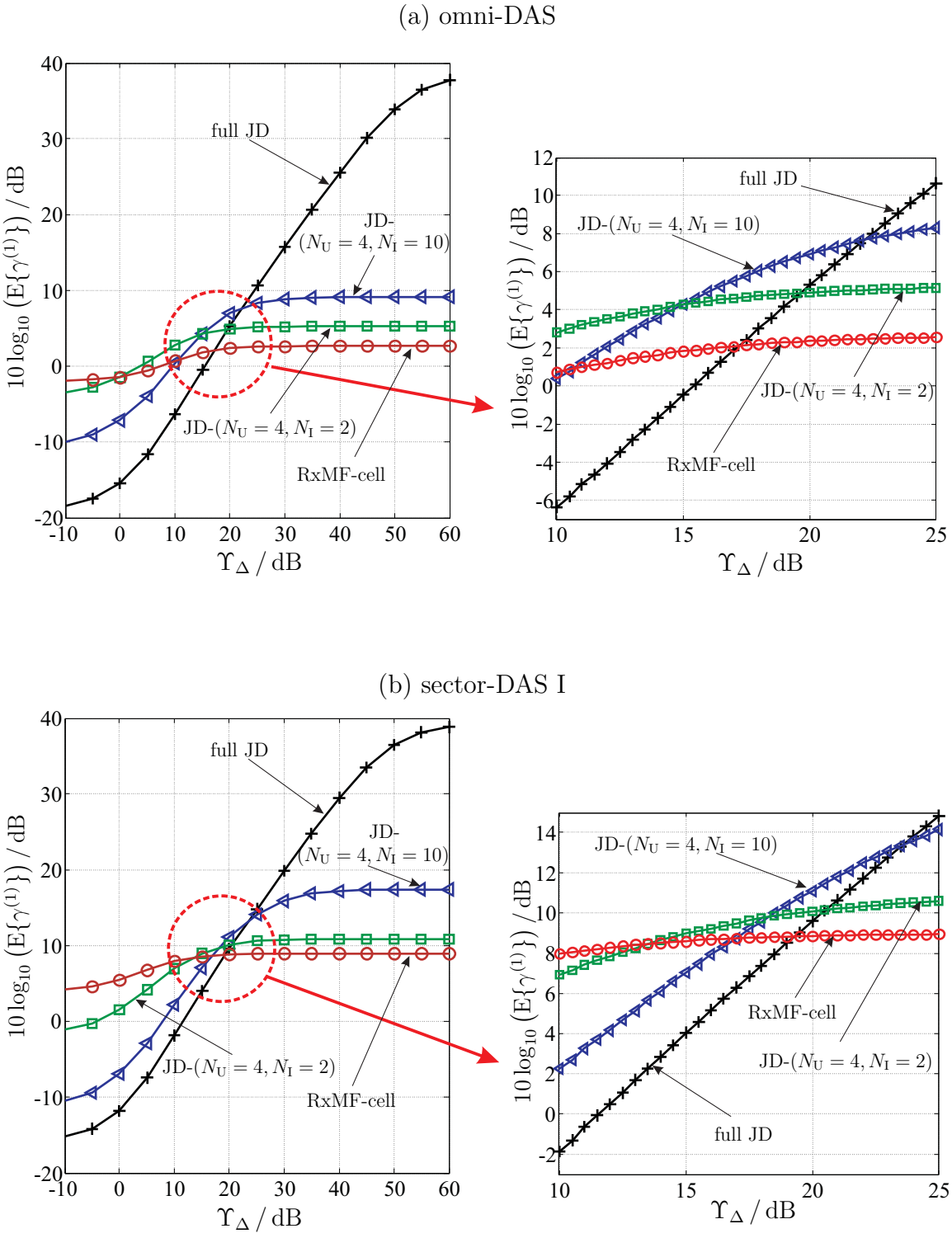

Figure 6.14. Average SINR $\mathrm{E}\{\gamma^{(1)}\}$ as a function of Υ_Δ in the UL, investigation on the impact of imperfect CSI on cooperative communication with different amount of significant CSI, $\Upsilon_N = 40\,\mathrm{dB}$ (interference-limited cellular system).

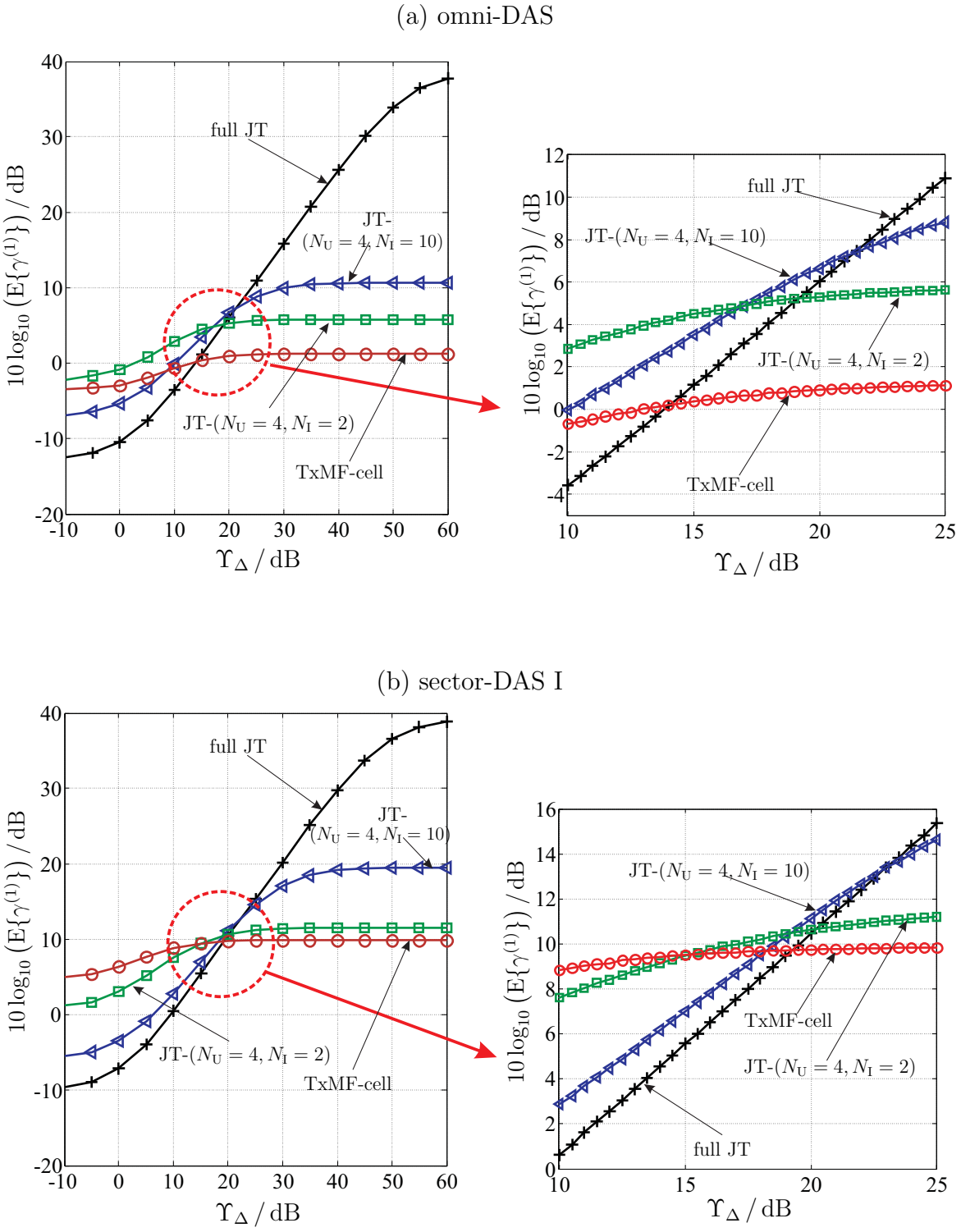

Figure 6.15. Average SINR $\mathrm{E}\{\gamma^{(1)}\}$ as a function of Υ_Δ in the DL, investigation on the impact of imperfect CSI on cooperative communication with different amount of significant CSI, $\Upsilon_N = 40\,\mathrm{dB}$ (interference-limited cellular system).

Chapter 7

Summaries

7.1 Summary in English

The reliability and the throughput of mobile radio cellular systems nowadays are mainly limited by multiuser interference. In future 4G mobile radio cellular networks considered as OFDM-MIMO systems, cooperative communication based on coordinated BSs is a very promising concept to perform inter-cell multiuser interference management. The present thesis deals with the concept of cooperative communication in a systematic way from its information-theoretic background to its practical system design.

The information-theoretic results in the present thesis show that the achievable rate region of multiple users can be significantly enlarged through cooperative reception and cooperative transmission as compared to that with no cooperation. At some operating points of interest, cooperative communication considering appropriately selected partial CSI achieves good system performance with little capacity loss as compared to that with full CSI. These results give good guidelines for a practical design of cooperative communication.

The main focus of this thesis is a practical design of the cooperative communication scheme with partial CSI, i.e., significant CSI and imperfect CSI, for future realistic mobile radio cellular systems. Practical constraints concerning the implementation complexity and the limited ability to track CSI are considered in the system design. A novel MS-oriented dynamic significant channel selection scheme distinguishing the significant useful channels from the significant interfering channels is proposed. With significant CSI corresponding to the selected significant channels, an efficient decentralized cooperative signal processing scheme is proposed. This scheme is based on coordinated BSs connected by backhaul links. In this way, JD for cooperative reception in the UL and JT for cooperative transmission in the DL are performed with a good compromise between system performance and implementation complexity. Furthermore, the impact of imperfectness of the CSI on the system performance is assessed. The question about how much CSI should be considered as a function of the extent of imperfectness of the CSI in JD/JT in order to achieve optimum system performance is answered based on numerical results. Additionally, numerical results show that the proposed intelligent signal processing technique can significantly benefit from the proposed smart BS-antenna-layout. Moreover, several advanced statistical signal processing schemes for multiuser detection are proposed.

7.2 Summary in German

Die Zuverlässigkeit und der Durchsatz in zellularen Mobilfunksystemen sind heutzutage hauptsächlich durch Mehrnutzerinterferenzen begrenzt. Zukünftige zellulare 4G Mobilfunksysteme können als OFDM-MIMO Systeme betrachtet werden. In solchen zukünftigen Mobilfunksystemen ist kooperative Kommunikation, basierend auf koordinierten BSen ein sehr viel versprechendes Konzept zum Interzellinterferenzmanagement. Die vorliegende Arbeit behandelt das Konzept der kooperativen Kommunikation auf eine systematische Art und Weise vom informationstheoretischen Hintergrund bis hin zum praktischen Systemdesign.

Die informationstheoretischen Ergebnisse der vorliegenden Arbeit zeigen, dass die erreichbare Ratenregion von mehreren Nutzern durch den Einsatz von kooperativem Empfang und kooperativem Senden, verglichen mit dem Fall, bei dem keine Kooperation stattfindet, signifikant vergrößert werden kann. In einigen interessanten Arbeitspunkten erreicht kooperative Kommunikation mit passend ausgewählter partieller Kanalkenntnis, verglichen mit dem Fall, bei dem die vollständige Kanalkenntnis genutzt wird, eine gute Performanz mit nur geringem Kapazitätsverlust. Diese Ergebnisse liefern gute Richtlinien für die praktische Implementierung von Systemen mit kooperativer Kommunikation.

Der Schwerpunkt der vorliegenden Arbeit liegt im praktischen Design kooperativer Kommunikationssysteme mit partieller Kanalkenntnis für zukünftige realistische zellulare Mobilfunksysteme. Hierbei bezeichnet partielle Kanalkenntnis signifikante Kanalkenntnis und imperfekte Kanalkenntnis. Beim Systemdesign werden zwei praktische Beschränkungen betrachtet. Zum einen ist die Komplexität der Implementierung und zum anderen ist die begrenzte Fähigkeit, die perfekte Kanalkenntnis zu erlangen, zu berücksichtigen. Eine neue MS-orientierte dynamische Technik um signifikante Kanäle auszuwählen wird vorgeschlagen. Dabei wird zwischen signifikanten Nutzkanälen und signifikanten Störkanälen unterschieden. Basierend auf der Kenntnis der ausgewählten signifikanten Kanäle wird eine effiziente dezentrale kooperative Signalverarbeitungstechnik vorgeschlagen. Diese vorgeschlagene Technik basiert auf koordinierten BSen, die über Backhaul Verbindungen miteinander kommunizieren. Auf diese Art und Weise wird JD für kooperatives Empfangen im UL und JT für kooperatives Senden im DL eingesetzt. Dabei wird ein guter Kompromiss zwischen Systemperformanz und Implementierungskomplexität erreicht. Weiterhin wird der Einfluss von imperfekter Kanalkenntnis auf die Systemperformanz bewertet. Die Frage wie viel Kanalkenntnis für JD/JT benötigt wird, um optimale Systemperformanz zu erreichen, wird numerisch beantwortet. Zusätzlich zeigen numerische Ergebnisse,

dass die vorgeschlagene intelligente Signalverarbeitungstechnik signifikant von dem vorgeschlagenen Layout der Antennen der BSen profitieren kann. Außerdem werden fortschrittliche statistische Signalverarbeitungstechniken für die Mehrnutzerdetektion vorgeschlagen.

Appendix A

Formulas and derivations

A.1 Formulas for calculating the Han-Kobayashi achievable rate region

A simplified explicit expression to compute the achievable rate region $\mathcal{R}(Z)$ defined in Section 3.2.4 is shown in the following. Considering the random variables Q, U_1, U_2, V_1, V_2, X_1 and X_2, $\mathcal{P}^*$ denotes the set of all distributions of the probability $Z = \Pr\{q\}\cdot\Pr\{u_1|q\}\cdot\Pr\{v_1|q\}\cdot\Pr\{u_2|q\}\cdot\Pr\{v_2|q\}\cdot\Pr\{x_1|u_1,v_1,q\}\cdot\Pr\{x_2|u_2,v_2,q\}$.

Theorem A.1. [HK81] The rate region $\mathcal{R}(Z)$ with any $Z \in \mathcal{P}^*$ is equal to the polyhedron consisting all pairs (R_1, R_2) with nonnegative real values satisfying

$$\begin{aligned} R_1 \le \rho_1, \quad R_2 \le \rho_2, \quad R_1 + R_2 \le \rho_{12}, \\ 2R_1 + R_2 \le \rho_{10}, \quad R_1 + 2R_2 \le \rho_{20}, \end{aligned} \tag{A.1}$$

where

$$\rho_1 = \sigma_1 + I(Y_1; U_1 \mid V_1V_2Q), \tag{A.2}$$

$$\rho_2 = \sigma_2 + I(Y_2; U_2 \mid V_1V_2Q), \tag{A.3}$$

$$\rho_{12} = \sigma_{12} + I(Y_1; U_1 \mid V_1V_2Q) + I(Y_2; U_2 \mid V_1V_2Q), \tag{A.4}$$

$$\begin{aligned} \rho_{10} = {} & 2\sigma_1 + 2I(Y_1; U_1 \mid V_1V_2Q) + I(Y_2; U_2 \mid V_1V_2Q) - [\sigma_1 - I(Y_2; V_1 \mid V_2Q)]^+ \\ & + \min\{\ I(Y_2; V_2 \mid V_1Q), \quad I(Y_2; V_2 \mid Q) + [I(Y_2; V_1 \mid V_2Q) - \sigma_1]^+, \\ & \qquad I(Y_1; V_2 \mid V_1Q), I(Y_1; V_1V_2 \mid Q) - \sigma_1\}, \end{aligned} \tag{A.5}$$

$$\begin{aligned} \rho_{20} = {} & 2\sigma_2 + I(Y_1; U_1 \mid V_1V_2Q) + 2I(Y_2; U_2 \mid V_1V_2Q) - [\sigma_2 - I(Y_1; V_2 \mid V_1Q)]^+ \\ & + \min\{\ I(Y_1; V_1 \mid V_2Q), \quad I(Y_1; V_1 \mid Q) + [I(Y_1; V_2 \mid V_1Q) - \sigma_2]^+, \\ & \qquad I(Y_2; V_1 \mid V_2Q), I(Y_2; V_1V_2 \mid Q) - \sigma_2\}, \\ & ([x]^+ = x, \text{ if } x \ge 0; \quad [x]^+ = 0, \text{ if } x < 0), \end{aligned} \tag{A.6}$$

with

$$\begin{aligned} \sigma_1 = {} & \min\{\ I(Y_1; V_1 \mid V_2Q), I(Y_2; V_1 \mid U_2V_2Q)\}, \\ \sigma_2 = {} & \min\{\ I(Y_2; V_2 \mid V_1Q), I(Y_1; V_2 \mid U_1V_1Q)\}, \\ \sigma_{12} = {} & \min\{\ I(Y_1; V_1V_2 \mid Q), I(Y_2; V_1V_2 \mid Q), I(Y_1; V_1 \mid V_2Q) + I(Y_2; V_2 \mid V_1Q), \\ & \qquad I(Y_2; V_1 \mid V_2Q) + I(Y_1; V_2 \mid V_1Q)\}. \end{aligned} \tag{A.7}$$

Details of the proof of Theorem A.1 can be found in [HK81]. Observing the relations between ρ_1, ρ_2, ρ_{12}, ρ_{10} and ρ_{20}, the polyhedron representing the region of $\mathcal{R}(Z)$ is determined by its 7 extreme points as

$$\begin{aligned} &A = (\rho_1, \rho_{10} - 2\rho_1), \quad B = (\rho_{10} - \rho_{12}, 2\rho_{12} - \rho_{10}), \quad C = (2\rho_{12} - \rho_{20}, \rho_{20} - \rho_{12}), \\ &D = (\rho_{20} - 2\rho_2, \rho_2), \quad E = (0, \rho_2), \quad G = (\rho_1, 0), \quad O = (0, 0). \end{aligned} \tag{A.8}$$

In the calculation of the achievable rate region for the two-user Gaussian IC, the relevant quantities concerning receiver 1 in Theorem A.1 can be calculated by

$$I(Y_1; U_1 \mid V_1V_2) = \varphi(\beta_1 P_1/(1 + a_{12}\beta_2 P_2)), \tag{A.9}$$

$$I(Y_1; V_1 \mid V_2) = \varphi(\bar{\beta}_1 P_1/(1 + \beta_1 P_1 + a_{12}\beta_2 P_2)), \tag{A.10}$$

$$I(Y_1; V_2 \mid V_1) = \varphi(a_{12}\bar{\beta}_2 P_2/(1 + \beta_1 P_1 + a_{12}\beta_2 P_2)), \tag{A.11}$$

$$I(Y_1; V_1V_2) = \varphi((\bar{\beta}_1 P_1 + a_{12}\bar{\beta}_2 P_2)/(1 + \beta_1 P_1 + a_{12}\beta_2 P_2)), \tag{A.12}$$

$$I(Y_1; V_1) = \varphi(\bar{\beta}_1 P_1/(1 + \beta_1 P_1 + a_{12} P_2)), \tag{A.13}$$

$$I(Y_1; V_2 \mid U_1V_1) = \varphi(a_{12}\bar{\beta}_2 P_2/(1 + a_{12}\beta_2 P_2)), \tag{A.14}$$

where $\varphi(x) = \log_2(1 + x)$, $\sigma^2(U_i) = \beta_i P_i$, $\sigma^2(V_i) = \bar{\beta}_i P_i$, $\beta_i + \bar{\beta}_i = 1$, $i = 1, 2$. Similarly, the relevant quantities concerning receiver 2 in Theorem A.1 can be calculated by applying the above equations from (A.9) to (A.14) with indices 1 and 2 exchanged with each other everywhere.

A.2 Dualities between uplink and downlink channel correlation matrices

Let's define

$$\underline{\mathbf{A}}_k = \left[\hat{\underline{\mathbf{H}}}_{\mathrm{UL,U}}\right]_k^{*\mathrm{T}} \hat{\underline{\mathbf{H}}}_{\mathrm{UL,I},k} = \left[\hat{\underline{\mathbf{H}}}_{\mathrm{U}}\right]_k^{*\mathrm{T}} \hat{\underline{\mathbf{H}}}_{\mathrm{I},k} \tag{A.15}$$

and

$$\underline{\mathbf{B}}_k = \hat{\underline{\mathbf{H}}}_{\mathrm{DL,I},k} \left[\hat{\underline{\mathbf{H}}}_{\mathrm{DL,U}}^{*\mathrm{T}}\right]_k = \hat{\underline{\mathbf{H}}}_{\mathrm{I},k}^{\mathrm{T}} \left[\hat{\underline{\mathbf{H}}}_{\mathrm{U}}^{*}\right]_k \quad . \tag{A.16}$$

The matrix operator $[\cdot]_k$ returns the k-th column of its argument as a column vector. It can be seen that

$$\underline{\mathbf{A}}_k = \underline{\mathbf{B}}_k^{\mathrm{T}} \tag{A.17}$$

always holds. The estimated channel correlation matrix $\hat{\underline{\mathbf{R}}}_{\mathrm{UL}}$ introduced in (4.59) can be expressed by

$$\hat{\underline{\mathbf{R}}}_{\mathrm{UL}} = \begin{pmatrix} \underline{\mathbf{A}}_1 \\ \vdots \\ \underline{\mathbf{A}}_K \end{pmatrix} \quad , \tag{A.18}$$

and the estimated channel correlation matrix $\hat{\underline{\mathbf{R}}}_{\mathrm{DL}}$ introduced in (5.36) can be expressed by

$$\hat{\underline{\mathbf{R}}}_{\mathrm{DL}} = \left(\underline{\mathbf{B}}_1, \ \ldots \ , \underline{\mathbf{B}}_K \right) \ . \tag{A.19}$$

Now we can easily obtain

$$\hat{\underline{\mathbf{R}}}_{\mathrm{UL}} = \begin{pmatrix} \underline{\mathbf{A}}_1 \\ \vdots \\ \underline{\mathbf{A}}_K \end{pmatrix} = \left(\underline{\mathbf{B}}_1, \ \ldots \ , \underline{\mathbf{B}}_K \right)^{\mathrm{T}} = \left(\hat{\underline{\mathbf{R}}}_{\mathrm{DL}} \right)^{\mathrm{T}} \ . \tag{A.20}$$

A.3 Estimated transmit power scaling matrix

It is assumed that the same data vector $\underline{\mathbf{d}} = (\underline{d}^{(1)} \ldots \underline{d}^{(K)})^{\mathrm{T}}$ with the covariance matrix $\mathbf{\Phi}_{\mathrm{d}} = \mathrm{E}\{\underline{\mathbf{d}}\,\underline{\mathbf{d}}^{*\mathrm{T}}\} = P_{\mathrm{d}}\mathbf{I}^{K\times K}$ is applied in both the UL and the DL. In the UL, with the simple transmitter, $\underline{\mathbf{s}} = \underline{\mathbf{d}}$ holds and the transmitted power for each data symbol k is $P_{\mathrm{s}}^{(k)} = P_{\mathrm{d}}$. In the DL, after introducing a diagonal scaling matrix $\hat{\mathbf{\Gamma}}$ with positive real-valued elements on its diagonal, the limiting value of transmitted vector in (5.41) is obtained as

$$\underline{\mathbf{s}}(\infty) = \hat{\underline{\mathbf{H}}}_{\mathrm{DL,U}}^{*\mathrm{T}} \left(\hat{\mathbf{G}}_{\mathrm{DL}} + \overline{\mathrm{diag}} \left(\hat{\underline{\mathbf{R}}}_{\mathrm{DL}} \right) \right)^{-1} \hat{\mathbf{\Gamma}} \cdot \underline{\mathbf{d}} \ . \tag{A.21}$$

The modulation matrix reads

$$\underline{\mathbf{M}} = \hat{\underline{\mathbf{H}}}_{\mathrm{DL,U}}^{*\mathrm{T}} \left(\hat{\mathbf{G}}_{\mathrm{DL}} + \overline{\mathrm{diag}} \left(\hat{\underline{\mathbf{R}}}_{\mathrm{DL}} \right) \right)^{-1} \hat{\mathbf{\Gamma}} \ . \tag{A.22}$$

The requirement to use the same transmit power per data symbol $P_{\mathrm{s}}^{(k)} = P_{\mathrm{d}}$ in the UL and in the DL leads to

$$\left[\underline{\mathbf{M}}^{*\mathrm{T}} \underline{\mathbf{M}} \right]_{k,k} = 1 \ , \tag{A.23}$$

which means that the norm of each column of the modulation matrix is kept to be 1 in order to keep the transmitted power per data symbol unmodified. From the condition

$$\begin{aligned} \left[\underline{\mathbf{M}}^{*\mathrm{T}} \underline{\mathbf{M}} \right]_{k,k} &= \left[\hat{\mathbf{\Gamma}} \left(\left(\hat{\mathbf{G}} + \overline{\mathrm{diag}} \left(\hat{\underline{\mathbf{R}}}_{\mathrm{DL}} \right) \right)^{-1} \right)^{*\mathrm{T}} \hat{\underline{\mathbf{H}}}_{\mathrm{DL,U}} \ \hat{\underline{\mathbf{H}}}_{\mathrm{DL,U}}^{*\mathrm{T}} \left(\hat{\mathbf{G}} + \overline{\mathrm{diag}} \left(\hat{\underline{\mathbf{R}}}_{\mathrm{DL}} \right) \right)^{-1} \hat{\mathbf{\Gamma}} \right]_{k,k} \\ &= 1 \ , \end{aligned} \tag{A.24}$$

one obtains

$$\begin{aligned} \hat{\mathbf{\Gamma}} &= \left(\mathrm{diag} \left(\left(\hat{\mathbf{G}} + \overline{\mathrm{diag}} \left(\hat{\underline{\mathbf{R}}}_{\mathrm{DL}}^{*\mathrm{T}} \right) \right)^{-1} \hat{\underline{\mathbf{H}}}_{\mathrm{DL,U}} \ \hat{\underline{\mathbf{H}}}_{\mathrm{DL,U}}^{*\mathrm{T}} \left(\hat{\mathbf{G}} + \overline{\mathrm{diag}} \left(\hat{\underline{\mathbf{R}}}_{\mathrm{DL}} \right) \right)^{-1} \right) \right)^{-\frac{1}{2}} \\ &= \left(\mathrm{diag} \left(\left(\hat{\mathbf{G}} + \overline{\mathrm{diag}} \left(\hat{\underline{\mathbf{R}}}^{*} \right) \right)^{-1} \hat{\underline{\mathbf{H}}}_{\mathrm{U}}^{\mathrm{T}} \ \hat{\underline{\mathbf{H}}}_{\mathrm{U}}^{*} \left(\hat{\mathbf{G}} + \overline{\mathrm{diag}} \left(\hat{\underline{\mathbf{R}}}^{\mathrm{T}} \right) \right)^{-1} \right) \right)^{-\frac{1}{2}} \\ &= \left(\mathrm{diag} \left(\left(\hat{\mathbf{G}} + \overline{\mathrm{diag}} \left(\hat{\underline{\mathbf{R}}} \right) \right)^{-1} \hat{\underline{\mathbf{H}}}_{\mathrm{U}}^{*\mathrm{T}} \ \hat{\underline{\mathbf{H}}}_{\mathrm{U}} \left(\hat{\mathbf{G}} + \overline{\mathrm{diag}} \left(\hat{\underline{\mathbf{R}}}^{*\mathrm{T}} \right) \right)^{-1} \right) \right)^{-\frac{1}{2}} \ . \end{aligned} \tag{A.25}$$

A.4 Eigenvalues of the loop matrix

As we know, the UL and the DL have the same estimated channel gain scaling matrix $\hat{\mathbf{G}}$ as shown in (6.6). Concerning the estimated channel covariance matrix $\underline{\hat{\mathbf{R}}}$, one can easily obtain

$$\overline{\mathrm{diag}}\left(\underline{\hat{\mathbf{R}}}\right) = \left(\overline{\mathrm{diag}}\left(\underline{\hat{\mathbf{R}}}^{\mathrm{T}}\right)\right)^{\mathrm{T}} \quad . \tag{A.26}$$

Assuming that $\underline{\mathbf{C}}$ and $\underline{\mathbf{D}}$ are two arbitrary N-by-N square matrices, it has been shown that $\underline{\mathbf{C}}$ and $\underline{\mathbf{C}}^{\mathrm{T}}$ have the same eigenvalues and that $\underline{\mathbf{C}}\,\underline{\mathbf{D}}$ and $\underline{\mathbf{D}}\,\underline{\mathbf{C}}$ have the same eigenvalues [HJ85]. From these results, one can easily derive that $(\underline{\mathbf{D}}\,\underline{\mathbf{C}})^{\mathrm{T}}$ has the same eigenvalues as $\underline{\mathbf{C}}\,\underline{\mathbf{D}}$. Assuming

$$\underline{\mathbf{C}} = \hat{\mathbf{G}}^{-1} \tag{A.27}$$

$$\underline{\mathbf{D}} = \overline{\mathrm{diag}}\left(\underline{\hat{\mathbf{R}}}\right) = \left(\overline{\mathrm{diag}}\left(\underline{\hat{\mathbf{R}}}^{\mathrm{T}}\right)\right)^{\mathrm{T}} \quad , \tag{A.28}$$

the loop matrices can be written as

$$\underline{\mathbf{L}}_{\mathrm{UL}} = \underline{\mathbf{C}}\,\underline{\mathbf{D}} \tag{A.29}$$

$$\underline{\mathbf{L}}_{\mathrm{DL}} = \underline{\mathbf{C}}^{\mathrm{T}}\,\underline{\mathbf{D}}^{\mathrm{T}} = (\underline{\mathbf{D}}\,\underline{\mathbf{C}})^{\mathrm{T}} \quad . \tag{A.30}$$

So obviously one can obtain the result that the loop matrices $\underline{\mathbf{L}}_{\mathrm{UL}}$ in the UL and $\underline{\mathbf{L}}_{\mathrm{DL}}$ in the DL have the same eigenvalues and then of course the same spectral radius.

Appendix B

List of frequently used abbreviations and symbols

B.1 Abbreviations

AWGN	additive white gaussian noise
B3G	beyond 3rd generation
BC	broadcast channel
BER	bit error rate
BS	base station
CCDF	complementary cumulative distribution function
CDMA	code division multiple access
CoMP	coordinated multi-point transmission
CP	cyclic prefix
CPRI	common public radio interface
CSI	channel state information
CU	central unit
DAS	distributed antenna system
DFT	discrete Fourier transform
DL	downlink
DPC	dirty-paper coding
IC	interference channel
ICI	inter-channel interference
IDFT	inverse-discrete Fourier transform
i.i.d.	independent and identically distributed
ISI	inter-symbol interference
JD	joint detection
JOINT	joint transmission and detection integrated network
JT	joint transmission
LTE	long term evolution
MAC	multiple access channel
MF	matched filtering
MIMO	multiple-input multiple-output
MMSE	minimum mean square error
MS	mobile station
OFDM	orthogonal frequency division multiplexing
OFDMA	orthogonal frequency division multiple access
OBSAI	open base station architecture initiative
PDF	probability density function
PIC	parallel interference cancellation

QoS	quality of service
SA	service area
SDMA	space division multiple access
SINR	signal-to-interference-plus-noise ratio
SIC	successive interference cancellation
SIR	signal-to-interference ratio
SISO	single-input single-output
SIMO	single-input multiple-output
SNR	signal-to-noise ratio
SVD	singular value decomposition
TDD	time division duplex
THP	Tomlinson-Harashima precoding
UL	uplink
ZF	zero forcing

B.2 Symbols

a_{ij}	channel gain between transmitter j and receiver i
A	amplitude of channel transfer function
$\underline{\mathbf{c}}_{k,\mathrm{BC}}$	transmit signature for user k in a BC
$\underline{\mathbf{c}}_{k,\mathrm{MAC}}$	receive signature for user k in a MAC
C	capacity
$\mathbb{C}$	set of complex-valued numbers
d	propagation distance
d_{B}	breakpoint distance in dual slope model
$\underline{d}^{(n_{\mathrm{us}})}$	data symbol of user n_{us}
$\underline{d}^{(k)}$	data symbol of MS k
$\hat{\underline{d}}^{(k)}$	estimated data symbol of MS k
$\hat{\underline{d}}^{(k)}(i)$	estimated data symbol of MS k in the i-th iteration
$\hat{\hat{\underline{d}}}^{(k)}(i)$	refined estimated data symbol of MS k in the i-th iteration
$\underline{\mathbf{d}}$	data vector
$\hat{\underline{\mathbf{d}}}$	estimated data vector
$\hat{\underline{\mathbf{d}}}(i)$	estimated data vector in the i-th iteration
$\hat{\hat{\underline{\mathbf{d}}}}(i)$	refined estimated data vector in the i-th iteration
$\mathbb{D}$	alphabet of data symbol $\underline{d}^{(k)}$
$\mathbb{D}^K$	alphabet of data vector $\underline{\mathbf{d}}$
$\underline{\mathbf{D}}$	linear demodulator matrix
$\underline{e}^{(n_{\mathrm{F}})}$	received signal on subcarrier n_{F} in an OFDM symbol
$\underline{e}^{(k_{\mathrm{A}})}$	received signal at BS antenna k_{A}
$\underline{e}^{(k)}$	received signal at MS k
$\underline{\mathbf{e}}$	received vector
Δf	frequency spacing between adjacent subcarriers

G	logarithmic path gain
$\bar{G}$	average logarithmic path gain
$\hat{\mathbf{G}}$	estimated channel gain scaling matrix
g	linear path gain
$\hat{g}^{(k)}$	estimated channel gain scaling factor for MS k
$\bar{g}$	average linear path gain
g_{R}	receive antenna gain
g_{T}	transmit antenna gain
$\underline{h}^{(\mu)}$	channel impulse response at time slot μ
$\underline{h}_{ij}$	channel coefficient between transmitter j and receiver i in an IC
$\underline{H}^{(n_{\mathrm{F}})}$	channel transfer function on subcarrier n_{F}
$\underline{H}(f)$	channel transfer function
$\underline{\mathbf{h}}_i$	channel vector corresponding to transmitter antenna i
$\underline{\mathbf{H}}$	channel matrix
$\underline{H}^{(k_{\mathrm{A}},k)}$	channel transfer function between BS antenna k_{A} and MS k in the system channel matrix $\underline{\mathbf{H}}$
$\hat{\underline{H}}^{(k_{\mathrm{A}},k)}$	estimate of $\underline{H}^{(k_{\mathrm{A}},k)}$
$\hat{\underline{\mathbf{H}}}$	estimated channel matrix
$\underline{\mathbf{H}}_{\mathrm{DL}}$	DL channel matrix
$\underline{\mathbf{H}}_{\mathrm{UL}}$	UL channel matrix
$\underline{H}_{\mathrm{DL}}^{(k,k_{\mathrm{A}})}$	DL channel coefficient between MS k and BS antenna k_{A}
$\hat{\underline{H}}_{\mathrm{DL}}^{(k,k_{\mathrm{A}})}$	estimate of $\underline{H}_{\mathrm{DL}}^{(k,k_{\mathrm{A}})}$
$\underline{H}_{\mathrm{UL}}^{(k_{\mathrm{A}},k)}$	UL channel coefficient between BS antenna k_{A} and MS k
$\hat{\underline{H}}_{\mathrm{UL}}^{(k_{\mathrm{A}},k)}$	estimate of $\underline{H}_{\mathrm{UL}}^{(k_{\mathrm{A}},k)}$
$\widetilde{\mathbf{H}}_{\mathrm{U}}$	significant useful channel indicator matrix for all MSs
$\underline{\mathbf{H}}_{\mathrm{U}}$	significant useful channel matrix for all MSs
$\hat{\underline{\mathbf{H}}}_{\mathrm{U}}$	estimated significant useful channel matrix for all MSs
$\widetilde{\mathbf{H}}_{\mathrm{I},k}$	MS-specific significant interfering channel indicator matrix for MS k
$\underline{\mathbf{H}}_{\mathrm{I},k}$	MS-specific significant interfering channel matrix for MS k
$\hat{\underline{\mathbf{H}}}_{\mathrm{I},k}$	estimated MS-specific significant interfering channel matrix for MS k
$\widetilde{\mathbf{H}}_{\mathrm{I}}$	combined significant interfering channel indicator matrix
$\underline{\mathbf{H}}_{\mathrm{I}}$	combined significant interfering channel matrix
$\hat{\underline{\mathbf{H}}}_{\mathrm{I}}$	estimated combined significant interfering channel matrix
$\mathbf{I}$	identity matrix
K	number of cells, which is equivalent to number of active MSs
K_{B}	number of BSs
K_{M}	number of MSs
K_{A}	number of BS antennas
L	number of iterations
$\underline{\mathbf{M}}$	linear modulator matrix
$\underline{n}^{(n_{\mathrm{F}})}$	noise signal on subcarrier n_{F} in an OFDM symbol
$\underline{n}^{(k_{\mathrm{A}})}$	noise signal at BS antenna k_{A} in the UL
$\underline{n}^{(k)}$	noise signal at MS k in the DL
$\underline{n}_j$	noise signal at receiver antenna j

$\underline{\mathbf{n}}$	noise vector
N_i	noise variance at receiver antenna i
N_0	the same noise variance at all receiver antennas
N_A	number of antennas at each BS
N_F	number of subcarriers
N_g	discrete length of the channel impulse response
N_I	number of significant interfering channels for every MS
N_IG	number of significant interfering channel groups for every MS
N_U	number of significant useful channels for every MS
N_UG	number of significant useful channel groups for every MS
N_us	number of users per cell
P_d	average transmit power of every data symbol
P	transmit sum power
P_k	transmit power for user k
$\tilde{P}_k$	optimum transmit power allocated to user k with available channel knowledge
Q	time-sharing random variable
$\underline{\mathbf{Q}}_i$	input covariance matrix for user i in a BC
$\mathcal{Q}$	set of random variable Q
r	cluster size
$\underline{r}^{(k)}$	matched filtering estimate for MS k
R_i	data rate of user i
$\mathbb{R}$	set of real-valued numbers
$\mathcal{R}_\mathrm{HK}$	the Han-Kobayashi achievable rate region for an IC
$\underline{\hat{\mathbf{R}}}$	estimated channel correlation matrix
$\underline{s}^{(n_\mathrm{F})}$	transmitted signal on subcarrier n_F in an OFDM symbol
$\underline{s}^{(k)}$	transmitted signal from MS k
$\underline{s}^{(k_\mathrm{A})}$	transmitted signal from BS antenna k_A
$\underline{\mathbf{s}}$	transmitted vector
S_i	data rate of private message from transmitter i in an IC
$\mathbf{\Phi}_\mathrm{n}$	covariance matrix of noise signals
$\mathbf{\Phi}_\mathrm{x}$	covariance matrix of input signals
$\underline{t}^{(k)}$	predistorted data symbol of MS k
$\underline{t}^{(k)}(i)$	predistorted data symbol of MS k in the i-th iteration
$\underline{\mathbf{t}}$	predistorted data vector
$\underline{\hat{\mathbf{t}}}(i)$	predistorted data vector in the i-th iteration
T_i	data rate of common message from transmitter i in an IC
T_d	original data symbol duration
T_s	OFDM symbol duration
U_i	random variable carrying private message from transmitter i
$\mathcal{U}_i$	set of random variable U_i
V_i	random variable carrying common message from transmitter i
$\mathcal{V}_i$	set of random variable V_i
W_i	message for user i from transmitter i
W_{ii}	private message for user i from transmitter i

W_{ij}	common message for users i and j from transmitter i
$\mathcal{W}_i$	message set for user i
$\underline{w}^{(\mu)}$	noise signal at time slot μ in an OFDM symbol
$\mathcal{X}_i$	set of input signal at transmitter antenna i
$\mathcal{X}_i^n$	set of input vector at transmitter antenna i
X_i	input signal variable at transmitter antenna i
$\mathbf{x}_i$	codeword for user i
$\underline{\mathbf{x}}$	channel input vector
$\underline{\tilde{\mathbf{x}}}$	channel input vector with cyclic prefix
$\underline{x}_i$	input signal from transmitter antenna i
$\underline{\hat{x}}_i$	estimated input signal from transmitter antenna i
$\underline{x}^{(\mu)}$	input symbol at time slot μ in an OFDM symbol
$\mathcal{Y}_i$	set of output signal at receiver antenna i
$\mathcal{Y}_i^n$	set of output vector at receiver antenna i
Y_i	output signal variable at receiver antenna i
$\underline{y}_i$	output signal at receiver antenna i
$\underline{y}^{(\mu)}$	output symbol at time slot μ in an OFDM symbol
$\underline{\mathbf{y}}$	channel output vector
$\underline{\tilde{\mathbf{y}}}$	channel output vector with cyclic prefix
$\underline{\mathbf{z}}$	colored/white Gaussian noise vector in a SIMO channel for one user
$\underline{\mathbf{K}}_{\mathrm{z}}$	covariance matrix of colored/white Gaussian noise vector in a SIMO channel for one user
α	path loss attenuation exponent
β	scaling factor
λ	system wavelength
λ_k	singular value of the channel matrix
$\gamma^{(k)}$	SINR of user k
$\gamma_{\mathrm{MAC}}^{(k)}$	SINR of user k in a MAC
$\gamma_{\mathrm{BC}}^{(k)}$	SINR of user k in a BC
$\gamma_{\mathrm{F}}^{(k)}$	SINR of user k which is firstly decoded in a two-user MAC applying the SIC strategy
$\gamma_{\mathrm{S}}^{(k)}$	SINR of user k which is secondly decoded in a two-user MAC applying the SIC strategy
$\gamma_{\mathrm{JD}}^{(k)}$	SINR of MS k applying JD in the UL
$\gamma_{\mathrm{JT}}^{(k)}$	SINR of MS k applying JT in the DL
$\mathbf{\Gamma}$	transmit power scaling matrix
$\underline{\mathbf{\Delta}}$	channel-error matrix
η	ratio of two numbers
ϵ_n	error probability
ρ_{s}	spectral radius
σ^2	variance of noise
σ_i^2	variance of noise at individual receiver i
$\hat{\sigma}_i^2$	estimated variance of noise at individual receiver i
σ_{G}^2	variance of logarithmic path gain
σ_{H}^2	variance of channel transfer function

σ_{Δ}^2	variance of channel error
$\sigma_{h_{ij}}^2$	variance of fading channel between transmitter j and receiver i
Υ	logarithmic ratio of two numbers
Υ_{N}	logarithmic ratio of the average receive signal power to the noise power
Υ_{Δ}	logarithmic ratio of the average receive signal power to the variance of channel estimation error
$\mathrm{diag}\,(\cdot)$	a diagonal matrix with the diagonal elements of its argument as its own diagonal entries
$\underline{\mathrm{diag}}\{\cdot\}$	a diagonal matrix with its argument elements as its own diagonal entries
$\overline{\mathrm{diag}}\,(\cdot)$	a matrix with 0's as its diagonal entries and the off-diagonal elements of its argument as its own off-diagonal entries
$\exp(\cdot)$	exponential function of its argument
$\mathrm{E}\,\{\cdot\}$	expectation of its argument
$\mathcal{F}^{-1}\,(\cdot)$	IDFT of its argument
$\mathcal{F}\,(\cdot)$	DFT of its argument
$\mathcal{O}(\cdot)$	computational complexity order of its argument
$\mathrm{p}(\cdot)$	probability density function of its argument
$\mathrm{p}(\cdot\|\cdot)$	conditional probability density function of its argument
$\Pr\{\cdot\}$	probability of its argument
$\Pr\{\cdot\|\cdot\}$	conditional probability of its argument
$\mathcal{Q}_{\mathrm{HD}}\,(\cdot)$	hard quantization function of its argument
$\sigma^2(\cdot)$	variance of a random variable of its argument
$(\cdot)^{\mathrm{T}}$	transposition of its argument
$(\cdot)^*$	conjugate of its argument
$(\cdot)^{*\mathrm{T}}$	conjugate transpose of its argument
$[\underline{\mathbf{A}}]_k$	the k-th column of the matrix $\underline{\mathbf{A}}$ as a column vector
$[\underline{\mathbf{a}}]_{\mu}$	the μ-th element of the vector $\underline{\mathbf{a}}$ as a scalar
$\odot$	element-wise multiplication
$\circledast$	circular convolution
$\mathcal{N}\,(\mu, \sigma^2)$	real Gaussian random variable with mean μ and variance σ^2
$\mathcal{CN}\,(0, \underline{\mathbf{K}})$	circularly symmetric Gaussian random vector with covariance matrix $\underline{\mathbf{K}}$ and mean zero
$\mathcal{CN}\,(0, \sigma^2)$	circularly symmetric complex Gaussian random variable with the real and imaginary parts are i.i.d. $\mathcal{N}\left(0, \frac{\sigma^2}{2}\right)$
$I(X;Y)$	mutual information of random variables X and Y
$I(X;Y\|Z)$	conditional mutual information of random variables X and Y given Z

Bibliography

[80299] *IEEE 802.11a Working Group, Part 11: Wireless LAN Medium Access Control (MAC) and Physical Layer (PHY) specifications–Amendment 1: High-Speed Physical Layer in the 5 GHz band*. 1999.

[80203] *IEEE 802.11g Working Group, Part 11: Wireless LAN Medium Access Control (MAC) and Physical Layer (PHY) specifications–Amendment 4: Further Higher-Speed Physical Layer Extension in the 2.4 GHz Band*. 2003.

[AEH06] Aktas, E.; Evans, J.; Hanly, S.: Distributed base station processing in the uplink of cellular networks. *Proc. IEEE International Conference on Communications(ICC'06)*, vol. 4, Istanbul, 2006, pp. 1641–1646.

[Ahl74] Ahlswede, R.: The capacity region of a channel with two senders and two receivers. *The Annals of Probability*, vol. 2, 1974, pp. 805–814.

[And05] Andrews, J. G.: Interference cancellation for cellular systems: A contemporary overview. *IEEE Wireless Communications*, vol. 12, 2005, pp. 19–29.

[AP05] Aalo, V.; Piboongungon, T.: On the multivariate generalized Gamma distribution with exponential correlation. *Proc. IEEE Global Telecommunications Conference (GLOBECOM '05)*, vol. 3, St. Loius, 2005, pp. 1229–1233.

[AVP06] Alecu, T. I.; Voloshynovskiy, S.; Pun, T.: The Gaussian transform of distributions: definition, computation and application. *IEEE Transactions on Signal Processing*, vol. 54, 2006, pp. 2976–2985.

[AWWD07] Ahrens, A.; Wei, X.; Weber, T.; Deng, S.: A novel decentralized MIMO-OFDM uplink detection scheme. *Proc. International ITG/IEEE Workshop on Smart Antennas (WSA'07)*, Vienna, 2007.

[B+07] Bublin, M.; et al.: Inter-cell interference management by dynamic channel allocation, scheduling and smart antennas. *Proc. 16th IST Mobile and Wireless Communications Summit*, Budapest, 2007.

[Ber74] Bergmans, P. P.: A simple converse for broadcast channels with additive white Gaussian noise. *IEEE Transactions on Information Theory*, vol. 20, 1974, pp. 279–280.

[BFKM93] Baier, P. W.; Felhauer, T.; Klein, A.; Mämmelä, A.: Survey of linear block estimation algorithms for the detection of spread spectrum signals transmitted over frequency selective channels. *IEICE Transactions on Communications*, vol. 76, 1993, pp. 825–834.

[Bin90] Bingham, J. A. C.: Multicarrier modulation for data transmission: An idea whose time has come. *IEEE Communications Magazine*, vol. 28, 1990, pp. 5–14.

[Blu03] Blum, R.: MIMO capacity with interference. *IEEE Journal on Selected Areas in Communications*, vol. 21, 2003, pp. 793–801.

[Car75] Carleial, A.: A case where interference does not reduce capacity. *IEEE Transactions on Information Theory*, vol. 21, 1975, pp. 569–570.

[Car78] Carleial, A. B.: Interference channel. *IEEE Transactions on Information Theory*, vol. 24, 1978, pp. 60–70.

[CDG00] Catreux, S.; Driessen, P.; Greenstein, L.: Simulation results for an interference-limited multiple-input multiple-output cellular system. *IEEE Communication Letters*, vol. 4, 2000, pp. 334–336.

[CG87] Costa, M. H. M.; Gamal, A. E.: The capacity region of the discrete and memoryless interference channel with strong interference. *IEEE Transactions on Information Theory*, vol. 33, 1987, pp. 710–711.

[Cha66] Chang, R. W.: Synthesis of band-limited orthogonal signals for multichannel data transmission. *Bell Systems Technical Journal*, vol. 45, 1966, pp. 1775–1796.

[Cho08] Choi, J.: Data detection with imperfect CSI using averaged likelihood function. *IEEE Transactions on Wireless Communications*, vol. 7, 2008, pp. 4117–4121.

[CMGEG08] Chong, H.; Motani, M.; Garg, H.; El Gamal, H.: On the Han-Kobayashi region for the interference channel. *IEEE Transactions on Information Theory*, vol. 54, 2008, pp. 3188–3195.

[Cos83] Costa, M. H. M.: Writing on dirty paper. *IEEE Transactions on Information Theory*, vol. 29, 1983, pp. 439–441.

[Cos85] Costa, M. H. M.: On the Gaussian interference channel. *IEEE Transactions on Information Theory*, vol. 31, 1985, pp. 607–615.

[COS91] COST231: *Urban transmission loss models for mobile radio in the 900- and 1800 MHz bands terrestrial radio access (UTRA).* Technical Report, 1991.

[Cov72] Cover, T. M.: Broadcast channels. *IEEE Transactions on Information Theory*, vol. 18, 1972, pp. 2–14.

[CRP09] *CPRI Specification V4.1.* 2009.

[CS00] Caire, G.; Shamai, S.: On achievable rates in a multi-antenna broadcast downlink. *Proc. 38th Annual Allerton Conference on Communications, Control and Computing*, Monticello, 2000, pp. 715–724.

[CS03] Caire, G.; Shamai, S.: On the achievable throughput of a multiantenna Gaussian broadcast channel. *IEEE Transactions on Information Theory*, vol. 49, 2003, pp. 1691–1706.

[CT06] Cover, T. M.; Thomas, J. A.: *Elements of Information Theory*. 2. edition. John Wiley & Sons, 2006.

[CTC91] Chow, P. S.; Tu, J. C.; Cioffi, J. M.: A discrete multitone transceiver system for HDSL applications. *IEEE Journal on Selected Areas in Communications*, vol. 9, 1991, pp. 895–908.

[CV93] Cheng, R.; Verdu, S.: Gaussian multiaccess channels with ISI: Capacity region and multiuser water-filling. *IEEE Transactions on Information Theory*, vol. 39, 1993, pp. 773–785.

[DKZ08] Du, J.; Kang, G.; Zhang, P.: Low complexity power allocation strategy for MIMO systems with imperfect CSI. *Electronics Letters*, vol. 44, 2008, pp. 651–652.

[DMP04] Dai, H.; Molisch, A.; Poor, H.: Downlink capacity of interference-limited MIMO systems with joint detection. *IEEE Transactions on Wireless Communications*, vol. 3, 2004, pp. 442–453.

[DSR98] Divsalar, D.; Simon, M. K.; Raphaeli, D.: Improved parallel interference cancellation for CDMA. *IEEE Transactions on Communications*, vol. 46, 1998, pp. 258–268.

[DWA09] Deng, S.; Weber, T.; Ahrens, A.: Capacity optimizing power allocation in interference channels. *International Journal of Electronics and Communications (AEÜ)*, vol. 63, 2009, pp. 139–147.

[Egg69] Eggleston, H. G.: *Convexity*. Cambridge: Cambridge University Press, 1969.

[EODD02] Emmanuelle, J.; Ovarlez, J.-P.; Declercq, D.; Duvaut, P.: Bayesian optimum radar detector in non-Gaussian noise. *Proc. IEEE International Conference on Acoustics, Speech, and Signal Processing (ICASSP'02)*, vol. 2, Orlando, 2002, pp. 1289–1292.

[ESZ05] Erez, U.; Shamai, S.; Zamir, R.: Capacity and lattice strategies for canceling known interference. *IEEE Transactions on Information Theory*, vol. 51, 2005, pp. 3820–3833.

[ETS97a] ETSI: *Digital video broadcasting (DVB); Framing structure, channel coding, and modulation for digital terrestial television.* Technical Report EN 300 744, European Telecommunication and Standardization Institute (ETSI), 1997.

[ETS97b] ETSI: *Radio broadcasting systems; digital audio broadcasting (DAB) to mobile, portable and fixed receivers*. Technical Report EN 300 401, European Telecommunication and Standardization Institute (ETSI), 1997.

[ETS99] ETSI: *Broadband radio access networks (BRAN); HIPERLAN Type 2 technical specification, Part I: physical layer*. 1999.

[ETW08] Etkin, R.; Tse, D.; Wang, H.: Gaussian interference channel capacity to within one bit. *IEEE Transactions on Information Theory*, vol. 54, 2008, pp. 5534–5562.

[FF08] Farhoodi, A. A.; Fazaelifar, M.: Sphere detection in MIMO communication systems with imperfect channel state information. *6th Annual Communication Networks and Services Research Conference (CNSR'08)*, Halifax, 2008, pp. 228–233.

[FG98] Foschini, G. J.; Gans, M. J.: On limits of wireless communications in a fading environment when using multiple antennas. *Wireless Personal Communications*, vol. 6, 1998, pp. 311–335.

[FGVW99] Foschini, G. J.; Golden, G. D.; Valenzuela, R. A.; Wolniansky, P. W.: Simplified processing for high spectral efficiency wireless communication employing multi-element arrays. *IEEE Transactions on Information Theory*, vol. 17, 1999, pp. 1841–1852.

[Fis02] Fischer, R. F. H.: *Precoding and Signal Shaping for Digital Transmission*. New York: John Wiley & Sons, 2002.

[FK03] Fazel, K.; Kaiser, S.: *Multi-Carrier and Spread Spectrum Systems*. Chichester: John Wiley & Sons, 2003.

[FWLH02] Fischer, R. F. H.; Windpassinger, C.; Lampe, A.; Huber, J. B.: Space-time transmission using Tomlinson-Harashima precoding. *Proc. 4. ITG Conference on Source and Channel Coding (SCC'02)*, Berlin, 2002, pp. 139–147.

[GJJV03] Goldsmith, A.; Jafar, S. A.; Jindal, N.; Vishwanath, S.: Capacity limits of MIMO channels. *IEEE Journal on Selected Areas in Communications*, vol. 21, 2003, pp. 684–702.

[GKGØ07] Gesbert, D.; Kiani, S.; Gjendemsjø, A.; Øien, G.: Adaptation, coordination, and distributed resource allocation in interference-limited wireless networks. *Proceedings of the IEEE*, vol. 95, 2007, pp. 2393–2409.

[GKH+07] Gesbert, D.; Kountouris, M.; Heath, R.; Chae, C.; Sälzer, T.: Shifting the MIMO paradigm. *IEEE Signal Processing Magazine*, vol. 24, 2007, pp. 36–46.

[God01] Godara, L. C.: *Handbook of Antennas in Wireless Communications*. CRC Press, 2001.

[Gol05] Goldsmith, A.: *Wireless Communications*. Cambridge: Cambridge University Press, 2005.

[GvL96] Golub, G. H.; van Loan, C. F.: *Matrix Computations*. 3. edition. Baltimore: Johns Hopkins University Press, 1996.

[GW96] Giallorenzi, T. R.; Wilson, S. G.: Suboptimum multiuser receivers for convolutionally coded asynchronous DS-CDMA systems. *IEEE Transactions on Communications*, vol. 44, 1996, pp. 1183–1196.

[Hag97] Hagenauer, J.: The turbo principle: Tutorial introduction and state of the art. *Proc. International Symposium on Turbo codes and Related Topics*, Brest, 1997, pp. 1–11.

[Har06] Harte, L.: *Introduction to 802.16 WiMAX, Wireless Broadband Technology, Operation and Services*. Althos Publishing, 2006.

[Hat80] Hata, M.: Empirical formula for propagation loss in land mobile radio services. *IEEE Transactions on Vehicular Technology*, vol. 29, 1980, pp. 317–325.

[HJ85] Horn, R. A.; Johnson, C.: *Matrix Analysis*. Cambridge: Cambridge University Press, 1985.

[HK81] Han, T. S.; Kobayashi, K.: A new achievable rate region for the interference channel. *IEEE Transactions on Information Theory*, vol. 27, 1981, pp. 49–60.

[HM72] Harashima, H.; Miyakawa, H.: Matched-transmission technique for channels with intersymbol interference. *IEEE Transactions on Communications*, vol. 20, 1972, pp. 774–780.

[HPS05] Hochwald, B. M.; Peel, C. B.; Swindlehurst, A. L.: A vector-perturbation technique for near-capacity multiantenna multiuser communication – part II: Perturbation. *IEEE Transactions on Communications*, vol. 53, 2005, pp. 537–544.

[HZW08] Huang, M.; Zhou, S.; Wang, J.: Analysis of Tomlinson-Harashima precoding in multiuser MIMO systems with imperfect channel state information. *IEEE Transactions on Vehicular Technology*, vol. 57, 2008, pp. 2856–2867.

[HZZW07] Huang, M.; Zhang, X.; Zhou, S.; Wang, J.: Tomlinson-Harashima precoding in multiuser MIMO systems with imperfect channel state information. *Proc. IEEE Global Telecommunications Conference, IEEE(GLOBECOM'07)*, Washington, D.C., 2007, pp. 2806–2810.

[IMW+09] Irmer, R.; Mayer, H.-P.; Weber, A.; Braun, V.; Schmidt, M.; Ohm, M.; Ahr, N.; Zoch, A.; Jandura, C.; Marsch, P.; Fettweis, G.: Multisite field trial for LTE and advanced concepts. *IEEE Communications Magazine*, vol. 47, 2009, pp. 92–98.

[INF01] Irmer, R.; Nahler, A.; Fettweis, G.: On the impact of soft decision functions on the performance of multistage parallel interference cancelers for CDMA systems. *Proc. IEEE 53th Vehicular Technology Conference (VTC'01-Spring)*, vol. 2, Rhodes, 2001, pp. 1513–1517.

[Irm05] Irmer, R.: *Multiuser Transmission in Code Division Multiple Access Mobile Communications Systems.* Dissertationen. Aachen: Shaker-Verlag, 2005.

[IUN03] Ivrlač, M.; Utschick, W.; Nossek, J.: Fading correlations in wireless MIMO communication systems. *IEEE Journal on Selected Areas in Communications*, vol. 21, 2003, pp. 819–828.

[J+08] Jing, S.; et al.: Multicell downlink capacity with coordinated processing. *EURASIP Journal on Wireless Communications and Networking*, 2008.

[JB04] Jorswieck, E. A.; Boche, H.: Performance analysis of capacity of MIMO systems under multiuser interference based on worst-case noise behavior. *EURASIP Journal on Wireless Communications and Networking*, vol. 2004, 2004, pp. 273–285.

[JKG+02] Joham, M.; Kusume, K.; Gzara, M. H.; Utschick, W.; Nossek, J. A.: Transmit Wiener filter for the downlink of TDD DS-CDMA systems. *Proc. IEEE 7th International Symposium on Spread Spectrum Techniques & Applications (ISSSTA'02)*, vol. 1, Prague, 2002, pp. 9–13.

[JTW+09] Jungnickel, V.; Thiele, L.; Wirth, T.; Haustein, T.; Schiffermüller, S.; Forck, A.; *et al.*: Coordinated multipoint trials in the downlink. *Proc. 5th IEEE Broadband Wireless Access Workshop (BWAWS), co-located with IEEE GLOBECOM'09*, Honolulu, Hawai, 2009.

[JUN05] Joham, M.; Utschick, W.; Nossek, J.: Linear transmit processing in MIMO communications systems. *IEEE Transactions on Signal Processing*, vol. 53, 2005, pp. 2700–2712.

[JVG04] Jindal, N.; Vishwanath, S.; Goldsmith, A.: On the duality of Gaussian multiple-access and broadcast channels. *IEEE Transactions on Information Theory*, vol. 50, 2004, pp. 768–783.

[Kay93] Kay, S. M.: *Fundamentals of Statistical Signal Processing: Estimation Theory.* Upper Saddle River, NJ: Prentice Hall, 1993.

[Kay98] Kay, S. M.: *Fundamentals of Statistical Signal Processing, Volume 2: Detection Theory.* Upper Saddle River, NJ: Prentice Hall, 1998.

[KB93] Klein, A.; Baier, P. W.: Linear unbiased data estimation in mobile radio systems applying CDMA. *IEEE Journal on Selected Areas in Communications*, vol. 11, 1993, pp. 1058–1066.

[KBB+05] Kaiser, T.; Bourdoux, A.; Boche, H.; Fonollosa, J. R.; Andersen, J. B.; Utschick, W.: *Smart Antennas: State of the Art.* New York: Hindawi Publishing Corporation, 2005.

[KF08] Khattak, S.; Fettweis, G.: Low backhaul distributed detection strategies for an interference limited uplink cellular system. *Proc. IEEE 67th Vehicular Technology Conference (VTC'08-Spring)*, Singapore, 2008, pp. 693–697.

[KFV06] Karakayali, M.; Foschini, G.; Valenzuela, R.: Network coordination for spectrally efficient communications in cellular systems. *IEEE Wireless Communications*, vol. 13, 2006, pp. 56–61.

[KFVY06] Karakayali, M.; Foschini, G.; Valenzuela, R.; Yates, R.: On the maximum common rate achievable in a coordinated network. *Proc. IEEE International Conference on Communications(ICC '06)*, vol. 9, Istanbul, 2006, pp. 4333–4338.

[KH95] Knopp, R.; Humblet, P.: Information capacity and power control in single cell multiuser communications. *IEEE International Conference on Communications (ICC)*, vol. 1, Seattle, 1995, pp. 331–335.

[Kha08] Khattak, S.: *Base Station Cooperation Strategies for Multi-user Detection in Interference Limited Cellular Systems*. Dissertationen. Dresden: Vogt Verlag, 2008.

[KK08a] Kühne, A.; Klein, A.: Throughput analysis of multi-user OFDMA-systems using imperfect CQI feedback and diversity techniques. *IEEE Journal on Selected Areas in Communications*, vol. 26, 2008, pp. 1440–1451.

[KK08b] Kühne, A.; Klein, A.: Adaptive MIMO-OFDM using OSTBC with imperfect CQI feedback. *Proc. International ITG/IEEE Workshop on Smart Antennas (WSA'08)*, Darmstadt, 2008.

[KKB96] Klein, A.; Kaleh, G. K.; Baier, P. W.: Zero forcing and minimum mean-square-error equalization for multiuser detection in code-division multiple access channels. *IEEE Transactions on Vehicular Technology*, vol. 45, 1996, pp. 276–287.

[Kle96] Klein, A.: *Multi-user Detection of CDMA Signals – Algorithms and Their Application to Cellular Mobile Radio*. Fortschrittberichte VDI, Reihe 10. Düsseldorf: VDI, 1996.

[KM00] Kowalewski, F.; Mangold, P.: Joint predistortion and transmit diversity. *Proc. IEEE Global Telecommunications Conference, IEEE(GLOBECOM'00)*, vol. 1, San Francisco, 2000, pp. 245–249.

[KM07] Kamoun, M.; Mazet, L.: Base-station selection in cooperative single frequency cellular network. *Proc. IEEE 8th Workshop on Signal Processing Advances in Wireless Communications (SPAWC'07)*, Helsinki, 2007.

[Kra06] Kramer, G.: Review of rate regions for interference channels. *Proc. 2006 Int. Zurich Seminar on Communications*, Zurich, 2006, pp. 162–165.

[KRF08] Khattak, S.; Rave, W.; Fettweis, G.: Distributed iterative multiuser detection through base station cooperation. *EURASIP Journal on Wireless Communications and Networking*, 2008.

[Küh06] Kühn, V.: *Wireless Communications over MIMO Channels*. West Sussex: Wiley, 2006.

[KZK03] Karagiannidis, G.; Zogas, D.; Kotsopoulos, S.: On the multivariate Nakagami-m distribution with exponential correlation. *IEEE Transactions on Communications*, vol. 51, 2003, pp. 1240–1244.

[LDYT05] Lindner, J.; Dangl, M.; Yacoub, D.; Teich, W.: Comparison of vector detection algorithms for MIMO-OFDM. *Frequenz*, vol. 59, 2005, pp. 137–146.

[Lin05] Lindner, J.: *Informationsübertragung*. Berlin: Springer-Verlag, 2005.

[LR99] Liberti, J. C.; Rappaport, T. S.: *Smart Antennas for Wireless Communications: IS-95 and Third Generation CDMA Applications*. Upper Saddle River: Prentice Hall, 1999.

[LWZ04] Liu, Y.; Weber, T.; Zirwas, W.: Uplink performance of a service area based multiuser mobile radio system. *Proc. 9th International OFDM-Workshop (InOWo'04)*, Dresden, 2004, pp. 17–21.

[MBQ04] Meurer, M.; Baier, P. W.; Qiu, W.: Receiver orientation versus transmitter orientation in linear MIMO transmission systems. *EURASIP Journal on Applied Signal Processing*, vol. 9, 2004, pp. 1191–1198.

[MBW+00] Meurer, M.; Baier, P. W.; Weber, T.; Lu, Y.; Papathanassiou, A.: Joint transmission: Advantageous downlink concept for CDMA mobile radio systems using time division duplexing. *Electronics Letters*, vol. 36, 2000, pp. 900–901.

[MF07a] Marsch, P.; Fettweis, G.: A decentralized optimization approach to backhaul-constrained distributed antenna systems. *Proc. 16th IST Mobile and Wireless Communications Summit*, Budapest, 2007.

[MF07b] Marsch, P.; Fettweis, G.: A framework for optimizing the uplink performance of distributed antenna systems under a constrained backhaul. *Proc. IEEE International Conference on Communications (ICC'07)*, Glasgow, 2007.

[MF08] Marsch, P.; Fettweis, G.: On multicell cooperative transmission in backhaul-constrained cellular systems. *Annals of Telecommunications*, vol. 63, 2008, pp. 253–269.

[MF09a] Marsch, P.; Fettweis, G.: On downlink network MIMO under a constrained backhaul and imperfect channel knowledge. *Proc. IEEE Global Telecommunications Conference (GLOBECOM'09)*, Honolulu, 2009.

[MF09b] Marsch, P.; Fettweis, G.: On uplink network MIMO under a constrained backhaul and imperfect channel knowledge. *Proc. IEEE International Conference on Communications (ICC'09)*, Dresden, 2009.

[MH94] Madhow, U.; Honig, M. L.: MMSE interference suppression for direct-sequence spread-spectrum CDMA. *IEEE Transactions on Communications*, vol. 42, 1994, pp. 3178–3188.

[MK09] Motahari, A.; Khandani, A.: Capacity bounds for the Gaussian interference channel. *IEEE Transactions on Information Theory*, vol. 55, 2009, pp. 620–643.

[Moh98] Moher, M.: An iterative multiuser decoder for near-capacity communications. *IEEE Transactions on Communications*, vol. 46, 1998, pp. 870–880.

[Mos96] Moshavi, S.: Multi-user detection for DS-CDMA communications. *IEEE Communications Magazine*, vol. 34, 1996, pp. 124–136.

[MW03] Meurer, M.; Weber, T.: Generalized data estimate refinement techniques for iterative multiuser detection in TD-CDMA including higher order modulation. *Proc. 10th International Conference on Telecommunications (ICT'03)*, vol. 2, Papeete, 2003, pp. 781–787.

[MWQ04] Meurer, M.; Weber, T.; Qiu, W.: Transmit nonlinear zero forcing: Energy efficient receiver oriented transmission in MIMO CDMA mobile radio downlinks. Sydney, 2004, pp. 260–269.

[NB02] Noll Barreto, A.: *Signal Pre-Processing in the Downlink of Spread-Spectrum Communications Systems*. Fortschrittberichte VDI, Reihe 10, no. 687. Düsseldorf: VDI-Verlag, 2002.

[NEHA08] Ng, B.; Evans, J.; Hanly, S.; Aktas, D.: Distributed downlink beamforming with cooperative base stations. *IEEE Transactions on Information Theory*, vol. 54, 2008, pp. 5491–5499.

[NK07] Nadarajah, S.; Kotz, S.: A supplement to the Gaussian transform of distributions. *IEEE Transactions on Signal Processing*, vol. 55, 2007, pp. 3537–3541.

[OBS09] *OBSAI Reference point 3 specification v4.1.* 2009.

[OOF68] Okumura, Y.; Omori, E.; Fukuda, K.: Field strength and its variability in VHF and UHF land mobile service. *Review Electrical Communication Laboratory*, vol. 16, 1968, pp. 825–873.

[OR05] Olonbayar, S.; Rohling, H.: Multiuser diversity and subcarier allocation in OFDM-FDMA systems. *10th International OFDM-Workshop (InOWo'05)*, Hamburg, 2005, pp. 275–279.

[Par92] Parsons, J. D.: *The Mobile Radio Propagation Channel*. London: Pentech Press, 1992.

[PBGH08] Papadogiannis, A.; Bang, H.; Gesbert, D.; Hardouin, E.: Downlink overhead reduction for multicell cooperative processing enabled wireless networks. *Proc. IEEE International Symposium on Personal, Indoor, Mobile Radio Communications (PIMRC'08)*, Cannes, 2008.

[PGH08] Papadogiannis, A.; Gesbert, D.; Hardoin, E.: A dynamic clustering approach in wireless networks with multi-cell cooperative processing. *Proc. IEEE International Conference on Communications (ICC'08)*, Beijing, 2008.

[PH94] Patel, P.; Holtzman, J.: Analysis of a simple successive interference cancellation schmene in a DS/CDMA system. *IEEE Journal on Selected Areas in Communications*, vol. 12, 1994, pp. 796–807.

[PHG09] Papadogiannis, A.; Hardoin, E.; Gesbert, D.: Decentralising multicell cooperative processing: A novel robust framework. *EURASIP Journal on Wireless Communications and Networking*, vol. 2009, 2009.

[Poo00] Poor, H. V.: Turbo multiuser detection: An overview. *Proc. IEEE 6th International Symposium on Spread Spectrum Techniques & Applications (ISSSTA'00)*, vol. 2, Parsippany, 2000, pp. 583–587.

[Poo04] Poor, H. V.: Iterative multiuser detection. *IEEE Signal Processing Magazine*, vol. 21, 2004, pp. 81–88.

[Rap01] Rappaport, T. S.: *Wireless Commnucations: Principles and Practice*. New Jersey: Prentice Hall PTR, 2001.

[Sas04] Sason, I.: On achievable rate regions for the Gaussian interference channel. *IEEE Transactions on Information Theory*, vol. 50, 2004, pp. 1345–1356.

[Sat77] Sato, H.: Two-user communication channels. *IEEE Transactions on Information Theory*, vol. 23, 1977, pp. 295–304.

[Sat78a] Sato, H.: On degraded Gaussian two-user channels. *IEEE Transactions on Information Theory*, vol. 24, 1978, pp. 637–640.

[Sat78b] Sato, H.: An outer bound to the capacity region of broadcast channels. *IEEE Transactions on Information Theory*, vol. 24, 1978, pp. 374–377.

[Sat81] Sato, H.: The capacity of the Gaussian interference channel under strong interference. *IEEE Transactions on Information Theory*, vol. 27, 1981, pp. 786–788.

[Sch05] Schwartz, M.: *Mobile Wireless Commnucations*. Cambridge: Cambridge University Press, 2005.

[SFGK00] Shiu, D.-S.; Foschini, G. J.; Gans, M. J.; Kahn, J. M.: Fading correlations and its effect on the capacity of multielement antenna systems. *IEEE Transactions on Communications*, vol. 48, 2000, pp. 502–513.

[Sha61] Shannon, C. E.: Two-way communication channels. *Proc. 4th Berkeley Symposium on Mathematical Statistics and Probability*, Berkeley, CA, 1961, pp. 611–644.

[SPSH04] Spencer, Q.; Peel, C.; Swindlehurst, A.; Haardt, M.: An introduction to the multi-user MIMO downlink. *IEEE Communications Magazine*, vol. 42, 2004, pp. 60–67.

[SSPS09] Simeone, O.; Somekh, O.; Poor, H.; Shamai, S.: Downlink multicell processing with limited-backhaul capacity. *EURASIP Journal on Advances in Signal Processing*, vol. 2009, 2009.

[SSSP08] Shamai, S.; Simeone, O.; Somekh, O.; Poor, H.: Joint multi-cell processing for downlink channels with limited-capacity backhaul. *Proc. IEEE Information Theory and Applications Workshop 2008*, San Diego, 2008, pp. 345–349.

[Ste96] Steil, A.: *Spektrale Effizienz digitaler CDMA–Mobilfunksysteme mit gemeinsamer Detektion.* Fortschrittberichte VDI, Reihe 10, no. 437. Düsseldorf: VDI-Verlag, 1996.

[SZ01] Shamai, S.; Zaidel, B.: Enhancing the cellular downlink capacity via co-processing at the transmitting end. *Proc. IEEE 53th Vehicular Technology Conference (VTC'01-Spring)*, vol. 3, Rhodes, 2001, pp. 1745–1749.

[Tac03] Tachikawa, K.: A perspective on the evolution of mobile communications. *IEEE Communications Magazine*, vol. 41, 2003, pp. 66–73.

[Tar07] Taricco, G.: Optimum receiver design and performance analysis for fully correlated rician fading MIMO channels with imperfect channel state information. *Proc. IEEE Global Telecommunications Conference, IEEE(GLOBECOM'07)*, Washington, D. C., 2007, pp. 1546–1550.

[Tel99] Telatar, E.: Capacity of multi-antenna Gaussian channels. *European Transactions on Telecommunications*, vol. 10, 1999, pp. 585–595.

[TH98] Tse, D.; Hanly, S.: Multiaccess fading channels-part I: Polymatroid structure, optimal resource allocation and throughput capacities. *IEEE Transactions on Information Theory*, vol. 44, 1998, pp. 2796–2815.

[TH99] Tse, D.; Hanly, S.: Linear multiuser receivers: Effective interference, effective bandwidth and user capacity. *IEEE Transactions on Information Theory*, vol. 45, 1999, pp. 641–675.

[Tom71] Tomlinson, M.: New automatic equalizer employing modulo arithmetic. *IEE Electronics Letters*, vol. 7, 1971, pp. 138–139.

[TPK09] Tölli, A.; Pennanen, H.; Komulainen, P.: SINR balancing with coordinated multi-cell transmission. *Proc. IEEE Wireless Communications Networking Conference (WCNC'09)*, Budapest, 2009.

[TR309] *3GPP TR 36.814 V1.0.0: Evolved universal terrestrial radio access (E-UTRA); further advancements for E-UTRA physical layer aspects (Release 9).* 2009.

[TV05] Tse, D.; Viswanath, P.: *Fundamentals of Wireless Communication*. Cambridge: Cambridge University Press, 2005.

[TXX+05] Tao, X.; Xu, J.; Xu, X.; Tang, C.; Zhang, P.: Group cell FuTURE B3G TDD system. *Proc. IEEE International Symposium on Personal, Indoor and Mobile Radio Communications (PIMRC'05)*, vol. 2, Berlin, 2005, pp. 967–971.

[VA90] Varanasi, M. K.; Aazhang, B.: Multistage detection in asynchronous code-division multiple-access communications. *IEEE Transactions on Communications*, vol. 38, 1990, pp. 509–519.

[Ver86] Verdú, S.: Minimum probability of error for asynchronous Gaussian multiple-access channels. *IEEE Transactions on Information Theory*, vol. 32, 1986, pp. 85–96.

[Ver98] Verdu, S.: *Multiuser Detection*. Cambridge: Cambridge University Press, 1998.

[VJ98] Vojčić, B.; Jang, W.: Transmitter precoding in synchronous multiuser communications. *IEEE Transactions on Communications*, vol. 46, 1998, pp. 1346–1355.

[VJG01] Vishwanath, S.; Jafar, S.; Goldsmith, A.: Optimum power and rate allocation strategies for multiple access fading channels. *Proc. IEEE 53th Vehicular Technology Conference (VTC'01-Spring)*, Rhodes, 2001, pp. 2888–2892.

[VJG03] Vishwanath, S.; Jindal, N.; Goldsmith, A.: Duality, achievable rates, and sum-rate capacity of Gaussian MIMO broadcast channels. *IEEE Transactions on Information Theory*, vol. 49, 2003, pp. 2658–2668.

[vNP00] van Nee, R. D. J.; Prasad, R.: *OFDM for Wireless Multimedia Communications*. Boston: Artech House, 2000.

[VTA01] Viswanath, P.; Tse, D. N.; Anantharam, V.: Asymptotically optimal water-filling in vector multiple-access channels. *IEEE Transactions on Information Theory*, vol. 47, 2001, pp. 241–267.

[WBR+] Wübben, D.; Böhnke, R.; Rinas, J.; Kühn, V.; Kammeyer, K.-D.: Efficient algorithm for decoding layered space-time codes. *IEE Electronics Letters*, vol. 37, pp. 1348–1350.

[WC00] Wang, X.; Chen, R.: Adaptive Bayesian multiuser detection for synchronous CDMA with Gaussian and impulsive noise. *IEEE Transactions on Signal Processing*, vol. 47, 2000, pp. 2013–2028.

[WCLM99] Wong, C. Y.; Cheng, R. S.; Lataief, K. B.; Murch, R. D.: Multiuser OFDM with adaptive subcarrier, bit, and power allocation. *IEEE Journal on Selected Areas in Communications*, vol. 17, 1999, pp. 1747–1758.

[WE71] Weinstein, S. B.; Ebert, P. M.: Data transmission by frequency-division multiplexing using the discrete Fourier transform. *IEEE Transactions on Communication Technology*, vol. 19, 1971, pp. 628–634.

[Web03] Weber, T.: *Interferenzreduktion in CDMA-Mobilfunksystemen - ein aktuelles Problem und Wege zu seiner Lösung.* Habilitation, Lehrstuhl für hochfrequente Signalübertragung und -verarbeitung, Technische Universität Kaiserslautern, 2003.

[WFH04a] Windpassinger, C.; Fischer, R.; Huber, J.: Lattice-reduction-aided broadcast precoding. *IEEE Transactions on Communications*, vol. 52, 2004, pp. 2057– 2060.

[WFH04b] Windpassinger, C.; Fischer, R. F. H.; Huber, J. B.: Precoding in multiantenna and multiuser communications. *Proc. 5th ITG Conference on Source and Channel Coding (SCC'04)*, Erlangen, 2004, pp. 403–408.

[WFVH04] Windpassinger, C.; Fischer, R. F. H.; Vencel, T.; Huber, J. B.: Precoding in multiantenna and multiuser communications. *IEEE Transactions on Wireless Communications*, vol. 3, 2004, pp. 1305–1316.

[WHG+10] Wang, C.-X.; Hong, X.; Ge, X.; Cheng, X.; Zhang, G.; Thompson, J.: Cooperative MIMO channel models: A survey. *IEEE Communications Magazine*, vol. 48, 2010, pp. 80 – 87.

[Win98] Winters, J.: Smart antennas for wireless systems. *IEEE Personal Communications Magazine*, vol. 5, 1998, pp. 23 – 27.

[WJLY09] Wang, Q.; Jiang, D.; Liu, G.; Yan, Z.: Coordinated multiple points transmission for LTE-advanced systems. *Proc. 5th International Conference on Wireless Communications, Networking and Mobile Computing (WiCom'09)*, Beijing, 2009.

[WM02] Weber, T.; Meurer, M.: Iterative multiuser detection for TD-CDMA exploiting data estimate refinement techniques. *Proc. IEEE 56th Vehicular Technology Conference (VTC'02-Fall)*, vol. 3, Vancouver, 2002, pp. 1642–1646.

[WMSL02] Weber, T.; Maniatis, I.; Sklavos, A.; Liu, Y.: Joint transmission and detection integrated network (JOINT), a generic proposal for beyond 3G systems. *Proc. 9th International Conference on Telecommunications (ICT'02)*, vol. 3, Beijing, 2002, pp. 479–483.

[WP99] Wang, X.; Poor, V. H.: Iterative (Turbo) soft interference cancellation and decoding for coded CDMA. *IEEE Transactions on Computers*, vol. 47, 1999, pp. 1046–1061.

[WRB+02] Wübben, D.; Rinas, J.; Böhnke, R.; Kühn, V.; Kammeyer, K.-D.: Efficient algorihtm for detecting layered space-time codes. *Proc. 4th ITG Conference on Source and Channel Coding (SCC'02)*, Berlin, 2002, pp. 399–405.

[WSM06] Weber, T.; Sklavos, A.; Meurer, M.: Imperfect channel state information in MIMO transmission. *IEEE Transactions on Communications*, vol. 54, 2006, pp. 543–552.

[WSS06] Weingarten, H.; Steinberg, Y.; Shamai, S.: The capacity region of the Gaussian multiple-input multiple-output broadcast channel. *IEEE Transactions on Information Theory*, vol. 52, 2006, pp. 3936–3964.

[WW08] Wei, X.; Weber, T.: MMSE detection based on noise statistics with random noise variance. *Proc. IEEE Vehicular Technology Conference (VTC'08-Fall)*, Calgary, 2008.

[WW10] Wei, X.; Weber, T.: Cooperative communication with partial channel-state information in multiuser MIMO systems. *International Journal of Electronics and Communications (AEÜ)*, 2010. accepted for publication.

[WWA07] Wei, X.; Weber, T.; Ahrens, A.: Decentralized signal processing for inter-cell interference cancellation with partial CSI. *Proc. 12th International OFDM-Workshop (InOWo'07)*, vol. 1, Hamburg, 2007, pp. 316–320.

[WWAD07] Wei, X.; Weber, T.; Ahrens, A.; Deng, S.: Decentralized interference management in mobile radio networks. *Frequenz*, vol. 61, 2007, pp. 259–269.

[WWC08] Wu, K.; Wang, L.; Cai, L.: Joint multiuser precoding and scheduling with imperfect channel state information at the transmitter. *Proc. IEEE 67th Vehicular Technology Conference (VTC'08-Spring)*, Singapore, 2008, pp. 265–269.

[WWKK08] Wei, X.; Weber, T.; Kühne, A.; Klein, A.: Optimum MMSE detection with correlated random noise variance in OFDM systems. *Proc. 13th International OFDM-Workshop (InOWo'08)*, vol. 1, Hamburg, 2008, pp. 138–142.

[WWKK09] Wei, X.; Weber, T.; Kühne, A.; Klein, A.: Joint transmission with imperfect partial channel state information. *Proc. IEEE Vehicular Technology Conference (VTC'09-Spring)*, Barcelona, 2009.

[WWWS09] Wei, X.; Weber, T.; Wolfgang, A.; Seifi, N.: Joint transmission with significant CSI in the downlink of distributed antenna systems. *Proc. IEEE International Conference on Communications (ICC'09)*, Dresden, 2009.

[XZ09] Xiao, S.-h.; Zhang, Z.-p.: Network multi-point coordinating downlink transmission with the clustered precoding design. *Proc. International Conference on Communications, Circuits and Systems (ICCCAS'09)*, Milpitas, 2009, pp. 128–132.

[YC01] Yu, W.; Cioffi, J. M.: Trellis precoding for the broadcast channel. *Proc. IEEE Global Telecommunications Conference (GLOBECOM'01)*, vol. 2, San Antonio, 2001, pp. 1344–1348.

[YC04] Yu, W.; Cioffi, J. M.: Sum capacity of Gaussian vector broadcast channels. *IEEE Transactions on Information Theory*, vol. 50, 2004, pp. 1875–1892.

[YCCG05] You, X.; Chen, G.; Chen, M.; Gao, X.: Toward beyond 3G: The FuTURE project in China. *IEEE Communications Magazine*, vol. 43, 2005, pp. 38–44.

[Yen01] Yener, A.; Yates, R. U. S.: Interference management for CDMA systems through power control,multiuser detection, and beamforming. *IEEE Transactions on Communications*, vol. 49, 2001, pp. 1227–1239.

[YRBC04] Yu, W.; Rhee, W.; Boyd, S.; Cioffi, J.: Iterative water-filling for vector multiple-access channels. *IEEE Transactions on Information Theory*, vol. 50, 2004, pp. 145–152.

[ZCA+09] Zhang, J.; Chen, R.; Andrews, J.; Ghosh, A.; Heath, R.: Networked MIMO with clustered linear precoding. *IEEE Transactions on Wireless Communications*, vol. 8, 2009, pp. 1910–1921.

[ZD04] Zhang, H.; Dai, H.: Cochannel interference mitigation and cooperative processing in downlink multicell multiuser MIMO networks. *EURASIP Journal on Wireless Communications and Networking*, vol. 2004, 2004, pp. 222–235.

[ZHG09] Zakhour, R.; Ho, Z.; Gesbert, D.: Distributed beamforming coordination in multicell MIMO channels. *Proc. IEEE Vehicular Technology Conference (VTC'09-Spring)*, Barcelona, 2009.

[ZLW01] Zeng, H. H.; Li, Y.; Winters, J. H.: Improved spatial-temporal equalization for EDGE: a fast selective-direction MMSE timing recovery algorithm and two-stage soft-output equalizer. *IEEE Transactions on Communications*, vol. 49, 2001, pp. 2124–2134.

[ZTZ+05] Zhang, P.; Tao, X.; Zhang, J.; Wang, Y.; Li, L.; Wang, Y.: A vision from the future: Beyond 3G TDD. *IEEE Communications Magazine*, vol. 43, 2005, pp. 38–44.

List of Figures

List of Tables

Thesen

1. Conventional mobile radio cellular systems are interference-limited.

2. The OFDMA transmission technique could be applied to eliminate the intracell interference with respect to inter-symbol interference and intracell multiuser interference.

3. Cooperative communication based on coordinated base stations (BSs) is a promising candidate for intercell interference management.

4. A two-user communication channel without any cooperation between transmitters or between receivers can be considered as a two-user interference channel. The Han-Kobayashi strategy achieves the best known inner bound for the capacity region of the interference channel.

5. A two-user communication channel with cooperative receivers can be considered a two-user multiple access channel with multiple antennas at the common receiver. The minimum mean square error detection combined with the successive interference cancellation strategy in the receiver achieves its capacity region.

6. A two-user communication channel with cooperative transmitters can be considered as a two-user broadcast channel with multiple antennas at the common transmitter. The dirty-paper coding strategy in the transmitter achieves its capacity region.

7. A two-user communication channel with full cooperation at both the transmitters and the receivers can be considered as a MIMO channel. Optimum power allocation based on the singular value decomposition of the channel matrix achieves its sum-capacity.

8. The cooperative communication scheme can significantly enlarge the achievable rate region of the interference channel as compared to the scheme with no cooperation.

9. At some operating points of interest, cooperative communication with appropriately selected partial channel state information achieves good system performance with little capacity loss as compared to that with full channel state information.

10. A practical cooperative communication scheme considering the channel knowledge, the signal processing algorithm and the decentralized implementation architecture is proposed for realistic cellular networks.

11. In order to make a good compromise between performance and complexity, the significant channel state information corresponding to the channels which play a significant role in the system performance is considered in joint detection and joint transmission.

12. According to the functionalities of physical channels, the significant useful channels are distinguished from the significant interfering channels for each mobile station (MS). A dynamic MS-oriented significant channel selection scheme is proposed.

13. The iterative zero-forcing joint detection with significant channel state information for interference cancellation is performed at the coordinated BSs to implement cooperative reception in the uplink.

14. The iterative zero-forcing joint transmission with significant channel state information for interference presubstraction is performed at the coordinated BSs to implement cooperative transmission in the downlink.

15. The decentralized implementation can make full use of the proposed iterative zero-forcing joint detection/transmission algorithm. The joint signal processing of all MSs is distributed to a parallel cooperative signal processing of individual MSs.

16. The joint detection/transmission scheme with dynamically selected MS-oriented significant channels outperforms the joint detection/transmission scheme with structure-oriented fixed significant channels.

17. The system performance can be improved by considering more significant interfering channels at the BSs corresponding to the significant useful channels.

18. Intelligent signal processing techniques can significantly benefit from smart BS-antenna-layouts.

19. The imperfectness of the channel state information has a great impact on both the significant channel selection and the joint detection/transmission.

20. The larger the imperfectness of the channel state information is, the less channel state information should be considered in joint detection/transmission to obtain the optimum system performance.

21. Advanced statistical signal processing schemes for multiuser detection exploiting the soft information could further improve the system performance.

Selbstständigkeitserklärung

Ich erkläre, diese Arbeit selbständig angefertigt und die benutzten Unterlagen vollständig angegeben zu haben.

Rostock, 14.07.2010

\- -

(Xinning Wei)